DISEASE DYNAMICS IN THE PRESENCE OF A RESERVOIR: A CASE STUDY OF BOVINE TUBERCULOSIS IN UK CATTLE INDUSTRY

SCOTT THOMAS BEE

Doctor of Philosophy

Institute of Computing Science and Mathematics
University of Stirling

August 2022

DECLARATION

I hereby declare that this thesis is entirely the result of my own work and includes nothing which is the outcome of any work done in collaboration except where specifically indicated within the text and bibliography.

I also declare that this thesis (or any significant part thereof) is not substantially the same as any that I have previously submitted, or that is being concurrently submitted, for a degree or diploma or other qualification at the University of Stirling or similar institution.

Stirling, May 2022

Scott Thomas Bee

ABSTRACT

Bovine tuberculosis (bTB) is one of the most complex, persistent and controversial problems facing the British cattle industry. For the last 20 years, increasing incidence rates have resulted in bTB becoming endemic in much of England (especially the southwest). Imperfect control strategies used to mitigate bTB effects often lead to cyclic disease behaviour, where once a farm is cleared of bTB infected cattle, the disease will continue to remerge some time later. This thesis explores one of bTB's primary open questions, what are the quantitative proportions each pathway contributes to persistent reinfection? The current data sets regarding residual disease are imperfect due to data gaps, high variability in disease parameters, and conflicts between data sets. These factors obscure the actual underlying mechanics of bTB within a herd, preventing the construction of optimal control strategies.

This thesis uses mathematical modelling to examine the primary disease mechanisms that result in residual disease remaining on a farm; latency, wildlife reservoir, and environmental contamination. Each of these disease mechanisms forms a chapter of the thesis, by focusing on each mechanism we can understand how they affect disease dynamics. After examining these mechanisms separately, this thesis considers their combined effect by numerically simulating bTB within a herd.

The first mathematical model investigates how imperfect testing and bTB's long latency period permits infection to remain on the farm. The highly variable latency period suggests that cattle may potentially be infected years before becoming infectious themselves. Additionally, imperfect disease diagnostic tools permit further transmission, as undiagnosed infected hosts may further spread bTB before being discovered and removed. The mathematical models derived from examining this mechanism uses a non-markovian exposure period, extending the exponentially distributed parameters to the Erlang distribution. The highly flexible and adjustable Erlang distribution means that we can further incorporate the variable nature of the latency period by adjusting the number of exposure compartments. In this chapter, we construct the SE^nTIRC model and perform mathematical analysis on the associated set of differential equations, examining the long term behaviour of solutions, system equilibria, and the threshold value for the system ($\mathcal{R}_0$). Afterwhich, we further extend the SE^nTIRC model, creating the SE^nT^mIRC model, which has Erlang distributed parameters for the entire latency period. Lastly, this chapter finishes by exploring how altering the latency period distribution

affects the long term disease dynamics of our model.

The next mechanism examined through mathematical modelling is wildlife reservoirs, exploring how they affect inter-herd disease dynamics. The interconnected disease dynamics between a herd and wildlife reservoirs create a continuous cycle of unobserved spill-over and spill-back between the two populations. This chapter studies this relationship through the construction of a multi-host system. The analysis of this model is similar to the previous chapter, as we examine the long term behaviour of solutions, system equilibria, and the threshold value for the system ($\mathcal{R}_0$). However, the interconnected system dynamics permit the system to backward bifurcate, a cumbersome phenomenon from a public health and control perspective. If the system undergoes backward bifurcation, the normal threshold ($\mathcal{R}_0$) of the system may not be enough to reduce the disease presence, as a further critical threshold is created. Further control measures must therefore be implemented to reduce the disease dynamics under this new lower threshold value. The nature and feasibility of backward bifurcation are therefore explored and discussed for this disease wildlife model.

The last mechanism explored is bTB's environmental contamination and its effect on disease transmission within the farm. The bacterium *M. bovis* can contaminate soil, troughs, cattle feed, hay, and various other materials for substantial periods of time. Even though the ecological literature heavily discusses environmental contamination, especially from the perspective of how the wildlife reservoirs and cattle interact, very little of the modelling literature discusses this component. This chapter poses and analyses a mathematical model incorporating environmental contamination as a component. Similar to the previous models, this model is analysed in terms of its long term behaviour of solutions, system equilibria, and the threshold value for the system ($\mathcal{R}_0$), where numerical simulations are also presented to give a more complete representation of the model dynamics.

The last model uses simulation techniques to investigate how the different model mechanisms expressed throughout this thesis work in conjunction. The other mechanisms were contemplated and considered through the lens of dynamical systems. If all model mechanisms were considered in conjunction, the resulting complexity of the set of differential equations would make the system very complicated to analyse, if not impossible, with currently available methods. However, through the use of simulations and their techniques, much of the underlying complexity can be mitigated. This simulation model explores three main research themes; badger contribution, culling rate, and residual disease. This simulation examines the associated wildlife reservoir's contribution to disease dynamics by considering how the system reacts if the wildlife reservoir is fully and partially excluded. The following section examines how the testing and detection strategy works by varying the test sensitivity and the

associated culling rate. Lastly, we attempt to quantify the different pathways in which residue disease is left on the farm.

Governments and Public Health officials can only construct optimal control strategies by completely understanding how bTB spreads and transmits. Quantifying these mechanisms will shed further light on these residual disease pathways, providing researchers with a clearer understanding of how to best mitigate bTB's effect. Only through the construction of better control mechanisms can we possibly eradicate the most complex, persistent and controversial problems facing the British cattle industry.

ACKNOWLEDGEMENTS

I would like to sincerely thank both my supervisors, Dr Anthony O'Hare and Prof Rachel Norman, for their time, patience, and support. I'm deeply grateful for the guidance and supervision they have given me over the years. Additionally, I would like to thank many others from Stirling University. Firstly, I would like to thank two of the most genuinely kind and helpful people I have ever encountered; Grace McArthur and Gemma Gardiner. Thanks for all the helpful advice and laughter over the years. I would also like to give special thanks to Mila Goranova, Ken Reid, and Paul McMenemy, for their time, wisdom, perspective, and friendship.

Thank you to my partner, Thomas Deveney, for constantly listening to me rant and talk things out, cracking jokes when things became too serious, and for all the sacrifices you have made. From the bottom of my heart, thanks for all your love, support, and encouragement.

Lastly, I'd like to express my deepest gratitude to my parents. Thanks to my mother, who taught me kindness, compassion and optimism. Thanks to my father for teaching me dedication and to never give up. Thanks for always having my best interest at heart and always believing in me. Thanks for everything!

DEDICATION

Calum Rowan

28/09/1992 - 20/08/2021

Who taught me that all problems can be solved by simply charging at them!

CONTENTS

LIST OF TABLES

Part I

INTRODUCTION

1

INTRODUCTION

1.1 RESERVOIR SYSTEMS

By the nature of disease evolution, it is advantageous for pathogens to infect multiple species. As infecting interconnected species, a disease can replicate and spread to previously unattainable susceptible hosts populations. This evolutionary advantage is believed to be why cross-species diseases are so prevalent, 61.6% of all human pathogens and 77.3% of all domestic livestock pathogens [1]. Similarly, the OIE (World Organisation for Animal Health) have also stated that 57 out of 70 diseases that cause the most significant impact internationally are these multi-host pathogens [2].

Epidemiologists need to understand the dynamics of infectious diseases in complex multi-host communities, in order to mitigate disease threats to public health, conservation efforts, and the global economy [3]. The CDC and the WHO indicate that this research will be vital to tackle the increasing number of new emerging diseases [4]. In light of antibiotic resistance, demographic changes, societal behaviour patterns, changes in ecology, and climate change, both institutions predict emerging diseases will become an increasing cause for concern [2]. These changes force native and foreign species to interact, enabling existing and newly evolved pathogens to emerge, into increasingly fragile ecological environments.

Cross-species pathogens pose complex challenges for complete disease eradication, especially where these species interact [5]. The interconnected disease dynamics between two populations may maintain the disease; as infection can spill-over and spill-back between the two distinct populations ("target population" and "reservoir"). If we consider the main population of concern as the target population, then a reservoir can be abstractly defined as:

> "one or more epidemiologically connected populations or environments in which the pathogen can be permanently maintained and from which infection is transmitted to the defined target population" [6].

Disease reservoirs play an essential role in maintaining multiple disease worldwide [7] and subsequently prevent the function of numerous disease control strategies [8], as gathering inter-species interaction data is impractical due to its inherent complexities [9], making reservoirs intrinsically difficult to identify. In many diverse situations, even when diseases are

assumed to be maintained by reservoirs, the exact wildlife species involved are rarely identified [6]. For example, the Ebola virus is an emerging disease in various regions and researchers strongly believe a yet unidentified reservoir has caused this spread and maintenance [10].

Once a reservoir population is identified, controlling the wildlife reservoir is often impractical; merely observing the population can prove challenging enough. This lack of disease surveillance within the reservoir population(s) facilitates a continuous unobserved cycle of spill-over and spill-back between the target population and the reservoir. Reservoirs therefore mask the true routes of infection by acting as a secure hidden source connected to the target population, consistently maintaining the disease. Moreover, reservoirs provide a hidden contagion pathway, as their interconnected nature also bridges different target sub-populations [6].

What tools do we have to mitigate the effects of the reservoir population? Ecologists and environmental agencies suggest governing officials have three main policy strategies available at their disposal; target control, decoupling control, and reservoir control [6]. Target control should be policy managers first protocol, where intervention is directed solely towards the target population. The main advantages of this approach are that we require no knowledge of complicated reservoir dynamics and usually can exert a more substantial influence over the target population. The next available tool is decoupling strategies, these aim to reduce cross-species interactions by enhancing environmental biosecurity measures (e.g. fences to reduce interactions). Lastly, policy makers may impose reservoir controls, which refers to the reduction of disease within the reservoir (e.g. culling/vaccination programmes).

To avoid unforeseen consequences, reservoir control should only be implemented when the reservoir structure, function, and interdependent dynamics are understood fully. However, if surveillance is poorly managed drastic actions are often taken to prevent an epidemic in the target population. Examples include: in Hong Kong (1998 & 2001) several million chickens were slaughtered to prevent a projected Influenza A virus outbreak [11], in Malaysia (1999) 1 million pigs were slaughtered due to the Nipah virus [12], and in 2001 the United Kingdom culled several million cattle to prevent a foot and mouth outbreak [13].

Under proper epidemiological governance, Haydon et al. proposed that the following three questions are answered before a combination of decoupling strategies and reservoir controls are implemented on wildlife reservoirs [6];

1. Is the transmission cycle wholly understood, including all reservoir populations?

2. Are the ramifications of the proposed interference comprehensively understood?

3. Does cost-benefit analysis indicate that the proposed actions have economic benefits, when considering the cost of culling and any required future interventions?

Haydon et al. argue that failure to answer these questions fully may lead to dire adverse consequences. For example, carnivore culling in Canada resulted in exploding moose and deer populations, where the subsequent grazing pressure and habitat damage had significant knock-on effects for the local ecological balance [8]. The resultant ecological damage required significant financial and conservation efforts, exceeding any financial benefits of the cull [14]. These questions force responsible parties to consider the associated disadvantages of culling programmes; hunting limitation, temporary effects if not sustained, increased dispersal and migration due to social disruptions, and compensatory reproduction [4]. These mitigating factors usually making such culling strategies disappointingly inefficient [8]. Culling a reservoir may temporarily reduce the spill-over and spill-back between the reservoir and target population by reducing their interactions, however, culling often increases the overall disease proportion within the reservoir population, as the resulting heightened migration causes an increase in inter-reservoir interactions. Hence, as the reservoir population grows, so does the disease proportion, intensifying the disease presence within the reservoir. Public officials must therefore be very considerate when culling a species, as the practice is often both expensive, ethically and ecologically unacceptable. However, even with proper diligence in constructing the culling regime structure, results are still far from reliable [8].

In summary, disease reservoirs exacerbate nearly all forms of disease transmission. By acting as an undetected source, reservoirs increase the target population's disease persistence and inhibit control strategies. Proposed reservoir control strategies must be exact and considered, otherwise they can have inefficient or even contrary results. As a result of humanity's destructive actions, the global burden of cross-species disease systems will become progressively more severe [4]. To prevent this increased mortality and morbidity will require a multi-faceted approach from Biologists, Veterinary professionals, Ecologists, Modellers, Biostatisticians, Public Health officials, and Policy Makers.

This thesis aims to develop mathematical models to understand the underlying dynamics of these systems through the lens of bovine tuberculosis within the British cattle industry. However, there are a multitude of reservoir systems out there; why has this specific system been chosen?

Bovine tuberculosis (bTB) is one of the most complex, persistent and controversial problems facing the British cattle industry, resulting in the slaughter of around 45,000 cattle each year [15]. The estimated average UK economic fallout has been costed at around £120 million each year since 2010. The cattle industry directly losses around £50 million through livestock

culling, liquidity issues, veternairy bills, and other associated cost [15]. The UK government incurs the remaining £70 million, where the majority of this costs takes the form farm reimbursement, farm subsidies, and testing costs [15]. The disease's complexity is derived from various compounding characteristics; long latency period, poor test sensitivity, environmental contamination, and high cattle trading migration; each of these complicating characteristics work in synergy to obscure the underlying disease dynamics. The remainder of this chapter will focus on bovine tuberculosis within the UK cattle industry, describing the current situation and discussing how these complicating characteristics impede disease surveillance and current control strategies.

1.2 BOVINE TUBERCULOSIS

Bovine tuberculosis (bTB) is a chronic respiratory disease induced by members of the *Mycobacterium tuberculosis* complex, predominately *Mycobacterium bovis* (*M. bovis*). This worldwide zoonotic pathogen infects a vast range of animals (practically all mammals) [16], however, cattle constitute the largest reservoir and primary source of infection for humans [17]. Other domesticated ruminates (e.g. sheep and goats) and wildlife species (e.g. wild boars, deer, and badgers) are also susceptible and commonly act as reservoirs themselves [18]. This contagious disease can be transmitted either directly or indirectly; direct transmission occurs when a host inhales infected aerosol (fomites), usually expelled by infectious agents exhaling or coughing [19]. Whereas indirect transmission results from a host interacting with contaminated material, usually through ingestion in the case of cattle [20].

Most developed countries have managed to mitigate or eliminate bovine TB from their cattle population, or have at least contained the disease to a limited number of regions. However, complete eradication of bTB is complicated by wildlife reservoirs maintaining the disease; European badgers in the UK [16], white-tailed deer in pockets of the USA [21] and brushtail possums in New Zealand [22], conversely, in many developing countries infection remains a severe and systemic problem for animal and human health with various factors fuelling this disparity; limited surveillance and control strategies, consumption of contaminated food sources, and inadequate public health facilities [23]. The regions experiencing the highest incidence of bovine tuberculosis throughout the world are within Africa and Asia (especially sub-Saharan Africa [24]. Moreover, agricultural professionals in these regions are at a notably higher risk, particularly if the occupation involves direct contact with cattle; farmers, milkmaids, abattoirs workers, or butchers [25]. Worryingly over the last decade, the number of animals and human cases in these regions have grown exponentially year on year [26].

1.2.1 *Mycobacterium Bovis*

The causal agent for bovine tuberculosis (bTB) is *Mycobacterium bovis*, which is one member of the *Mycobacterium tuberculosis* complex. Below are the most notable species and subspecies with their primary host populations in brackets; *M. tuberculosis* (humans - Worldwide), *M. canettii* (Humans - Horn of Africa), *M. africanum* (Humans - West Africa), *M. pinnipedii* (Seals), *M. microti* (Voles and other small rodents) and *M. caprae* (goats, cattle and other ruminants) [27]. [1] *Mycobacterium bovis* is not the only causal agent of bovine tuberculosis, as in central Europe *M. caprae* has caused bTB, albeit significantly fewer cases when compared to *M. bovis*. However, *M. caprae* does not constitute an obstacle to disease control, as it presents similarly to *M. bovis* and the same diagnostic test will identify the host as a positive reactor [29].

Mycobacterium bovis predominately infects cattle but does induce natural cases in humans, although this number is significantly higher in developing countries that consume raw meats and unpasteurised milk [30]. Whereas, for human cases the most notable member of the *Mycobacterium tuberculosis* complex is *M. tuberculosis* itself. This pathogen induces a staggeringly high number of tuberculosis cases and is endemic in various regions worldwide [31]. Currently, *M. tuberculosis* is estimated to have infected one-quarter of the global population [32], although 20 years ago this number was closer to one-third [33]. Even though *M. tuberculosis* has a low mortality rate, due to the high incidence rate the disease still causes 1.18 million human deaths per year (2019), making it the 13^{th} most common cause of death worldwide [34].

Both *M. bovis* and *M. tuberculosis* pathogens induce a slow and progressive disease with similar clinical symptoms: a general state of illness, persistent cough, high temperature, pneumonia, weight loss, tiredness, fatigue, and eventually death [35]. One fundamental characteristic of tuberculosis progression is its extensive variability in the observed latency period, where the disease may remain dormant for years before becoming active [32]. As bTB progresses within the host, granulomas develop within the host respiratory system [35]. These lesions allow the disease to persist and continually replicates *M. bovis*, infecting the host further. Theoretically, tuberculous lesions can form in most body tissues, however, these lesions are predominately found in the upper respiratory system, lungs' interior, and lymph nodes (especially in the thorax) but can also be found in the intestines, liver, spleen, pleura, and peritoneum [36]. In most cases, tuberculosis is a chronic disease and can be burdensome to identify by clinical symptoms alone. Infected hosts may shed the bacteria before the appearance of clinical signs; even in advanced cases where lesions have formed in multiple organs,

1 Interestingly, only recently have both *M. caprae* and *M. pinnipedi* been distinguished from *M. bovis*. Gene sequencing technology (16S rRNA) is a tool to identify bacteria at the species level and differentiate between closely related bacterial species. Microbiologists managed to distinguish between these two strains but found the strains have identical 16s RNA sequences with over 99.9% of their genome sequenced [28].

clinical symptoms may still be lacking [36].

1.3 PUBLIC HEALTH SIGNIFICANCE

From a public health perspective, *M. tuberculosis* induces the majority of human cases worldwide but *M. bovis* still poses a risk to human health within specific regions of the developing world. Researchers estimated that *M. bovis* induces around 3.1% of the total human tuberculosis cases globally [37]. However, this statistic has a high regional dependency, as similar estimations predict that *M. bovis* contributes to less than 1% of total cases in developed nations, whereas this may be as high as 30% in developing countries (particularly sub-Saharan Africa; Tanzania, Nigeria, and Ethiopia) [30]. What causes this disparity between developing and developed nations?

1.3.1 *Developed Countries*

Most developed countries have managed to mitigate or eliminated bovine TB from their livestock populations through enforcing safeguards; systematic surveillance projects, regular meat inspection, and the pasteurisation of dairy products. These simple measures have managed to reduce the risk of infection to humans substantially, only a few occupations remain at risk; farmers, veterinary workers, abattoir workers, and butchers [38]. Besides farmers, the next occupation at most risk is abattoir workers (especially meat handlers) [16]. Previously employees have contracted tuberculosis through inhalation of aerosols or accidental inoculation via skin contact while processing contaminated carcasses [16]. Nevertheless, cases in these occupations are still rare and continually declining due to informational campaigns regarding the zoonotic risks of bovine tuberculosis [39]. Furthermore, in light of increasing bTB cases among cattle in the United Kingdom, the Food Standards Agency have implemented new measures to monitor meat contamination [40]. The Food Standards Agency stress that the cooking process purges *M. bovis* from meat and the public health risk is minimal. As according to the Food Standards Agency there are "no known cases where TB has been transmitted through eating meat and the risk of infection from eating meat, even if raw or undercooked, remains extremely low." [40].

1.3.2 *Developing Countries*

In the developing world, *M. bovis* is still a prominent public health risk for both animals and humans [41]. As we shall see, this disparity in disease incidence rates can be attributed to a lack of resources to prevent disease transmission, differing husbandry and cultural practices, and other compounding public health problems.

In developing countries, many regions and communities simply do not have the technology, finances or required labour to achieve disease surveillance, never mind combat TB's effects. For this reason, the preventative measures enacted in developed countries such as systematic testing, regular meat inspection, and pasteurisation of dairy products are rarely accomplished [42]. The second major contributing factor which increases exposure is differing husbandry and cultural practices. Worldwide, most humans contract bTB by interacting with cattle, other domesticated ruminates (e.g. sheep and goats), and wildlife species (e.g. wild boars, deer, and badgers). Community exposure risk is therefore intrinsically higher in regions which share communal living spaces with livestock or if regional cuisine contains dishes with soured milk, raw and exotic meats [26]. In addition, the factors compound with differences in wildlife density and behaviour, average health and sanitation, and labour-intensive farming, meaning that virtually all of the population is at risk of infection [43].

Additionally, tuberculosis is only one of the various public health problems facing developing countries. If multiple diseases are endemic they may co-infect hosts, exacerbating infection dynamics. A particularly apt example is HIV and tuberculosis, as these pathogens form a deadly human syndemic, acting in synergy to magnify the burden of disease [44]. HIV and tuberculosis is the quintessential example of this behaviour, the immune deficiency caused by HIV increase both the susceptibility and chance of tuberculosis becoming active [44]. This dual co-infection proliferates both diseases and further weakens the population. This behaviour is particularly apparent in sub-Saharan Africa, where there exists a strong positive correlation between both cases and deaths of tuberculosis patients with HIVs [44].

The myriad of differences presented here illustrates why *M. bovis* still constitutes a severe public health risk in the developing world (particularly in Africa). Conversely, in developed countries the number of human cases are significantly lower [38], as these countries have the available resources to actively managed the disease. Undoubtedly, there exists a strong relationship between a country's relative wealth and its effectiveness in disease management. In the following section, we shall discuss how the disease affects nations' economies, where again, this discussion is divided between the developing and developed countries.

1.4.1 *Incidence rates in Developed Countries*

In most developed countries the number of zoonotic TB cases are minimal, as most have either managed to eradicate or at least control bTB within their cattle populations [45]. The low public health risk associated with reduced infection rates has led developed countries to focus on restricting trade from infected herds and extending surveillance programs (both national and international).

Member State (MS)	OTF status	N (prevalence %) of infected herds in OTF regions	N (prevalence %) of test-positive herds in non-OTF regions
Austria		3 (0.005)	– (*)
Belgium		6 (0.023)	–
Bulgaria	■	–	8 (0.011)
Croatia	■	–	3 (0.013)
Cyprus	■	–	0
Czech Republic		0	–
Denmark		0	–
Estonia		0	–
Finland		0	–
France		123 (0.066)	–
Germany		6 (0.004)	–
Greece	■	–	131 (0.715)
Hungary		2 (0.012)	–
Ireland	■	–	5,573 (5.046)
Italy	▨	9 (0.020)	232 (0.576)
Latvia		0	–
Lithuania		0	–
Luxembourg		0	–
Malta	■	–	0
Netherlands		0	–
Poland		14 (0.003)	–
Portugal	▨	0	77 (0.252)
Romania	■	–	34 (0.007)
Slovakia		0	–
Slovenia		1 (0.003)	–
Spain	▨	0	2,384 (2.291)
Sweden		0	–
United Kingdom	▨	8 (0.060)	10,359 (12.226)
EU Total		**172 (0.015)**	**18,801 (1.93)**

(*): –: not applicable (no such regions).
OTF: Officially bovine tuberculosis free (status for freedom from bovine tuberculosis, in cattle).
□, All regions of the MS are OTF.
▨, Not all regions of the MS are OTF.
■ No region of the MS is OTF.

Figure 1.1: The current OTF status of European countries with associated incident percentages of herds and regions.

The European Union requires all countries to follow specific requirements if some of their farms are not "Officially Tuberculosis Free" (OTF). As of 2020, table 1.1 shows that eleven countries still have non-OTF farms [46]. Out of these eleven countries, seven have no regions declared bTB free; Bulgaria, Croatia, Cyprus, Greece, Ireland, Malta, and Romania. Whereas in the other four countries bTB is only endemic in specific regions; Italy, Spain, Portugal and the United Kingdom [46].

The legislation of the European Union requires all countries with non-OTF farms to impose tuberculosis eradication programs that operate according to a specific framework. Following this mandate, farms with livestock must test their whole cattle herd using the single intradermal comparative cervical tuberculin test (SICCT) routinely, usually at least once a year [47]. The SICCT test and other diagnostics factors will be discussed in detail in section 1.7. Under the following conditions a farm will lose its OTF status; failure to follow regulations, a

single positive reactor is discovered, or *M. bovis* is identified in cultures grown from suspicious lesions discovered at the abattoir [48]. If any of these criteria are met, a farm is categorised as OTFW (OTF-withdrawn). Once a farm has lost its OTF status, they are prohibited from participating in livestock trading for any purpose (buying or selling). In order to regain the OTF status, a farm must pass two consecutive whole herd tests within a 60 days period [49]. The associated cost of surveillance and maintenance of bTB in some European countries has been criticised by governments [46], especially if there is little history of bTB. However, various studies have indicated that bTB would become endemic once again in historically active regions without such measures [46].

1.4.2 *Incidence rates in Developing Countries*

Calculating the economic impact of human bTB in developing countries is exceptionally troublesome to measure accurately due to unreliable and inconsistent datasets [24]. The exact impact may be difficult to determine, however research indicates that bTB and other systemic diseases have a high associated economic burden for developing countries [30]. From a public health point of view, high workforce morbidity rates cause significant economic inefficiencies that developing countries could repurpose associated health expenditure funds; treatment costs, health workers wages, prescriptions, medical equipment, etc [30]. Other economic benefits would also result from reducing morbidity rates; for example, improved average health quality would positively influence workforce productivity [26].

While there is much discussion in the literature regarding the severe economic burden to the agricultural sector [24], [41], [23], lacking the availability of a reliable and cost-effective diagnostic test, true incidence levels among cattle herds remain obscured [24]. With little confidence in the accuracy of our current estimates of cattle incidence rates, accurate costs of the disease cannot be achieved. Even from the limited surveillance accomplished, current estimates of prevalence levels vary considerably; for example, in central Africa, bTB prevalence rates range from 0.2% to 19.9% [23]. Nonetheless, even though exact incidence rates are not known explicitly, virtually all literature indicates that *M. bovis* and its effects are at least prevalent in all major livestock-producing developing countries, especially in sub-Saharan Africa [41], [26].

1.5 RESERVOIRS

Species and subspecies within the *M. tuberculosis* complex tend to infect a single primary host population [27]. In humans, infections are produced by *M. tuberculosis*, M. canettii, and M. africanum [27]. Similarly in animal populations, seals are infected by M. pinnipedii, voles by

M. microti, and goats/sheep by M. caprae [50], [27]. However, Mycobacteria bovis is somewhat unique in its ability to infect a vast number of hosts effectively, its extensive host range consists of domesticated livestock (notably ruminants, e.g. sheep, goats, buffalo, and deer) and wildlife species (e.g. badgers, boar, possums, greater kudu, warthog, and lechwe) [51]. There are documented cases where other tuberculosis species have infected other animal species, yet it is rare for the disease to be maintained out-with their primary host population [51]. In the above examples, bTB cases are not just spill-over from cattle populations, instead *M. bovis* is maintained within these populations [51]. Importantly, the inherent isolation exhibited between these host species is unlikely to indicate cross-species adaption, rather particular strains of *M. bovis* have crossed into these different species [52].

It is becoming increasingly apparent from bTB eradication programs worldwide (North America, Spain, New Zealand, and Australia) that implemented control mechanics not addressing the reservoir population are ineffective at eradicating the disease [53]. In order to eradicate bTB, governments must design and execute adequate control mechanics which tackle both the disease in the target population and the reservoir population.

A particularly apt example of this phenomenon is the badger's wildlife reservoir in the United Kingdom and the Republic of Ireland. Badgers are currently the only documented wildlife reservoir and are considered the main barriers preventing the eradication of bTB among livestock populations [54]. The same European Union regulation has reduced incidence in most European Union countries, however, within the UK, average number of cases have been increasing year on year from the 1970's [55]. Infected badgers presents complex challenges to disease eradication in the UK, as they can live asymptomatically throughout their natural lives and shed *M. bovis* through their urine, faeces, sputum and saliva [18]. The disease poses no obstacles to either breeding or migration, therefore it will likely spread bTB to other badgers and cattle. Once a badger within a sett becomes infected, it is not long until the infection spreads to the remaining members due to the close and confined nature of badger burrows [54]. Transmission is also likely between neighbouring badger setts because of badgers strong territorial nature, as during territorial disputes biting exchanges a high bacterial load [20]. Therefore, badgers exhibit prototypical behaviour associated with a reservoir. Once a badger is infected, it begins spreading the disease among the local reservoir population, from there it spreads to both the target population and to further subsets of the badger population.

1.6 EPIDEMIOLOGY

Transmission of bovine tuberculosis occurs when bacteria aerosols are exhaled directly from an infected host's respiratory tract. These aerosols linger in the air as contaminated fine dust

particles (fomite particles); susceptible hosts' respiratory systems then become exposed after inhaling the pathogen [56]. Analogously, bTB may also be contracted by ingesting contaminated material as sputum and salvia contaminate the surrounding objects and the environment [56]. After initial exposure a host is classified as infectious once they begin exhaling the pathogen, which requires lesions to form in a host's lungs and lymph nodes. Statistics from abattoir inspection studies suggest that between 40% and 73% of all reactors have lung lesions, although it is believed that this percentage is much higher as many of such lesions are too small to be identified by the human eye [57]. Moreover, the location of these lesions also plays an essential role in transmission, as further laboratory examination of carcasses found that around one-fifth of positive reactors shed *M. bovis* primarily from their upper respiratory tract [56]. These cattle play an important role in disease transmission and are referred to as superspreaders, as hosts are more likely to shed *M. bovis* in both frequency and quantities [56].

After contracting bTB the rate at which the disease progresses is highly variable with various risk factors, as the disease may take a few weeks to a lifetime for clinical signs to manifest [58]. As the reactivation of latent bTB may occur years after initial infection [59], this grants the opportunity for bTB to spread throughout a herd unnoticed before the onset of clinical signs appears. The latency effect of bTB therefore obscures disease dynamics and contributes to one of the main unanswered questions facing disease eradication:

> On a farm recently categorised as OTF, do subsequent breakdowns result from an adjacent badger reservoir or from an undiagnosed latent infected cattle (originating from the farm or undetected cattle introduced via inter-farm trade)?

Due to the poor sensitivity and specificity, modern diagnostic tools do not allow us to rule out the existence of unidentified infectious cattle remaining in the herd after testing [43]. However, what the literature does suggests is that high volume livestock trading, proximity to an infected wildlife reservoir, and remaining undiagnosed cattle all play an integral role in the disease dynamics [60][61]. Unfortunately, the relative percentage effect that each of these contributes still remains unknown and without these percentages, policy makers will continue to implement imperfect disease control strategies.

1.6.1 *Transmission*

As the last section indicates, there still exists some unanswered questions within the literature regarding transmission. Another such critical question is what percentage of hosts contract the disease through inhalation or ingestion? The OIE states that worldwide, bTB among cattle is

mainly a respiratory disease and subsequently contracted as such [62]. Transmission therefore must primarily result from direct and sustained contact with an infectious host. The opposite view is that indirect transmission also plays a vital role, defined as ingestion or inhalation of contaminants from materials such as herd feed, troughs, other farm equipment, and pastures [20]. Direct contact transmission constituted the vast majority of transmissions [63][62], which is evident throughout the modelling literature as most only consider direct contacts [64], [65]. However, this belief has recently been called into question, especially regarding how the disease spreads between herd and reservoir. Several more recent observational studies have shown that badgers and cattle tend to avoid each other [54], [66]. If badgers and cattle interact so infrequently, how is the dual dynamics of spill-over and spill-back maintained? An increasing amount of research implies that badgers and cattle interact indirectly through the shared environment [66]. Researchers have therefore been considering, if contamination of the shared medium may facilitate the spread of disease between these species, is the same true for cattle?

Much of the previous epidemiological and modelling literature does not adequately incorporate the idea of the shared environment into the conceptual notion of a reservoir. The environmental contamination is an important mechanic in the spread of bTB, as it obfuscates actual underlying dynamics, facilitating future infections even after complete removal of all infectious cattle. This disagreement within the literature is a still an active area of research with various open questions remaining.

1.6.1.1 *Cattle to Cattle Transmission*

The most prolific transmission pathway for spreading bTB throughout a herd is cattle to cattle transmission, as according to the analyses presented in [17], 94.3 % of all UK bTB cases result from cattle to cattle transmission. The remaining 5.7% of cases are as a result of wildlife reservoirs. Cattle to cattle transmission is comprised of the following components; within-herd transmission (at both pasture and housing), over the fence transmission, livestock trading transmission, vertical disease transmission, and environmental contamination [17]. Each of these factors plays an essential role in disease transmission, nevertheless most bTB cases are contracted on the farm from infected individual(s) within the herd, either through direct contact or environmental contamination.

Alluded to earlier, there is currently a debate on the proportion of the disease transmitted between cattle through ingestion or inhalation. Until somewhat recently, indirect transmission was not considered a contributing factor and was believed to be a rare occurrence. Although, as reservoirs transmission occurs through a shared medium [66], some open questions have

begun to arise. The majority of papers addressing this dispute have indicated that indirect transmission plays an important role but direct transmission between cattle is still far more likely. However as there is still little quantitative evidence regarding the exact percentage each contributes, the debate is ongoing. The primary reasons supporting the direct transmission pathway are; the reduced bacterial load required for infection and the location of lesions found during cattle necropsies [48], [9]. Researchers have demonstrated experimentally that fewer bacilli are needed to transmit the disease via inhalation, in contrast to the much higher bacterial load needed to transmit the disease through ingestion [20]. Furthermore, statistics from abattoir investigations indicated the distribution of contagious lesions are predominantly confined to the upper respiratory system indicating infections occur through inhalation [67]. Although, lesion detection preformed by the human eye are unreliable, further laboratory investigations are required to quantify the distribution [48].

1.6.1.2 *Inter-farm Dynamics*

How then does infection spread from farm to farm? The main two transmission pathways are over the fence infection transmission or cattle movement due to livestock trading.

Over the fence refers to infection jumping from one farm to another, either through cattle interacting directly at farm boundaries or by airborne transmission. Several studies have demonstrated that farms are at an increased risk of infection depending on the proximity to contagious premises [19]. It is common practice for farms in both the UK and Ireland to share a boundary with adjacent herds, presenting a potential risk of cross-infection [19],[17]. In Ireland, around a quarter of incidents (23% - 25%) were attributed to this cross-infection at boundaries [17]. Moreover, farms adjacent to a contagious herd were four times more likely to sustain bTB themselves [17]. Similarly in Northern Ireland, around 40% of breakdowns were attributed to the presence of a neighbouring herd experiencing a breakdown [17].

The second main mechanism is cattle trading, the literature suggests the current high volume of trading facilitates the spread of bTB both nationally and internationally [23]. Moreover, cattle trade is averagely increasing year on year within the EU at both a national and international level [68]. By utilising molecular epidemiology techniques, phenotype studies have indicated that cattle movements are the root cause of most breakdowns in previously unaffected herds [69]. Before legislation enforcing coupled pre-movement and post-movement testing, cattle sold from high incident areas in England to Scotland (bTB free) were around four times more likely to induce a breakdown than those from other herds [69]. Cattle movements have the additional hazard of being the only transmission mechanism with the ability to transport the disease long distances, granting the disease the opportunity to become endemic within

new regions. This phenomenon was demonstrated after the foot-and-mouth outbreak within the UK in 2001. Nationwide restocking transported bTB infected cattle to new previously unaffected susceptible herds, allowing bTB a foothold in new regions and in many of these regions the disease still persists currently [18].

In 2006-2009, APHA (animal and plant health agency) implemented changes in UK cattle trading legislation, requiring pre-movement and post-movement testing. Similar legislation (Council Directive 64/432/EEC) has since been introduced within the European Union. As a result of this new legislation, the associated risk of cattle movements on bTB levels has been substantially reduced in the UK and EU [70][68]. However, with current diagnostic tools we currently cannot concretely say an individual cow is free from bTB at the point of trade [17] as current screening tests for bTB focus on testing of herds rather than individuals [68]. Hence, cattle movements will continue to propagate the spread of bTB until we develop improved screening techniques. Newer EU trade agreements attempt to minimise exposure by increasingly utilising concepts like regionalisation, zoning, and compartmentalisation as principles of disease control [68], however, this only mitigates bTB transmission and does not prevent it entirely.

1.6.1.3 *Vertical disease transmission*

Vertical disease transmission (VDT) is defined inconsistently within the literature, certain definitions only refer to transmission from mother to offspring during either pregnancy or childbirth. Whereas other definitions also consider short-term post-parturition infections related to the mother's behaviour (pseudo-vertical disease transmission). Vertical disease transmission (VDT) is not a significant factor for the transmission of bTB in the UK [16]. A large cohort study in Northern Ireland results indicate that there exists no statistical evidence that a positive reactor's offspring are more likely to become infected themselves [71].

Conversely, pseudo-VDT is a prominent infection route worldwide, as calves may become infected by drinking contaminated milk directly from their mothers. Direct udder-feeding is still common in the developing world and is one of the main reasons for their relatively higher incidence rates [72]. Alternatively, in most developed countries (including the UK), the pseudo-VDT pathway has been all but eradicated, as newborn heifers are separated from their mothers at birth and are kept separate until their first calving [73]. Additionally, calves are supplied with a substitute feed instead of cow's milk [74], both of these measures prevent the risk of pseudo-vertical disease transmission.

1.6.1.4 *Wildlife Reservoir*

In both the UK and Ireland, the European badger (*Meles meles*) is the main reservoir for bTB and is often noted as the main obstacle in eradicating bTB in domesticated livestock [73]. Badgers play an essential role in the inter-farm community dynamics of bTB and this claim has been well documented in the literature utilising molecular testing techniques [75]. Whole Genome Sequencing (WGS) is increasingly being used to study the forensic epidemiology of bacterial pathogens, as these diagnostic tools are especially useful when analysing unobserved reservoir populations [76]. As WGS techniques allows epidemiologists to glean insight about the reservoir indirectly. Phenotype studies indicate that bTB is continuously in a state of spilling over and spilling back between the target population and reservoir [75]. Their results indicate that 40% of the badger samples taken were indistinguishable from the sample sequenced in cattle, implying close inter-community spreading occurs [76]. In the same study, no sequenced sample from badgers were more than four mutational steps away from the nearest reactor cow. As discussed previously, only 5.7% of infections in cattle are as a result of badger interaction, although notably, these new cattle cases are estimated to subsequently generate around 52% of the total bTB cases observed [17].

Evidently, badgers transmit *M. bovis* to cattle and there is strong observational evidence indicating that cattle likewise transmit *M. bovis* to badgers [77]. Despite this, numerous uncertainties and inconsistencies remain with such findings. Various studies have indicated that direct contact between badger and cattle is infrequent [63], [78]. For the most part, both badger and cattle tend to avoid each other [79],[66]. For example, ecologists used a combination of GPS monitoring collars and contact collars in [66] to examine the underlying interaction between badgers and cattle. Across four sites, the researchers monitored 421 collared cattle for a total of 8551 collar days, 53 contact-collared badgers for 8308 collar days, and 54 GPS-collared badgers for 7176 days. They found no direct contact between cattle and badgers during the entire study, where direct contact is the required distance for the aerosol transmission to occur (proximity of 1.5 m) [66]. What makes this mutual avoidance even more striking is that the same study also concluded that badgers preferred habitat is in fact cattle pastures [66]. Clearly, inter-population spread between badgers and cattle is more likely to occur through the shared environmental landscape, rather than direct contact.

1.6.1.5 *Environmental Contamination*

The previous GPS monitoring collars and contact collars study [66] suggests direct transmission may be rare, where some ecologists have went as far to even suggest non-existent

[80]. How then does the disease contamination result in cross species inter-community spread?

M. bovis can survive in the environment as fine dust particles or it may contaminate either pastures or water sources [20]. If *M. bovis* undergoes aerosolisation, it has been demonstrated experimentally that these contaminated aerosols linger in the air for 12-24 hours and is resistant to associated environmental decay [19]. Furthermore, this infection interval is expected to be considerably longer if cattle are housed permanently indoors, due to the poor ventilation associated with housing pens [20]. The estimated decay rate of bTB contaminants in some environmental matrix (e.g. feed, hay, soil, or water) is exceptionally variable, lasting anywhere between a couple of days to two years [16]. Contamination of these environmental matrices occurs by infected cattle excreting M.bovis through their urine, faeces, saliva, nasal secretion, and sputum [19]. One USA (Michigan) study found that *M. bovis* remains viable and pathogenic for 88 days in soil and 58 days in both water and hay [62]. Whereas similar studies in the UK have found the bacteria may remain present in pastures and soils for around six months [79]. The survival and persistence of *M. bovis* rises in other mediums such as faeces (8-9 months) and dry cattle feed (9 months) when stored indoors [79],[19]. The different time intervals are likely due to the UK climate, multiple studies have found that tubercle bacilli best survive in cool, shaded, and moist environments [20]. Under laboratory conditions, researchers have demonstrated that *M. bovis* remains viable up to twice as long if within a shaded environment [16]. Consequentially, similar field studies imply longer survival times during the winter months; GB [79], New Zealand [81], Michigan [62], and Australia [82].

Contamination of drinking water has also been identified as a typical transmission pathway between local wildlife and cattle (white-tailed deer in the USA [83] and boar in Spain [84]). Infected hosts shed *M. bovis* through nasal and oral secretion into communal water sources, often supporting reservoir and target population interaction. In the UK, communal water sources are not considered a significant risk factor in reservoir and target population interaction, as most cattle drink from self-contained troughs. However, livestock troughs have yet to be examined thoroughly in the literature and may be a more substantial source of contamination than currently thought. Defra suggests that troughs may be contaminated by saliva and sputum, advising regular cleaning and disinfection of water troughs and avoiding stagnation if possible [85]. Furthermore, in separate advice regarding badger biosecurity measures, Defra suggests raising water troughs to at least 80cm to prevent badger contamination [16]. Defra advises similar measures should be implemented regarding feeder rings, as these have also been suggested as a potential source of contamination [16].

1.6.2 *Transmission Summary*

Effective management of infectious disease relies upon fully understanding the mechanisms behind how a particular pathogen transmits. Lacking a comprehensive understanding of the primary infectious routes, public health officials may implement ineffective management strategies endangering the lives of humans, domestic livestock and local wildlife. Unfortunately, discovering an accurate quantitative description of the transmission mechanisms have yet to be fully achieved due to various discussed complications [65]. The main transmission pathways are known; cattle to cattle transmission, inter-farm transmission, wildlife reservoir, and environmental transmission, however, the exact percentage that each contribute still eludes researchers. Without a clearer conceptual picture of bovine tuberculosis transmission and persistence, public health officials will not be able to fully control or eradicate bovine tuberculosis from the UK cattle industry.

1.6.3 *Risk Factors*

In an epidemiological context, susceptible refers to an individual within a population that could potentially become infectious [86]. What makes such an individual more susceptible or resistant remains unclear, as there is relatively limited knowledge about susceptibility at a granular level. Below we shall discuss the general factors associated with variability and resistance of bTB broadly in two main themes; animal level and herd management level.

1.6.3.1 *Animal level*

GENETICS, SEX, BREED AND FARM TYPE Through the study of genetic engineering, researchers are striving to determine what proportion of a host's susceptibility/resistance is as a result of the host's genetic makeup. With this knowledge, scientists could isolate which gene variations result in this resistance and subsequently create a breeding program to mitigate bTB within the cattle population [18]. The genetic differences within species seem to be responsible for significant variation in the heritability of susceptibility to bTB [87]. UK and Ireland studies have examined the genetic variation of dairy cattle population (mainly Holstein Friesian pure breeds or mixed breeds) and found that between 16% and 18% of variance in bTB resistance was estimated to be heritable when diagnosed with the SICCT test [88]. Comparatively, less is known regarding beef cattle due to the lack of investigation, although one Irish study found similar variation among the various beef breeds and estimated the heritability of susceptibility to be 13% [89].

Many open questions regarding how bovine tuberculosis resistance differs between the sexes remain, the different functions and husbandry practises between the sexes prevents the construction of informative comparisons. These inherent differences are compounded when we consider farm management type between dairy cattle or beef cattle. As bulls and steers (castrated males) are only used within the beef farming industry, comparatively in the UK, most dairy cows and heifers never even interact with males as they are inseminated artificially [90].

Dairy cattle tend to experience elevated incident rates due to higher herd density, contact rates, and average life expectancy [91]. Researchers believe that these differences are responsible for the higher incidence rates exhibited in dairy cattle herds [91], as comparatively, dairy cattle older than two years are 40% more likely to be infected compared to similar beef cattle [91]. At the same time, young calves on either a dairy herd or beef herd experienced a similar level of infection [91]. As a result of these differences, the majority of the literature suggests that on average males experience lower level of incidences of bTB [91], [92] and ,[93] however, none of the papers noted above, considered for the differing function and husbandry practises between the sexes. Therefore, currently this literature does not demonstrate any intrinsic difference in susceptibility to bTB between male and female livestock.

MATURITY, HEALTH, AND BEHAVIOUR One consistent thread throughout the literature is that cattle's relative risk and susceptibility increase with age [91]. UK surveillance data suggests that the relationship between incidents and age increases monotonically for the first 24-36 months, after which incident rates begin to level off [91]. This relationship arises from the fact that cattle past the age of three are more sensitive to the SICCT test, increasing the likelihood of detection [91]. The positive correlation between incidents and longevity most likely arises from prolonged exposure to routes of infection; within-herd infection, wildlife reservoir infection, and environmental contamination. The longer a host lives, the higher the probability of contracting the disease and overcoming the variable latency period. Additionally as cattle reach late adulthood their susceptibility increases due to a weakening of their cellular immunity response [94]. However, this weakening effect is not as pronounced compared to humans as livestock rarely reach their nature longevity [94].

Cattle's immune response directly affects their susceptibility and is conditional on various factors, not just age. Poor nutritional conditions can suppress a cattle immune system, increasing the susceptibility to bTB and the likelihood that latent bTB activates [87]. Poor health also negatively affects diagnostic tools, as there exists a positive correlation between responsiveness to the SICCT test and body condition index in lactating Holstein-Friesian UK dairy cows [95], implying cattle with a more susceptible disposition are less likely to respond to the SICCT

test accurately. On the other hand, two separate Irish studies concluded there existed no significant differences in cattle susceptibility if fed either an energy-restricted or unrestricted diet [96],[97]. Further research is required to discover the immunological consequences that nutritional and body conditions have on susceptibility.

The host constitution is not the only factor at play, as host behaviour similarly has a profound effect on susceptibility. Throughout the different stages of maturity in the cattle life cycle, their inter-host and environmental contact networks vary tremendously. Cattle are inquisitive by nature, particularly calves and younger dominant cows will examine and investigate new objects in their surroundings [98]. Observational studies have shown these cattle were most likely to approach badgers and possible contamination sources (e.g. badger latrines) [63]. This pattern also holds true for inter-host connections, UK studies using contact data loggers have shown that younger adults have the highest number of connections with other cattle [63]. The heterogeneous characteristic of contact networks has a profound effect on cattle susceptibility, as seen in a New Zealand study, which found that 86% of positive reactors originated from the herd's top 20% most interconnected cattle [98].

1.6.3.2 *Herd-level*

HERD CHARACTERISTICS The literature is virtually unanimously agreed that incidence rates of bTB increase as herd size does; this holds true regardless of geographical region or relative local prevalence [99]. Dynamic modelling has shown that as herd size grows, so does the number of potential within-herd connections, increasing the opportunity for transmission to occur [100]. Consequentially, numerous papers indicate a positive correlation between herd size and the likelihood of a breakdown. However, herd size is not an independent factor but rather it constitutes various other positively correlated contributing risk factors; farm management style, farm acreage, neighbouring farms, geographical location, livestock density and trade movements [16]. This umbrella term of herd size may then be misleading, as these constituting factors are more likely to induce a varied number of cases in different scenarios. For example, farms with the largest herd size often have the highest herd density; under cramped conditions livestock are in contact for prolonged periods of time which exacerbates bTB transmission. Alternatively, due to the imperfect sensitivity and specificity of the diagnostic test, false-positive diagnosis increases with herd size, increasing the likelihood of a breakdown irrespective of incidence levels within the farm.

The farm production type also influences the same risk combination seen by the proxy of herd size, as comparatively, dairy herds have a higher risk of infection than beef herds [101]. Many of the same underlying factors contributing to herd size are more frequently found in the dairy herd management style; elevated herd size, herd density, trading volume, and

contact per day [16]. A UK study using surveillance data found that most of the supplementary incidence of bTB in dairy farm compared to beef farms could be attributed to increased herd size and location of dairy herds within the UK [100].

FARM MANAGEMENT Understanding the relationship between transmission and susceptibility allows farmers to implement 'good' farm management. Organising and operating a farm with proper disease prevention has been shown to maximise animal welfare, production and profits [102], as good farm management and a high standard of hygiene may prevent or reduce the risk of having a herd breakdown [18]. In a UK study, farms exhibiting poor management techniques were at an enhanced risk of having persistent breakdowns. This study specifically highlighted the following issues; wildlife reservoirs having access to farm buildings and feed stores, cattle grazing at pasture margins, and badger activity in pastures [20]. Recently, the role of farm management is more apparent due to "big agriculture"; large farming conglomerates have increased their market share over the last 30 years [103]. These farms tend to be poorly managed from a disease mitigation point of view, as these herds tend to have increased contact rates and stress levels, increasing overall herd susceptibility [103].

1.6.4 *Risk Factors Summary*

This section demonstrates that the various risk factors associated with bTB are complex and interwoven. Differing herd elements have a profound effect on bTB's disease progression, where independent cattle characteristics are not the only factor affecting bTB's expression, the farm type and management style also contribute. Hence, the individual risk factors affecting a singular farm vary tremendously from farm to farm. The UK control strategy should therefore not be designed broadly but instead, control strategies should be individually tailored for each farm's differing risk factors.

1.7 DIAGNOSTICS

How do we determine if a cow is infected with bovine tuberculosis? As we shall see, the accurate detection of bTB in cattle remains exceptionally challenging. The imperfect nature of current diagnostic tools play an integral role in the high level of persistence seen in the southwest of England's dairy farms [104]. At present, there exists no singular test available with the ability to accurately identify all infectious hosts within a herd [105]. Most surveillance programs within the wider developed world rely solely on two main detection pathways; whole herd testing using the tuberculin skin test (TST) and abattoir examination of carcasses for symptomatic lesions [106]. Where suspected lesions are subsequently confirmed for *M.*

bovis by growing bacterial cultures [43],[100]. In this section, we shall illustrate the associated weaknesses of the different available tests; tuberculin skin test, Gamma-interferon assay, post-mortem investigations, and lastly, we shall discuss a vaccine and its effects on diagnostics.

1.7.1 *Tuberculin Skin Test*

Under European Union Legislation, there are only two legally approved diagnostic tests permitted to detect bTB within cattle; Gamma-interferon assay and the Tuberculin Skin Test (TST) (Mantoux Test). However, the inherent advantages of TST's relatively low cost and ease of administration has led to it becoming the international standard test for conducting whole-herd tests [107]. The test works by eliciting a delayed hypersensitivity reaction to an intradermal injection consisting of bovine tuberculin, which is a protein synthesised from mycobacterial cultures [108]. If the host's immune system recognises the tuberculin antigens, the infected host's body mounts an inflammatory response and begins swelling at the injection site. Inflammation peaks between 2-3 days later and rapidly declines thereafter [106]. If a host is bTB free, the host body is not sensitive to bovine tuberculin and therefore elicits no local inflammatory response. By examining the injection site, members of the veterinarian profession can distinguish if a host is infected or not.

There are two primary forms of the TST, either the single intradermal skin test or the single intradermal comparative tuberculin test (SICCT test). The single intradermal skin test injects one dose of *M. bovis* tuberculin, whereas, the single intradermal comparative tuberculin test (SICCT) compares the host's different responses to two injections (one injection of *M. bovis* tuberculin and M. avium tuberculin) [105]. The SICCT test is standard in the UK as it facilitates the differentiation of hosts infected with *M. bovis* or hosts infected with another mycobacterium [106]. The UK national eradication program runs in accordance with the European Union Council Directive 64/432/EEC (EU,1980), which regulates the TST test boundary for determining when a host is a positive reactor. Under this legislation, a host is considered a positive reactor for the SICCT test if the inflammation response is at least 4mm greater than the reaction at the avian tuberculin injection site [109]. An inconclusive result refers to an inflammatory response between 1 to 4 mm and such cattle must be retested [109]. If one host is inconclusive twice or more, the host is deemed a positive reactor [109]. The level of inflammation recorded during the SICCT test is indicative of the severity of disease progression within the host, as hosts that react strongly to the SICCT test tend to have visible disease markers discovered during post-mortem examination [110].

Within the literature, it is generally accepted that newly infected hosts will remain undetected using SICCT for some time [101]. Under experimental conditions cattle were inoculated

with the *M. bovis* pathogen, three weeks after initial exposure some cattle began being positively identified by the SICCT test [111]. Similarly, official OIE guidelines state that for SICCT test to detect infected hosts, there is between a three to six week development period before the delayed hypersensitivity reaction will occur [111]. Although various authors have expressed dubiety in these time frames, suggesting further study into the factors affecting the incubation period is required [18]. For example, there are numerous cases of bTB becoming active years after initial infection [112]. Therefore, there still remains extreme variations in the required duration period before test results are reliable.

In addition to these findings, extensive evidence indicates that the SICCT test may become ineffective and even unresponsive to chronically inflicted hosts [16]. Livestock with advanced cases of bTB may become so immunocompromised that their body fails to produce an inflammatory response. Cattle in this stage are classified as anergic hosts and their lack of reaction effectively nullifying the SICCT test results. However, anergic hosts are rarely discovered within developed countries, as earlier surveillance programs will likely detect such hosts before they become anergic [16].

Often within high incidence areas, once cases of bTB are detected within a farm, the infection typically persists [113]. Infected herds must be continually retested until they successfully complete two consecutive whole-herd tests that are clear of reactors and are within 60 of each other [18]. Often with each subsequent whole herd test, new unidentified infected hosts are discovered [113]. However, recent research indicates that the inter-testing interval plays a vital role in the sensitivity of the SICCT test. If infected cattle undergo two consecutive tests a short time apart, the second test often fails to detect bTB [114]. The desensitisation of the test is most intense in the first seven days after administration [114], although, some studies state that such mitigation effects on test sensitivity are only diminished after 60 days [114]. Other studies have suggested this weakening effect has a prolonged residual effect, especially on borderline cases [115]. Moreover, recent work has indicated that enforcing a minimum 60 day inter-test interval, which many researchers have suggested, would not be sufficient to mitigate the effects [115]. As laboratory experiments and observational data have shown that continually testing at a 60 day interval leads to desensitisation of future tests [115].

As numerous compounding factors may adversely affect the SICCT test's inherent reliability, estimating the associated sensitivity has proven to be challenging [108]. The varied range of cattle breeds creates difficulties in sampling, as no easily accessible subset of cattle would provide an accurate proxy for the entire worldwide cattle population. Estimating test sensitivity for cattle from one particular area may vary significantly in different areas or countries, especially those with differing farm management styles, husbandry practises, reservoir popu-

lations, etc [105]. To truly determine the average sensitivity for the entire cattle population of the UK, a larger cross-sectional sample of cattle would be required to be simultaneously tested. After which, the entire sample would have to be slaughtered so that post-mortem investigations could accurately verify these test results. By developing mycobacterial cultures for these hosts, we could accurately determine the test's sensitivity. Although, even with the high confidence attached to post-mortem investigation, no test is perfect, these test imperfections would introduce systematic errors into our predicted sensitivity. Such studies have been completed, although the sample sizes are often far too small or focus on dairy cattle from high incidence areas. The results of these studies are inconsistent and provide a considerable variation in estimated sensitivity, ranging from 51% to 89% under the standard SICCT interpretation [116].

There exists a secondary classification procedure for the SICCT test referred to as "severe interpretation", where a host is identified as a positive reactor if they only react to the bovine tuberculin or if there is a 2mm discrepancy between the bovine tuberculin and avian tuberculin injection sites [18]. However, by employing the severe interpretation, we increase the SICCT sensitivity at the detriment of specificity. For example, one study estimated the standard tests sensitivity to be within the range 70% to 89% and under the severe interpretation, this range increased to be between 78% to 91% [18]. However, in the same study, the SICCT's specificity reduced from 99.98 $\pm$ 0.004% to 99.91 $\pm$ 0.013% [18]. Undeniably, using the severe interpretation would increase the number of cattle detected considerably, although the subsequent numbers of false positives reactors culled would be impractical.

1.7.2 *Gamma-interferon assay*

Gamma-interferon blood assay is the second test approved by the EU directive 64/432 annexe B [117], designed to act as a supplementary test to the TST. When used in conjunction with the tuberculin skin test (TST) it enhances the likelihood of detecting TB-infected hosts [105]. The gamma-interferon test is based on measuring the emission levels of a cytokine called 'interferon gamma' (IFNγ). IFNγ is emitted from infected cattle's white blood cells when stimulated with bovine and avian tuberculins (the same as used in the tuberculin skin test) [118]. The associated level of IFNγ emitted determines if the host is considered as a positive reactor. Where a host is considered a positive reactor if their blood samples emit a comparatively higher level of IFNγ in response to bovine tuberculin compared to avian tuberculin [118].

The true strength of the gamma-interferon test is its ability to detect bTB earlier and with significantly higher sensitivity [105]. The gamma-interferon test is able to detect infection in the first 2-5 weeks, often before the host has become infectious [67]. For example, a Northern

Ireland study discovered IFNγ positive animals were at a significantly higher risk of failing a subsequent SICCT, indicating IFNγ ability to identify early-stage infections [119]. The IFNγ test sensitivity is also favourable, researchers estimate the sensitivity ranges from 73% to 100% (median 87.6%) [120]. By the quantitative nature of the IFNγ test, results are more objective and no longer clouded by differing test interpretations often seen in TST test data [43].

The IFNγ test has numerous advantages compared to the TST test, however, there are also various disadvantages; cost, complexity, and specificity. The inherent complexity in the IFNγ testing procedure makes it an expensive test. For example, the requirement for cultures to be developed under laboratory conditions within 24 hours drives up procedural costs. Another disadvantage is the reduction in specificity, with some researchers indicating IFNγ testing specificity range is from 85% to 99.6% (median 96.6%) [120]. The significant reduction in specificity when compared to the SICCT (standard interpretation), would therefore lead to the slaughter of an unacceptably high number of false-positive hosts.

Considering the associated cost-benefit analysis of both tests, researchers advise parallel testing to utilise both test's advantages. Implementing IFNγ as an ancillary test can optimally detect infections improving overall sensitivity, specificity and detection interval. Moreover, parallel testing increases the general diagnostic sensitivity, identifying otherwise undetected hosts [105]. In a similar fashion, other epidemiological studies have demonstrated that the ancillary use of gamma-interferon test in parallel to SICCT can reduce the proportion of false-negative outcomes (i.e. non-reactor cases) from the SICCT [121]. Lastly, parallel tests allow earlier detection at the expense of specificity. However, if suspected cattle are isolated and removed before becoming sources of infection, we reduce the likelihood of persistent herd breakdowns [67].

1.7.3 *Post-mortem Investigations*

The few inconsistent clinical markers of bovine tuberculosis make a diagnosis via clinical examination extremely challenging [122]. Direct detection of the pathogen can only be accurately achieved during a post-mortem investigation, where suspected infected tissue can be sampled. Positive identification of the organism is accomplished through either cultivating bacterial cultures or molecular techniques such as polymerase chain reaction (PCR). In the UK, PCR tests are used much less frequently due to their relatively poor performance in terms of sensitivity, specificity, and reliability [122].

Although both techniques may fail to detect *M. bovis* directly due to poor sampling, samples with low organism numbers may not develop sufficiently or sample contaminants may prevent

efficient PCR reactions [123]. Increasing the number of samples using multiple lesion locations may increase the likelihood of detection, however this approach may be impractical due to both time and financial constraints [122]. Another reason post-mortem investigations may fail to successfully diagnose bTB is the pathological lesions must be visible to the sample. Lesions may be absent or too small to detect with the naked eye, introducing uncertainty into subsequent results [123].

1.7.4 *Vaccination*

There are currently numerous proposed bTB vaccines for cattle on the market, however experimental trials have concluded that the best available is the BCG vaccine (bacille Calmette-Guerin) [124]. This vaccine induces antibodies through inoculation of a live attenuated strain of *M. bovis*, the immunological response against this weakened antigen provides the antibodies which prevent future infections [125]. The results from cattle trials show variable efficacy, where the differences in vaccine variability are attributed to differing vaccine formulations, inoculation entry points, and exposure to environmental mycobacteria [125].

The BCG vaccine is currently not in use in the UK, not because of financial constraints as one may expect, but rather the vaccines legality. Currently under EU legislation it is illegal to vaccinate cattle[2], as it compromises the diagnostic powers of other immunological tests. As the vaccine is comprised of live *M. bovis*, the resultant antibodies would interact with the tuberculin used in both the tuberculin skin test and gamma-interferon test [124]. Therefore, either of these diagnostic tools would no longer be able to distinguish between BCG vaccinated cattle and infected cattle. Development of other diagnostic tests hope to circumvent this problem, the so-called DIVA antigens (differential diagnosis of infected individuals from vaccinated individuals) are being designed with the ability to distinguish between BCG vaccinated and infected cattle [126]. As these new diagnostic tools are still in development, they may help in future but researchers believe they are at least five years off (not including the associated time to become EU and internationally approved) [16].

If administered to wildlife reservoirs, vaccines are predicted to have a higher impact in a more reasonable time frame [125], although to date very few studies have examined the effect of vaccination in badgers. The studies which have examined badger vaccination do generally note a reduction in incidence rates among the badger population and therefore vaccines would reduce the risk to the cattle population [127]. The most comprehensive source of wildlife

2 The UK in all likelihood will continue to follow the EU laws, even though they officially left the EU on the 31st of January 2020. As the UK exports most of its cattle products to the EU, failure to comply with EU legislation may result in associated barriers or tariffs.

vaccination examinations is from the simulation model literature. Several regionally specific simulations do indicate a radical reduction of bTB incidences within the badger population [128]. However, there is a small caveat regarding simulations; if simulations fail to account for any unforeseen possible future outcomes their predictions may be wildly wrong. Therefore, researchers must be very considered before implementing wildlife vaccines while only using simulation evidence as justification.

1.7.5 *Diagnostics Summary*

From a diagnostic point of view, both the tuberculin skin test (TST) and the Gamma-interferon test (IFNγ) suffer from insufficiently quantified sensitivity and specificity. Moreover, the current quantitative estimates predict an overall poor sensitivity (51% to 89%). The available tests fail to provide a sufficiently high standard of accuracy, especially regarding sensitivity, facilitating a persistent cycle of reinfections that obscures the true routes of transmission.

A breakthrough in either diagnostic tests or cattle vaccination will provide an invaluable tool for the eradication of bovine tuberculosis. However, in the shorter term researchers should focus their attention on badger vaccinations and their ramifications. As the current literature implies this could be an effective measure of mitigating bTB, by decoupling the inter-population dynamics of the UK's cattle and badger populations.

1.8 BOVINE TUBERCULOSIS IN THE UNITED KINGDOM

Bovine tuberculosis (bTB) is one of the most complex, persistent and controversial inter-species diseases facing the UK governments and the wider British cattle industry, costing the country an estimated £120 million per year [129]. Despite continual implementation of large scale and expensive control mechanics since the 1950s, both the United Kingdom (UK) and Ireland have failed to eradicate the disease. In the last 35 years, bovine tuberculosis (bTB) incidences have been exponentially growing within the UK and is now endemic in the majority of southwest England and south Wales. Researchers have only partially explained this growth and various questions remain open. The obscurity surrounding transmission pathways and high associated government expense has led to this issue becoming highly politicised, making it burdensome to implement new scientifically accurate policies [18]. In this section we examine the disease's origin, first from a global prospective and later we focus on the UK. What effect did bTB have on the UK's history and how did the disease become endemic?

1.8.1 *History of Bovine Tuberculosis*

The exact origin of bovine tuberculosis is hard to pinpoint due to the disease's age, as tuberculosis has been discovered in remains from over 9,000 years ago (predating written records). The first mention of tuberculosis originate from classical antiquity (8^{th} century BC - 6^{th} century AD), stating that the disease had been present in the Mediterranean peninsula for aeons [39]. Historians believe that bTB originated in the Mediterranean peninsula or the Horn of Africa, first spreading slowly to northern regions of Italy, then to western Europe (including the United Kingdom). The disease was later spread globally through European colonialism [130].

The first substantial scientific study of tuberculosis began in late nineteenth century, where in 1881, the great scientific figure Robert Koch[3] discovered that "tubercle bacillus" is the leading cause of tuberculosis in humans [124]. The term "tuberculosis" is even derived from its namesake "tubercle", which are nodules formed in an infected host's lymph nodes [124]. The corresponding causal bacterium that causes tuberculosis in cattle (*M. bovis*) was then subsequently discovered in 1898. However, biologists were aware of tuberculosis in an ecological setting before the discovery of *M. bovis* [39]; Dr Duncan Hutcheon made the first documented record of tuberculosis in animals in 1880[4] [131],[124].

1.8.2 *History of Bovine Tuberculosis in the United Kingdom*

Historically, tuberculosis has greatly impacted public health in the UK, especially during the industrialisation era when incident rates exploded [132]. As urbanisation began, humans moved into large cities where conditions were crowded and insanitary, providing fertile ground for the disease to grow [132]. One compounding factor was the consumption of contaminated milk, as ingesting unpasteurised milk was commonplace at the time (especially in preadolescents and children) [55],[132]. The milk's high bacterial load led to acute cases that were often fatal in children and the elderly [133]. Studies have shown that in this period, there existed a strong correlation between human and cattle infection levels [41].

3 Robert Koch made many great scientific discoveries through his lifetime and is one of the principal founders of modern bacteriology.

4 Dr D. Hutcheon was a pioneering Colonial Veterinary Surgeon in South Africa, who elucidated many previously unidentified diseases in livestock.

However, the continued spill-over from the infected cattle into the UK populace began to decline after 1935, with the invention of pasteurisation and the tuberculin skin test (TST)[5] [55]. Pasteurisation eradicates bacteria from contaminated milk by rapidly heating the milk for only a short period of time. By the 1960s, when this practice had became enshrined in law, the causal transmission pathway of contaminated milk had virtually been eliminated [43]. Similarly, the TST enabled the government to begin screening cattle, through routine testing the disease could start to be controlled.

The TST has undergone continual refinement in its formulation and standardisation, which has significantly influenced how the test is interpreted and administered. Nevertheless, the basic fundamentals of the TST remain unchanged and it is still the main tool used for surveillance today. When first implemented in the late 1930's/early 1940's the UK was currently engaged in World War II, therefore it was deemed impracticable to cull all identified reactors [45]. Alternatively, the government set up a voluntary scheme ("attested herd scheme") to mitigate the disease's spread and identify uninfected herds [49]. Farmers within the scheme would voluntarily eradicate bTB from their herds leading to complete eradication in certain regions. The scheme had progressively started to successfully manage the disease and was slowing further spread [49]. However, after a period the uptake of the voluntary scheme had begun to slow, especially as certain regions resisted compliance [49].

Throughout the 1950s, the government changed its previous strategy and began enforcing scheme membership for farms within certain regions [49]. These actions and regulatory changes culminated in 1960, when the government required all farms to become "attested" by the 1^{st} of October (i.e. all cattle herds were subjected to regular tuberculin skin tests, where all positive reactors were subsequently culled) [49]. In conjunction with these new measures, the government began enforcing herd depopulation on farms with either unacceptably high incidence rates or persistent reinfections [16]. The test and slaughter strategy had a profound effect on bTB within the UK, progressively reducing incident rates, where in the 1970s and early 1980s bTB had nearly been eradicated [16]. Incidence rates in the UK fell sharply in a reasonably short period; in 1961 nearly 15,000 positive reactors were slaughtered (16.2 reactors per 10,000 TST's) and by 1982 this number was slashed to just 569 (2.3 reactors per 10,000 TST's) [49]. Throughout the 1970s, at some time all herds in the UK had been cleared of bTB, although unfortunately, these farms were not all clear at the same time [55]. Persistent regional infection in Cornwall and Gloucestershire prevented eradication, despite

5 The test was first developed in 1909 by Austrian scientist Clemins von Pirquet. This work predominately built on Robert Koch's discovery that infected hosts exhibit tuberculin hypersensitivity, which is the core mechanism the test depends on [134].

the continued implementation of more frequent whole herd tests [55],[135].

In the 1970s, the perspective surrounding persistent reinfection changed, as the wild Eurasian badgers (*Meles meles*) were identified as potential reservoirs for the disease [135]. This paradigm shift altered the focus onto badgers; could they contribute or even cause these persistent regional infections? This new attitude persuaded the UK government to act, from 1973 to 1998 the current control strategies were augmented with successive wildlife culling, intended to curtail the reservoir population in areas of persistent reinfection. Despite all these control strategies, incidence rates began creeping up in the mid to late 1980s. In particular regions, the reinfection cycle became increasingly onerous to deal with, infections seem to persist and resisted eradication. By the 1990s, the annual increase of cases had grown to around 18%, consequentially the government commissioned the Krebs report to determine the role of badgers in bTB transmission [55]. The report recommended a large-scale field trial of badger culling, so the government implemented the Randomised Badger Culling Trials (RBCT). The trial's aim was to quantify badger's contribution to bTB infections and elucidate the effects of reservoir depopulation. The RBCT subsequently ran for the next decade (1998-2007), incurring a £50 million taxpayer cost [55]. The findings of the study were published in June 2007 and the report explicitly stated that:

> "The sum of evidence strongly supports the view that, in Britain, badgers are a significant source of infection in cattle. Most of this evidence is indirect, consisting of correlations rather than demonstrations of cause and effect; but in total the available evidence, including the effects of completely removing badgers from certain areas, is compelling. " [136]

The results of the 10-year "randomised badger culling trials" showed that widespread coordinated culls of thousands of badgers resulted in a 16% reduction in new infections [136].

The Krebs report has been highly controversial with many wildlife advocates and scientists disputing its findings [43],[16]. One of the loudest voices of opposition is Professor Lord John Krebs, who was the government adviser responsible for the initial scientific review in the 1990s. Lord Krebs said the trial evidence should be interpreted as an argument against culling;

> " The trial evidence should be interpreted as an argument against culling. You cull intensively for at least four years, you will have a net benefit of reducing TB in cattle of 12% to 16%. So you leave 85% of the problem still there, having gone to a huge amount of trouble to kill a huge number of badgers. " [137]

and

> "It doesn't seem to be an effective way of controlling the disease" [137]

Lord Krebs has since amplified voices within the scientific community, echoing the opinion that the development of a vaccine was crucial in the long term. Furthermore, better "biosecurity" measures would decouple cattle and badger interaction in the short term and prevent further reinfections [136],[137].

The bTB situation worsened in 2001, as the foot and mouth epidemic (FMD) started spreading rapidly around the country. Whole herds were slaughtered to prevent further spread and during this time bTB testing was temporarily suspended [138]. The high levels of undiagnosed bTB in conjunction with the restocking of FMD affected herds from high incidence areas led to a 24% increase in positive reactor identified the following year [138]. From 2001 the number of incidences began to grow exponentially, reaching around 40,000 positive reactors slaughtered in 2008. Since this period, incidence rates have fluctuated but remain relatively constant, with 39,243 cattle slaughtered out of 9,050,158 tests administered in the 12 months from June 2020 to June 2021 [139].

What does the situation look like in 2022? Once again, bovine tuberculosis is endemic in much of the southwest of England and south Wales [139]. In an effort to meet the UK target to be "Officially Bovine Tuberculosis Free (OTF) status for England by 2038", current government control strategies are being augmented with another set of local badger culls. However, researchers and invested parties have questioned the basis for these culls, expressing claims that these measures have been implemented on political grounds rather than on epidemiological [140]. Only time will tell the effects these badger culls have. What we can say with some certainty is bovine tuberculosis is a complex disease and without a change in strategy, new diagnostic tools, vaccine discovery, or an enhanced understanding of transmission pathways, bTB is likely to remain problematic for many years to come.

Table 1.1 Summary Timeline

1880	Tuberculosis in animals was first referenced in South Africa by veterinary surgeon Dr Duncan Hutcheon.
1881	Robert Koch discovered tubercle bacillus was the main cause of tuberculosis in humans.
1898	The corresponding causal bacterium agent (*M. bovis*) which induces tuberculosis in cattle was discovered.
1909	The test was first developed in 1909 by Austrian scientist Clemins von Pirquet. This work predominately built on Robert Koch's discovery that infected hosts exhibit tuberculin hypersensitivity, which is the core mechanism the test depends on [134].
1935	The invention of pasteurisation began eradicating *M. bovis* from contaminated milk. As pasteurisation became more commonplace it began eliminating this transmission pathway.
1935	The tuberculin skin test (TST) began to be used as a screening tool in the United Kingdom.
1940	The voluntary "attested herd scheme" was implemented. This scheme encouraged and supported farmers in their attempt to eradicate bovine tuberculosis from within their own herds.
1960	By the 1st October, all of the UK became "attested", legally requiring all cattle herds to be regularly tested using the tuberculin skin testing (TST), where any positive reactors identified were immediately slaughtered.
1971	*M. bovis* was detected in a wild Eurasian badger on a Gloucestershire farm. This discovery fundamentally changed the perspective surrounding persistent reinfections and the infection cycle of bovine tuberculosis.
1973	Badger culling strategies began being implemented in conjunction with cattle test and slaughter regimes.
1982	Herds with high infections or persistent infections were depopulated. The measures resulted in the lowest recorded incidence rates of bovine tuberculosis, only 569 positive reactors were discovered (or 2.3 positive reactors per 10000 tests).

Table 1.2 Summary Timeline

1998	From the Kerb's report, the RBCT (randomised badger culling trial) was set up to quantify the impact of badgers on disease incidence levels.
2001	Due to foot and mouth outbreak all tuberculin skin test were suspended and numerous herds were culled to prevent spread. The high volume of cattle trading in the next year, attempting to repopulate culled herds, led to a 24% increase in positive reactors identified in 2002. From here, the number of incidences began to grow exponentially year on year.
2007	The RBCT report explicitly stated that badgers contribute to the infection cycle and that they increased infection persistence.
2009	The whole of Scotland became official bTB free (OTF).
2012	The think tank (Bow Group) urged the government to reconsider its plans to cull thousands of badgers to control bovine TB, stating the findings of RBCT report implies culling does not work. Their report consisted of a foreword by singer Brian May and contributions from many leading tuberculosis scientists (including Lord Krebs).
2012	UK MPs vote to abandon badger culls entirely (147 to 28).
2013	Two new pilot badger culls go ahead in the summer of 2013 in Somerset and Gloucestershire.
2020	Badger culls were expanded, leading to the slaughter of over 100,000 badgers. Activist groups widely condemn this expansion due to the lack of science. This action results in the UK government admitting failings and saying they shall focus more on vaccination in future.

1.9 SUMMARY AND THESIS OBJECTIVES

Bovine tuberculosis is one of the complex and costly diseases facing the UK, posing significant challenges to the cattle industry, veterinary profession, UK government, and scientific community. Throughout this literature review, we have described and examined the various associated risk factors, diagnostic tools, and transmission pathways of bovine tuberculosis in the UK cattle industry. In recent years, there have been tremendous breakthroughs in our understanding of the disease progression cycle and diagnostic performance factors. Although, many open questions still remain. The most crucial open questions that prevent disease eradication are connected to the continuous cycle of reinfection exhibited within many herds.

Once a herd is deemed OTF, what causes the resurgence of bTB within the herd? Various uncertainties mask the true infection transmission routes, these prevent researchers from fully understanding disease resurgence. These ambiguous factors come in three primary forms:

1. **Imperfect Diagnostics Tools**: The standard diagnostic test's low sensitivity and high variability in the latency periods mask infection sources. Subsequent herd breakdowns may result from previous infections, as latency cattle may become infectious years after initial exposure. Additionally, the imperfect diagnostic tools permit the importing of undiagnosed cattle through livestock trading, improving testing capabilities would therefore reduce inter-herd transmission.

2. **Wildlife Reservoir**: If a herd has a connected wildlife reservoir, it may act as a disease source, maintaining the disease and infecting new hosts. This continuous spillover from the wildlife population causes persistent reinfections.

3. **Environmental Transmission**: If infected hosts have contaminated the environment, new hosts may continue to be infected even after successfully removing all infected hosts from the farm.

Each of these factors; imperfect diagnostics, wildlife reservoir, and environmental contamination, play an integral role in the transmission of bovine tuberculosis in the UK cattle industry, although the interconnected relationship between evidence, uncertainty, and risk makes it nearly impossible to tell what each factor contributes. Each of these factors forms a central theme of this thesis, where each chapter develops a further understanding of these factors in further detail.

1.9.1 *Thesis Objectives*

The structure of this thesis is as follows:

In chapter two, we review the history of mathematical epidemiology, examining what types of modelling techniques exist and how they are used to understand disease transmission dynamics. After which, we discuss the various theorems, definitions, and mathematical tools required to illustrate the dynamics behind the epidemiological models constructed in this thesis. Particularly, we focus on the factors that affect the behaviour of long term solutions; basic reproduction number, disease-free equilibria, endemic equilibrium, and their stability.

In chapter three, we examine the role of bTB's highly variable latency period in persistent breakdowns. This chapter extends the SETIR model, the standard prototypical disease dynamic model for bovine tuberculosis, by incorporating more exposure compartments. Through augmenting the SETIR model, we alter how the system incorporates its latency period, changing the distribution from an exponential distribution to the Erlang distribution. This highly flexible distribution allows the incorporation of more realistic exposure periods. In total, this chapter analyses three different systems, each an extension of the previous. Firstly, to illustrate the basic fundamental properties of the prototypical model, we examine the SE_1E_2TIRC model 3.1. The next system extends the exposure compartment of the system (E) to incorporate Erlang distributed parameters (SE^nTIR model 3.3). The next extension is similar, the new SE^nTIR model is further extended such that the entire latency period (exposed E and test sensitive T) has Erlang distributed parameters. Each extension enables the modeller to incorporate more complexity and realism.

In chapter four, we examine the role of the wildlife reservoir in bTB's transmission dynamics by constructing and analysing a mathematical model. The model's demographics are constrained, such that both species are analysed at their respective equilibriums. In this multi-host system, we consider the spill-over and spill-back between a herd and wildlife reservoir, analysing this model's long term solutions and the system properties which affect their behaviour; basic reproduction number, disease-free equilibria, endemic equilibrium, and stability. Moreover, the analysis discusses the backward bifurcation present in the model's dynamics, where we discuss the conditions in which the backward bifurcation exists and the feasibility of these conditions.

In chapter five, we explore the biological contamination properties of bovine tuberculosis in bTB's transmission dynamics by constructing the SETIB model. As we will discuss in the literature review, infected cattle shed fomites and infect not just each other but they also

contaminate the environment. This contamination of soil, troughs, cattle feed, hay, and various other materials have an incredibly variable decay rate. This chapter extends the basic SETIR model by incorporating a compartment for the background environmental contamination. This multi-transmission pathway model considers both direct cattle to cattle transmission and infections from the contaminated environment $B(t)$. The fundamental properties of this model are analysed; disease-free equilibrium, endemic equilibrium, the basic reproductive number, and the long term behaviour of our solutions. After which, we examine the SETIB system with bTB parameters through numerical analysis, comparing and contrasting how the system dynamics alter when examining different environmental contamination parameters.

In chapter six, we explore how the different model mechanics expressed throughout this thesis work in conjunction with each other. The other thesis chapters contemplated and considered models through the lens of dynamical systems. However, the underlying complexity of considering all mechanisms simultaneously would be incredibly difficult to analyse. In order to mitigate much of the underlying complexity, we instead use simulation techniques. In this simulation, we examine three main research themes: wildlife reservoir's contribution, testing and detection strategy, and persistent reinfections. The first section considers persistent reinfections, using system parameters from the literature we aim to quantify the contribution proportions of each different mechanic (e.g. latency, wildlife reservoir, and environmental contamination). The second section examines badger's contribution by investigating the change in dynamics by fully and partially excluding the wildlife reservoir from the farm, representing how the disease dynamics are affected by a farm increasing bio-security measures.

In chapter seven, we summarise all the findings throughout this thesis and conclude with a critical discussion of this thesis' limitations and possible future directions. The focus is on how the results and modelling approaches from this thesis can be used to support the development of more sophisticated epidemiological models in the future.

2

MATHEMATICAL TOOLS AND FRAMEWORK

2.1 INTRODUCTION

Through formulating our epidemiological models in the language of mathematics, models can be scientifically analysed and studied. However, to understand these epidemiological models, various theorems, definitions, concepts, and mathematical tools are required. This chapter begins by discussing epidemiological modelling; what types of modelling techniques exist? How are these models used to understand disease dynamics and improve control strategies? Afterwards, this chapter reviews the required mathematical theory used throughout this thesis. This description shall centre around the general mathematical epidemiology framework of non-linear dynamical systems, in which our models are constructed, discussing their dynamics, basic reproduction number, equilibria, and stability.

2.2 A BRIEF HISTORY OF MATHEMATICAL EPIDEMIOLOGY

Infectious diseases have been an unpleasant part of everyday life as long as humans and animals have roamed the earth. Most diseases go by unnoticed or cause relatively minor issues (e.g. the common cold) with no long-term detrimental damage. However, other infectious diseases can be substantially worse, causing discomfort, distress, disability, or even death. Human history is littered with various examples of diseases causing death and destruction on an unprecedented scale. For example, the estimated death toll of the bubonic plague in Europe was between 25-50 million (around 35% of Europe's total population) [141]. Similarly, historians indicate that in the 14^{th} century a combination of smallpox, salmonella enterica, and other diseases eradicated around 15 million Aztecs in 5 years (around 80% of the total population) [142].

Even since the turn of the millennium, there have been multiple disease outbreaks; foot-and-mouth, SARS, influenza, and Ebola, although these diseases pale in comparison to COVID-19 [143]. In December 2019, the first identified human case occurred in Wuhan (China) and from there the coronavirus spread worldwide [143]. The World Health Organisation (WHO) has since declared COVID-19 a pandemic [143], resulting in 515,192,979 cases and has killed 6,254,140 people globally as of the 9/05/2022 [143]. The COVID-19 zoonosis stands for

"coronavirus disease 2019" and is an infectious disease caused by the RNA virus, "severe acute respiratory syndrome coronavirus 2" (SARS-CoV-2)[1].

These risks to public health have been a strong motivator for humans to understand how infectious diseases are transmitted. How do diseases spread throughout a community? What factors influence the prevalence of a disease? By comprehending how a disease spreads, humans aspire to control disease transmission or at least mitigate the detrimental health effects. Mathematical epidemiology has been incrementally developed from this need, predominately over the last century. This field has evolved from a few overly simplified modelling techniques into the complex and technical field we see today.

The founder of mathematical epidemiology is widely regarded as Daniel Bernoulli, [2] who in 1760 developed a model to show that inoculation against smallpox would improve the life expectancy of the general population [145]. This model was a monumental milestone in mathematical epidemiology, although excluding work by John Snow (1855)[3] and William Farr (1840)[4] this research went quiet until the twentieth century, as the underlying theory of disease mechanics such as germ theory, were still under development.

At the beginning of the twentieth-century mathematical epidemiology began to develop, as several breakthroughs in the theory of differential equations facilitated the construction of deterministic modelling. In 1906, Hamer used this new theory to postulate a fundamental tenet of mathematical epidemiology, the mass-action principle [146]. This principle relates the disease incidence rate in a fixed population to the number of current cases (I), the number of susceptible people (S), and the infection transmission parameter (β). The infection transmission parameter β is the average number of contacts per person per time, multiplied by the probability of disease transmission during a single contact.

1 Initially researchers believed it originated in bats, although in February 2020 a virus sample obtained from a sunda pangolin implied they were the species of origin. The virus sample collected from the pangolin had a viral nucleic acid sequence "99% identical" to SARS-CoV-2. [144]

2 Some historians dispute Bernoulli as the founder of mathematical epidemiology, as around a century earlier J. Graunt (the founder of demography) conducted the first empirical analysis of an epidemic. Using data from London's Bill of Mortality, he estimated the death rates of diseases using basic statistical analysis. Despite this, most dispute this claim due to the empirical nature of Graunt's research. Bernoulli's approach was different, as it attempted to model smallpox through mathematical formulation. From this theoretical viewpoint, Bernoulli tried to understand the underlying disease mechanics.

3 John Snow identified the transmission mechanics of cholera through the use of data collection and construction of the first dot map. The dot map identified the location of cholera cases, which illustrated that cases seemed to cluster around specific water pumps. By petitioning the council to remove the handle, he saved lives and proved his hypothesis: cholera is spread via water.

4 Through fitting normal curves to epidemic data, Farr was able to predict disease numbers for an upcoming quarter. Farr could then distinguish between average case numbers and an upcoming outbreak.

$$\frac{dI}{dt} = \beta SI$$

The mass-action principle is still a fundamental assumption made in numerous deterministic models today [64].

In 1911, R. Ross and G. Macdonald developed the first vector-host model to study malaria transmission and discussed its threshold properties [147]. The initial formulation of this model used probabilistic arguments, however, their model is intrinsically deterministic as given a particular initial condition, all future states can be calculated for this original state. In 1927, this model was generalised by Kermack and McKendrick, who developed the first compartmental model that separated individuals into three compartments; susceptible (S), infectious (I), and removed R[5] [148]. Their general SIR epidemic model is represented by the following non-linear system of ordinary differential equations

$$\begin{aligned}
\frac{dS}{dt} &= -\beta SI \\
\frac{dI}{dt} &= \beta SI - \gamma I \\
\frac{dR}{dt} &= \gamma I
\end{aligned}$$

where $S(t), I(t), R(t)$ denotes the number of susceptible, infected, and removed with respect to time t. A typical individual starts within the susceptible category and remains so until successfully infected. The rate individuals become infected is then assumed to follow the mass-action principle and hence susceptible individuals become infected according to the β parameter. Similarly, infected individuals transition to the removed compartment (R) at the recovery rate γ, where this transitional parameters represent the proportion of infected individuals recovering or dying from the disease per unit of time. [6]

These models constructed by Ross, MacDonald, Kermack, and M^{c}Kendrick initiated a flurry of advances, developing mathematical epidemiology from its initial empirical approach towards the mathematical rigours and analytical field we see today. Epidemiological models constructed in this quantitative framework allowed researchers to investigate the underlying disease transmission mechanics. Given appropriate data to estimate model parameters (e.g. contact rates, removal rates, birth, and death rates), researchers can use these simplistic models

5 The removed compartment R may represent individuals that have recovered from the disease and are no longer susceptible. However, it may also represent removed individuals who have succumbed to the disease.

6 An alternative view is that these transitional parameters control the average length of time an individual spends in the infectious state. This length of time is a random variable according to an exponential distribution with γ as its rate parameter. Hence, the expected time an individual remains within the infectious compartment is $\frac{1}{\gamma}$.

to estimate the long term behaviour of these systems.

The development of mathematical epidemiology slowed during the second world war, afterwards research continued throughout the subsequent decades, albeit at a slower pace. In the 1980s, mathematical epidemiology underwent a resurgence, breakthroughs in other fields such as dynamical systems, graph theory, and computer science unlocked other techniques that could extend and enhance models. This rejuvenation is widely regarded to have occurred due to three parallel developments:

1. Significant developments in pure mathematics sparked exciting work not just in mathematical epidemiology but also modelling theory as a whole. Mathematical ideas from differential geometry, topology, and algebra were amalgamated with the pre-existing theory of non-linear dynamical systems to produce a wave of theoretical developments. New ideas related to chaos, strange attractors, and fractals caused subsequent advances in applied mathematics.

2. The development of computer science and the adoption of digital computers provided researchers with a plethora of new techniques. Researchers could now use computers to numerically analyse problems that were previously intractable to standard mathematical techniques. Moreover, the development of computers opened up a whole new field of enquiry for mathematical epidemiology, as they provided researchers with the ability to simulate complex systems. Furthermore, digital computers meant that scientific data could now be collected, processed, and proliferated significantly quicker.

3. Enhanced computer power also spurred significant development in various supporting fields, most notably computers revolutionised graph theory. Graphs or the more modern term "networks" were now able to be generated and analysed with millions of nodes, a feat that would not have been possible previously.

These developments allowed researchers to investigate a wide range of phenomena, incorporating more realism and complexity into their models:

- **Host Heterogeneity models:** Models incorporating age-structure, host-vector models, multi-group models and non-Markovian models.

- **Spatial Models:** Models incorporating graph theory, patch models, and non-linear reaction-diffusion equations.

- **Stochastic Models**: Models framed as probabilistic models, branching processes models, stochastic ODE and PDE models, and numerical simulations.

Mathematical epidemiologists armed with both the new theoretical and previously existent theory made great strides in tackling pandemics such as AIDS, malaria and smallpox

[86]. The enhanced predictive powers of mathematical modelling informed policymakers, allowing them to implement informed and effective control strategies. A particular poignant demonstration comes from Somalia in 1977, where after a concerted effort by the academic community and W.H.O, the last known natural case of smallpox was treated [149],[150]. Previously, smallpox was an acutely painful and debilitating disease, resulting in extensive scarring and occasionally blindness [149],[150]. In the last 100 years of its existence, it is estimated to have killed 500 million people [150]. In the 1980s, the World Health Organisation (W.H.O) certified the global eradication of smallpox, and this is widely regarded as one of the greatest achievements of humankind.

In the 21st century, mathematical modelling of infectious diseases is a matter of compromise. With the invention of new techniques and methodologies researchers are afforded more options, allowing them to construct more bespoke and complex models for specific diseases. Especially with the advent of computational models, it is possible to perform large scale complex simulations of an entire epidemic. Therefore, it is now up to the researcher whether a disease is better understood computationally, deterministically, spatially, stochastically, etc. This does not come without drawbacks, as in a perfect world, incorporating more realism would produce better models. However, in the real world, model complexity causes problems; either the model's complexity masks the system's underlying causal relations or the models are mathematically intractable.

Simplistic models that focus solely on primary disease transmission mechanics may sacrifice accuracy and predictive power due to the exclusion of such secondary effects. Yet, their simplicity allows researchers to analytically describe the fundamental principles that guide disease transmission. Understanding these characteristics allow us to broadly articulate "When will an epidemic occur?", "How large will the epidemic be?" and "How long may it last?" Fundamentally the researcher will always be restrained, as no matter how suitable a particular model is for a given disease, the researcher must always consider will the results be both mathematically traceable and interpretable? Therefore, researchers must always construct models with the right amount of complexity, where the relative balance depends on the individual questions being asked.

2.3 Mathematical epidemiological models: non-linear differential equations framework

The required mathematical theory used throughout this thesis is discussed within this section, focusing on the mathematical framework of non-linear dynamical systems and how they are

constructed. First, the dynamical framework of differential equations and their properties are discussed; well posed, feasibility region, non-autonomous systems and species demographics. Afterwards, these non-linear dynamical systems are examined in terms of their dynamics; system attractors, stability, and bifurcation.

2.3.1 *Non-linear Dynamical Systems and their associated Qualitative Behaviour*

Dynamical systems abstractly model how a system in a given state will evolve over time provided it follows certain rules, described by either a set of differential equations or difference equations. Abstractly, a state is defined by a n-tuple whose elements are real numbers (a vector) often conceptualised as a point in an associated state space (geometrical manifold). This thesis (unless otherwise stated) exclusively focuses on dynamical systems whose evolution is governed by a set of continuously deterministic differential equations of the form:

$$\frac{dx}{dt} = \dot{x} = f(x, t; \mu) \tag{2.1}$$

Where x is some open set in the n-dimensional real coordinate space (i.e. $x \in U \subset \mathbb{R}^n$). Our independent variable t is constrained to the one dimensional case $t \in \mathbb{R}^1$. Similarly, μ is some open set in the q-dimensional real coordinate space (i.e. $\mu \in V \subset \mathbb{R}^p$), where q represent the number of parameters of our associated system. A solution to a given dynamical system is a map x:

$$\begin{aligned} x : I &\to \mathbb{R}^n, \\ t &\mapsto x(t) \end{aligned}$$

Where some interval $I \subset \mathbb{R}^n$ is "mapped" into $\mathbb{R}^n$, such that $x(t)$ satisfies the associate set of differential equations. A geometric integration of this map x is a curve in $\mathbb{R}^n$ and then our dynamical system represents the associated tangent vector corresponding to every point in the curve. The phase space of our dynamical system is the space of its dependent variables (i.e. $\mathbb{R}^n$)[7]. The goal of dynamic system theory is to understand the geometry of solution curves in the phase space.

2.3.1.1 *Well Posed*

For a system to be both mathematically valid and biologically significant, the system must be well-posed. The mathematical term well-posed means that for a given system, a unique solu-

7 In many applications the phase space of a dynamical system is more general that $\mathbb{R}^n$; spherical, cylindrical or toroidal. Throughout this thesis, the set of phase spaces will be restricted to open sets in $\mathbb{R}^n$ representing the possible n parameter values.

tion must exist and the solution's behaviour changes continuously with the initial conditions. The well-posed requirement is vital for several theorems used throughout this thesis. Without this requirement, the consequences may be detrimental to the system's long-term predictions and contradict much of the underlying system's biological properties.

The methodology used throughout this thesis is standard within the literature, by showing a function is Lipschitz continuous (see below) then the ODE $\frac{dx}{dt} = f(x, t; \mu)$ can be solved uniquely for any initial condition (at least locally). Lets us examine these in more formal language:

Definition 2.3.1 *Let* $D \in \mathbb{R} \times \mathbb{R}^n$ *be a closed rectangle with* $(t_0, y_0) \in D$. *Let* $f : D \to \mathbb{R}^n$ *be a function that is continuous in* t *and Lipschitz continuous in* x. *Hence for our equations;*

$$x'(t) = f(x, t; \mu), \qquad \textit{where } x(t_0) = x_0.$$

there exists some $\epsilon > 0$ *such that the initial value problem has a unique solution* $x(t)$ *on the interval* $[t_0 - \varepsilon, t_0 + \varepsilon]$.

Where a real-valued function is defined as Lipschitz continuous if:

Definition 2.3.2 *A real-valued function* $f : \mathbb{R} \to \mathbb{R}$ *is called Lipschitz continuous if there exists a positive real constant* K *such that, for all real* x_1 *and* x_2,

$$|f(x_1) - f(x_2)| \leqslant K|x_1 - x_2|$$

This is a particularly useful property, as it implies that every function that has a bounded first derivative is Lipschitz continuous. By the nature of these mathematical epidemiological systems the population demographics inherently are bounded, as a result we can use the total bound for the population as our constant K.

Similarly, since population demographics are inherently bounded, there often exists a bounded positive invariant region, where trajectories of the system are attracted.

Definition 2.3.3 *Let* $\dot{x} = f(x, t; \mu)$ *be a dynamical system, where* $x(t, x_0)$ *is a trajectory, and* x_0 *is the initial point. A set* Ω *is said to be positively invariant if* $x_0 \in \Omega$ *implies that* $x(t, x_0) \in \Omega \ \forall t \geqslant 0$

This is important as for a system to be biologically sound, solutions originating from non-negative initial conditions must remain non-negative for all future time. As in these systems, dependent variables represent physical quantities of hosts such as humans, badgers, or cattle. This requirement restricts the biologically unrealistic possibility of a negative number of cattle

within a herd.

In other words, once a trajectory of the system enters Ω, it will never leave it again. Throughout this thesis we shall restrict our analysis to the positive invariant Ω, which we shall refer to as feasibility regions.

2.3.1.2 *Non-Autonomous System: Species Demographics*

In general, many epidemiological models do not explicitly incorporate species demographics; such models require the disease to work on a much shorter time scale (e.g. influenza). Omitting species' demographics requires the disease to operate on a shorter time scale than the interval in which demographics alter. However, if the disease operates in a time frame more comparable to the host's lifespan, then species demographic must be incorporated. As the incubation period of bTB may last up to 7 years [43], then the demography of the population cannot be ignored. This thesis predominantly incorporates species' demographics using the simplified logistic model (see [86]), assuming that a herd has constant births and proportional deaths. Hence,

$$\frac{dN(t)}{dt} = \Lambda - \mu N(t)$$

As a result, all models used throughout this thesis are systems of non-autonomous differential equations. A system of differential equations $\frac{dx}{dt} = f(x, t; \mu)$ is defined as non-autonomous if the $f(x, t; \mu)$ explicitly depends on time t. Non-autonomous systems tend to be more difficult to analyse and are often not subject to the theory of autonomous systems. To circumvent this increased complexity, the associated limiting system is considered instead. If a system depends only on time through the overall population dynamics function $N(t)$ and has a limit as time goes to infinity (namely $N(t) \implies \frac{\Lambda}{\mu}$), then the reduced limiting system can be examined instead. Non-autonomous systems with an autonomous limiting system are called asymptotically autonomous; these reduced systems are often easier to solve and are still informative from the point of view of the dynamics. Although, when do the global dynamics of the asymptotically autonomous represent the original non-autonomous system.

Theorem 2.3.1 *Assume that* $\frac{dx}{dt} = f(x, t; \mu)$ *is a non-autonomous system such that* $x \in R^n$ *and* $y = g(y)$ *is the limiting autonomous system. Let* Ω *be the* Ω*-limit set of a forward bounded solution* x *of the non-autonomous system. Assume that there exists a neighbourhood of* Ω *that contains at most finitely many equilibria of the autonomous system. Then the following trichotomy holds:*

1. Ω *consists of the equilibrium of the autonomous system.*

2. *Ω is a union of periodic orbits of the autonomous system and possible centres that are surrounded by periodic orbits of the autonomous system lying in Ω.*

3. *Ω contains equilibria of the autonomous system that are cyclically chained to each other in Ω by orbits of the autonomous system.*

If the non-autonomous system is uniformly bounded, then the above theorem implies that the Ω-limit set of the non-autonomous system can be understood through analysing the Ω-limit set of the autonomous system. As a result, this thesis focuses on analysing the asymptotically autonomous versions of our non-autonomous systems.

2.3.2 *Attractors and their Stability*

An important concept in the discussion of deterministic non-linear dynamical systems is an attractor. An attractor is a geometric object embedded within the phase space that attracts all trajectories with a given domain. The prototypical attractor is that of an equilibrium $\bar{\mathbf{x}}(t) \in \mathbb{R}^n$, where roughly speaking, an equilibrium is a point in the phase space such that it will remain stationary for all time t. More precisely, for the dynamical system $\dot{\mathbf{x}} = f(\mathbf{x}, t; \mu)$, then the rate that the dynamical system variables change at a equilibrium point $\bar{\mathbf{x}}$ is zero (i.e. $f(\bar{\mathbf{x}}, t; \mu) = 0$ for all time t). An equilibrium $\bar{\mathbf{x}}(t)$ is said to be stable if solutions that are sufficiently close to the equilibrium remain close to $\bar{\mathbf{x}}(t)$ for all future time t. Stable equilibria $\bar{\mathbf{x}}(t)$ are described as asymptotically stable if these sufficiently close solutions do not just remain close but rather converge to the equilibrium $\bar{\mathbf{x}}(t)$ as time tends to infinity $t \to \infty$.

An example of a more complex attractor is a stable limit cycle, this is a closed curve $\mathcal{C}$ in the phase space in which trajectories both inside and outside approach $\mathcal{C}$. These stable limit cycle exhibit periodic behaviour, where there exist some period t_0 such that $x(t + t_0) = x(t)$ for all time $t \in \mathbb{R}$. For more detailed definitions for attractors, limit cycles, equilibria, and stability see [151].

2.3.2.1 *Determining Stability*

Let $\bar{\mathbf{x}} \in \mathbb{R}^n$ be a given equilibrium point for a n dimensional dynamical system. In order to understand the nature of the solutions local to $\bar{\mathbf{x}}$, the equilibrium point's stability must be determined. By understanding how the attractors affect the phase space, insight into the long term behaviour of our solutions and dynamics are gained.

The classical method to determine stability is construct a new solution $\mathbf{x}(t)$ by introducing a small perturbation $\boldsymbol{\epsilon}(t) = (\epsilon_1, \epsilon_2, \ldots, \epsilon_n)(t)$ at the equilibrium $\bar{\mathbf{x}}$, hence the solution can be defined as $\mathbf{x}(t) = (x_1, x_2, \ldots, x_n)(t)$, where $x_i(t) = \bar{x}_i(t) + \epsilon_i(t)$ for all $i \in n$. By determining

if this small perturbation either grows or decays gives insight into the local dynamics. Starting with the general definition of a dynamical system definition,

$$\frac{d\mathbf{x}}{dt} = \dot{\mathbf{x}} = f(\mathbf{x}, t)$$

The system can be linearised via a Taylor expansion to produce the following approximation,

$$\frac{d\boldsymbol{\epsilon}}{dt} \approx f(\bar{\mathbf{x}}, t) + Df(\bar{\mathbf{x}}, t) \cdot (\mathbf{x} - \bar{\mathbf{x}})$$

Where $f(\bar{\mathbf{x}}, t) = 0$ for all t, as it is an equilibrium point and by definition $\mathbf{x} - \bar{\mathbf{x}} = \boldsymbol{\epsilon}$. Thus,

$$\frac{d\boldsymbol{\epsilon}}{dt} \approx Df(\bar{\mathbf{x}}, t) \cdot \boldsymbol{\epsilon}$$

Where $Df(\bar{\mathbf{x}}, t)$ denotes the Jacobian Matrix $\mathbb{J}$ of $f(\mathbf{x}, t)$ evaluated at the equilibrium $\bar{x}$.

The equilibrium point $\bar{x}$ is then stable if all eigenvalues of the Jacobian Matrix $\mathbb{J}$ have negative real parts, as all sufficiently close trajectories will therefore approach the equilibrium point. If on the other hand, there exists an eigenvalue with a positive real part, then the system is considered unstable.

An important caveat is the behaviour of our original dynamical system must match the behaviour of our new linearised system. The Hartman Grobman theorem implies this is true as long as the equilibrium point $\bar{\mathbf{x}}$ is hyperbolic, where an equilibrium point is hyperbolic if and only if all eigenvalues of the linearised system do not lie on the imaginary axis (i.e. $Re(\lambda_i) \neq 0$, $\forall i \in \{1, \ldots, n\}$). If this condition is met, then the equilibrium's phase space is topologically equivalent to the phase space of the linearised system [151]. Hence, this implies the linearised system will realistically capture the qualitative patterns of behaviour of the original non-linear system and consequently the stability behaviour of our equilibrium point $\bar{\mathbf{x}}$.

2.3.2.2 *Routh-Hurwitz Criterion*

As described above, the signs of the eigenvalues of the linearised system determine the stability of an equilibrium point. Therefore, the roots of the n^{th}-degree characteristic polynomial of our given system must be determined to give the eigenvalues. For higher dimension systems (particularly for $n > 4$), factoring the polynomial can be challenging; as there is no methodology to deduce the roots of the polynomial unless it is in very specific forms[8].

8 As Galois theory has shown that there is no explicit formula to factor the roots of a quintic polynomial (polynomial of degree 5) or any other polynomial with a higher degree.

However, the Routh-Hurwitz criterion determines the sign of the roots without calculating the roots themselves, thus, circumventing this complication.

Definition 2.3.4 *For a given n^{th}-degree polynomial with real coefficients* $P(\lambda)$,

$$P(\lambda) = \lambda^n + a_1\lambda^{n-1} + \cdots + a_{n-1}\lambda + a_n$$

Where a ***Hurwitz matrix*** *(H) of the coefficients* a_i *of the characteristic polynomial is defined as:*

$$H_1 = (a_1), \quad H_2 = \begin{pmatrix} a_1 & 1 \\ a_3 & a_2 \end{pmatrix}, \quad H_3 = \begin{pmatrix} a_1 & 1 & 0 \\ a_3 & a_2 & a_1 \\ a_5 & a_4 & a_3 \end{pmatrix}$$

Therefore, the n^{th} dimensional Hurwitz matrix can be defined as follows:

$$H_n = \begin{pmatrix} a_1 & 1 & 0 & 0 & \cdots & 0 \\ a_3 & a_2 & a_1 & 1 & \cdots & 0 \\ a_5 & a_4 & a_3 & a_2 & \cdots & 0 \\ \vdots & \vdots & \vdots & \vdots & \ddots & \vdots \\ 0 & 0 & 0 & 0 & \cdots & a_n \end{pmatrix}$$

Theorem 2.3.2 *The Routh-Hurwitz Criteria states that all roots of the polynomial* $P(\lambda)$ *are negative or have a negative real part if and only if the determinants of every Hurwitz matrices are positive,* $\Delta H_j > 0$, *for j = 1,...,n.*

For the proof, see the original paper by Adolph Hurwitz from 1895 [152]. This criterion implies all eigenvalues are negative if all coefficients of the polynomial are positive, $a_i > 0$ for all $i = 1, \ldots, n$ and all secondary conditions are met. Table 2.1 gives the additional requirements for polynomials of degrees three to five, which ensure the roots are either negative or have negative real parts.

n	Routh-Hurwitz criterion additional conditions
3	$a_1 a_2 > a_3$
4	$a_1 a_2 a_3 > a_3^2 + a_1^2 a_4$
5	$a_1 a_2 a_3 > a_3^2 + a_1^2 a_4$,
	$(a_1 a_4 - a_5)\left(a_1 a_2 a_3 - a_3^2 - a_1^2 a_4\right) > a_5 \left(a_1 a_2 - a_3\right)^2 + a_1 a_5^2$

Table 2.1: Routh-Hurwitz criteria for polynomials of degree 5 and under.

2.3.2.3 *Lyapunov Functions*

An alternative approach to determining the stability of an equilibrium point is the indirect method of Lyapunov. A particular strength of this method is that the equilibrium points are not required to be hyperbolic. The basic idea of the method is given a n-dimensional vector field, an equilibrium point $\bar{\mathbf{x}}$ is stable if there exists a neighbourhood $\mathcal{U}$ around $\bar{x}$, such that orbits starting inside $\mathcal{U}$ will remain so for all positive time t[9]. The theory progresses by showing that the vector field of the boundary of our neighbourhood $\mathcal{U}$ is either tangential to the boundary or is directed inwards toward our equilibrium $\bar{x}$. As this boundary $\mathcal{U}$ is constricted and shrunk down onto $\bar{x}$, the vector field should continue to point inward or tangential.

More concretely, let our potential Lyapunov function, $V(\mathbf{x})$ define a scalar-valued function (i.e. $V : \mathcal{U} \to \mathbb{R}^1$ for some domain $\mathcal{U} \subset \mathbb{R}^n$.) which is at least $\mathcal{C}^1$ (zero and first derivatives are continuous). Where the function should be zero at the equilibrium point $V(\bar{x}) = 0$. Otherwise the function should be a constant $V(\mathbf{x}) = C$, where C form a closed curve containing $\bar{x}$ for different values of C. Therefore our scalar-valued function should be positive in some neighbourhood $\mathcal{U}$ around $\bar{x}$ (i.e. $V(\mathbf{x}) > 0$, $\forall x \in \mathcal{U}$).

Now by taking the gradient of our scalar-valued function V, then we obtain a vector which is perpendicular to the tangent curve, ∇V, whose direction is pointing towards increasing V along each curve $V = C$. Therefore, to ensure solution vector's point tangential or inwards toward to the boundary $\mathcal{U}$, then we require,

$$\nabla V(\mathbf{x}) \cdot \dot{\mathbf{x}} \leqslant 0$$

Theorem 2.3.3 *Consider the following vector field:*

$$\dot{\mathbf{x}} = f(x) \qquad x \in \mathbb{R}^n$$

Where $\bar{\mathbf{x}}$ is an equilibrium point in our vector space. If there exist a Lyapunov function $V : \mathcal{U} \to \mathbb{R}$, that is $\mathcal{C}^1$ function defined on a neighbourhood $\mathcal{U}$ around $\bar{x}$ such that;

1. $V(\bar{\mathbf{x}}) = 0$ *and* $V(\mathbf{x}) > 0 \qquad \forall\, \mathbf{x} \in \mathcal{U} - \{\bar{x}\}$
2. $\dot{V}(\mathbf{x}) \leqslant 0 \qquad \forall\, \mathbf{x} \in \mathcal{U} - \{\bar{x}\}$

Then $\bar{\mathbf{x}}$ is stable. Lastly if in condition 2, the derivative of the scalar-valued function is strictly negative $\dot{V}(\mathbf{x}) \leqslant 0$, $\forall \mathbf{x} \in \mathcal{U} - \{\bar{x}\}$ then $\bar{\mathbf{x}}$ is asymptotically stable.

9 Throughout much of the literature, the definitions of orbit and trajectory are often conflated. An orbit of a point x_0 is the set of points in the phase space that lies on a trajectory passing through x_0. In contrast, a trajectory is a function $x(t)$ that represents the solution of a differential equation starting from the initial condition x_0. Hence, a trajectory is a function that has an orbit as an image set.

The original proof can be found in [153], however, for a more modern and succinct proof see [151].

2.3.2.4 *Mathematical Epidemiology Equilibrium*

These equilibria play an essential role in the long term disease dynamic of many mathematical epidemiological systems. In mathematical epidemiology there are specific names for certain equilibria; disease free equilibrium ($\mathcal{DFE}$) and endemic equilibrium ($\mathcal{EE}$).

Definition 2.3.5 *The **disease free equilibrium** ($\mathcal{DFE}$) represents the system where there is no disease present in the system.*

Definition 2.3.6 *The **endemic equilibrium** ($\mathcal{EE}$) represents the system in which there is some disease present in the system.*

For example, let us consider the non-linear SIR model discussed earlier, where a host can be either susceptible $S(t)$, infected $I(t)$, or removed (R). Therefore, if this system had 100 hosts the disease free equilibrium would be $\mathcal{DFE} = (S, I, R) = (100, 0, 0)$. Whereas, the endemic equilibrium represents the system with some positive number of infected host ($I \geqslant 0$), for example $\mathcal{EE} = (S, I, R) = (78, 10, 12)$.

2.3.2.5 *Frequency vs Density Dependence Infection Rates*

The infection transmission parameter β is the average number of contacts per person per time c, multiplied by the probability of disease transmission during a single contact $P_{transmission}$.

$$\beta = c \times P_{transmission} \qquad \frac{dI}{dt} = \beta SI$$

The infection transmission parameter β does come in different forms, particularly when considering how β varies with time. There exist two main forms density-dependent transmission and frequency-dependent transmission.

Density dependence transmission considers how the system dynamics alter as the population changes over time. For example, in various epidemiological systems if the number of people in a certain area doubled, so to would the number of contacts c per unit time, increasing disease transmission. Therefore, in density-dependent transmission, the per capita contact rate c between susceptible (S) and infected (I) individuals depends on the population density.

Whereas in frequency-dependent transmission, the per capita contact rate c between susceptible (S) and infected (I) individuals does not depend on the population density. Frequency-dependent is therefore often used to model the spread of sexually transmitted diseases, vector-borne diseases, and in general populations with a heterogeneous contact structure REF. These two different philosophies represent the two extremes and various other constructions for the effective contact parameter c exist that are somewhere between the two. It's then up to the individual modeller to analyse disease data and select the appropriate contact form for that specific disease.

In the subsequent subsection 2.3.1.2, we discuss how this thesis focuses on asymptotically autonomous versions of the non-autonomous systems analysed in this thesis. As a result, our systems do not consider how our model dynamics vary in time, therefore, both the frequency and density-dependent formulation for the infection transmission parameter are equivalent [154].

2.3.3 *Bifurcation and the Basic Reproductive Number $\mathcal{R}_0$*

After describing both the disease-free equilibrium ($\mathcal{DFE}$) and the endemic equilibrium ($\mathcal{EE}$), a natural question arises: for a given initial condition, when will the system approach either the $\mathcal{DFE}$ or the $\mathcal{EE}$? This question depends on the fundamental epidemiological concept of the Basic Reproductive Number $\mathcal{R}_0$. Comprehending the concept of $\mathcal{R}_0$ will allow us to understand the stability of our equilibrium and when it changes, as the basic reproductive number $\mathcal{R}_0$ gives the point in which the system bifurcates between two different system behaviours.

2.3.3.1 *Basic Reproduction Number $\mathcal{R}_0$*

The basic reproductive number ($\mathcal{R}_0$) is a fundamental concept of epidemiological systems and is defined in an epidemiological setting as follows:

Definition 2.3.7 *The basic reproduction number $\mathcal{R}_0$ is a dimensionless quantity defined as the expected number of secondary cases produced by a single (typical) infectious individual in a completely susceptible population.*

The $\mathcal{R}_0$ of a specific epidemic system is comprised of the system parameters, however generally speaking, it will be composed of the following factors in some form:

$$\mathcal{R}_0 \propto \left(\frac{\text{infection}}{\text{contact}}\right) \times \left(\frac{\text{contact}}{\text{time}}\right) \times \left(\frac{\text{time}}{\text{infection}}\right)$$

$$\mathcal{R}_0 \propto \qquad \tau \qquad \times \qquad c \qquad \times \qquad d$$

where,

- τ is the transmission rate (i.e. the probability of an infected host successfully passing the infection to a susceptible host during contact).
- c is the average contact rate between susceptible and infected individuals.
- d is the average duration of a host's infectious period.

In the last century, during the development of mathematical epidemiology, it has become apparent that understanding $\mathcal{R}_0$ and its effects on epidemic systems is crucial in allowing researchers to control and mitigate epidemics. As $\mathcal{R}_0$ acts as a bifurcation point for a system, it generally determines which of the following behaviour will occur.

$$\text{If } \mathcal{R}_0 > 1 \implies \text{The number of infected will tend to increase, as each infected will pass the disease onto more than one other individual on average.}$$

$$\text{If } \mathcal{R}_0 < 1 \implies \text{The number of infected will tend to decrease, as each infected will pass the disease onto less than one other individual on average.}$$

2.3.3.2 *Calculating $\mathcal{R}_0$: Next Generation Matrix*

In the literature, there are a myriad of different techniques to calculate $\mathcal{R}_0$. For simple models with few heterogeneous features, the $\mathcal{R}_0$ can be calculated by examining the associated Jacobian for the system. The Jacobian approach works well for models in which the necessary and sufficient conditions for the stability of the Jacobian can be reduced to a single condition. The Jacobian method often fails mathematically in more complex systems, particularly ones with substantial heterogeneity included, such as multiple types of infected hosts or multiple heterogeneous populations.

As an alternative, the next-generation matrix was introduced by Diekmann and Heesterbeek in the 1990s [155]. This technique defines $\mathcal{R}_0$ as a demographic process, where new infections are regarded as offspring produced from consecutive generations of infected individuals. If subsequent generations are growing in size, that signifies an epidemic. The rate at which each successive generation grows is the mathematical characterisation of $\mathcal{R}_0$.

Therefore, for compartmental models where different types of hosts are considered in discrete categories, one can define a matrix that relates the number of newly infected individuals to the various compartments. This approach is the basis for the next generation matrix $\mathbf{FV^{-1}}$, where the reproduction number $\mathcal{R}_0$ is then defined as the spectral radius of the next-generation matrix.

Definition 2.3.8 *Let* $\sigma(FV^{-1}) = \{\lambda_1, \ldots, \lambda_n\}$ *be the (real or complex) eigenvalues of a matrix* $FV^{-1} \in \mathbb{C}^{n\times n}$*, then its spectral radius* $\rho(FV^{-1})$ *is defined as the maximum of the absolute values of the eigenvalues:*

$$\rho(FV^{-1}) = \sup\{|\lambda| : \lambda \in \sigma(FV^{-1})\}$$

For example, let there exist some system where there are two discrete types of infected hosts; population one and population two (e.g. Mosquitoes and humans, men and women, or as in this thesis, cattle and badgers). The next-generation matrix ($\mathbf{FV^{-1}}$) entries $a_{ij} \in \mathbf{FV^{-1}}_{n\times n}$ are simply the system's reproduction number only considering each population separately.

$$\mathbf{FV^{-1}} = \begin{pmatrix} \mathcal{R}_{11} & \mathcal{R}_{21} \\ \mathcal{R}_{12} & \mathcal{R}_{22} \end{pmatrix}$$

Hence, the entry $\mathcal{R}_{11}$ is the expected number of secondary infections in population one caused by a singular infected individual within population one, again assuming that population one is entirely susceptible. Similarly, the entry $\mathcal{R}_{12}$ is the expected number of secondary infections in population two caused by a singular infected individual in population one. Hence, each element of $\mathbf{FV^{-1}}_{n\times n}$ is a reproduction number in and of itself (see [86] for more information).

2.3.3.3 *Calculation of the Next Generation Matrix*

Various techniques have been developed to derive the next generation matrix from compartmental models (e.g. Castillo-Chavez, Feng and Huang approach [156]). Predominately, these techniques augment the Van den Driessche and Watmough approach [157] (e.g. by incorporating incubation stages, where hosts have been infected but are not yet infectious). This thesis predominately uses the Van den Driessche and Watmough approach [157] to construct the next-generation matrix.

THE VAN DEN DRIESSCHE AND WATMOUGH APPROACH The Van den Driessche and Watmough approach begins by separating an arbitrary epidemiological system into two

categories; one category represents non-infected individuals ($\mathbf{y}$), and the second category represents infectious individuals ($\mathbf{x}$).

1. First step: Reformulate our original dynamical system into the following format;

$$\dot{x_i} = f_i(\mathbf{x}, \mathbf{y}) = F_i(\mathbf{x}, \mathbf{y}) - V_i(\mathbf{x}, \mathbf{y})$$
$$\dot{y_j} = g_j(\mathbf{x}, \mathbf{y})$$

   The following functions $F_i(\mathbf{x}, \mathbf{y})$ and $V_i(\mathbf{x}, \mathbf{y})$ represents new infections and remaining transitional terms respectfully. Although please note, the decomposition of our system into the following form is not unique and this can lead to a slightly different interpretation of the basic reproduction number being produced. Before continuing with this explanation, our system of ordinary differential equations must meet the following conditions;

   - $F_i(0, \mathbf{y}) = 0$, meaning that all new infections are in fact secondary infections. This rules out the option of hosts becoming infected spontaneously.
   - $F_i(\mathbf{x}, \mathbf{y}) \geqslant 0$ for all $\mathbf{x}, \mathbf{y} \geqslant 0$ Similarly, this condition enforces infections are a continuous process and do not vanish from the system.
   - $V_i(0, \mathbf{y}) = 0$ for $y \geqslant 0$ and $i \in \{1, 2, \ldots, n\}$. This states that no individuals migrate between compartments unless there is disease present within the system.
   - $V_i(\mathbf{x}, \mathbf{y}) \leqslant 0$ whenever $\mathbf{x}_i = 0$ for all $i \in \{1, 2, \ldots, n\}$. This condition implies that if no new infection occurs, transitional compartment must reduce in size.
   - $\sum_{i=1}^{n} V_i(\mathbf{x}, \mathbf{y}) \geqslant 0$ for all $\mathbf{x}, \mathbf{y} \geqslant 0$, hence the total outflow of infected compartments is positive.

2. Second step: lets assume for the disease free system $\dot{\mathbf{y}} = g(0, \mathbf{y})$ there exists a disease free equilibrium $\mathbf{DFE} = (0, y_0)$. Where all solutions with initial conditions of the form $(0, \mathbf{y})$ approach the $\mathbf{DFE} = (0, y_0)$ as time $t \to \infty$.

3. Third step: Determine the following two matrices F and V

$$F = \left[\frac{\partial F_i(0, y_0)}{\partial x_j}\right] \qquad \text{and} \qquad V = \left[\frac{\partial V_i(0, y_0)}{\partial x_j}\right]$$

   where these matrices are the linearisations of our system around the disease free equilibrium $\mathbf{DFE} = (0, y_0)$.

4. Fourth step: The last step in this methodology is to obtain the spectral radius of the next generation matrix $\mathbf{FV^{-1}}$, giving us the basic reproduction formulation $\mathcal{R}_0$. Therefore, the basic reproductive number is defined as the following,

$$\mathcal{R}_0 = \rho(\mathbf{FV}^{-1})$$

The above description has outlined the Van den Driessche and Watmough approach, used to find the next generation matrix and the basic reproductive number for the system. For a detailed proof of this theorem see the following Diekmann, Heesterbeek, and Metz paper [155]. Although, let us briefly outline the underlying mechanics which makes this work. Recall, by the Hartman Grobman theorem, the system behaviour near equilibrium points is determined by the eigenvalues of the linearised system, evaluated at the equilibrium point (Jacobian). Moreover, if all the corresponding eigenvalues of the Jacobian all have negative real parts, then the system is stable near the equilibrium point. Conversely, if any eigenvalue of the Jacobian has positive real parts then the system is said to be unstable.

The Diekmann, Heesterbeek, and Metz paper [155] proves there exists an equivalence between the spectral bound of the original linearised system $m(F-V)$ and the spectral radius of the next generation matrix FV^{-1}.

Theorem 2.3.4 *The spectral bound of the linearized matrix* $m(F-V)$ *evaluated at the disease free equilibrium* $\mathcal{DFE}$ *sign is determined by the spectral radius of the next generation matrix* $\rho(FV^{-1})$ *. As there exists the following correspondence:*

1. $m(F-V) < 0$ *if and only if* $\rho(FV^{-1}) < 1$

2. $m(F-V) > 0$ *if and only if* $\rho((FV^{-1}) > 1$

Where the spectral bound is defined as follows:

Definition 2.3.9 *The* ***spectral bound*** *of a matrix A is denoted by*

$$m(A) = \sup\{Re(\lambda) : \lambda \in \sigma(A)\}$$

Where $\sigma(A)$ *is the spectrum of the matrix* A *(i.e. Matrix A's set of eigenvalues* $\sigma(A) = \{|\lambda_1|, \ldots, |\lambda_n|)$ *and* $Re(\lambda)\}$ *is the real component of the eigenvalue. Hence, the spectral bound of a matrix is the maximum real part of the matrix's spectrum.*

Recall, the spectral radius of a matrix is the largest absolute value of its eigenvalues.

As the above theorem demonstrates, $\rho(FV^{-1})$ behaves precisely as the threshold property generally associated with the basic reproductive number. For example, consider a system in which $\rho(FV^{-1}) < 1$, this implies the spectral bound of matrix $m(F-V) < 0$ meaning all corresponding eigenvalues are negative. This implies that the $\mathcal{DFE}$ is locally asymptotically stable due to the real part of all eigenvalues being negative. For a more detailed analysis of the next-generation matrix and a proof of the above theorem, please see [86].

In summary, $\mathcal{R}_0$ was defined as the number of secondary infections that one infective host individual will produce in an entirely susceptible host population during its typical infected lifespan. The concept of the next-generation approach is different, as it defines the reproduction number as the number of secondary infections generated per stage. The next generation matrix approach means it is now possible to construct a threshold quantity $\mathcal{R}_0$ for a multitude of systems, where previous simpler techniques would have failed. The disadvantage of the next-generation approach is that the reproduction number obtained through this technique is often harder to interpret biologically.

2.3.4 *Bifurcations*

The qualitative structure of dynamical systems can change as parameters are varied, particularly in higher dimensional systems, equilibrium points can change their stability. These behavioural changes in the dynamics are referred to as "bifurcation" and the associated parameter values in which they occur are called "bifurcation points". In many epidemiological systems there exist only one bifurcation point (when the basic reproductive number equals one $\mathcal{R}_0 = 1$), if the basic reproductive number is above that point the disease free equilibrium $(\mathcal{DFE})$ becomes unstable and the endemic equilibrium $(\mathcal{EE})$ becomes stable.

There are multiple types of bifurcations; however, this thesis shall only describe relevant bifurcations; transcritical bifurcation and backward bifurcation.

2.3.4.1 *Transcritical Bifurcation*

Transcritical bifurcations in dynamical system are characterised by the behaviour that a particular equilibrium point exists for all parameter values. For example in most mathematical epidemiological systems, there shall always exist a disease-free equilibrium $(\mathcal{DFE})$ point relating to zero infection. This principle holds for the majority of epidemiological systems, as if there are no infectious hosts in the system, then how can any new hosts become infected? Let us consider the following example of a dynamical system[10]:

Transcritical Bifurcation's Normal Form:

$$\dot{x} = rx - x^2$$

10 This example is in fact the normal form for a transcritical bifurcation. All systems that undergo a transcritical bifurcation are locally topologically equivalent to this normal form, when considered locally around the equilibrium point.

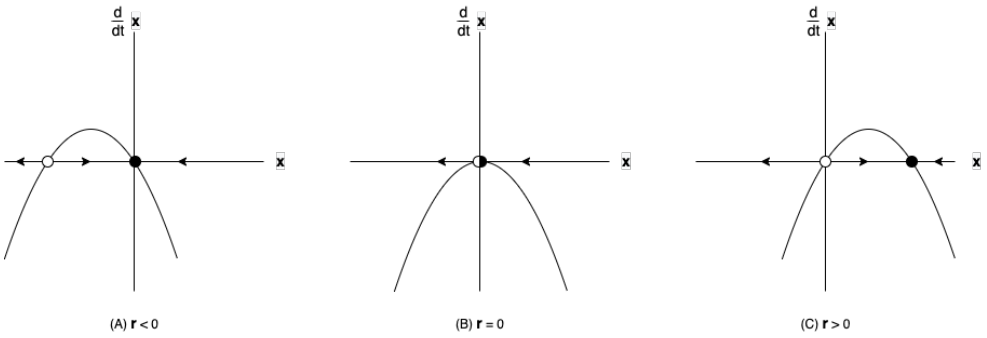

Figure 2.1: Diagram of a transcritical bifurcation, where r represents the parameter shift through a bifurcation point occurring at $r = 0$. In this diagram, black dots represent a stable equilibrium, white dots represent unstable, and both black and white represent semi-stable. As we can see in figure (A) (when $r < 0$), the equilibrium point at the origin is stable and there exist an unstable equilibrium point in the negative domain. As our parameter r approaches zero, these two equilibrium points become closer and closer together. Figure (B) represents the system when $r = 0$, as this demonstrates, the two equilibrium points merge and become one semi-stable equilibrium point at the bifurcation point. The last figure (C), represents how the system changes as r increases past zero. Now the equilibrium point at the origin is now unstable and a stable equilibrium point exists in the positive domain.

The above figure and equation demonstrate that for all values of r the vector field has a constant equilibrium point at $\bar{x} = 0$. More specifically, if r is increased through its bifurcation point ($r = 0$) the stability of our two equilibrium points switch. As r continues to increase through zero and becomes positive $r > 0$, a new stable equilibrium point appears in the positive domain, removing the previous unstable equilibrium point in the negative domain.

2.3.4.2 *Backward Bifurcation*

Transcritical bifurcations are not the only type of bifurcation that occurs in mathematical epidemiology models, there exist models which "backward bifurcate". In these systems, two endemic equilibrium ($\mathcal{EE}$) exists before the system has reached its bifurcation point ($\mathcal{R}_0 = 1$) for a range of basic reproductive values $\mathcal{R}_0$ values. If we define $\mathcal{R}_0^*$ as the critical point in which two endemic equilibria exist, such that these equilibria no longer exist for any basic reproductive number lower than $\mathcal{R}_0^*$. Consequentially, there exist two endemic equilibria within the following range:

$$\mathcal{R}_0^* < \mathcal{R}_0 < 1$$

Typically, one of these endemic equilibria ($\mathcal{EE}$) is stable and the other is unstable. There exist fundamental differences between systems that undergo transcritical bifurcations and

backward bifurcations[11]. As can be seen in the following example, backward bifurcation can have serious consequences related to disease control.

Consider the canonical example of a backward bifurcation:

$$\dot{x} = rx + x^3 - x^5$$

In this bifurcation, the competing growth rates of our different polynomial powers generate the behaviour demonstrated in the bifurcation diagram below, where the arrows indicate the direction of travel for our system trajectories as r and x vary.

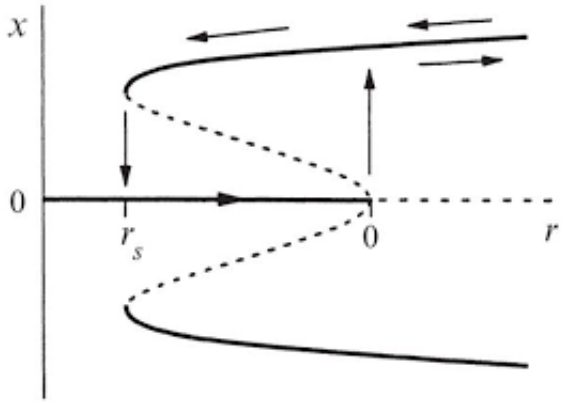

Figure 2.2: The bifurcation diagram associated with a higher order backward bifurcation.

For small x and negative $r < 0$, the origin is locally stable and two branches extended backwards representing unstable fixed points. Although as x increases, the quintic power x^5 becomes dominant, resulting in these branches curving and becoming stable at $r = r_s$.

Transcritical bifurcations and backward bifurcations demonstrate quantitatively different dynamics. The main differences between these two bifurcations are the following:

1. Under a transcritical bifurcation, the system can have two globally attracting equilibria depending if $\mathcal{R}_0$ is above or below one (the disease-free equilibrium ($\mathcal{DFE}$) and the endemic equilibrium ($\mathcal{EE}$)). Whereas, if a system backward bifurcates and is within the range $\mathcal{R}_0^* < \mathcal{R}_0 < 1$ then there exists three equilibria; two stable equilibria ($\mathcal{DFE}$ and $\mathcal{EE}_1$) with a second unstable endemic equilibrium ($\mathcal{EE}_2$). The second unstable endemic equilibrium $\mathcal{EE}_2$ exists on the boundary of attraction between the other two stable equilibria ($\mathcal{DFE}$ and $\mathcal{EE}_1$). As a result, systems that backward bifurcate can only ever be locally stable in the range $\mathcal{R}_0^* < \mathcal{R}_0 < 1$.

11 Note on naming convention, there exist a myriad of different names given to super-critical and sub-critical pitchfork bifurcations due to the numerous areas of application of dynamical systems. On the whole, super-critical and sub-critical pitchfork bifurcations are more standard than their forward and backward counterparts. However, this thesis shall use the name transcritical and backward bifurcation to remain consistent with the mathematical epidemiology literature.

2. Under a transcritical bifurcation, the endemic equilibrium is created continuously, whereas a backward bifurcation exhibits qualitatively different behaviour. Within the interval where multiple equilibria exist $\mathcal{R}_0^* < \mathcal{R}_0 < 1$, the system may jump from the origin to the non-zero stable equilibrium point ($\mathcal{EE}_1$) if the system experiences a perturbation of significant enough magnitude to move the system above the unstable equilibrium $\mathcal{EE}_2$. Additionally, as the basic reproductive number increases past unity ($\mathcal{R}_0 > 1$), the system will discontinuously jump from the stable origin point to the higher amplitude equilibrium point ($\mathcal{EE}_1$).

From a control theory perspective, backward bifurcations are more problematic to manage as given a sufficiently large perturbation in $\mathcal{R}_0^* < \mathcal{R}_0 < 1$ or if $\mathcal{R}_0 > 1$ the system will jump to the other stable endemic equilibrium point ($\mathcal{EE}_)$. After which the basic reproductive number $\mathcal{R}_0$ must be reduced further, it now must reduce past the original threshold of 1 to $\mathcal{R}_0^*$ before the system returns to the disease free equilibrium ($\mathcal{DFE}$).

Paradoxically, this behaviour is typical in systems that incorporate imperfect vaccination [158], [159], [160]. Whereas the same systems that exclude the vaccination effects have a transcritical bifurcation. The existence of backward bifurcation are common in the following literature threads;

- Models incorporating exogenous re-infection [161].
- Models including public health campaigns to improve the education of numerous sexually transmitted diseases [162].
- Models incorporating resistance and immunity mechanisms [163].
- Models that incorporate multi-group mechanisms, especially those with asymmetries between groups [164].

2.4 CONCLUSION

This chapter has reviewed the history of mathematical epidemiology, examining what types of modelling techniques exist and how they are used to understand the disease transmission dynamics. From there, we discussed the various theorems, definitions, concepts, and mathematical tools to illustrate how the dynamical system framework models epidemiological systems. Particularly, we focused on the factors that affect the behaviour of long terms solutions; basic reproduction number, disease-free equilibria, endemic equilibrium, and their stability. This chapter has given us the required mathematical theory to present the various mathematical models constructed throughout this thesis.

Part II

MY CONTRIBUTION

3

CHAPTER 3: BOVINE TUBERCULOSIS' LATENCY PERIOD PROPERTIES

3.1 INTRODUCTION

In this chapter, we examine the standard foundational description of the infection cycle used throughout the literature, the SETIRC model [64]. This model captures the essential features of bovine tuberculosis (bTB) transmission within a herd of susceptible cattle, which many other researchers have extended and built upon [165]. In the standard SETIRC model, hosts can exist in one of six distinct compartments; Susceptible $(S(t))$, Exposed $(E(t))$, Test Sensitive $(T(t))$, Infectious $(I(t))$, Relapsed $(R(t))$, or Culled $(C(t))$. The SETIRC model, like all models, is built upon various underlying assumptions and through investigating these assumptions we aim to extend and improve the model. This chapter explores bTB's highly variable latency period and examines how the SETIRC model incorporates this latency mechanic. After which, we directly develop upon this SETIRC epidemiological model by augmenting its latency mechanic, altering the mechanic to incorporate more realistic latency distribution periods. Understanding this new augmented model will provide further insights into the role latency plays in the spread of bovine tuberculosis disease in the UK cattle industry.

In the SETIRC model, the latency mechanic consists of two compartments Exposed $(E(t))$ and Test Sensitive $(T(t))$ that are each controlled by exponentially distributed parameters. As we shall discuss, exponentially distributed parameters imperfectly capture the underlying latency period distribution, instead, the latency transmission interval time can be modelled to follow an Erlang distribution, a more flexible and adaptable family of distributions. In our extension, the SETIRC model's exposure period distribution is adapted to fit the Erlang distribution by increasing the number of exposure compartments. This augmented model more accurately captures the highly variable time required for an exposed individual to progress to clinical disease and become infectious.

The first section of this chapter briefly discusses the SETIRC model, explaining how the system's differential equations are constructed and how they model bTB's infection cycle. The next section examines bTB's highly variable latency interval, discussing the underlying biological factors that influence this period and the literature's discourse regarding the latency interval range. After which, we examine and improve upon the underlying latency mechanic

of the SETIRC model. Firstly, we discuss the advantages and disadvantages of exponentially distributed parameters in the original SETIRC model, illustrating how they imperfectly capture bTB's disease dynamics. Secondly, we introduce the Erlang distribution and illustrate why this distribution more accurately incorporates the underlying biology of bTB.

In order to demonstrate how changing the latency distribution alters the system dynamics three separate models are introduced and subsequently contrasted. Firstly, a model similar to the SETIRC model based on a paper by Agusto et al. [64] is adapted and discussed, namely the SE_1E_2TIRC model. The mathematical analysis focuses on the system's equilibria, stability, basic reproductive number, and bifurcation type. The first extension of this model considers how the system will change if the exposed compartment $E(t)$ has an Erlang distributed inter-compartment period (referred to as the SE^nTIRC model). The last model further extends the SE^nTIRC model, where now both the exposure and test compartment have an Erlang distributed inter-compartment period (referred to as the SE^nT^mIRC model). In the last section of this chapter, we compare and contrast the different systems, focusing on how altering the number of latency compartments changes the system dynamics.

3.2 BRIEF DESCRIPTION OF THE SETIRC MODEL

A brief introduction into the SETIRC model goes as follows; the model's cattle population is comprised of six distinct compartments; Susceptible $S(t)$, Exposed $E(t)$, Test Sensitive $T(t)$, Infectious $I(t)$, Relapse $R(t)$, and Culled $C(t)$. The susceptible compartment $S(t)$ represents disease-free and healthy cattle that may contract the disease in the future. After cattle contract the disease, two separate compartments represent the substantial incubation period of the bTB; exposed compartment $E(t)$ and test sensitive compartment $T(t)$. The host's first compartment after being infected is exposed $E(t)$, at which time the SICCT test cannot detect the host's bTB antigens. After some time, the host then transitions to the second incubation compartment test sensitive $T(t)$, at which point the host has had sufficient immunological activity for the SICCT test to positively identify them.

The next stage in the infection cycle is infectious $I(t)$, where the host will begin infecting other cattle with bovine tuberculosis (bTB). However, the literature suggests that infectious individuals are only intermittently infectious [166], and a sufficient immunological response may suppress the disease for short periods [165]. Therefore, hosts will transfer to the non-infectious relapse compartment ($R(t)$) intermittently. Hosts will therefore begin oscillating between these two states until removed from the system; infectious ($I(t)$) and relapse ($R(t)$).

Throughout the entire infectious cycle, cattle undergo regular SICCT testing in accordance with the current UK surveillance and detection strategy. The cull rate of this strategy depends on their current infection state, where cattle in the test sensitive ($T(t)$), infectious ($I(t)$), and relapse ($R(t)$) compartments will be detected as positive reactors and culled at rate τ_2. Although the SICCT test's imperfect specificity can return a false positive result, therefore cattle in the other compartments will also be culled at rate τ_1.

The herd's total cattle population ($N(t)$) is conserved and maintained at constant by recruiting new hosts Λ (e.g. births or livestock purchasing), where we assume all recruited hosts are susceptible. These newly recruited hosts replace the natural removals that occur with the herd at a rate μ (e.g. deaths and livestock selling), which occurs regardless of the infection stage. However, cattle detected and culled through testing are not replenished immediately, as this assumption allows the proposed model to obtain the relative population portion of culled cattle and circumvent the additional complexity associated with species demographics. Therefore, cattle that have been culled are still counted in the herd total cattle population ($N(t)$) and are removed at the same rate μ.

For a more in-depth discussion of the original model, please see [64], although further discussion of the model's differential equations will be given in section 3.4.2. Before discussing the underlying latency mechanics of the different models, let us first discuss and inspect the complicating latency factors associated with bTB.

3.3 THE COMPLEX NATURE OF BOVINE TUBERCULOSIS LATENCY PERIOD

There is an extensive discussion regarding the bTB latency period in the literature, although the exact quantitative ranges of the latency period distribution are still largely uncertain [58]. A significant proportion of bTB's modelling papers often derived latency parameter values from a paper indicating the total latency range is between 87-226 days [167]. However, numerous prominent biological researchers refute this upper bound, stating that the upper range of 226 days under-represents extreme cases [168]. For example, researchers have demonstrated experimentally that bovine tuberculosis may remain dormant for at least seven years [167], [169]. As most commercial cattle are permitted only to live between five and six years, this implies cattle may remain in the exposed stage for their entire lives [170].

Biologists suggest that the significant variation in exposure times is due to Mycobacteria bovis biological make-up, as it grants the bacterium the ability to remain dormant for extended periods of time [171]. Under laboratory conditions, M. bovis may enter a dormant state that is both biochemically and morphologically distinct from its respective growing states [172].

Biologists and other veterinarian researchers widely believe this behaviour occurs in so-called "wild" M. bovis as well [172]. In this dormant state, cattle's immune system controls further growth and prevents clinical symptoms from developing [171]. Bovine tuberculosis remains dormant until the cattle enter a state of immuno-suppression, at which point the disease begins growing and can no longer be contained by the host's intrinsic defences [171]. Once bTB has activated, the literature suggests the time taken to achieve maximum immune response is within the range of 8 to 65 days [173],[65]. Influential factors that weaken the immune system further alter the variation seen within the latency period (e.g. stress, pregnancy, lactation, age, and poor nutrition) [16]. The literature also distinguishes the following factors as significant; route of infection, herd-level demographics, and breed [105]. These compounding factors exemplify the difficulty in accurately measuring the extensive latency period distribution associated with bovine tuberculosis infected cattle.

However, researchers are starting to become more confident in the little knowledge they do have regarding the latency period distribution. For example, more recent research into the highly variable latency period has shown it exhibits the heavy-tailed phenomena, meaning that its probability distribution tails are not exponentially bounded [93]. Similarly, more recent longitudinal studies have illustrated that extreme cases are more common than previously believed [112].

This section has demonstrated the complex nature of bTB's latency period and highlighted some of the compounding factors adding to this complexity. How then does the SETIRC model incorporate this highly dependent system mechanic? The next subsection of this chapter examines this question in detail by exploring the underlying assumptions of this latency mechanic, illustrating why exponentially distributed parameters are so frequently used and highlighting their advantages and disadvantages.

3.3.1 *Models and their Underlying Assumptions*

As with all mathematical models, their construction requires a series of assumptions to be made. In the case of the SETIRC model and in general, most mathematical epidemiological models have at least one of the following assumptions:

1. Infection occurs through horizontal transmission; hosts infect each other through direct connections. Secondly, infection occurs according to the mass action principle, where the rate susceptible hosts acquire the disease is given by the force of infection $\lambda = \frac{\beta I}{N}$, controlled by the effective transmission rate β.

2. The population of hosts are homogeneously mixed, where all individuals are equally likely to connect regardless of individual traits or current classification.

3. Infection is only maintained in the system and no outside sources are considered (i.e. this assumption requires all entering recruited hosts to be susceptible).

4. Infection is usually only considered to originate from one population instead of being considered a multi-host system, excluding infection entering from a nearby subpopulation. This approach is common in bTB modelling, as some models ignore the effects of a wildlife reservoir.

5. Models incorporating species demographics only consider the total population remaining at a constant, where the variation of the total population over time is disregarded.

6. Individuals progress from the different compartments proportional to the population size. For instance in the SETIRC model, the rate at which hosts progress from the exposed compartment ($E(t)$) to the test sensitive compartment ($T(t)$) occurs at rate $\gamma E(t)$. As we shall see, the linear recovery rate γ implies that the host's recovery time occurs according to an exponential distribution.

For researchers to draw relevant conclusions about the usability of a model, they require reliable information regarding the model's associated assumptions. Each of the above assumptions will differ from the actual underlying dynamics in a particular fashion; further examination and improvement of these assumptions can more accurately capture the underlying disease dynamics.

The next subsection focuses on number six of our assumptions list, exponentially distributed parameters. As shall be demonstrated, in the SETIRC system exponentially distributed parameters are used to control the length of time the host remains in a compartment. We shall examine how exponentially distributed parameters incorporate the bTB highly latency variability. Furthermore, in the subsequent section we examine how the system can be augmented to incorporate more realism.

3.3.2 *Exponential Distributed Parameters*

The exponential distribution is a widely used continuous distribution used to model the time elapsed between two events. In the underlying structure of the SETIRC model, the rate at which cattle progress through the exposed stage is controlled by the latency parameter γ, where γE gives the proportion of hosts transferring to the next compartment per unit time. A consequence of this assumption is exposed hosts transition to the test sensitive compartment

in accordance with the exponential cumulative probability distribution. In the following section, we shall show how the proportional removal of an exposed individual by a scale parameter leads to these exponentially distributed parameters.

Let us consider the following differential equation, similarly to the SETIRC system in which hosts are only removed from a compartment according to the γ parameter.

$$\frac{dE(t)}{dt} = -\gamma E(t)$$

After solving the differential equation, the number of exposed hosts within this compartment at time t is given by,

$$E(t) = E_0 e^{-\gamma t} \qquad \text{Where } E(0) = E_0 \text{ for t= 0}$$

The expression $e^{-\gamma t}$ gives the proportion of the population that remains in the exposed compartment $E(t)$ after some time t, as $\frac{E(t)}{E_0} = e^{-\gamma t}$.

In the language of probability, the probability a host remains in the exposed compartment at time $t \geqslant 0$ given that they were in the compartment at time $t = 0$ is given by $e^{-\gamma t}$. The probability distribution $F(t)$ given below represents the probability that a host progresses to the next compartment in the time interval $[0, t)$.

$$F(t) = \begin{cases} 1 - e^{-\gamma t}, & \text{for } t \geqslant 0 \\ 0, & \text{for } t < 0 \end{cases}$$

This probability distribution $F(t)$ is in fact, the exponential cumulative probability distribution., therefore, we can now see that the assumption of proportional removal rates is the same as assuming that the exposure time interval has an exponential distribution.

Using this information, we can determine that the expected time interval hosts remain in the exposed compartment. Firstly, the probability density function of the exponential distribution ($f(t) = \frac{d}{dt}F(t)$) is given by:

$$f(t) = \begin{cases} \gamma e^{-\gamma t}, & \text{for } t \geqslant 0 \\ 0, & \text{for } t < o \end{cases}$$

Therefore, the average exposure time interval is

$$\mathbb{E} = \int_{-\infty}^{\infty} t f(t) dt = \frac{1}{\gamma}$$

meaning that the expected time interval that hosts remain in the exposed compartment is $\frac{1}{\gamma}$.

Even though the exponential distribution is frequently used throughout the mathematical epidemiological literature, it is not fully biological realistic due to various reasons. For example, the exponential distribution's memoryless property implies that the remaining time in the exposed stage is independent of entry time, which is unrealistic in terms of disease progression. If this was true, a host exposed a long time ago would have the same expected progression time as a newly exposed host.

A more accurate description would be to measure the real probability density function (pdf) of the exposure period and include this explicitly in the model. However, solving an ODE system with a built-in arbitrary distribution is a difficult task; therefore, we approximate the true probability density function (pdf) with a linear combination of Erlang distributions [1].

3.3.3 *Erlang distributed Parameters*

The SETIRC model's latency mechanic can therefore be augmented by changing its exposure latency period from being exponentially distributed to Erlang distributed. This change in distribution is achieved by sub-dividing the exposure compartment $E(t)$ into n sub-stages, where each sub-stage has the same disease progression parameter γ. This subdivision transforms the latent exposure period into an Erlang distributed parameter, a highly flexible distribution which is better suited to mimic a variety of biologically continuous delays. Let us now examine the Erlang distribution, what makes this distribution better suited?

The Erlang distribution is a two-parameter family of continuous probability distributions that is a special case of the well-known gamma distribution. The Erlang distribution discretises the gamma distribution, meaning that the shape parameter of the Erlang distribution is restricted to some positive number K (i.e. $K \in \mathbb{N}$). The probability density function of the Erlang distribution is given by:

$$g(t; K, \gamma) = \begin{cases} \frac{\gamma^K t^{K-1} e^{-\gamma t}}{(K-1)!} & \text{for } t, \gamma \geqslant 0, \text{for } K \in \mathbb{N} \\ 0 & \text{for } t < 0. \end{cases}$$

The parameter K is called the shape parameter and represents the number of exposed compartments in the system. The γ parameter is the rate parameter and it controls the average period of time that hosts remain in one singular exposure compartment. By adjusting the two Erlang distribution parameters (γ and K), we can more accurately incorporate the true exposure distribution.

1 For more information on how to incorporate an arbitrary exposed time distribution into the SETIRC model, Driessche et al. analysed a similar model using an arbitrary exposed time distribution in their paper[165].

Under the Erlang distrubtion, the expected time interval in which the hosts remain exposed is given by:

$$\mathbb{E} = \int_{-\infty}^{\infty} tg(t)dt = \frac{K}{\gamma}$$

The Erlang distribution is a generalisation of the exponential distribution, as the Erlang distribution is simply the sum of K independent exponential variables with mean $\frac{1}{\gamma}$ each, where if $K = 1$, the Erlang distribution simplifies to the exponential distribution. Therefore, we can augment our model by incorporating more exposure compartments in the SETIRC system, further capturing the inherent latency sensitivity seen with the bovine tuberculosis disease in the UK cattle industry.

In the next three sections we introduce three separate models, namely the SE_1E_2TIRC model, SE^nTIRC model, and the SE^nT^mIRC model. First the SE_1E_2TIRC model is constructed, which is similar to the SETIRC model and is based on a paper by Agusto et al. [64] is adapted and discussed. The next model we consider is the SE^nTIRC model, this extends the system such that the exposure compartment $E(t)$ has an Erlang distributed inter-compartment period. The next model extends the system once more, where now both the exposure and test compartment are fitted with Erlang distributed inter-compartment periods (referred to as the SE^nT^mIRC model).

3.4 sE_1E_2TIRC system

This section introduces the SE_1E_2TIRC model, which captures the fundamental characteristic of how bTB spreads among a herd of cattle. Where this model is similar to the SETIRC model, however, instead of just regurgitating similar analysis, we introduce the first extension towards Erlang distributed parameters (i.e. instead of a singular exposure compartment ($E(t)$), there are two ($E(t)_1$ and $E(t)_2$)). The model is first developed and constructed in the framework of differential equations, where the analysis begins by discussing the system's feasibility region and the well-posed nature of solutions. From here the analysis discusses this system's long term dynamic of solutions; focusing on the system's equilibria, stability, and basic reproductive number.

3.4.1 *Mathematical Model Formulation*

The inter-herd disease dynamics are described using a cattle population compartmental model, where the total cattle population at time t is denoted by $N(t)$ and cattle are separated into the following mutually distinct compartments; Susceptible $S(t)$, Exposed $E_1(t)$ and $E_2(t)$, Test

sensitive $T(t)$, Infectious $I(t)$, Relapse $R(t)$ or Culled $C(t)$. Therefore, the species' population dynamics that govern the number of cattle within the herd are constrained as follows:

$$N(t) = S(t) + E_1(t) + E_2(t) + T(t) + I(t) + R(t) + C(t)$$

The herd's total cattle population is conserved and maintained at constant by recruiting new hosts Λ (i.e. births or livestock purchasing), where we assume all recruited hosts are susceptible. These new recruited hosts replace the natural removals (deaths and livestock selling) that occur at a rate μ regardless of the infection stage. Therefore, the total host population changes according to the following simplified logistic differential equation:

$$\frac{dN(t)}{dt} = \Lambda - \mu(S(t) + E_1(t) + E_2(t) + T(t) + I(t) + R(t) + C(t)) = \Lambda - \mu N(t)$$

The susceptible compartment $S(t)$ represents disease-free and healthy cattle that may succumb to the disease in future. After accounting for newly recruited cattle Λ and natural deaths μ, the susceptible host population is reduced by susceptible cattle contracting the disease. Infections occur according to the mass action principle, where the rate susceptible acquire the disease is given the force of infection $\lambda = \frac{\beta I}{N}$ that is controlled by the effective transmission rate β. Further reduction occurs by the culling of cattle that return a false positive result on the SICCT test, the rate at which false-positive reactors are culled is τ_1. Therefore, the rate of change for the susceptible population is modelled by the continuous non-linear differential equation:

$$\frac{dS}{dt} = \Lambda - \frac{\beta I}{N} S - (\mu + \tau_1) S$$

The exposed compartment represents cattle who have yet to mount a sufficient immune response to the M. bovis bacterium to be successfully detected by the SICCT test. The exposure period is augmented from the original SETIRC model, in our new SE_1E_2TIRC model the exposure period has two separate compartments, $E_1(t)$ and $E_2(t)$, where they both have the same removal rate γ. Similarly to the susceptible compartment $S(t)$, the exposed compartments ($E_1(t)$ and $E_2(t)$) are reduced by natural deaths $\mu(t)$ and false-positive test reactors $\tau_1(t)$. Hence, the differential equations controlling the exposed compartments are given by:

$$\frac{dE_1}{dt} = \frac{\beta I}{N} S - (\mu + \tau_1 + \gamma) E_1$$

$$\frac{dE_2}{dt} = \gamma E_1 - (\mu + \tau_1 + \gamma) E_2$$

The test sensitive population $T(t)$ is increased by those progressing from the second exposed compartment $E_2(t)$. The population is reduced by natural death μ and cattle progressing to the infectious stage, which occurs at rate σ. In the test sensitive compartment $T(t)$ the behaviour differs from the previously exposed compartments, as these cattle are considered to have mounted a sufficient immune response to be detected successfully by the SICCT test.

Therefore, the SICCT test can detect test sensitive cattle and hence they are subsequently culled and removed at rate τ_2.

$$\frac{dT}{dt} = \gamma E_2 - (\mu + \tau_2 + \sigma)T$$

The last two active states a host can enter are infectious $I(t)$ and relapse $R(t)$, where hosts exhibit oscillatory behaviour, cycling between these two compartments ($I(t)$ and $R(t)$). As cattle progress into the infectious compartment $I(t)$, the infectious population is reduced by natural deaths μ, testing τ_2, and cattle progressing to the relapse compartment $R(t)$ at rate ν. However, relapse cattle $R(t)$ may return to the infectious compartment $I(t)$ and hence the infectious population gains the relapsing hosts occurring at rate α.

$$\frac{dI}{dt} = \sigma T + \alpha R - (\mu + \tau_2 + \nu)I$$

Relapse host progress from being infectious at rate ν and are removed according to natural deaths μ, relapsing hosts α, and positive reactors τ_2.

$$\frac{dR}{dt} = \nu I - (\mu + \tau_2 + \alpha)R$$

Lastly, all cattle that have tested positive, regardless of whether they are actual positive reactors or false-positive reactors, progress to the culled compartment $C(t)$. This compartment illustrates the resulting economic damage to a herd, where similarly, cattle in the compartment are removed at the same rate as natural deaths μ. This methodology restricts the population to a constant, reducing demographic system complexity.

$$\frac{dC}{dt} = \tau_1(S + E_1 + E_2) + \tau_2(T + I + R) - \mu C$$

To summarise, this SE_1E_2TIRC model encapsulates a simplified representation of the transmission dynamics of bTB in a single herd. Above, we have formulated the system where each compartment's governing differential equation has been given. The differential equations have been collected below with the associated flow diagram.

3.4.2 *SE_1E_2TIRC System's Differential Equations*

$$
\begin{aligned}
\frac{dS}{dt} &= \Lambda - \frac{\beta I}{N}S - (\mu + \tau_1)S \\
\frac{dE_1}{dt} &= \frac{\beta I}{N}S - (\mu + \tau_1 + \gamma)E_1 \\
\frac{dE_2}{dt} &= \gamma E_1 - (\mu + \tau_1 + \gamma)E_2 \\
\frac{dT}{dt} &= \gamma E_2 - (\mu + \tau_2 + \sigma)T \\
\frac{dI}{dt} &= \sigma T + \alpha R - (\mu + \tau_2 + \nu)I \\
\frac{dR}{dt} &= \nu I - (\mu + \tau_2 + \alpha)R \\
\frac{dC}{dt} &= \tau_1(S + E_1 + E_2) + \tau_2(T + I + R) - \mu C
\end{aligned}
\tag{3.1}
$$

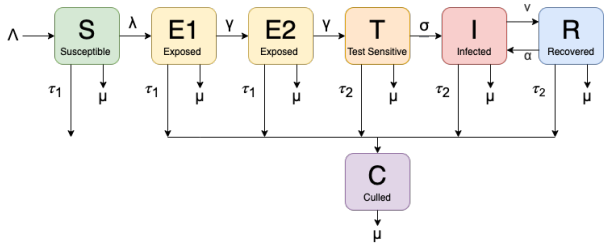

Figure 3.1: Flow chart of the transmission dynamics of the SE_1E_2TIRC model.

3.4.3 *Mathematical Model Properties*

Let us now investigate the model properties of the SE_1E_2TIRC system. In this section, we shall demonstrate the well posed nature of solutions and construct the system feasibility region.

Theorem 3.4.1 *All solutions for our SE_1E_2TIRC system 3.1 which have initial conditions originating within $\mathbb{R}^7_+$ are bounded.*

$$\mathbb{R}^7_+ = \{N(S, E_1, E_2, T, I, R, C) | S \geqslant 0, E_1 \geqslant 0, E_2 \geqslant 0, T \geqslant 0, I \geqslant 0, R \geqslant 0, C \geqslant 0\}$$

Proof 3.4.1 *Let $N\big(S(t), E_1(t), E_2(t), T(t), I(t), R(t), C(t)\big)$ be an arbitrary solution of the SE_1E_2TIRC system 3.1 with a non-negative initial conditions. The population of the herd is given by $N(t)$, where*

$$N(t) = S(t) + E_1(t) + E_2(t) + T(t) + I(t) + R(t) + C(t)$$

Hence,

$$\frac{dN}{dt} = \Lambda - \mu(S + E_1 + E_2 + T + I + R + C) = \Lambda - \mu N(t)$$

By Grönwall lemma, if $x(t)$ is a function satisfying $\frac{dx}{dt} \leqslant ax + b$, where $x(0) = x_0$ and both a and b are constants, then for all time $t \geqslant 0$:

$$x(t) \leqslant x_0 e^{at} + \frac{b}{a}\big(e^{at} - 1\big)$$

therefore,

$$0 \leqslant N\big(S(t), E_1(t), E_2(t), T(t), I(t), R(t), C(t)\big) \leqslant \frac{\Lambda}{\mu}\big(1 - e^{-\mu t}\big) + N(0)e^{-\mu t}$$

Hence,

$$0 \leqslant \limsup_{t\to\infty} N(t) \leqslant \frac{\Lambda}{\mu}$$

Therefore all solutions of the SE_1E_2TIRC system 3.1 that originate in $\mathbb{R}^7_+$ are attracted to the following positive invariant region,

$$\Omega = \left\{N(S, E_1, E_2, T, I, R, C) \in \mathbb{R}^7_+ \mid N \leqslant \frac{\Lambda}{\mu}\right\}$$

The SE_1E_2TIRC system 3.1 is therefore bounded, additionally, since the limit of the supremum of $N(t)$ is independent of the initial conditions then the system is uniformly bounded. As all solutions beginning in our positive invariant region Ω are trapped there, the analysis will be restricted to this feasibility region.

Now that we have shown that solutions are uniformly bounded, the next stage is to show that the SE_1E_2TIRC model's solutions are well posed (i.e. exist and are unique depending on initial conditions).

Theorem 3.4.2 *The SE_1E_2TIRC system's (3.1) solutions are well posed.*

Proof 3.4.2 *As the right hand side of system 3.1 are continuously differentiable functions on*

$$\mathbb{R}^7_+ = \{N(S, E_1, E_2, T, I, R, C) \mid S \geqslant 0, E_1 \geqslant 0, E_2 \geqslant 0, T \geqslant 0, I \geqslant 0, R \geqslant 0, C \geqslant 0\}$$

and as the above theorem indicates, the first derivative of our system is uniformly bounded. This condition implies that the system equation are Lipschitz continuous and with this condition, we can apply the Picard Lindelöf theorem that proves unique solutions exists for the SE_1E_2TIRC system 3.1.

The SE_1E_2TIRC model is therefore well posed and any solution with initial conditions originating in Ω will remain in this feasibility region for all future time. Now, lets turn our attention the the system equilibrium and the basic reproductive number that bifurcates the system.

3.4.4 *Disease free equilibrium $\mathcal{DFE}$ and the Basic Reproductive Number $\mathcal{R}_0$*

In this section we discuss the disease free equilibrium $\mathcal{DFE}$ and the associated basic reproductive number $\mathcal{R}_0$ of the system. After first examining the disease free equilibrium $\mathcal{DFE}$, from here we derive the system's basic reproductive number $\mathcal{R}_0$. The basic reproductive number

$\mathcal{R}_0$ then permits us to discuss the stability of the disease free equilibrium $\mathcal{DFE}$. Where we show both locally and globally that if $\mathcal{R}_0 < 1$ then solutions are asymptotically attracted to the disease free equilibrium $\mathcal{DFE}$.

The disease-free equilibrium $\mathcal{DFE}$ represents the system absent of disease and therefore for the SE_1E_2TIRC system 3.1, the $\mathcal{DFE}$ is given by:

$$\mathcal{DFE} = (\overline{S}, \overline{E_1}, \overline{E_2}, \overline{T}, \overline{I}, \overline{R}, \overline{C}) = \left(\frac{\Lambda}{\mu}, 0, 0, 0, 0, 0, 0\right)$$

Where the over line notation denote that the compartment is at equilibrium (e.g. $\overline{S}$ represents the susceptible compartment at equilibrium). As we are examining the limiting system of this system, we assume that the total population of the herd is at $\frac{\Lambda}{\mu}$ at time equal to zero (i.e. $N(t) = \frac{\Lambda}{\mu}$ when $t = 0$). Therefore, this make sense that the disease-free equilibrium $\mathcal{DFE}$, the entire herd consists only of susceptible hosts.

Let us now determine the basic reproductive number $\mathcal{R}_0$ for the SE_1E_2TIRC system, by using the Van den Driesche and Watmough approach to generate the next generation matrix.

Theorem 3.4.3 *For the given SE_1E_2TIRC system 3.1, where initial conditions originate in the positively invariant set Ω, the basic reproductive number is:*

$$\mathcal{R}_0 = \frac{\beta\gamma^2\sigma\kappa_4}{\kappa_1^2\kappa_2(\kappa_3\kappa_4 - \nu\alpha)}$$

Proof 3.4.3 *The basic reproductive number $\mathcal{R}_0$ is calculated using the Van den Driesche and Watmough approach, which has been extensively discussed in section 2.3.3.3 and therefore this analysis shall be condensed.*

The basic reproductive number $\mathcal{R}_0$ is the spectral radius of the next generation matrix given by FV^{-1}, hence the basic reproductive number is the following:

$$\mathcal{R}_0 = \rho(FV^{-1})$$

Let us now generate the matrices F and V for SE_1E_2TIRC system. Recall these matrices are generated from the linearization of the system equations evaluated at the disease free equilibrium ($\mathcal{DFE}$). Where the two matrices F and V decouple the system, as matrix F's elements are only the parameters which induce new infections and the matrix V's elements are all other parameters. These matrices for the SE_1E_2TIRC system have been calculated below:

$$F = \begin{pmatrix} 0 & 0 & 0 & \beta & 0 & 0 \\ 0 & 0 & 0 & 0 & 0 & 0 \\ 0 & 0 & 0 & 0 & 0 & 0 \\ 0 & 0 & 0 & 0 & 0 & 0 \\ 0 & 0 & 0 & 0 & 0 & 0 \end{pmatrix} \quad \textit{and} \quad V = \begin{pmatrix} k_1 & 0 & 0 & 0 & 0 & 0 \\ -\gamma & k_1 & 0 & 0 & 0 & 0 \\ 0 & -\gamma & k_2 & 0 & 0 & 0 \\ 0 & 0 & -\sigma & k_3 & -\alpha & 0 \\ 0 & 0 & 0 & -\nu & k_4 & 0 \\ -\tau_1 & -\tau_1 & -\tau_2 & -\tau_2 & -\tau_2 & \mu \end{pmatrix}$$

Where the infectious category is considered to be E_1,E_2,T,I,R,C *and is calculated in this order. A quick note of notation, in this analysis the following expression have been used:*

$$\kappa_0 = (\mu + \tau_1) \qquad \kappa_1 = (\mu + \tau_1 + \gamma) \quad \kappa_2 = (\mu + \tau_2 + \sigma) \qquad \kappa_3 = (\mu + \tau_2 + \nu) \quad \kappa_4 = (\mu + \tau_2 + \alpha)$$

These expression originate from the differential equations, where each represent the non-infectious compartment removal parameters. For example, κ_0 *represents the non-infectious compartment removal parameters for the susceptible compartment, which are natural death parameter* μ *and false positive culling rate* τ_1.

The next generation matrix FV^{-1} *for the* SE_1E_2TIRC *system is therefore defined as follows:*

$$FV^{-1} = \begin{pmatrix} \frac{\beta\gamma^2\sigma\kappa_4}{\kappa_1^2\kappa_2(\kappa_3\kappa_4-\nu\alpha)} & \frac{\beta\gamma\sigma\kappa_4}{\kappa_1\kappa_2(\kappa_3\kappa_4-\nu\alpha)} & \frac{\beta\sigma\kappa_4}{\kappa_2(\kappa_3\kappa_4-\nu\alpha)} & \frac{\beta\kappa_4}{(\kappa_3\kappa_4-\nu\alpha)} & \frac{\beta\alpha}{(\kappa_3\kappa_4-\nu\alpha)} & 0 \\ 0 & 0 & 0 & 0 & 0 & 0 \\ 0 & 0 & 0 & 0 & 0 & 0 \\ 0 & 0 & 0 & 0 & 0 & 0 \\ 0 & 0 & 0 & 0 & 0 & 0 \end{pmatrix}$$

By the properties of eigenvalues, clearly the $\mathcal{R}_0$ *for the* SE_1E_2TIRC *system is defined as:*

$$\mathcal{R}_0 = \rho(FV^{-1}) = \frac{\beta\gamma^2\sigma\kappa_4}{\kappa_1^2\kappa_2(\kappa_3\kappa_4 - \nu\alpha)}$$

By the properties of the next generation matrix, we have shown that given the basic reproductive number is less than unity ($\mathcal{R}_0 < 1$) then the disease free equilibrium $\mathcal{DFE}$ is locally asymptotically stable. However, as the remaining of this section will show this analysis can be extended, as given that our basic reproductive number is less than unity (i.e. $\mathcal{R}_0 < 1$), then the following theorem proves all solutions in the feasibility region Ω are globally asymptotically attracted to the $\mathcal{DFE}$.

Theorem 3.4.4 *For the given* SE_1E_2TIRC *system 3.1, where initial conditions originate in the positively invariant set* Ω*, the disease free equilibrium* $\mathcal{DFE}$ *is globally asymptotically stable (GAS) in* Ω *whenever* $\mathcal{R}_0 < 1$.

Proof 3.4.4 *Theorem shall be proved by the existence of the following Lyapunov function:*

$$\mathcal{F} = \left(\beta\gamma\sigma\kappa_4\right)E_1 + \left(\beta\sigma\kappa_1\kappa_4\right)E_2 + \left(\beta\sigma\frac{\kappa_1^2\kappa_4}{\gamma}\right)T + \left(\beta\frac{\kappa_1^2\kappa_2\kappa_4}{\gamma}\right)I + \left(\beta\frac{\alpha\kappa_1^2\kappa_2}{\gamma}\right)R$$

Where as we shall demonstrate, that $\frac{d\mathcal{F}}{dt} \leqslant 0$ *for* $\mathcal{R}_0 < 1$ *which implies the system is globally asymptotically stable (GAS).*

$$\begin{aligned}
\frac{d\mathcal{F}}{dt} &= \left(\beta\gamma\sigma\kappa_4\right)\dot{E_1} + \left(\beta\sigma\kappa_1\kappa_4\right)\dot{E_2} + \left(\beta\sigma\frac{\kappa_1^2\kappa_4}{\gamma}\right)\dot{T} + \left(\beta\frac{\kappa_1^2\kappa_2\kappa_4}{\gamma}\right)\dot{I} + \left(\beta\frac{\alpha\kappa_1^2\kappa_2}{\gamma}\right)\dot{R} \\
&= \beta\gamma\sigma\kappa_4\left(\frac{\beta I}{N}S - \kappa_1 E_1\right) + \beta\sigma\kappa_1\kappa_4\left(\gamma E_1 - \kappa_1 E_2\right) \\
&\quad + \beta\sigma\frac{\kappa_1^2\kappa_4}{\gamma}\left(\gamma E_2 - \kappa_2 T\right) + \beta\frac{\kappa_1^2\kappa_2\kappa_4}{\gamma}\left(\sigma T + \alpha R - \kappa_3 I\right) + \beta\frac{\alpha\kappa_1^2\kappa_2}{\gamma}\left(\nu I - \kappa_4 R\right)
\end{aligned}$$

After collecting the different variables of our system together and rearranging terms, we obtain the following:

$$\begin{aligned}
\frac{d\mathcal{F}}{dt} &= \beta\gamma\sigma\kappa_4\left(\frac{\beta I}{N}S\right) + E_1\left(\beta\sigma\gamma\kappa_1\kappa_4 - \beta\sigma\gamma\kappa_1\kappa_4\right) + E_2\left(\beta\sigma\kappa_1^2\kappa_4 - \beta\sigma\kappa_1^2\kappa_4\right) \\
&\quad + T\left(\beta\sigma\frac{\kappa_1^2\kappa_2\kappa_4}{\gamma} - \beta\sigma\frac{\kappa_1^2\kappa_2\kappa_4}{\gamma}\right) + I\left(\beta\alpha\nu\frac{\kappa_1^2\kappa_2}{\gamma} - \beta\frac{\kappa_1^2\kappa_2\kappa_3\kappa_4}{\gamma}\right) \\
&\quad + R\left(\alpha\beta\frac{\kappa_1^2\kappa_2\kappa_4}{\gamma} - \alpha\beta\frac{\kappa_1^2\kappa_2\kappa_4}{\gamma}\right) \\
&= \beta\gamma\sigma\kappa_4\left(\frac{\beta I}{N}S\right) + I\left(\beta\alpha\nu\frac{\kappa_1^2\kappa_2}{\gamma} - \beta\frac{\kappa_1^2\kappa_2\kappa_3\kappa_4}{\gamma}\right) \\
&= \left(\beta\gamma\sigma\kappa_4\left(\frac{S}{N}\right) + \frac{\kappa_1^2\kappa_2}{\gamma}\left(\alpha\nu - \kappa_3\kappa_4\right)\right)\beta I \\
&= \frac{\kappa_1^2\kappa_2}{\gamma}(\kappa_3\kappa_4 - \alpha\nu)\left(\mathcal{R}_0\left(\frac{S}{N}\right) - 1\right)\beta I \\
&\leqslant \kappa_1\kappa_2(\kappa_3\kappa_4 - \alpha\nu)\left(\mathcal{R}_0 - 1\right)\beta I
\end{aligned}$$

Where if we examine our the following term $\kappa_3\kappa_4 - \alpha\nu$*, we can see that it is always positive. As if we input the other variable expressions for* κ_3 *and* κ_4*, we obtain the following:*

$$\kappa_3\kappa_4 - \alpha\nu = (\mu + \tau_2 + \nu)(\mu + \tau_2 + \alpha) - \alpha\nu = (\mu + \tau_2 + \nu)(\mu + \tau_2) + \alpha(\mu + \tau_2) > 0$$

Therefore, our Lyapunov function is negative if our basic reproductive number is less than one (i.e. $\dot{\mathcal{F}} \leqslant 0$ *for* $\mathcal{R}_0 < 1$*, as* $S \leqslant N$ *in* Ω*). This Lyapunov function has shown that the* $\mathcal{DFE}$ *is globally asymptotically stable (GAS) if* $\dot{\mathcal{F}} < 0$ *then it remains to show when* $\dot{\mathcal{F}} = 0$*.*

Notice that $\dot{\mathcal{F}} = 0$ *if and only is* $I = 0$ *or* $S\mathcal{R}_0 = N$*. Given that our initial condition are in* Ω *and as our model parameters are non-negative, then it follows from the system differential equations* 3.1*, that if* $I = 0$*, this implies* $(E_1, E_2, T, R, C) \to (0, 0, 0, 0, 0)$ *as* $t \to \infty$*. Hence, as the total population* $N(t)$ *is a conserved quantity, then* $S \to N$ *and* $C \to 0$ *as* $t \to \infty$*. Thereby the LaSalle's invariance principle,* $\dot{\mathcal{F}} = 0$ *implies that system 3.1's disease free equilibrium* $\mathcal{DFE}$ *is asymptotically stable. Hence, as this is true for both* $I > 0$ *and* $I = 0$*, the disease free equilibrium* $\mathcal{DFE}$ *is globally asymptotically stable (GAS) in* Ω *whenever* $\mathcal{R}_0 < 1$*.*

3.4.5 *Endemic Equilibrium and its Stability*

Let us now consider the SE_1E_2TIRC model's system dynamics when the basic reproductive number is greater than unity (i.e. $\mathcal{R}_0 > 1$), what does this mean for the long term solutions? As we shall show in this section, solutions are globally attracted to the endemic equilibrium ($\mathcal{EE}$). Where the endemic equilibrium represents disease being maintained in the system at a particular endemic level, that continuously depends on system parameters. The definition of the endemic equilibrium ($\mathcal{EE} = (\overline{S}, \overline{E_1}, \overline{E_2}, \overline{T}, \overline{I}, \overline{R}, \overline{C})$) for the SE_1E_2TIRC system 3.1 is given below:

$$\overline{E_1} = \frac{\overline{\lambda^{**}}}{\kappa_1}\overline{S}, \qquad \overline{E_2} = \frac{\gamma}{\kappa_1}\overline{E_1}, \qquad \overline{T} = \frac{\gamma}{\kappa_2}\overline{E_2}, \qquad \overline{I} = \frac{\sigma}{\left(\frac{\nu\alpha}{\kappa_4} - \kappa_3\right)}\overline{T}, \qquad \overline{R} = \frac{\nu}{\kappa_4}\overline{I}$$
$$\overline{C} = \frac{\tau_1}{\mu}\left(\overline{S} + \overline{E_1} + \overline{E_2}\right) + \frac{\tau_2}{\mu}\left(\overline{T} + \overline{I} + \overline{R}\right)$$

At the endemic equilibrium, the force of infection for the SE_1E_2TIRC system 3.1 is denoted by the following expression:

$$\overline{\lambda^{**}} = \frac{\beta\overline{I}}{\overline{N}}$$

The equilibrium points of a system are simply obtained from considering the entire SE_1E_2TIRC system at rest (i.e. $\dot{S} = 0, \dot{E_1} = 0, \ldots, C(t) = 0$). The endemic equilibrium for the SE_1E_2TIRC system can be expressed explicitly as:

$$\begin{aligned}
\overline{S} &= \frac{\Lambda}{(\overline{\lambda^{**}} + \kappa_0)} \\
\overline{E_1} &= \frac{1}{\kappa_1}\left(\frac{\overline{\lambda^{**}}\Lambda}{(\overline{\lambda^{**}} + \kappa_0)}\right) \\
\overline{E_2} &= \frac{\gamma}{\kappa_1^2}\left(\frac{\overline{\lambda^{**}}\Lambda}{(\overline{\lambda^{**}} + \kappa_0)}\right) \\
\overline{T} &= \frac{\gamma^2}{\kappa_2\kappa_1^2}\left(\frac{\overline{\lambda^{**}}\Lambda}{(\overline{\lambda^{**}} + \kappa_0)}\right) \\
\overline{I} &= \left(\frac{\kappa_4\sigma}{\kappa_4\kappa_3 - \alpha\nu}\right)\left(\frac{\gamma^2}{\kappa_2\kappa_1^2}\right)\left(\frac{\overline{\lambda^{**}}\Lambda}{(\overline{\lambda^{**}} + \kappa_0)}\right) \\
\overline{R} &= \left(\frac{\nu\sigma}{\kappa_4\kappa_3 - \alpha\nu}\right)\left(\frac{\gamma^2}{\kappa_2\kappa_1^2}\right)\left(\frac{\overline{\lambda^{**}}\Lambda}{(\overline{\lambda^{**}} + \kappa_0)}\right) \\
\overline{C} &= \frac{\tau_1}{\mu}\left(1 + \frac{\overline{\lambda^{**}}}{\kappa_1} + \frac{\gamma\overline{\lambda^{**}}}{\kappa_1^2}\right)\left(\frac{\Lambda}{(\overline{\lambda^{**}} + \kappa_0)}\right) \\
&\quad + \frac{\tau_2}{\mu}\left(1 + \frac{\kappa_4\sigma}{\kappa_3\kappa_4 - \alpha\nu} + \frac{\nu\sigma}{\kappa_3\kappa_4 - \alpha\nu}\right)\left(\frac{\gamma^2}{\kappa_2\kappa_1^2}\right)\left(\frac{\overline{\lambda^{**}}\Lambda}{(\overline{\lambda^{**}} + \kappa_0)}\right)
\end{aligned} \tag{3.2}$$

Now through the use of Lyapunov functions, we shall prove the globally asymptotically stable (GAS) nature of the SE_1E_2TIRC system's solutions.

Theorem 3.4.5 *For the given SE_1E_2TIRC system 3.1, where initial conditions originate in the positively invariant set Ω, the endemic equilibrium $\mathcal{EE}$ is globally asymptotically stable (GAS) in Ω whenever $\mathcal{R}_0 > 1$.*

Proof 3.4.5 *If the basic reproductive number is above unity ($\mathcal{R}_0 > 1$) then our unique endemic equilibrium exists ($\mathcal{EE}$) and the following non-linear Lyapunov function proves it is globally asymptotically stable (GAS).*

$$\begin{aligned}\mathcal{F} = {} & \overline{S}\left(\frac{S}{\overline{S}} - \ln\frac{\overline{S}}{S}\right) + \overline{E_1}\left(\frac{E_1}{\overline{E_1}} - \ln\frac{\overline{E_1}}{E_1}\right) + \frac{\kappa_1}{\gamma}\overline{E_2}\left(\frac{E_2}{\overline{E_2}} - \ln\frac{\overline{E_2}}{E_2}\right) + \frac{\kappa_1^2}{\gamma^2}\overline{T}\left(\frac{T}{\overline{T}} - \ln\frac{\overline{T}}{T}\right) \\ & + \frac{\kappa_1^2\kappa_2}{\gamma^2\sigma}\overline{I}\left(\frac{I}{\overline{I}} - \ln\frac{\overline{I}}{I}\right) + \left(\frac{\kappa_1^2\kappa_2\kappa_3}{\gamma^2\sigma\nu} - \frac{\beta\overline{S}}{N\nu}\right)\overline{R}\left(\frac{R}{\overline{R}} - \ln\frac{\overline{R}}{R}\right)\end{aligned}$$

Therefore, the differentiated Lyapunov Function is given by:

$$\begin{aligned}\dot{\mathcal{F}} = {} & \left(1 - \frac{\overline{S}}{S}\right)\dot{S} + \left(1 - \frac{\overline{E_1}}{E_1}\right)\dot{E_1} + \frac{\kappa_1}{\gamma}\left(1 - \frac{\overline{E_2}}{E_2}\right)\dot{E_2} + \frac{\kappa_1^2}{\gamma^2}\left(1 - \frac{\overline{T}}{T}\right)\dot{T} + \frac{\kappa_1^2\kappa_2}{\gamma^2\sigma}\left(1 - \frac{\overline{I}}{I}\right)\dot{I} \\ & + \left(\frac{\kappa_1^2\kappa_2\kappa_3}{\gamma^2\sigma\nu} - \frac{\beta\overline{S}}{N\nu}\right)\left(1 - \frac{\overline{R}}{R}\right)\dot{R}\end{aligned}$$

By expanding the brackets we obtain the following:

$$\begin{aligned}\dot{\mathcal{F}} = {} & \dot{S} - \left(\frac{\overline{S}}{S}\right)\dot{S} \\ & + \dot{E_1} - \left(\frac{\overline{E_1}}{E_1}\right)\dot{E_1} \\ & + \frac{\kappa_1}{\gamma}\dot{E_2} - \frac{\kappa_1}{\gamma}\left(\frac{\overline{E_2}}{E_2}\right)\dot{E_2} \\ & + \frac{\kappa_1^2}{\gamma^2}\dot{T} - \frac{\kappa_1^2}{\gamma^2}\left(\frac{\overline{T}}{T}\right)\dot{T} \\ & + \frac{\kappa_1\kappa_2}{\gamma^2\sigma}\dot{I} - \frac{\kappa_1\kappa_2}{\gamma^2\sigma}\left(\frac{\overline{I}}{I}\right)\dot{I} \\ & + \left(\frac{\kappa_1^2\kappa_2\kappa_3}{\gamma^2\sigma\nu} - \frac{\beta\overline{S}}{N\nu}\right)\dot{R} - \left(\frac{\kappa_1^2\kappa_2\kappa_4}{\gamma^2\sigma\nu} - \frac{\beta\overline{S}}{N\nu}\right)\left(\frac{\overline{R}}{R}\right)\dot{R}\end{aligned}$$

Therefore, let us define the following sub-functions, $\dot{\mathcal{F}_1}$ and $\dot{\mathcal{F}_2}$, that when added together equal to our original Lyapunov function $\mathcal{F}$.

$$\dot{\mathcal{F}} = \dot{\mathcal{F}_1} + \dot{\mathcal{F}_2}$$

Where,

$$\dot{\mathcal{F}_1} = \frac{\beta I\overline{S}}{N} - \frac{\beta IS}{N} + \dot{E_1} + \frac{\kappa_1}{\gamma}\dot{E_2} + \frac{\kappa_1^2}{\gamma^2}\dot{T} + \frac{\kappa_1^2\kappa_2}{\gamma^2\sigma}\dot{I} + \left(\frac{\kappa_1^2\kappa_2\kappa_3}{\gamma^2\sigma\nu} - \frac{\beta\overline{S}}{N\nu}\right)\dot{R}$$

$$\dot{\mathcal{F}_2} = \dot{S} - \left(\frac{\overline{S}}{S}\right)\dot{S} - \frac{\beta I\overline{S}}{N} + \frac{\beta IS}{N} - \left(\frac{\overline{E_1}}{E_1}\right)\dot{E_1} - \frac{\kappa_1}{\gamma}\left(\frac{\overline{E_2}}{E_2}\right)\dot{E_2} - \frac{\kappa_1^2}{\gamma^2}\left(\frac{\overline{T}}{T}\right)\dot{T} - \frac{\kappa_1^2\kappa_2}{\gamma^2\sigma}\left(\frac{\overline{I}}{I}\right)\dot{I} - \left(\frac{\kappa_1^2\kappa_2\kappa_3}{\gamma^2\sigma\nu} - \frac{\beta\overline{S}}{N\nu}\right)\left(\frac{\overline{R}}{R}\right)\dot{R}$$

Lets begin to analyse $\dot{\mathcal{F}_2}$. The first part of our analysis is to show the following equality holds:

$$\dot{S} - \left(\frac{\overline{S}}{S}\right)\dot{S} - \frac{\beta I\overline{S}}{N} + \frac{\beta IS}{N} = \frac{\beta I\overline{S}}{N}\left(1 - \frac{\overline{S}}{S}\right) + \kappa_0\overline{S}\left(2 - \frac{\overline{S}}{S} - \frac{S}{\overline{S}}\right)$$

If you consider the susceptible compartment $S(t)$ at the equilibrium ($\mathcal{EE}$) we obtain the following expression for the recruitment parameter, $\Lambda = \beta\frac{\overline{SI}}{N} + \kappa_0\overline{S}$, using this we can obtain the expression:

$$\begin{aligned}\dot{S} - \left(\frac{\overline{S}}{S}\right)\dot{S} - \frac{\beta I\overline{S}}{N} + \frac{\beta IS}{N} &= \left(\Lambda - \frac{\beta IS}{N} - \kappa_0 S\right) - \left(\Lambda\left(\frac{\overline{S}}{S}\right) - \frac{\beta I\overline{S}}{N} - \kappa_0\overline{S}\right) - \frac{\beta I\overline{S}}{N} + \frac{\beta IS}{N} \\ &= \left(\frac{\beta\overline{SI}}{N} + \kappa_0\overline{S} - \kappa_0 S\right) - \left(\frac{\beta\overline{SI}}{N}\left(\frac{\overline{S}}{S}\right) - \kappa_0\overline{S}\left(\frac{\overline{S}}{S}\right) - \kappa_0\overline{S}\right) \\ &= \frac{\beta\overline{SI}}{N}\left(1 - \frac{\overline{S}}{S}\right) + \kappa_0\overline{S}\left(2 - \frac{S}{\overline{S}} - \frac{\overline{S}}{S}\right)\end{aligned}$$

Using the above expression, our sub-Lyapunov function $\dot{\mathcal{F}}_2$ becomes the following:

$$\begin{aligned}\dot{\mathcal{F}}_2 = {} & \frac{\beta\overline{IS}}{N}\left(1 - \frac{\overline{S}}{S}\right) + \kappa_0\overline{S}\left(2 - \frac{\overline{S}}{S} - \frac{S}{\overline{S}}\right) - \left(\frac{\overline{E_1}}{E_1}\right)\dot{E_1} - \frac{\kappa_1}{\gamma}\left(\frac{\overline{E_2}}{E_2}\right)\dot{E_2} - \frac{\kappa_1^2}{\gamma^2}\left(\frac{\overline{T}}{T}\right)\dot{T} \\ & - \frac{\kappa_1^2\kappa_2}{\gamma^2\sigma}\left(\frac{\overline{I}}{I}\right)\dot{I} - \left(\frac{\kappa_1^2\kappa_2\kappa_3}{\gamma^2\sigma\nu} - \frac{\beta\overline{S}}{N\nu}\right)\left(\frac{\overline{R}}{R}\right)\dot{R}\end{aligned}$$

From considering our system of differential equations at equilibrium, we obtain the following equalities that will aid our analysis.

$$\kappa_1\overline{E_1} = \frac{\beta\overline{SI}}{N}, \qquad \kappa_1\overline{E_2} = \gamma\overline{E_1}, \qquad \kappa_2\overline{T} = \gamma\overline{E_2}, \qquad \kappa_3\overline{I} = \alpha\overline{R} + \sigma\overline{T}, \qquad \nu\overline{I} = \kappa_4\overline{R}$$

Using these equalities and substituting the respective differential equations, the following relations can be obtained:

$$\begin{aligned}-\left(\frac{\overline{E_1}}{E_1}\right)\dot{E_1} &= \frac{\beta\overline{IS}}{N}\left(1 - \frac{\overline{E_1}}{E_1}\frac{S}{\overline{S}}\frac{I}{\overline{I}}\right) \\ -\frac{\kappa_1}{\gamma}\left(\frac{\overline{E_2}}{E_2}\right)\dot{E_2} &= \frac{\beta\overline{IS}}{N}\left(1 - \frac{\overline{E_2}}{E_2}\frac{E_1}{\overline{E_1}}\right) \\ -\frac{\kappa_1^2}{\gamma^2}\left(\frac{\overline{T}}{T}\right)\dot{T} &= \frac{\beta\overline{IS}}{N}\left(1 - \frac{\overline{T}}{T}\frac{E_2}{\overline{E_2}}\right) \\ -\frac{\kappa_1^2\kappa_2}{\gamma^2\sigma}\dot{I} &= \frac{\beta\overline{IS}}{N}\left(1 - \frac{\overline{I}}{I}\frac{T}{\overline{T}}\right) + \frac{\kappa_1^2\kappa_2\alpha}{\gamma^2\sigma}\overline{R}\left(1 - \frac{\overline{I}}{I}\frac{R}{\overline{R}}\right) \\ -\left(\frac{\kappa_1^2\kappa_2\kappa_3}{\gamma^2\sigma\nu} - \frac{\beta\overline{S}}{N\nu}\right)\left(\frac{\overline{R}}{R}\right)\dot{R} &= \frac{\kappa_1\kappa_2\alpha}{\gamma^2\sigma}\overline{R}\left(1 - \frac{I}{\overline{I}}\frac{\overline{R}}{R}\right)\end{aligned}$$

Therefore, after substituting in the above expressions, our sub-function $\dot{\mathcal{F}}_2$ can be written in the following form:

$$\begin{aligned}\dot{\mathcal{F}}_2 = {} & \frac{\beta\overline{IS}}{N}\left(5 - \frac{\overline{S}}{S} - \frac{\overline{E_1}}{E_1}\frac{S}{\overline{S}}\frac{I}{\overline{I}} - \frac{\overline{E_2}}{E_2}\frac{E_1}{\overline{E_1}} - \frac{\overline{T}}{T}\frac{E_2}{\overline{E_2}} - \frac{\overline{I}}{I}\frac{T}{\overline{T}}\right) \\ & + \frac{\kappa_1^2\kappa_2\alpha}{\gamma^2\sigma}\overline{R}\left(2 - \frac{\overline{I}}{I}\frac{R}{\overline{R}} - \frac{I}{\overline{I}}\frac{\overline{R}}{R}\right) \\ & + \kappa_0\overline{S}\left(2 - \frac{\overline{S}}{S} - \frac{S}{\overline{S}}\right)\end{aligned}$$

Lets now consider our other sub-function $\dot{\mathcal{F}}_1$ where using the equalities from above, the following relationship is attained:

$$\begin{aligned}\frac{\kappa_1^2\kappa_2\kappa_3\kappa_4}{\gamma^2\sigma\nu}\overline{R} = \frac{\kappa_1^2\kappa_2\kappa_3}{\gamma^2\sigma}\overline{I} = \frac{\kappa_1^2\kappa_2}{\gamma^2\sigma}\left(\alpha\overline{R}+\sigma\overline{T}\right) = \frac{\kappa_1^2\kappa_2\alpha}{\gamma^2\sigma}\overline{R} + \frac{\kappa_1^2\kappa_2}{\gamma^2}\overline{T} = \frac{\kappa_1^2\kappa_2\alpha}{\gamma^2\sigma}\overline{R} + \frac{\beta\overline{SI}}{N}\\ = \frac{\kappa_1^2\kappa_2\alpha}{\gamma^2\sigma}\overline{R} + \frac{\beta\overline{S}}{N\nu}\kappa_4\overline{R}\end{aligned}$$

With this expression in hand, we can use it to show that the sub-function is equal to zero ($\dot{\mathcal{F}}_1 = 0$).

$$\begin{aligned}\dot{\mathcal{F}}_1 &= \dot{E_1} + \frac{\kappa_1}{\gamma}\dot{E_2} + \frac{\kappa_1^2}{\gamma^2}\dot{T} + \frac{\kappa_1^2\kappa_2}{\gamma^2\sigma}\dot{I} + \left(\frac{\kappa_1\kappa_2\kappa_3}{\gamma^2\sigma\nu} - \frac{\beta\overline{S}}{N\nu}\right)\dot{R} + \frac{\beta I\overline{S}}{N} - \frac{\beta IS}{N}\\ &= \frac{\beta IS}{N} - \frac{\beta IS}{N} + E_1\left(\frac{\kappa_1}{\gamma}\gamma - \kappa_1\right) + E_2\left(\frac{\kappa_1^2}{\gamma^2}\gamma - \frac{\kappa_1}{\gamma}\kappa_1\right) + T\left(\frac{\kappa_1^2\kappa_2}{\gamma^2\sigma}\sigma - \frac{\kappa_1^2\kappa_2}{\gamma^2}\right)\\ &\quad + I\left(\frac{\kappa_1^2\kappa_2\kappa_3}{\gamma^2\sigma\nu}\nu - \frac{\kappa_1^2\kappa_2\kappa_3}{\gamma^2\sigma} - \frac{\beta\overline{S}}{N\nu}\nu + \frac{\beta\overline{S}}{N}\right) + R\left(-\frac{\kappa_1^2\kappa_2\kappa_3\kappa_4}{\gamma^2\sigma\nu} + \frac{\kappa_1^2\kappa_2\alpha}{\gamma^2\sigma} + \frac{\beta\overline{S}}{N\nu}\kappa_4\right)\\ &= R\left(-\frac{\kappa_1^2\kappa_2\kappa_3\kappa_4}{\gamma^2\sigma\nu} + \frac{\kappa_1^2\kappa_2\alpha}{\gamma^2\sigma} + \frac{\beta\overline{S}}{N\nu}\kappa_4\right)\\ &= \left(\frac{R}{\overline{R}}\right)\left(-\frac{\kappa_1^2\kappa_2\kappa_3\kappa_4}{\gamma^2\sigma\nu}\overline{R} + \frac{\kappa_1^2\kappa_2\alpha}{\gamma^2\sigma}\overline{R} + \frac{\beta\overline{S}}{N\nu}\kappa_4\overline{R}\right)\\ &= 0\end{aligned}$$

Therefore, the original Lyapunov function $\dot{\mathcal{F}}$ that is given by $\dot{\mathcal{F}} = \dot{\mathcal{F}}_1 + \dot{\mathcal{F}}_2$ has the following form:

$$\begin{aligned}\dot{\mathcal{F}} &= \frac{\beta\overline{IS}}{N}\left(5 - \frac{\overline{S}}{S} - \frac{\overline{E_1}}{E_1}\frac{S}{\overline{S}}\frac{I}{\overline{I}} - \frac{\overline{E_2}}{E_2}\frac{E_1}{\overline{E_1}} - \frac{\overline{T}}{T}\frac{E_2}{\overline{E_2}} - \frac{\overline{I}}{I}\frac{T}{\overline{T}}\right)\\ &\quad + \frac{\kappa_1^2\kappa_2\alpha}{\gamma^2\sigma}\overline{R}\left(2 - \frac{\overline{I}}{I}\frac{R}{\overline{R}} - \frac{I}{\overline{I}}\frac{\overline{R}}{R}\right)\\ &\quad + \kappa_0\overline{S}\left(2 - \frac{\overline{S}}{S} - \frac{S}{\overline{S}}\right)\end{aligned}$$

Using the fact that the arithmetic mean is greater than or equal to the geometric mean, the following inequalities hold:

$$\begin{aligned}5 - \frac{\overline{S}}{S} - \frac{\overline{E_1}}{E_1}\frac{S}{\overline{S}}\frac{I}{\overline{I}} - \frac{\overline{E_2}}{E_2}\frac{E_1}{\overline{E_1}} - \frac{\overline{T}}{T}\frac{E_2}{\overline{E_2}} - \frac{\overline{I}}{I}\frac{T}{\overline{T}} &\leqslant 0\\ 2 - \frac{\overline{I}}{I}\frac{R}{\overline{R}} - \frac{I}{\overline{I}}\frac{\overline{R}}{R} &\leqslant 0\\ 2 - \frac{\overline{S}}{S} - \frac{S}{\overline{S}} &\leqslant 0\end{aligned}$$

For example, given that the arithmetic mean is greater than or equal to the geometric mean this implies,

$$\begin{aligned}\frac{S}{2} + \frac{\overline{S}}{2} &\geqslant \sqrt{S\overline{S}}\\ S^2 + \overline{S}^2 + 2S\overline{S} &\geqslant 4S\overline{S}\\ \frac{S}{\overline{S}} + \frac{\overline{S}}{S} &\geqslant 2\end{aligned}$$

Clearly, this implies that $2 - \frac{S}{\bar{S}} - \frac{\bar{S}}{S} \leqslant 0$.

The above Lyapunov function $\dot{\mathcal{F}} < 0$ *therefore shows that given that the model parameters are non-negative and given initial conditions are in* Ω*, then the unique endemic equilibrium* $\mathcal{EE}$ *is globally asymptotically stable (GAS) when it exists (i.e. when* $\mathcal{R}_0 > 1$*).*

3.4.6 *Conclusion*

For the SE_1E_2TIRC system 3.1, where initial conditions originate in the positively invariant set Ω, the dynamics and equilibrium of the system are completely determined by the basic reproductive number $\mathcal{R}_0$. Where the entire long term behaviour of the SE_1E_2TIRC system can be defined as follows:

- If $\mathcal{R}_0 < 1$, all solutions within the feasibility region Ω asymptotically approach the disease free equilibrium ($\mathcal{DFE}$).
- If on the other hand $\mathcal{R}_0 > 1$, all solutions within $\Omega \setminus \mathcal{DFE}$ approach the unique endemic equilibrium ($\mathcal{EE}$).

3.5 GENERALISING THE MATHEMATICAL MODEL

Let us now consider and analyse the generalised SE^nTIRC model where this model incorporates Erlang distributed exposure latency periods. The inter-herd disease dynamics are described using a cattle population compartmental model similar to the SE_1E_2TIRC system. However, instead of two exposure compartments there exists an arbitrary number of exposure compartments (n). Through better encapsulating this highly variable latency period, we can examine and understand what effect latency has on model predictions.

3.5.1 *Mathematical Model Formulation*

In the following section, we define the non-linear differential equations of the SE^nTIRC system. By incorporating more exposure compartments the total cattle population $N(t)$ at time t is now governed by the following population constraint:

$$N(t) = S(t) + \sum_{i=1}^{n} E_i(t) + T(t) + I(t) + R(t) + C(t)$$

The differential equations governing the generalised SE^nTIRC remain the same as the SE_1E_2TIRC system, except for the exposure compartment E and the culled compartment C.

When cattle first become exposed and progress into the first exposed compartment E_1, the differential equation has the following form:

$$\frac{dE_1}{dt} = \frac{\beta I}{N} S - (\mu + \tau_1 + \gamma) E_1$$

However, now cattle progress through another $n-1$ exposure compartments ($E_2, \ldots, E_n$), where each compartment progression occurs according to the same parameter γ. In each exposure compartment, host are still removed due to natural deaths μ and false-positive test reactors τ_1, hence, the differential equations controlling the other exposure compartments are given by:

$$\frac{dE_i}{dt} = \gamma E_{i-1} - (\mu + \tau_1 + \gamma) E_i \qquad \text{Where } i \in 2, 3, \ldots, n$$

The culled compartment $C(t)$ differential equation must also be altered to accommodate these new exposure compartments.

$$\frac{dC}{dt} = \tau_1 \left(S + \sum_{i=1}^{n} E_i \right) + \tau_2 (T + I + R) - \mu C$$

The SE^nTIRC set of non-linear differential equations are therefore defined as follows:

$$\begin{aligned}
\frac{dS}{dt} &= \Lambda - \frac{\beta I}{N} S - (\mu + \tau_1) S \\
\frac{dE_1}{dt} &= \frac{\beta I}{N} S - (\mu + \tau_1 + \gamma) E_1 \\
\frac{dE_2}{dt} &= \gamma E_1 - (\mu + \tau_1 + \gamma) E_2 \\
&\vdots \\
\frac{dE_n}{dt} &= \gamma E_{n-1} - (\mu + \tau_1 + \gamma) E_n \\
\frac{dT}{dt} &= \gamma E_n - (\mu + \tau_2 + \sigma) T \\
\frac{dI}{dt} &= \sigma T + \alpha R - (\mu + \tau_2 + \nu) I \\
\frac{dR}{dt} &= \nu I - (\mu + \tau_2 + \alpha) I \\
\frac{dC}{dt} &= \tau_1 \left(S + \sum_{i=1}^{n} E_i \right) + \tau_2 (T + I + R) - \mu C
\end{aligned} \tag{3.3}$$

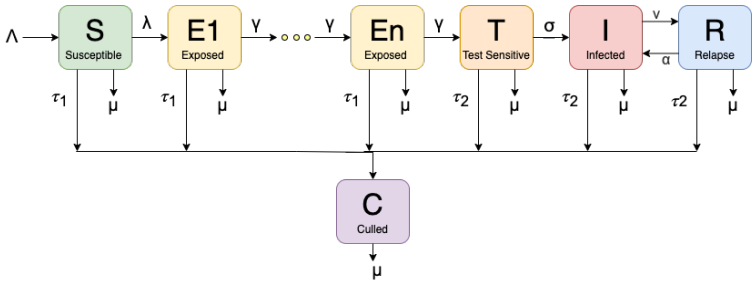

Figure 3.2: Flow chart of the transmission dynamics of the SE^nTIRC model.

In the following subsection, similar analysis shall be preformed for the SE^nTIRC model, as was performed for the SE_1E_2TIRC model. First we examine the model properties, proving that the system's solutions for the augmented system (SE^nTIRC) are still well posed. The analysis then leads on to the exploration of the long term solutions behaviour, investigating this system's basic reproductive number ($\mathcal{R}_0$) and system equilibria ($\mathcal{DFE}$ and $\mathcal{EE}$).

3.5.2 *Mathematical Model Properties*

Let us now investigate the model properties of the SE^nTIRC system. In this section, we shall demonstrate the well posed nature of solutions and construct the system feasibility region.

Theorem 3.5.1 *All solutions for our SE^nTIRC system 3.3 which have initial conditions originating in $\mathbb{R}^{n+5}_+$ are bounded.*

$$\mathbb{R}^{n+5}_+ = \{N(S, E_1, \ldots, E_n, T, I, R, C) \mid S \geqslant 0, E_i \geqslant 0, T \geqslant 0, I \geqslant 0, R \geqslant 0, C \geqslant 0, \forall i \in \{1, \ldots, n\}\}$$

Proof 3.5.1 *Let $N\big(S(t), E_1(t), \ldots, E_n(t), T(t), I(t), R(t), C(t)\big)$ be an arbitrary solution of the SE^nTIRC system 3.3 with non-negative initial conditions. The population of the herd is given by $N(t)$, where*

$$N(t) = S(t) + \sum_{i=1}^{n} E_i(t) + T(t) + I(t) + R(t) + C(t)$$

Hence, the rate of change of the herd population is given by,

$$\frac{dN}{dt} = \Lambda - \mu\left(S + \sum_{i=1}^{n} E_i(t) + T + I + R + C\right) = \Lambda - \mu N(t)$$

By Grönwall lemma, if $x(t)$ is a function satisfying $\frac{dx}{dt} \leqslant ax + b$, where $x(0) = x_0$ and both a and b are constants, then for all time $t \geqslant 0$:

$$x(t) \leqslant x_0 e^{at} + \frac{b}{a}(e^{at} - 1)$$

Therefore, our cattle population for the system is bounded as follows:

$$0 \leqslant N\big(S(t), E_1(t), \ldots, E_n(t), T(t), I(t), R(t), C(t)\big) \leqslant \frac{\Lambda}{\mu}(1 - e^{-\mu t}) + N(0)e^{-\mu t}$$

This implies that all long term solutions for the SE^{n}TIRC system 3.3 are bounded by the herds population at equilibrium (i.e. $\overline{N} = \frac{\Lambda}{\mu}$)

$$0 \leqslant \limsup_{t\to\infty} N(t) \leqslant \frac{\Lambda}{\mu}$$

Therefore all solutions of the system 3.3 that originate in $\mathbb{R}_+^{n+5}$ are attracted to the following positive invariant region:

$$\Omega_n = \left\{ N(S, E_1, \ldots, E_n, T, I, R, C) \in \mathbb{R}_+^{n+5} \;\middle|\; N \leqslant \frac{\Lambda}{\mu} \right\}$$

The SE^{n}TIRC system 3.3 is therefore bounded, additionally, since the limit of $\sup N(t)$ is independent of the initial conditions then the system is uniformly bounded. Now that we have shown that solutions are uniformly bounded, the next stage is to show that the SE^{n}TIRC model solutions are well posed (i.e. exist and are unique depending on initial conditions).

Theorem 3.5.2 *The SE^{n}TIRC system (3.3) is well posed.*

Proof 3.5.2 *As the right hand side of system 3.3 are continuously differentiable functions on the domain:*

$$\mathbb{R}_+^{n+5} = \{N(S, E_1, \ldots, E_n, T, I, R, C) \;|\; S \geqslant 0, E_i \geqslant 0, T \geqslant 0, I \geqslant 0, R \geqslant 0, C \geqslant 0, \forall i \in \{1, \ldots, n\}\}$$

and as the above theorem indicates that the first derivative of our system is uniformly bounded. This condition implies that the system equation are Lipschitz continuous and with this condition, we can apply the Picard Lindelöf theorem that proves unique solutions exist for the SE^{n}TIRC system 3.3.

The SE^{n}TIRC model is therefore well posed and any solution with initial conditions originating in Ω_n will remain in this feasibility region for all future time. Now, lets turn our attention the the system equilibrium and the basic reproductive number that bifurcates the system.

3.5.3 *Disease free equilibrium $\mathcal{DFE}$ and the Basic Reproductive Number $\mathcal{R}_0$*

In this section we discuss the disease free equilibrium $\mathcal{DFE}$ and the associated basic reproductive number $\mathcal{R}_0$ of the SE^{n}TIRC system. Where we begin by first examining the disease free equilibrium $\mathcal{DFE}$, from here we derive the system's basic reproductive number. The basic reproductive number then permits us to discuss the stability of the disease free equilibrium $\mathcal{DFE}$, where we show both locally and globally that if $\mathcal{R}_0 < 1$ then solutions are asymptotically attracted to the disease free equilibrium $\mathcal{DFE}$.

The disease free equilibrium $\mathcal{DFE}$ represents the system absent of disease and is the same for the SE^nTIRC system 3.3 as it was for the SE_1E_2TIRC system. The entire herd consists of only susceptible cattle at the $\mathcal{DFE}$, hence the disease free equilibrium $\mathcal{DFE}$ is given by:

$$\mathcal{DFE} = (\overline{S}, \overline{E_1}, \ldots, \overline{E_n}, \overline{T}, \overline{I}, \overline{R}, \overline{C}) = \left(\frac{\Lambda}{\mu}, 0, 0, \ldots, 0\right)$$

Let us now determine the basic reproductive number $\mathcal{R}_0$ for the system by using the Van den Driesche and Watmough approach to generate the next generation matrix.

Theorem 3.5.3 *For the given SE^nTIRC system 3.3, where initial conditions originate in the positively invariant set Ω_n, the basic reproductive number is:*

$$\mathcal{R}_0 = \frac{\gamma^n}{\kappa_1^n}\left(\frac{\beta\sigma\kappa_4}{\kappa_2(\kappa_3\kappa_4 - \nu\alpha)}\right)$$

Proof 3.5.3 *The basic reproductive number $\mathcal{R}_0$ is calculated by the Van den Driesche and Watmough approach. This method has been extensively discussed in section 2.3.3.3 and therefore this analysis shall be condensed.*

The basic reproductive number $\mathcal{R}_0$ is the spectral radius of the next generation matrix given by FV^{-1}, hence the basic reproductive number is denoted by:

$$\mathcal{R}_0 = \rho(FV^{-1})$$

Where the matrices F and V are generated from the linearisation of the system equations evaluated at the disease free equilibrium. Where the two matrices F and V decouple the system, as matrix F's elements are only the parameters which induce new infections and the matrix V's elements are all other parameters. However, lets consider the form that the F matrix takes for our arbitrary system that has n-dimensional latency compartments (SE^nTIRC). If the matrix order is considered to be $E_1, \ldots, E_n, T, I, R, C$ then the matrix F will be a $n+4$ dimensional square matrix. However, as there exists only a single infection transmission pathway (cattle to cattle) in the F matrix, it has the following simple formula,

$$F_{[i,j]} = \begin{cases} \beta & \textit{if i=1 and j=n+2} \\ 0 & \textit{otherwise} \end{cases}$$

This simply formula confirms that all new infectious enter into the first row, which corresponds to the exposure compartment E_1.

$$F = \begin{pmatrix} 0 & \ldots & 0 & \beta & 0 & 0 \\ 0 & \ldots & 0 & 0 & 0 & 0 \\ \vdots & \vdots & \vdots & \vdots & \vdots & \vdots \\ 0 & 0 & 0 & 0 & 0 & 0 \end{pmatrix}$$

Therefore, as there only exists one non-zero element of matrix F*, the next generational matrix* FV^{-1} *will consist entirely of one row of* V^{-1}*. As the only non-zero element (*β*) of F is positioned at* $F[1, n+2]$ *this implies the next generation matrix will consist of* β *times the* $n+2$ *row of the inverse of matrix V. Hence, the next generation matrix has the following form:*

$$FV^{-1} = \beta \begin{pmatrix} V^{-1}_{[n+2,1]} & V^{-1}_{[n+2,2]} & \cdots & V^{-1}_{[n+2,n+4]} \\ 0 & 0 & \dots & 0 \\ \vdots & \vdots & \vdots & \vdots \\ 0 & 0 & 0 & 0 \end{pmatrix}$$

By the properties of eigenvalues, if the next generation matrix FV^{-1} *has the above form then the spectral radius of this matrix* FV^{-1} *is given by the first element of the next generation matrix (i.e.* $\rho(FV^{-1}) = a_{11} \in FV^{-1}$*). This element corresponds to the the first element of the* $n+2$ *row of the inverse of matrix V and hence, the basic reproductive number for the system* $\mathcal{R}_0$ *is given by:*

$$\mathcal{R}_0 = \rho(FV^{-1}) = \beta V^{-1}_{[n+2,1]}$$

Lets us now turn our focus to generating the inverse of the matrix V. First, let us begin by commenting on the last row of our matrix V, this corresponds to the cull compartment and it wont effect the $n+2$ *row of the inverse of matrix V. As a result, we will excluded this row to reduce matrix size in this discussion.*

In our analysis of matrix V, we consider the matrix in an associated block form, where a block matrix is a matrix whose elements are themselves matrices, which are called sub-matrices. By allowing a matrix to be viewed at different levels of abstraction, the block matrix viewpoint enables more transparent proofs of results. Let us first define our matrix V as a block matrix, consisting of 4 sub-matrices, namely A,B,C,D.

$$V = \begin{pmatrix} A & B \\ C & D \end{pmatrix}$$

Where the sub-matrix A represents the transfer between the exposure compartments and the test sensitive compartments. As a result, the matrix is a $n+1$ *dimension square matrix, that is in lower triangular form.*

$$A = \begin{pmatrix} \kappa_1 & 0 & 0 & & & \\ -\gamma & \kappa_1 & 0 & & & \\ 0 & -\gamma & \kappa_1 & & & \\ & & & \ddots & & \\ & & & \kappa_1 & 0 & 0 \\ & & & -\gamma & \kappa_1 & 0 \\ & & & 0 & -\gamma & \kappa_2 \end{pmatrix} \qquad A_{[i,j]} = \begin{cases} \kappa_1 & \textit{if } i = j \ \forall i, j \in \{1, \ldots, n\} \\ \kappa_2 & \textit{if } i = j = n+1 \\ -\gamma & \textit{if } i = j+1 \\ 0 & \textit{otherwise} \end{cases}$$

The sub-matrix B represents the transfer (excluding new infectious hosts) of hosts coming from either the infectious or relapse compartments to the exposure and test sensitive compartments. As the system of differential equations for the SE^{n}TIRC system 3.3 show, no such transfer occur. Therefore, it should be clear to see that the sub-matrix B is a zero matrix of dimensions $[n+1, 2]$*:*

$$B = \begin{pmatrix} 0 & 0 \\ \vdots & \vdots \\ 0 & 0 \end{pmatrix}$$

The sub-matrix C represents the transfer of hosts from the exposure and test sensitive compartments to either infectious or relapse compartments. Through examining the SE^{n}TIRC differential equations, it can be seen that this only occurs when host progress from the test sensitive T *compartment to the infectious compartment* I*. Therefore, the sub-matrix C has only one non-zero element* σ *at the position* $[1, n+1]$*.*

$$C = \begin{pmatrix} 0 & \ldots & 0 & -\sigma \\ 0 & \ldots & 0 & 0 \end{pmatrix} \qquad C_{[i,j]} = \begin{cases} -\sigma & \textit{if } i = 1 \textit{ and } j = n+1 \\ 0 & \textit{otherwise} \end{cases}$$

Lastly the sub-matrix D represents the transfer between the infectious or relapse compartments. Through examining the SE^{n}TIRC differential equations, it can be seen that the sub-matrix D has the following form:

$$D = \begin{pmatrix} \kappa_3 & -\alpha \\ -\nu & \kappa_4 \end{pmatrix}$$

In this block form, the next step in the analysis is to use a standard block form inversion, where the following formula allows us to obtain the inverse for our matrix V.

Theorem 3.5.4 *Let* $A \in \mathbb{F}^{n\times n}, B \in \mathbb{F}^{n\times m}, C \in \mathbb{F}^{m\times n}$*, and* $D \in \mathbb{F}^{m\times m}$*. If* A *and* $D - CA^{-1}B$ *are non-singular, then the following formula holds:*

$$\mathbf{V^{-1}} = \begin{bmatrix} \mathbf{A} & \mathbf{B} \\ \mathbf{C} & \mathbf{D} \end{bmatrix}^{-1} = \begin{bmatrix} \mathbf{A^{-1}} + \mathbf{A^{-1}B}\left(\mathbf{D} - \mathbf{CA^{-1}B}\right)^{-1}\mathbf{CA^{-1}} & -\mathbf{A^{-1}B}\left(\mathbf{D} - \mathbf{CA^{-1}B}\right)^{-1} \\ -\left(\mathbf{D} - \mathbf{CA^{-1}B}\right)^{-1}\mathbf{CA^{-1}} & \left(\mathbf{D} - \mathbf{CA^{-1}B}\right)^{-1} \end{bmatrix}$$

For a proof of this statement please see [174]. As our block matrix B is the zero matrix, therefore we must show that A *and* D *are non-singular for this formula to hold, which will be completed in this analysis. Additional as the block matrix B is the zero matrix, this above condition can be simplified to the following:*

$$\mathbf{V^{-1}} = \begin{bmatrix} \mathbf{A} & \mathbf{B} \\ \mathbf{C} & \mathbf{D} \end{bmatrix}^{-1} = \begin{bmatrix} \mathbf{A^{-1}} & 0 \\ -\mathbf{DCA^{-1}} & \mathbf{D^{-1}} \end{bmatrix}$$

Therefore, let us begin by constructing the inverses for the our defined sub-matrices A, D *to construct* A^{-1}, D^{-1}*, and* $-DCA^{-1}$*.*

By the properties of matrices, the inverses of our sub-matrix A is defined as follows:

$$A = \begin{pmatrix} \kappa_1 & 0 & 0 & & & \\ -\gamma & \kappa_1 & 0 & & & \\ 0 & -\gamma & \kappa_1 & & & \\ & & & \ddots & & \\ & & & \kappa_1 & 0 & 0 \\ & & & -\gamma & \kappa_1 & 0 \\ & & & 0 & -\gamma & \kappa_2 \end{pmatrix} \quad \textit{and} \quad A^{-1} = \begin{pmatrix} \frac{1}{\kappa_1} & 0 & 0 & & \dots & 0 \\ \frac{\gamma}{\kappa_1^2} & \frac{1}{\kappa_1} & 0 & & & \vdots \\ \frac{\gamma^2}{\kappa_1^3} & \frac{\gamma}{\kappa_1^2} & \frac{1}{\kappa_1} & & & \\ & & & \ddots & & \\ \vdots & & & & \frac{1}{\kappa_1} & 0 \\ \frac{\gamma^n}{\kappa_1^n \kappa_2} & \dots & & & \frac{\gamma}{\kappa_1 \kappa_2} & \frac{1}{\kappa_2} \end{pmatrix}$$

Where this inverse can easily be verified and can be proven using straight forward induction.

The next sub-matrix we find the inverse for is D:

$$D = \begin{pmatrix} \kappa_3 & -\alpha \\ -\nu & \kappa_4 \end{pmatrix} \quad \textit{and} \quad D^{-1} = \frac{1}{\kappa_4\kappa_3 - \nu\alpha} \begin{pmatrix} \kappa_4 & \alpha \\ \nu & \kappa_3 \end{pmatrix}$$

Now that we have the inverse for both our sub-matrices A and D, the next step in obtaining the next generation matrix is to calculate $-D^{-1}CA^{-1}$*. The first step in acquiring* $-D^{-1}CA^{-1}$ *is to calculate* $-D^{-1}C$*. Simple matrix multiplication demonstrates that* $-D^{-1}C$ *is given by:*

$$-D^{-1}C = \frac{1}{\kappa_4\kappa_3 - \nu\alpha} \begin{pmatrix} 0 & \dots & 0 & \kappa_4\sigma \\ 0 & \dots & 0 & \nu\sigma \end{pmatrix}$$

Hence,

$$-D^{-1}CA^{-1} = \frac{1}{\kappa_4\kappa_3 - \nu\alpha}\begin{pmatrix} \frac{\gamma^n}{\kappa_1^n\kappa_2}\kappa_4\sigma & \frac{\gamma^{n-1}}{\kappa_1^{n-1}\kappa_2}\kappa_4\sigma & \dots & \frac{\kappa_4\sigma}{\kappa_2} \\ \frac{\gamma^n}{\kappa_1^n\kappa_2}\nu\sigma & \frac{\gamma^{n-1}}{\kappa_1^{n-1}\kappa_2}\nu\sigma & \dots & \frac{\nu\sigma}{\kappa_2} \end{pmatrix}$$

Therefore, this last result is the final step in calculating the next inverse of our matrix V, therefore we are finally able to calculate the next generation matrix FV^{-1}*. As discussed previous the next generation matrix consists of the* $n+2$ *row of the inverse of V, therefore it consists of the first row of both* $-D^{-1}CA^{-1}$ *and* $D^{-}1$*.*

$$FV^{-1} = \frac{\beta}{\kappa_4\kappa_3 - \nu\alpha}\begin{pmatrix} \frac{\gamma^n}{\kappa_1^n\kappa_2}\kappa_4\sigma & \frac{\gamma^{n-1}}{\kappa_1^{n-1}\kappa_2}\kappa_4\sigma & \dots & \frac{\kappa_4\sigma}{\kappa_2} & \frac{\kappa_4}{\beta} & \frac{\alpha}{\beta} \\ 0 & 0 & \dots & 0 & 0 & 0 \\ \vdots & \vdots & \ddots & \vdots & \vdots & \vdots \\ 0 & 0 & 0 & 0 & 0 & 0 \end{pmatrix}$$

Finally by the products of eigenvalues, the spectral radius of the next generation matrix is clearly its first element and hence the basic reproductive number for the SE^nTIRC *system 3.3 is as follows:*

$$\mathcal{R}_0 = \rho(FV^{-1}) = \left(\frac{\gamma^n}{\kappa_1^n\kappa_2}\right)\frac{\beta\kappa_4\sigma}{\kappa_4\kappa_3 - \nu\alpha}$$

The basic reproductive number $\mathcal{R}_0$ for the given n dimensional SE^nTIRC system correctly corresponds to the basic reproductive number for the SE_1E_2TIRC system given earlier and the SETIRC model given in [64]. The expression for the n dimensional system makes intuitive sense as well, because as the system grows the basic reproductive system is only alter by increasing the number of $\frac{\gamma}{\kappa_1}$ expressions in front of the previous basic reproductive number. The $\frac{\gamma}{\kappa_1}$ expression represents the proportion of cattle that will make it to the next exposure compartment, therefore the basic reproductive number must incorporate this expression.

We have therefore shown that given the basic reproductive number is less than unity ($\mathcal{R}_0 < 1$) then the disease free equilibrium $\mathcal{DFE}$ is locally asymptotically stable. In the remaining of this section, we explore the globally asymptotically stable nature of all solutions in the feasibility region Ω_n given that $\mathcal{R}_0 < 1$.

Theorem 3.5.5 *For the given* SE^nTIRC *system 3.3, where initial conditions originate in the positively invariant set* Ω_n*, the disease free equilibrium* $\mathcal{DFE}$ *is globally asymptotically stable (GAS) in* Ω_n *whenever* $\mathcal{R}_0 < 1$*.*

Proof 3.5.4 *This theorem shall be proved by the existence of the following Lyapunov function:*

$$\mathcal{F} = \sum_{i=1}^{n} X_i E_i + X_{n+1}T + X_{n+2}I + X_{n+3}R$$

Where the expressions $X_1, X_2, \ldots, X_{n+3}$ are defined as follows:

$$X_i = \beta\sigma\kappa_4 \frac{\kappa_1^{i-1}}{\gamma^{i-2}} \qquad \forall i \in \{1, \ldots, n+1\}$$
$$X_{n+2} = \beta\kappa_2\kappa_4 \frac{\kappa_1^n}{\gamma^{n-1}}$$
$$X_{n+3} = \beta\kappa_2\alpha \frac{\kappa_1^n}{\gamma^{n-1}}$$

Let us now differentiate our Lyapunov function $\mathcal{F}$ with respect to time. After expanding the Lyapunov function and some rearrangement, we obtain $\mathcal{F}$ in the following form:

$$\dot{\mathcal{F}} = X_1\beta I\left(\frac{S}{N}\right) + \sum_{i=1}^{n}\left(\gamma X_{i+1} - \kappa_1 X_i\right)E_i + \left(\sigma X_{n+2} - \kappa_2 X_{n+1}\right)T + \left(\nu X_{n+3} - \kappa_3 X_{n+2}\right)I + \left(\alpha X_{n+2} - \kappa_4 X_{n+3}\right)R$$

As a result of our choice of X_i expressions, the following expressions are equal to zero.

$$\sum_{i=1}^{n}\left(\gamma X_{i+1} - \kappa_1 X_i\right)E_i = 0 \qquad \text{as } \gamma X_{i+1} = \beta\sigma\kappa_4\left(\frac{\kappa_1^i}{\gamma^{i-2}}\right) = \kappa_1 X_i \quad \forall i \in \{1, \ldots, n\}$$
$$\left(\sigma X_{n+2} - \kappa_2 X_{n+1}\right)T = 0 \qquad \text{as } \sigma X_{n+2} = \beta\sigma\kappa_2\kappa_4\left(\frac{\kappa_1^n}{\gamma^{n-1}}\right) = \kappa_2 X_{n+1}$$
$$\left(\alpha X_{n+2} - \kappa_4 X_{n+3}\right)R = 0 \qquad \text{as } \alpha X_{n+2} = \beta\alpha\kappa_2\kappa_4\left(\frac{\kappa_1^n}{\gamma^{n-1}}\right) = \kappa_4 X_{n+3}$$

Therefore, our function $\dot{\mathcal{F}}$ can be simplified to the following form:

$$\dot{\mathcal{F}} = X_1\beta I\left(\frac{S}{N}\right) + \left(\nu X_{n+3} - \kappa_3 X_{n+2}\right)I$$

The next step in the analysis is to enter our system parameter values instead of the X_i parameters. After doing so the Lyapunov function has the following form:

$$\begin{aligned}
\dot{\mathcal{F}} &= \left(\beta\gamma\sigma\kappa_4\left(\frac{S}{N}\right) + \kappa_2(\alpha\nu - \kappa_3\kappa_4)\left(\frac{\kappa_1^n}{\gamma^{n-1}}\right)\right)\beta I \\
&= \kappa_2(\kappa_3\kappa_4 - \alpha\nu)\left(\frac{\kappa_1^n}{\gamma^{n-1}}\right)\left(\frac{\beta\sigma\kappa_4\gamma^n}{\kappa_1^n\kappa_2(\kappa_3\kappa_4 - \alpha\nu)}\left(\frac{S}{N}\right) - 1\right)\beta I \\
&= \kappa_2(\kappa_3\kappa_4 - \alpha\nu)\left(\frac{\kappa_1^n}{\gamma^{n-1}}\right)\left(\mathcal{R}_0\left(\frac{S}{N}\right) - 1\right)\beta I \\
&\leqslant \kappa_2(\kappa_3\kappa_4 - \alpha\nu)\left(\frac{\kappa_1^n}{\gamma^{n-1}}\right)\left(\mathcal{R}_0 - 1\right)\beta I
\end{aligned}$$

Where as show in the previous analysis of the SE_1E_2TIRC model, the term $\kappa_3\kappa_4 - \alpha\nu$ is always positive.

$$\kappa_3\kappa_4 - \alpha\nu = (\mu + \tau_2 + \nu)(\mu + \tau_2 + \alpha) - \alpha\nu = (\mu + \tau_2 + \nu)(\mu + \tau_2) + \alpha(\mu + \tau_2) > 0$$

Our Lyapunov function is negative if our basic reproductive number is less than one (i.e. $\dot{\mathcal{F}} \leqslant 0$ for $\mathcal{R}_0 < 1$, as $S \leqslant N$ in Ω_n). Therefore, this Lyapunov function shows that the $\mathcal{DFE}$ is globally asymptotically stable (GAS) if the basic reproductive number is less than one ($\mathcal{R}_0 < 1$).

3.5.4 *Endemic Equilibrium and its Stability*

Let now examine the dynamics when the basic reproductive number is greater than unity (i.e. $\mathcal{R}_0 > 1$), what does this mean for the long term solutions? As we shall show in this section, solutions are globally attracted to the endemic equilibrium ($\mathcal{EE}$). Where the endemic equilibrium represents the disease being maintained in the system at a particular endemic level, that continuous depends on system parameters. The definition of the endemic equilibrium for the SE^nTIRC system 3.3 is given below:

$$\mathcal{EE} = (\overline{S}, \overline{E_1}, \ldots, \overline{E_n}, \overline{T}, \overline{I}, \overline{R}, \overline{C})$$

$$\overline{S} = \frac{\Lambda}{(\overline{\lambda^{**}} + \kappa_0)}, \qquad \overline{E_i} = \frac{\gamma^{i-1}}{\kappa_1^i}\overline{\lambda^{**}S}, \qquad \overline{T} = \frac{\gamma}{\kappa_2}\overline{E_n}, \qquad \overline{I} = \frac{\sigma}{\left(\kappa_3 - \frac{\nu\alpha}{\kappa_4}\right)}\overline{T}, \qquad \overline{R} = \frac{\nu}{\kappa_4}\overline{I}$$

$$\overline{C} = \frac{\tau_1}{\mu}\left(\overline{S} + \sum_{i=1}^{n}\overline{E_i}\right) + \frac{\tau_2}{\mu}(\overline{T} + \overline{I} + \overline{R})$$

At the endemic equilibrium, the force of infection for the SE^nTIRC system 3.3 is denoted by the following expression:

$$\overline{\lambda^{**}} = \frac{\beta\overline{I}}{\overline{N}}$$

This endemic equilibrium for the SE^nTIRC system can be expressed explicitly as:

$$\mathcal{EE} = (\overline{S}, \overline{E_1}, \ldots, \overline{E_n}, \overline{T}, \overline{I}, \overline{R}, \overline{C})$$

$$\overline{S} = \frac{\Lambda}{(\overline{\lambda^{**}} + \kappa_0)}$$

$$\overline{E_i} = \frac{\gamma}{\kappa_1}\overline{E_{i-1}} = \frac{\gamma^{i-1}}{\kappa_1^{i-1}}\overline{E_1} = \frac{\gamma^{i-1}}{\kappa_1^i}\left(\frac{\overline{\lambda^{**}}\Lambda}{\overline{\lambda^{**}} + \kappa_0}\right)$$

$$\overline{T} = \frac{\gamma^n}{\kappa_1^n\kappa_2}\left(\frac{\overline{\lambda^{**}}\Lambda}{\overline{\lambda^{**}} + \kappa_0}\right)$$

$$\overline{I} = \left(\frac{\kappa_4\sigma}{\kappa_4\kappa_3 - \alpha\nu}\right)\overline{T} = \left(\frac{\kappa_4\sigma}{\kappa_4\kappa_3 - \alpha\nu}\right)\left(\frac{\gamma^n}{\kappa_1^n\kappa_2}\right)\left(\frac{\overline{\lambda^{**}}\Lambda}{\overline{\lambda^{**}} + \kappa_0}\right)$$

$$\overline{R} = \left(\frac{\nu\sigma}{\kappa_4\kappa_3 - \alpha\nu}\right)\overline{T} = \left(\frac{\nu\sigma}{\kappa_4\kappa_3 - \alpha\nu}\right)\left(\frac{\gamma^n}{\kappa_1^n\kappa_2}\right)\left(\frac{\overline{\lambda^{**}}\Lambda}{\overline{\lambda^{**}} + \kappa_0}\right)$$

$$\overline{C} = \frac{\tau_1}{\mu}\left(1 + \overline{\lambda^{**}}\sum_{i=1}^{n}\frac{\gamma^{i-1}}{\kappa_1^i}\right)\left(\frac{\Lambda}{\overline{\lambda^{**}} + \kappa_0}\right) + \frac{\tau_2}{\mu}\left(1 + \frac{\sigma(\kappa_4 + \nu)}{\kappa_4\kappa_3 - \alpha\nu}\right)\left(\frac{\gamma^n}{\kappa_2\kappa_1^n}\right)\left(\frac{\overline{\lambda^{**}}\Lambda}{\overline{\lambda^{**}} + \kappa_0}\right)$$

Where, the following parameter are described the same as before:

$$\kappa_0 = (\mu + \tau_1) \qquad \kappa_1 = (\mu + \tau_1 + \gamma) \quad \kappa_2 = (\mu + \tau_2 + \sigma) \qquad \kappa_3 = (\mu + \tau_2 + \nu) \quad \kappa_4 = (\mu + \tau_2 + \alpha)$$

Similarly to the previous analysis, let us now determine the stability condition of the endemic equilibrium $(\mathcal{EE})$ through the use of Lyapunov functions.

Theorem 3.5.6 *For the given SE^nTIRC system 3.3, where initial conditions originate in the positively invariant set Ω_n, the endemic equilibrium $\mathcal{EE}$ is globally asymptotically stable (GAS) in Ω whenever $\mathcal{R}_0 > 1$.*

Proof 3.5.5 *If the basic reproductive number is above unity ($\mathcal{R}_0 > 1$) then our unique endemic equilibrium exists ($\mathcal{EE}$) and the following non-linear Lyapunov function proves it is globally asymptotically stable (GAS).*

$$\begin{aligned}\mathcal{F} = {} & \overline{S}\left(\frac{S}{\overline{S}} - \ln\frac{\overline{S}}{S}\right) + \sum_{i=1}^{n}\left(\frac{k_1^{i-1}}{\gamma^{i-1}}\right)\overline{E_i}\left(\frac{E_i}{\overline{E_i}} - \ln\frac{\overline{E_i}}{E_i}\right) + \frac{\kappa_1^n}{\gamma^n}\overline{T}\left(\frac{T}{\overline{T}} - \ln\frac{\overline{T}}{T}\right) \\ & + \frac{\kappa_1^n\kappa_2}{\gamma^n\sigma}\overline{I}\left(\frac{I}{\overline{I}} - \ln\frac{\overline{I}}{I}\right) + \left(\frac{\kappa_1^n}{\gamma^n}\frac{\kappa_2\kappa_3}{\sigma\nu} - \frac{\beta\overline{S}}{N\nu}\right)\overline{R}\left(\frac{R}{\overline{R}} - \ln\frac{\overline{R}}{R}\right)\end{aligned}$$

Therefore, the differentiated Lyapunov Function is given by:

$$\dot{\mathcal{F}} = \left(1 - \frac{\overline{S}}{S}\right)\dot{S} + \sum_{i=1}^{n}\left(\frac{\kappa_1^{i-1}}{\gamma^{i-1}}\right)\left(1 - \frac{\overline{E_i}}{E_i}\right)\dot{E_i} + \frac{\kappa_1^n}{\gamma^n}\left(1 - \frac{\overline{T}}{T}\right)\dot{T} + \frac{\kappa_1^n\kappa_2}{\gamma^n\sigma}\left(1 - \frac{\overline{I}}{I}\right)\dot{I} + \left(\frac{\kappa_1^n\kappa_2\kappa_3}{\gamma^n\sigma\nu} - \frac{\beta\overline{S}}{N\nu}\right)\left(1 - \frac{\overline{R}}{R}\right)\dot{R}$$

By expanding the brackets we obtain,

$$\begin{aligned}\dot{\mathcal{F}} = {} & \dot{S} - \left(\frac{\overline{S}}{S}\right)\dot{S} \\ & + \sum_{i=1}^{n}\left(\frac{\kappa_1^{i-1}}{\gamma^{i-1}}\right)\dot{E_i} - \sum_{i=1}^{n}\left(\frac{\kappa_1^{i-1}}{\gamma^{i-1}}\right)\left(\frac{\overline{E_i}}{E_i}\right)\dot{E_i} \\ & + \frac{\kappa_1^n}{\gamma^n}\dot{T} - \frac{\kappa_1^n}{\gamma^n}\left(\frac{\overline{T}}{T}\right)\dot{T} \\ & + \frac{\kappa_1^n\kappa_2}{\gamma^n\sigma}\dot{I} - \frac{\kappa_1^n\kappa_2}{\gamma^n\sigma}\left(\frac{\overline{I}}{I}\right)\dot{I} \\ & + \left(\frac{\kappa_1^n\kappa_2\kappa_3}{\gamma^n\sigma\nu} - \frac{\beta\overline{S}}{N\nu}\right)\dot{R} - \left(\frac{\kappa_1^n\kappa_2\kappa_4}{\gamma^n\sigma\nu} - \frac{\beta\overline{S}}{N\nu}\right)\left(\frac{\overline{R}}{R}\right)\dot{R}\end{aligned}$$

Lets define the following sub-functions, $\dot{\mathcal{F}_1}$ and $\dot{\mathcal{F}_2}$.

$$\dot{\mathcal{F}} = \dot{\mathcal{F}_1} + \dot{\mathcal{F}_2}$$

$$\dot{\mathcal{F}_1} = \frac{\beta I\overline{S}}{N} - \frac{\beta IS}{N} + \sum_{i=1}^{n}\left(\frac{\kappa_1^{i-1}}{\gamma^{i-1}}\right)\dot{E_i} + \frac{\kappa_1^n}{\gamma^n}\dot{T} + \frac{\kappa_1^n\kappa_2}{\gamma^n\sigma}\dot{I} + \left(\frac{\kappa_1^n\kappa_2\kappa_3}{\gamma^n\sigma\nu} - \frac{\beta\overline{S}}{N\nu}\right)\dot{R}$$

$$\dot{\mathcal{F}_2} = \dot{S} - \left(\frac{\overline{S}}{S}\right)\dot{S} - \frac{\beta I\overline{S}}{N} + \frac{\beta IS}{N} - \sum_{i=1}^{n}\left(\frac{\kappa_1^{i-1}}{\gamma^{i-1}}\right)\left(\frac{\overline{E_i}}{E_i}\right)\dot{E_i} - \frac{\kappa_1^n}{\gamma^n}\left(\frac{\overline{T}}{T}\right)\dot{T} - \frac{\kappa_1^n\kappa_2}{\gamma^n\sigma}\left(\frac{\overline{I}}{I}\right)\dot{I} - \left(\frac{\kappa_1^n\kappa_2\kappa_3}{\gamma^n\sigma\nu} - \frac{\beta\overline{S}}{N\nu}\right)\left(\frac{\overline{R}}{R}\right)\dot{R}$$

Lets begin to analyse $\dot{\mathcal{F}_2}$. As shown in the analysis of the SE_1E_2TIRC model, the following equality holds:

$$\dot{S} - \left(\frac{\overline{S}}{S}\right)\dot{S} - \frac{\beta I\overline{S}}{N} + \frac{\beta IS}{N} = \frac{\beta I\overline{S}}{N}\left(1 - \frac{\overline{S}}{S}\right) + \kappa_0\overline{S}\left(2 - \frac{\overline{S}}{S} - \frac{S}{\overline{S}}\right)$$

Hence,

$$\dot{\mathcal{F}_2} = \frac{\beta I\overline{S}}{N}\left(1 - \frac{\overline{S}}{S}\right) + \kappa_0\overline{S}\left(2 - \frac{\overline{S}}{S} - \frac{S}{\overline{S}}\right) - \sum_{i=1}^{n}\left(\frac{\kappa_1^{i-1}}{\gamma^{i-1}}\right)\left(\frac{\overline{E_i}}{E_i}\right)\dot{E_i} - \frac{\kappa_1^2}{\gamma^2}\left(\frac{\overline{T}}{T}\right)\dot{T} - \frac{\kappa_1^2\kappa_2}{\gamma^2\sigma}\left(\frac{\overline{I}}{I}\right)\dot{I} - \left(\frac{\kappa_1^2\kappa_2\kappa_3}{\gamma^2\sigma\nu} - \frac{\beta\overline{S}}{N\nu}\right)\left(\frac{\overline{R}}{R}\right)\dot{R}$$

The following equalities will aid our analysis.

$$\kappa_1\overline{E_1} = \frac{\beta\overline{S}\overline{I}}{N}, \qquad \left(\frac{\kappa_1^i}{\gamma^{i-1}}\right)\overline{E_i} = \left(\frac{\kappa_1^{i-1}}{\gamma^{i-1}}\right)\left(\kappa_1\overline{E_i}\right) = \left(\frac{\kappa_1^{i-1}}{\gamma^{i-1}}\right)\left(\gamma\overline{E}_{i-1}\right) = \kappa_1\overline{E_1} = \frac{\beta\overline{S}\overline{I}}{N}$$

$$\kappa_2\overline{T} = \left(\frac{\kappa_1^n}{\gamma^{n-1}}\right)\overline{E_n}, \qquad \kappa_3\overline{I} = \alpha\overline{R} + \sigma\overline{T}, \qquad \nu\overline{I} = \kappa_4\overline{R}$$

Using these equalities, the following relations can be obtained:

$$\begin{aligned}
-\left(\frac{\overline{E_1}}{E_1}\right)\dot{E_1} &= \frac{\beta I\overline{S}}{N}\left(1 - \frac{\overline{E_1}}{E_1}\frac{S}{\overline{S}}\frac{I}{\overline{I}}\right)\\
-\frac{\kappa_1^{i-1}}{\gamma^{i-1}}\left(\frac{\overline{E_i}}{E_i}\right)\dot{E_i} &= \frac{\beta I\overline{S}}{N}\left(1 - \frac{\overline{E_i}}{E_i}\frac{E_{i-1}}{\overline{E_{i-1}}}\right)\\
-\frac{\kappa_1^n}{\gamma^n}\left(\frac{\overline{T}}{T}\right)\dot{T} &= \frac{\beta I\overline{S}}{N}\left(1 - \frac{\overline{T}}{T}\frac{E_n}{\overline{E_n}}\right)\\
-\frac{\kappa_1^n\kappa_2}{\gamma^n\sigma}\dot{I} &= \frac{\beta I\overline{S}}{N}\left(1 - \frac{\overline{I}}{I}\frac{T}{\overline{T}}\right) + \frac{\kappa_1^n\kappa_2\alpha}{\gamma^n\sigma}\overline{R}\left(1 - \frac{\overline{I}}{I}\frac{R}{\overline{R}}\right)\\
-\left(\frac{\kappa_1^n\kappa_2\kappa_3}{\gamma^n\sigma\nu} - \frac{\beta\overline{S}}{N\nu}\right)\left(\frac{\overline{R}}{R}\right)\dot{R} &= \frac{\kappa_1^n\kappa_2\alpha}{\gamma^n\sigma}\overline{R}\left(1 - \frac{I}{\overline{I}}\frac{\overline{R}}{R}\right)
\end{aligned}$$

Therefore, our sub-function $\dot{\mathcal{F}_2}$ can be written in the following form:

$$\begin{aligned}
\dot{\mathcal{F}_2} = \frac{\beta I\overline{S}}{N}&\left(n + 3 - \frac{\overline{S}}{S} - \sum_{i=2}^{n-1}\frac{\overline{E_i}}{E_i}\frac{E_{i-1}}{\overline{E_{i-1}}} - \frac{\overline{E_n}}{E_n}\frac{T}{\overline{T}} - \frac{\overline{T}}{T}\frac{E_n}{\overline{E_n}} - \frac{\overline{I}}{I}\frac{T}{\overline{T}}\right)\\
&+ \frac{\kappa_1^n\kappa_2\alpha}{\gamma^n\sigma}\overline{R}\left(2 - \frac{\overline{I}}{I}\frac{R}{\overline{R}} - \frac{I}{\overline{I}}\frac{\overline{R}}{R}\right)\\
&+ \kappa_0\overline{S}\left(2 - \frac{\overline{S}}{S} - \frac{S}{\overline{S}}\right)
\end{aligned}$$

Lets now consider our other sub-function $\dot{\mathcal{F}}_1$. Using the equalities from above, the same relationship from the analysis of the SE_1E_2TIRC model is attained:

$$\frac{\kappa_1^n\kappa_2\kappa_3\kappa_4}{\gamma^n\sigma\nu}\overline{R} = \frac{\kappa_1^n\kappa_2\alpha}{\gamma^n\sigma}\overline{R} + \frac{\beta\overline{S}}{N\nu}\kappa_4\overline{R}$$

This is used below to show that the sub-function is equal to zero ($\dot{\mathcal{F}}_1 = 0$).

$$\begin{aligned}
\dot{\mathcal{F}}_1 &= \frac{\beta I\overline{S}}{N} - \frac{\beta IS}{N} + \sum_{i=1}^{n}\left(\frac{\kappa_1^{i-1}}{\gamma^{i-1}}\right)\dot{E}_i + \left(\frac{\kappa_1^n}{\gamma^n}\right)\dot{T} + \left(\frac{\kappa_1^n\kappa_2}{\gamma^n\sigma}\right)\dot{I} + \left(\frac{\kappa_1^n\kappa_2\kappa_3}{\gamma^n\sigma\nu} - \frac{\beta\overline{S}}{N\nu}\right)\dot{R} \\
&= -\frac{\beta IS}{N} + \left(\frac{\beta IS}{N} - \kappa_1 E_1\right) + \sum_{i=2}^{n}\left(\frac{\kappa_1^{i-1}}{\gamma^{i-1}}\right)\left(\gamma E_{i-1} - \kappa_1 E_i\right) \\
&\quad + \left(\frac{\kappa_1^n}{\gamma^n}\right)\left(\gamma E_n - \kappa_2 T\right) + \left(\frac{\kappa_1^n\kappa_2}{\gamma^n\sigma}\right)\left(\sigma T + \alpha R - \kappa_3 I\right) + \frac{\beta I\overline{S}}{N} + \left(\frac{\kappa_1^n\kappa_2\kappa_3}{\gamma^n\sigma\nu} - \frac{\beta\overline{S}}{N\nu}\right)\left(\nu T - \kappa_4 R\right) \\
&= \sum_{i=1}^{n} E_i\left(\frac{\kappa_1^{i-1}}{\gamma^{i-1}}\right)\left(\frac{\kappa_1}{\gamma}\gamma - \kappa_1\right) + T\left(\frac{\kappa_1^n}{\gamma^n}\right)\left(\frac{\kappa_2}{\sigma}\sigma - \kappa_2\right) \\
&\quad I\left(\frac{\kappa_1^n\kappa_2\kappa_3}{\gamma^n\sigma\nu}\nu - \frac{\kappa_1^n\kappa_2\kappa_3}{\gamma^n\sigma} - \frac{\beta\overline{S}}{N\nu}\nu + \frac{\beta\overline{S}}{N}\right) + R\left(-\frac{\kappa_1^n\kappa_2\kappa_3\kappa_4}{\gamma^n\sigma\nu}\overline{R} + \frac{\kappa_1^n\kappa_2\alpha}{\gamma^n\sigma}\overline{R} + \frac{\beta\overline{S}}{N\nu}\kappa_4\overline{R}\right) \\
&= \overline{R}\left(\frac{R}{\overline{R}}\right)\left(-\frac{\kappa_1^n\kappa_2\kappa_3\kappa_4}{\gamma^n\sigma\nu}\overline{R} + \frac{\kappa_1^n\kappa_2\alpha}{\gamma^n\sigma}\overline{R} + \frac{\beta\overline{S}}{N\nu}\kappa_4\overline{R}\right) \\
&= 0
\end{aligned}$$

Therefore, the original Lyapunov function $\dot{\mathcal{F}}$ such that $\dot{\mathcal{F}} = \dot{\mathcal{F}}_1 + \dot{\mathcal{F}}_2$, is the following:

$$\begin{aligned}
\dot{\mathcal{F}} &= \frac{\beta I\overline{S}}{N}\left(n + 3 - \frac{\overline{S}}{S} - \sum_{i=2}^{n-1}\frac{\overline{E_i}}{E_i}\frac{E_{i-1}}{\overline{E_{i-1}}} - \frac{\overline{E_n}}{E_n}\frac{T}{\overline{T}} - \frac{\overline{T}}{T}\frac{E_n}{\overline{E_n}} - \frac{\overline{I}}{I}\frac{T}{\overline{T}}\right) \\
&\quad + \frac{\kappa_1^n\kappa_2\alpha}{\gamma^n\sigma}\overline{R}\left(2 - \frac{\overline{I}}{I}\frac{R}{\overline{R}} - \frac{I}{\overline{I}}\frac{\overline{R}}{R}\right) \\
&\quad + \kappa_0\overline{S}\left(2 - \frac{\overline{S}}{S} - \frac{S}{\overline{S}}\right)
\end{aligned}$$

Using the fact that the arithmetic mean is greater than or equal to the geometric mean, the following inequalities hold:

$$\begin{aligned}
n + 3 - \frac{\overline{S}}{S} - \sum_{i=2}^{n-1}\frac{\overline{E_i}}{E_i}\frac{E_{i-1}}{\overline{E_{i-1}}} - \frac{\overline{E_n}}{E_n}\frac{T}{\overline{T}} - \frac{\overline{T}}{T}\frac{E_n}{\overline{E_n}} - \frac{\overline{I}}{I}\frac{T}{\overline{T}} &\leqslant 0 \\
2 - \frac{\overline{I}}{I}\frac{R}{\overline{R}} - \frac{I}{\overline{I}}\frac{\overline{R}}{R} &\leqslant 0 \\
2 - \frac{\overline{S}}{S} - \frac{S}{\overline{S}} &\leqslant 0
\end{aligned}$$

The above Lyapunov function is negative ($\dot{\mathcal{F}} < 0$), therefore this shows that given that the model parameters are non-negative and given initial conditions are in Ω_n, then the unique endemic equilibrium $\mathcal{EE}$ is globally asymptotically stable (GAS) when it exists (i.e. when $\mathcal{R}_0 > 1$).

3.5.5 *SE^nTIRC Model Summary*

In this section we have examined the latency mechanic of the SE^nTIRC system 3.3. By augmenting this model, we have altered the system's latency period distribution, changing from the exponential distribution to the Erlang distribution. This highly flexible distribution further incorporates bTB's extensive latency period into the model.

So far in this chapter we have analysed two different systems, namely the SE_1E_2TIRC 3.1 system and the SE^nTIRC system 3.3. In this analysis we have shown that for any system, no matter the number of exposure compartment n, long term solution's behaviour are completely determined by the basic reproductive number $\mathcal{R}_0$. Where given initial conditions originate in the positively invariant set Ω_n, either one of two states occur:

- For $\mathcal{R}_0 < 1$, all solutions within Ω_n approach the disease free equilibrium ($\mathcal{DFE}$).

- For $\mathcal{R}_0 > 1$, all solutions within $\Omega_n \setminus \mathcal{DFE}$ approach the unique endemic equilibrium ($\mathcal{EE}$).

3.6 BOVINE TUBERCULOSIS' sE^nT^mIRC MODEL EXTENSION

In the previous sections, we examined the bTB latency mechanic and extended the SETIRC model into the SE^nTIRC model. However, the most natural question arises: "Why has only the exposed compartment been extended?". To fully explore how the latency period affects the bTB transmission, we must extend the test sensitive compartment in a similar fashion.

This section aims to directly develop the previous SE^nTIRC epidemiological model into the SE^nT^mIRC epidemiological model by further amending its latency mechanic. However, as the nature of this extension (i.e. the SE^nTIRC system to the SE^nT^mIRC system) is very similar to the previous extension (SE_1E_2TIRC system to the SE^nTIRC system), therefore, so too is the underlying analysis. In this section, we perform the same analysis for the SE^nT^mIRC system as was completed for the previous SE^nTIRC system however the proofs of this analysis are attached as an appendix due to their similarity to the previous section's analysis. The proofs of all theorems can be found in appendix A.

Therefore, this section consists of a brief description of the SE^nT^mIRC system, describing the associated differential equations and giving a schematic representation of the system. Afterwhich, the analysis of the SE^nT^mIRC model is summarised and similarly to the SE^nTIRC

model, each of our equilibrium ($\mathcal{DFE}$ and $\mathcal{EE}$) are globally attractive depending on the system's $\mathcal{R}_0$.

3.6.1 *Mathematical Model Formulation*

Let us now consider and analyse the generalised SE^nT^mIRC model that further augments the latency mechanic, incorporating Erlang distributed test sensitive latency periods. The inter-herd disease dynamics used to describe a cattle population compartmental model are similar to the SE^nTIRC model. However, instead of a singular test sensitive compartment there exists an arbitrary number of test sensitive compartments (m). This model augmentation further incorporates the highly variable total latency period by allowing the modeller to incorporate a more realistic latency distribution.

3.6.2 *SE^nT^mIRC system's differential equations*

In this section we define the non-linear differential equations of the SE^nT^mIRC system. The total cattle population $N(t)$ at time t is now governed by the following population constraint:

$$N(t) = S(t) + \sum_{i=1}^{n} E_i(t) + \sum_{j=1}^{m} T_j(t) + I(t) + R(t) + C(t)$$

The differential equations governing the generalised SE^nT^mIRC remain the same as the SE^nTIRC system, except for the test sensitive compartment T and the culling compartment C.

When cattle first become test sensitive after the n different exposure compartments, they progress into the first of m test sensitive compartment T_1. Where the differential equation has the following form:

$$\frac{dT_1}{dt} = \gamma E_n - (\mu + \tau_2 + \sigma)T_1$$

However, now cattle progress through another $m-1$ test sensitive compartments ($T_2, \ldots, T_m$), where each compartment progression occurs according to the same parameter σ. In each test sensitive compartment, host are still removed due to natural deaths μ and positive test reactors τ_2. Hence, the differential equations controlling the other test sensitive compartments are given by:

$$\frac{dT_j}{dt} = \sigma T_{j-1} - (\mu + \tau_2 + \sigma)T_j \qquad \text{Where } j \in 2, 3, \ldots, m$$

The culled compartment $C(t)$ differential equation must also be altered to accommodate the new test sensitive compartments.

$$\frac{dC}{dt} = \tau_1\left(S + \sum_{i=1}^{n} E_i\right) + \tau_2\left(\sum_{j=1}^{m} T_j + I + R\right) - \mu C$$

The SE^nT^mIRC set of non-linear differential equations are therefore defined as follows:

$$\begin{aligned}
\frac{dS}{dt} &= \Lambda - \frac{\beta I}{N}S - (\mu + \tau_1)S \\
\frac{dE_1}{dt} &= \frac{\beta I}{N}S - (\mu + \tau_1 + \gamma)E_1 \\
\frac{dE_2}{dt} &= \gamma E_1 - (\mu + \tau_1 + \gamma)E_2 \\
&\vdots \\
\frac{dE_n}{dt} &= \gamma E_{n-1} - (\mu + \tau_1 + \gamma)E_n \\
\frac{dT_1}{dt} &= \gamma E_n - (\mu + \tau_2 + \sigma)T_1 \\
\frac{dT_2}{dt} &= \sigma T_1 - (\mu + \tau_2 + \sigma)T_2 \\
&\vdots \\
\frac{dT_m}{dt} &= \gamma T_{m-1} - (\mu + \tau_2 + \gamma)T_m \\
\frac{dI}{dt} &= \sigma T_m + \alpha R - (\mu + \tau_2 + \nu)I \\
\frac{dR}{dt} &= \nu I - (\mu + \tau_2 + \alpha)I \\
\frac{dC}{dt} &= \tau_1\left(S + \sum_{i=1}^{n} E_i\right) + \tau_2\left(\sum_{j=1}^{m} T_j + I + R\right) - \mu C
\end{aligned} \tag{3.4}$$

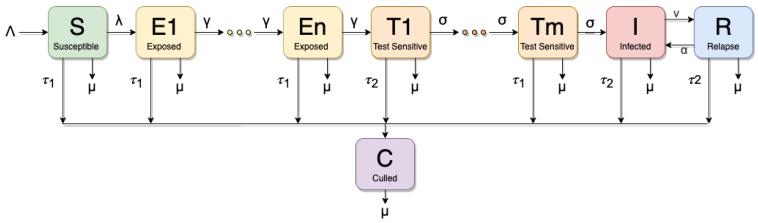

Figure 3.3: Flow chart of the transmission dynamics of the SE^nT^mIRC model.

3.7 SE^nT^mIRC MATHEMATICAL ANALYSIS SUMMARY

In this section we summarise all analysis for the SE^nT^mIRC system, exploring the long term behaviour of solutions, investigating the system's basic reproductive number ($\mathcal{R}_0$) and system equilibria ($\mathcal{DFE}$ and $\mathcal{EE}$)

Theorem 3.7.1 *All solutions for our SE^nT^mIRC system 3.4 which have initial conditions originating within $\mathbb{R}_+^{n+m+4}$ are bounded in the positive invariant set:*

$$\Omega_{n+m} = \left\{ N(S, E_1, \ldots, E_n, T_1, \ldots, T_m, I, R, C) \in \mathbb{R}_+^{n+m+4} \mid N \leqslant \frac{\Lambda}{\mu} \right\}$$

Where the solutions of the SE^nT^mIRC system (3.4) are well posed in nature.

Theorem 3.7.2 *The disease-free equilibrium $\mathcal{DFE}$ for the SE^nT^mIRC system 3.4 the $\mathcal{DFE}$ is given by:*

$$\mathcal{DFE} = (\overline{S}, \overline{E_1}, \ldots, \overline{E_n}, \overline{T_1}, \ldots, \overline{T_m}, \overline{I}, \overline{R}, \overline{C}) = \left(\frac{\Lambda}{\mu}, 0, 0, \ldots, 0\right)$$

Where, for the given SE^nT^mIRC system 3.4, where initial conditions originate in the positively invariant set Ω_{n+m}, the basic reproductive number is:

$$\mathcal{R}_0 = \frac{\gamma^n \sigma^m}{\kappa_1^n \kappa_2^m} \left(\frac{\beta \kappa_4}{\kappa_2(\kappa_3 \kappa_4 - \nu\alpha)} \right) \tag{3.5}$$

Theorem 3.7.3 *For the given SE^nT^mIRC system 3.4, where initial conditions originate in the positively invariant set Ω_{n+m}, the disease free equilibrium $\mathcal{DFE}$ is globally asymptotically stable (GAS) in Ω_{n+m} whenever $\mathcal{R}_0 < 1$. Similarly, the endemic equilibrium $\mathcal{EE}$ is globally asymptotically stable (GAS) in Ω_{n+m} whenever $\mathcal{R}_0 > 1$.*

3.8 MODEL COMPARISON

This section illustrates the different dynamics present in our various models by comparing and contrasting these systems. Through the use of numerical examples, we will compare how the different system's equilibrium changes in relation to the number of compartments. This section demonstrates that increasing the number of compartments alters the system dynamics by "drawing out" the system, which means the system takes longer to reach equilibrium.

In order to simplify this discussion, this section focuses on how varying the n exposure compartments alters the dynamics of the SE^nTIRC model, as the extension from the SE^nTIRC system 3.3 to the SE^nT^mIRC system 3.4 alters the dynamics in a similar fashion.

3.8.1 *Comparison Between our Different Models*

The most natural question arising from this analysis is, how does varying the number of exposure compartments E_n alter the results and dynamics of our models? As discussed in this section, the amount the dynamics of our different systems alter heavily depends on the γ

and κ_1 parameters.

In order to see this change in dynamics, let us first consider how we could compare SE^nTIRC models with a different number of exposure compartments n. For the system to represent the same epidemiological situation, let us first fix the average time an individual is considered exposed. To demonstrate the differences in dynamics, let us consider two SE^nTIRC models, one model that has only one exposed compartment and the other has an arbitrary n exposed compartments. If the average exposure time of the original exponential distributed parameter (i.e. when $n = 1$) is given by $\frac{1}{\gamma_1}$ and for this to match the average exposure time for the Erlang distributed parameters case ($\frac{n}{\gamma_n}$), the following equivalence must hold:

$$\frac{1}{\gamma_1} = \frac{n}{\gamma_n} \quad \Longrightarrow \quad \gamma_1 = \frac{\gamma_n}{n}$$

Where γ_n corresponds to the equivalent average exposure transition parameter for the SE^nTIRC system 3.3 with n compartments (γ_n). However, if the equivalence in total average exposure time is maintained, this forces the systems to have different $\mathcal{R}_0$ values. Recall the basic reproductive number for the system with n compartment is given by:

$$\mathcal{R}_0 = \frac{\gamma^n}{\kappa_1^n}\left(\frac{\beta\sigma\kappa_4}{\kappa_2(\kappa_3\kappa_4 - \nu\alpha)}\right)$$

Consider, if we force the average exposed time to be the same for any number of compartments and if we assume that basic reproductive numbers of the two system are equivalent then this implies:

$$\mathcal{R}_0^1 = \frac{\gamma_1}{\mu+\tau_1+\gamma_1}\left(\frac{\beta\sigma\kappa_4}{\kappa_2(\kappa_3\kappa_4 - \nu\alpha)}\right) = \mathcal{R}_0^n = \left(\frac{\gamma_n}{\mu+\tau_1+\gamma_n}\right)^n\left(\frac{\beta\sigma\kappa_4}{\kappa_2(\kappa_3\kappa_4 - \nu\alpha)}\right)$$

$$\frac{\gamma_1}{\mu+\tau_1+\gamma_1} = \left(\frac{\gamma_n}{\mu+\tau_1+\gamma_n}\right)^n$$

$$\frac{\gamma_1}{\mu+\tau_1+\gamma_1} = \left(\frac{n\gamma_1}{\mu+\tau_1+n\gamma_1}\right)^n$$

The superscript above the $\mathcal{R}_0$ indicates the number of exposed compartments (i.e. $\mathcal{R}_0^1$ implies that the system has only one exposed compartment).

Clearly, the basic reproductive numbers do not equal each other, as this equality is incorrect. Hence, for the n different systems, if we assume a constant expected exposure time, then the $\mathcal{R}_0$ of each system are different. Therefore, these systems cannot be directly compared due to their different bifurcation points. In the remaining of this section, we shall explore how the system's dynamics change by fixing the expected exposure period and varying the number of compartments n.

3.8.2 *Variation of the Dynamics for the SE^{n}TIRC System*

In this section we demonstrate how increasing the number of exposure compartments alters the underlying system dynamics. This discussion shall focus on two main research questions:

- How does increasing the number of compartments n affect the latency period distribution?
- How does increasing the number of compartments n affect the long term behaviour of solutions for the SE^{n}TIRC system?

Before we can discuss how the SE^{n}TIRC system changes and adapts, we must first explain how increasing compartment numbers affects the following expression $\left(\frac{\gamma}{\kappa_1}\right)$, as we shall see, this is an integral expression for this discussion. Let us begin by examining what the parameter $\left(\frac{\gamma}{\kappa_1}\right)$ represents, by the properties of the exponential distribution, this parameter is the proportion of cattle that progress to the test sensitive compartment T(t) instead of either dying (μ) or being culled (τ_1). However, through a small amount of manipulation, this parameter can be examined from the perspective of latency period length; this perspective better describes these parameters in terms of the underlying biology. Let us define the parameters γ and $\tau_1 + \mu$ in the following forms:

1. $\frac{1}{\gamma}$ is the expected period of time a host will remain in an exposed compartment before progress onto the next compartment.
2. $\frac{1}{\tau_1+\mu}$ is the expected period of time a host can remain in the exposed compartment before being removed from the system (either from natural death μ or from being culled τ_1).

The relative exposed duration proportion, is the average time a host remains in the exposed compartment divided by the average time a host can remain in the exposed compartment before being removed by death (μ) or culling (τ_1). Therefore, this parameter represents the expected portion of a cattle lifetime in which it will remain in the exposed compartment.

$$\left(\frac{\frac{1}{\gamma}}{\frac{1}{\mu+\tau_1}}\right) = \left(\frac{\mu+\tau_1}{\gamma}\right)$$

In the case of the SE^{n}TIRC system, if the parameter value $\left(\frac{\mu+\tau_1}{\gamma}\right)$ is high, this indicates a long exposure period, as it takes a larger percentage of its natural lifespan to progress from the exposure compartment. If we explore our parameter value $\left(\frac{\gamma}{\kappa_1}\right)^n$ for the SE^{n}TIRC system, we shall see this parameter heavily depends on this relative proportion $\frac{\tau_1+\mu}{\gamma}$

$$\left(\frac{\gamma}{\kappa_1}\right)^n = \left(\frac{\gamma}{\mu+\tau_1+\gamma}\right)^n = \left(\frac{1}{1+\frac{\mu+\tau_1}{\gamma}}\right)^n = \left(1-\frac{\frac{\mu+\tau_1}{\gamma}}{1+\frac{\mu+\tau_1}{\gamma}}\right)^n$$

The last equality below is achieved using partial fractions. Clearly, the dynamics of each case heavily depend on theses two parameters; number of compartments n and relative exposed duration proportion $\frac{\mu+\tau_1}{\gamma}$. As demonstrated in figure 3.4, the higher both the relative exposed duration proportion $\frac{\mu+\tau_1}{\gamma}$ and number of compartments n are, the lower the $\left(\frac{\gamma}{\kappa_1}\right)^n$ parameter becomes. For example, if we consider a disease which has a relative exposed duration proportion of 5% and then we vary the number of compartment n, we see that parameter $\frac{\gamma^n}{\kappa_1^n}$ drops from 0.952 if n is equal to one, to 0.6139 is n equals 10.

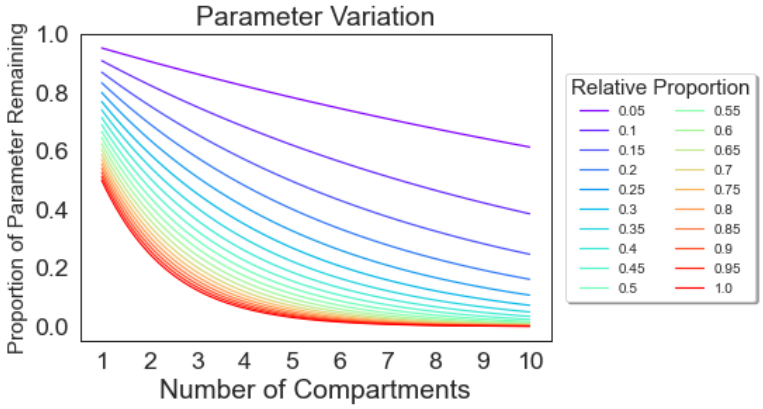

Figure 3.4: The parameter variation of $\left(\frac{\gamma}{\kappa_1}\right)$ as we vary the number of compartments verse the relative percentage of the expected latency period per average host lifespan.

Therefore, the parameter $\left(\frac{\gamma}{\kappa_1}\right)^n$ decreases as the n parameter grows, however, how quickly this decreases depends on how large the relative exposed duration proportion is $(\frac{\mu+\tau_1}{\gamma})$. This means this parameter $\left(\frac{\gamma}{\kappa_1}\right)^n$ is more sensitive to diseases that have a long incubation period. Now that we understand this parameter in greater detail, this permits us to discuss how this parameter changes the system dynamics.

3.8.2.1 *Latency Distribution*

In order to further understand the relationship between system dynamics and number of compartments let us analysis two questions:

- How does increasing the number of compartments n affect the latency period distribution?
- How does increasing the number of compartments n affect the infection levels of the SE^nTIRC system?

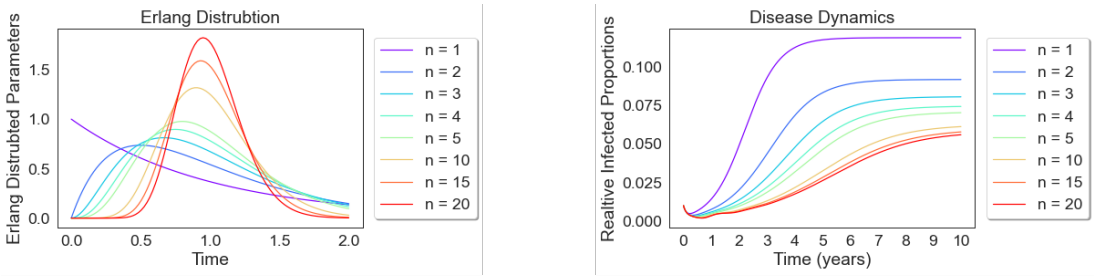

Figure 3.5: The left figure are Erlang distributed variables for varying shape parameter (n). Where each of these different Erlang distributed variables have a constant expected interval waiting time of 1. The right figure represents how the dynamics of the SE^nTIRC system changes as the number of compartment increases.

Firstly, as the left plot of figure demonstrates, as we increase the number of compartments n the exposure distribution becomes increasingly centred around the expected value of the system $\frac{1}{\gamma}$. Incorporating Erlang distribution therefore gives researchers the ability to fit exposure parameters more accurately.

Secondly, how does increasing compartments number n affect the infection levels of the SE^nTIRC system? The figure on the right-hand side demonstrates two changes in dynamics. The figure demonstrates that as the compartment numbers increase, the system takes longer to reach the endemic equilibrium and the corresponding endemic equilibrium level for the infectious compartment diminishes in size.

Let us first examine why the system takes longer to reach the endemic equilibrium. As the left plot of figure demonstrates, as we increase the compartment numbers the system becomes increasingly centred on the expected value. This phenomenon is what induces this delay, as for larger compartment numbers, a relatively smaller number of cattle will progress through the exposure period quickly, meaning relatively more cattle take longer to become test sensitive, extending the time for the system to reach the endemic equilibrium.

Moreover, why does extending compartment numbers correspond to a lower level of infection in the endemic equilibrium? To see the root cause of this effect, let us examine the basic reproductive number and endemic equilibrium:

$$\mathcal{R}_0 = \frac{\gamma^n}{\kappa_1^n}\left(\frac{\beta\sigma\kappa_4}{\kappa_2(\kappa_3\kappa_4 - \nu\alpha)}\right)$$

$$
\begin{aligned}
\mathcal{EE} &= (\overline{S}, \overline{E_1}, \ldots, \overline{E_n}, \overline{T}, \overline{I}, \overline{R}, \overline{C}) \\
\overline{S} &= \frac{\Lambda}{(\overline{\overline{\lambda^{**}}} + \kappa_0)} \\
\overline{E_i} &= \frac{\gamma^{i-1}}{\kappa_1^i} \overline{\lambda^{**}}\ \overline{S} \\
\overline{T} &= \frac{\gamma^n}{\kappa_1^n \kappa_2} \overline{\lambda^{**}}\ \overline{S} \\
\overline{I} &= \left(\frac{\kappa_4 \sigma}{\kappa_4 \kappa_3 - \alpha\nu}\right)\left(\frac{\gamma^n}{\kappa_1^n \kappa_2}\right) \overline{\lambda^{**}}\ \overline{S} \\
\overline{R} &= \left(\frac{\nu\sigma}{\kappa_4 \kappa_3 - \alpha\nu}\right)\left(\frac{\gamma^n}{\kappa_1^n \kappa_2}\right) \overline{\lambda^{**}}\ \overline{S} \\
\overline{C} &= \frac{\tau_1}{\mu}\left(1 + \overline{\overline{\lambda^{**}}} \sum_{i=1}^{n} \frac{\gamma^{i-1}}{\kappa_1^i}\right)\overline{S} + \frac{\tau_2}{\mu}\left(1 + \frac{\sigma(\kappa_4 + \nu)}{\kappa_4 \kappa_3 - \alpha\nu}\right)\left(\frac{\gamma^n}{\kappa_2 \kappa_1^n}\right) \overline{\lambda^{**}}\ \overline{S}
\end{aligned}
$$

The reason for the lower endemic equilibrium infection level is the $\left(\frac{\gamma}{\kappa_1}\right)^n$ expression discussed previously. As can be seen in both the basic reproductive number $\mathcal{R}_0$ and the endemic equilibrium levels for non-susceptible hosts, these properties are both reduced by the $\left(\frac{\gamma}{\kappa_1}\right)^n$ expression. Therefore, the reduction seen in the SE^{n}TIRC model endemic level is similarly controlled by the number of compartments n and relative exposed duration proportion $\frac{\mu+\tau_1}{\gamma}$, as these parameters control the $\left(\frac{\gamma}{\kappa_1}\right)^n$ expression.

The amount the system dynamics change is, therefore, more pronounced when these parameters are high (n and $\frac{\mu+\tau_1}{\gamma}$). What does this mean in terms of the underlying biology? Model dynamics change significantly for diseases with long exposure periods and if their latency distribution is heavily centred around the expected value.

3.8.2.2 *SE^{n}T^{m}IRC model Extension*

In the SE^{n}T^{m}IRC model, the system dynamics are adjusted in a similar fashion. Where, if the total expected latency period is fixed, increasing latency compartments number (n and m) both lowers endemic equilibrium infection levels and this system takes longer to reach the equilibrium. Although the effects are now more pronounced, as now the system is reduced by both $\left(\frac{\gamma}{\kappa_1}\right)^n$ and $\left(\frac{\sigma}{\kappa_2}\right)^m$. Likewise, the $\left(\frac{\sigma}{\kappa_2}\right)^m$ expression is controlled by the number of compartments m and relative test sensitive duration proportion $\frac{\mu+\tau_2}{\sigma}$, as these parameter control the $\left(\frac{\sigma}{\kappa_2}\right)^m$ expression. The reason for this similarly arise from the nature of Erlang distributed parameters, as by extending the SE^{n}TIRC system to the SE^{n}T^{m}IRC system doesn't alter the total latency period distribution, only gives the researcher more control. The reason the total latency period distribution remains the same is that the summation of two independent Erlang distribution variables is itself Erlang[2].

2 This is a commonly used property of the gamma distribution, as Erlang is a special case of the gamma distribution this property applies to the Erlang distribution also.

If $X \sim \text{Erlang}(a_1, b)$ and $Y \sim \text{Erlang}(a_2, b)$ and both X and Y are independent variables then $X + Y \sim \text{Erlang}(a_1 + a_2, b)$.

3.9 CONCLUSION

In this chapter we have examined the latency mechanic of the SE_1E_2TIRC model 3.4. By augmenting this model, we have altered how the system incorporates the latency period distribution, changing it from the exponential distribution to the Erlang distribution, allowing the incorporation of more realistic latency periods. From there we analysed two different extensions of the SE_1E_2TIRC model 3.4, firstly this system was extended to the SE^nTIRC system 3.3 and then to the SE^nT^mIRC system 3.4. Where in both systems, their analysis shows that no matter the number of exposure compartments n or test sensitive compartments m, the long term solution's behaviours are completely determined by the basic reproductive number $\mathcal{R}_0$. Where given initial conditions originating in the positively invariant set Ω_{n+m}, either one of two behaviours occur:

- For $\mathcal{R}_0 < 1$, all solutions within Ω_{n+m} approach the disease free equilibrium ($\mathcal{DFE}$).

- For $\mathcal{R}_0 > 1$, all solutions within $\Omega_{n+m} \setminus \mathcal{DFE}$ approach the unique endemic equilibrium ($\mathcal{EE}$).

However, the basic reproductive number $\mathcal{R}_0$ is reliant on the original parameters and the number of compartments that control how long hosts remain in the latency period (n,m). By varying the number of compartments (n,m) we alter the latency distribution, changing both the basic reproductive number and the system dynamics. This system extension allows modellers to more accurately encapsulate as much biological realism as possible, producing more realistic predictions.

4

CHAPTER 4: BOVINE TUBERCULOSIS AND WILDLIFE RESERVOIRS

In this chapter, the inter-herd dynamics are examined between a single herd adjacent to a self-sustaining badger set. The long term infection dynamics are investigated with a special focus on the system bifurcation type. This model further develops our understanding of bTB's spill-over and spill-back between these two populations.

The model structure is based on the commonly used vector host mathematical epidemiological model with incorporated demographics effects. The focus of our investigation is to understand both the threshold condition and the global system behaviour.

4.1 WILDLIFE RESERVOIR MODEL

This section shall present and describe a wildlife reservoir epidemic model with direct and wildlife transmission, where the dynamics of the herd are loosely based on the SETIRC model. Several simplifying assumptions have had to been assumed to reduce the complexity of this model, therefore the model has the following assumptions:

1. The wildlife population $N_b(t)$ is separated into two distinct compartments $S_b(t)$ and $I_B(t)$ representing the susceptible and infectious badgers respectively.

2. To simplify the associated population dynamics, both populations are consider to be at equilibrium, this means that the analysis is of the asymptotically autonomous system. Where similar to the previous model, the cattle total population $N_h(t)$ is at equilibrium when $N_h(t) = \frac{\Lambda_h}{\mu_h}$. Likewise, the wildlife reservoir population is at equilibrium when $N_b(t) = \frac{\Lambda_b}{\mu_b}$.

3. Susceptible host have two infection channels; direct (cattle to cattle transmission) and indirect (through wildlife infection). Where both the direct and indirect transmission works according to the mass action principle. The rate of transmission between cattle is denoted by β_{hh}, where the subscripts represent infection is host to host. Therefore, direct transmission works according to $\beta_{hh}S_hI_h$. Similarly, the rate of transmission from badger to cattle is given by β_{bh} and as a result the indirect transmission infection force is given by $\beta_{bh}S_hI_b$.

4. The relapse compartment R and culling compartment C of the system has been removed to reduce the inherent complexity of the system. As adding more compartments increases the dimensional size, making the associated system more complex to analyse.

4.2 MATHEMATICAL MODEL FORMULATION

The inter-herd disease dynamics are described using a cattle population compartmental model similar to the SETIRC model. The total cattle population at time t is denoted by $N_h(t)$, where the subscript defines which population we are referring too (h subscript for cattle host population and b subscript for badger population). In this model cattle are separated into the following mutually distinct compartments; Susceptible $S_h(t)$, Exposed $E_h(t)$, Test sensitive $T_h(t)$, or Infected $I_h(t)$. Therefore, the first system constraint is the cattle population dynamics;

$$N_h(t) = S_h(t) + E_h(t) + T_h(t) + I_h(t)$$

Similarly for the badger population, the total badger population at time t is denoted by $N_b(t)$, where the only compartments are Susceptible $S_b(t)$ and Infected $I_b(t)$. Therefore, the second system constraint is the badger population dynamics;

$$N_b(t) = S_b(t) + I_b(t)$$

Let us now examine the associated differential equations for each of the following populations, cattle and badger.

4.2.1 *Construction of the Wildlife Reservoir Differential Equations*

Let us consider the susceptible cattle population, after accounting for newly recruited cattle Λ_h and natural deaths μ_h, the susceptible host population is reduced after susceptible cattle contract the disease. Infections occur from both the wildlife reservoir population and cattle population, these infections occurs according to the mass action principle. The effective transmission rate for cattle to cattle transmissions is given by β_{hh} and similarly, the effective transmission rate for badger population is given by β_{bh}. The rate of change of the susceptible population is therefore modelled by the continuous non-linear differential equation:

$$\frac{dS_h}{dt} = \Lambda_h - \left(\beta_{hh}\frac{I_h}{N_h} + \beta_{bh}\frac{I_b}{N_b}\right)S_h - \mu_h S$$

Cattle that contract the disease progress to the exposed compartments E_h and remain there until the disease progresses to test sensitive compartment (γ_h) or until they die a natural death (μ_h). The γ_h progression parameter is the transition rate between the exposed E_h to the test

sensitive T_h compartment. The differential equation controlling the exposed compartments is given by:

$$\frac{dE_h}{dt} = \left(\beta_{hh}\frac{I_h}{N_h} + \beta_{bh}\frac{I_b}{N_b}\right)S_h - (\mu_h + \gamma_h)E_h$$

The test sensitive population T_h is increased by those cattle progressing from the exposed compartment E_h and the population is reduced by natural deaths μ_h and cattle progressing to the infected stage, which occurs at the rate σ_h.

$$\frac{dT_h}{dt} = \gamma_h E_h - (\mu_h + \sigma_h)T_h$$

As the test sensitive T_h cattle progress into the infected compartment, they enter into the last compartment of this system. The only way hosts are removed from the infected compartment is by dying a natural death occurring at rate μ_h.

$$\frac{dI_h}{dt} = \sigma_h T_h - \mu_h I_h$$

Similarly, for the susceptible badger population, badgers are recruited through births at Λ_b and die natural deaths at rate μ_b. The susceptible badger population is reduced after susceptible badgers contract the disease, although these cattle become infected immediately. The continuous non-linear differential equation controlling the badger population are therefore modelled by:

$$\frac{dS_b}{dt} = \Lambda_b - \beta_{hb}S_b\frac{I_h}{N_h} - \mu_b S_b$$
$$\frac{dI_b}{dt} = \beta_{hb}S_b\frac{I_h}{N_h} - \mu_b I_b$$

Therefore, the following system of non-linear differential equation represent the inter-species dynamics of bovine tuberculosis:

$$\begin{aligned}
\frac{dS_h}{dt} &= \Lambda_h - \left(\beta_{hh}\frac{I_h}{N_h} + \beta_{bh}\frac{I_b}{N_b}\right)S_h - \mu_h S_h \\
\frac{dE_h}{dt} &= \left(\beta_{hh}\frac{I_h}{N_h} + \beta_{bh}\frac{I_b}{N_b}\right)S_h - (\gamma_h + \mu_h)E_h \\
\frac{dT_h}{dt} &= \gamma_h E_h - (\sigma_h + \mu_h)T_h \\
\frac{dI_h}{dt} &= \sigma_h T_h - \mu_h I_h
\end{aligned} \tag{4.1}$$

$$\frac{dS_b}{dt} = \Lambda_b - \beta_{hb}S_b\frac{I_h}{N_h} - \mu_b S_b$$
$$\frac{dI_b}{dt} = \beta_{hb}S_b\frac{I_h}{N_h} - \mu_b I_b$$

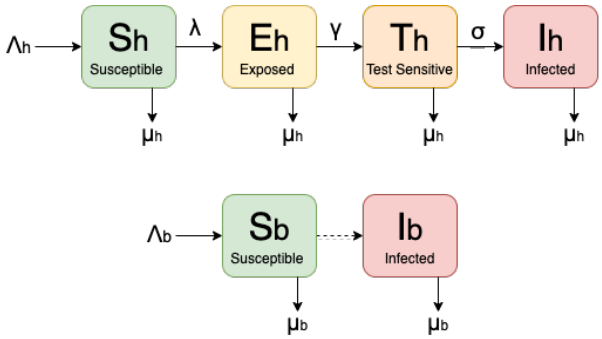

Figure 4.1: Flow chart of the transmission dynamics of the Wildlife Reservoir model.

4.2.2 *Mathematical Model Properties*

Let us begin our analysis by examining the required mathematical properties of the model such as well posed and feasibility region.

Theorem 4.2.1 *All solutions for our wildlife reservoir system (4.1) which have initial conditions originating within* $\mathbb{R}^6_+$ *are bounded.*

$$\mathbb{R}^6_+ = \{N(S_h, E_h, T_h, I_h, S_b, I_b) | S_h \geqslant 0, E_h \geqslant 0, T_h \geqslant 0, I_h \geqslant 0, S_b \geqslant 0, I_b \geqslant 0\}$$

Proof 4.2.1 *Let* $N\big(S_h(t), E_h(t), T_h(t), I_h(t), S_b(t), I_b(t)\big)$ *be an arbitrary solution of the wildlife reservoir system (4.1) with a non-negative initial conditions. The total population of the herd and wildlife reservoir is given by* $N(t) = N_h(t) + N_b(t)$*, where*

$$N_h(t) = S_h(t) + E_h(t) + T_h(t) + I_h(t)$$
$$N_b(t) = S_b(t) + I_b(t)$$

Hence,

$$\frac{dN_h}{dt} = \Lambda_h - \mu_h(S_h + E_h + T_h + I_h) \qquad = \Lambda_h - \mu_h N_h(t)$$
$$\frac{dN_b}{dt} = \Lambda_b - \mu_b(S_b + I_b) \qquad = \Lambda_b - \mu_h N_b(t)$$

By Grönwall's lemma,

$$0 \leqslant N_h\big(S_h(t), E_h(t), T_h(t), I_h(t)\big) \qquad \leqslant \frac{\Lambda_h}{\mu_h}\big(1 - e^{-\mu_h t}\big) + N_h(0)e^{-\mu_h t}$$
$$0 \leqslant N_b\big(S_b(t), I_b(t)\big) \qquad \leqslant \frac{\Lambda_b}{\mu_b}\big(1 - e^{-\mu_b t}\big) + N_b(0)e^{-\mu_b t}$$

Hence,

$$0 \leqslant \limsup_{t\to\infty} N_h(t) \leqslant \frac{\Lambda_h}{\mu_h}$$
$$0 \leqslant \limsup_{t\to\infty} N_b(t) \leqslant \frac{\Lambda_b}{\mu_b}$$

By definition $N(t) = N_h(t) + N_b(t)$*, therefore the total population is also bounded.*

$$0 \leqslant \limsup_{t\to\infty} N(t) \leqslant \frac{\Lambda_h}{\mu_h} + \frac{\Lambda_b}{\mu_b}$$

Therefore all solutions of the system 4.1 that originate in $\mathbb{R}^6_+$ *are attracted to the following positive invariant region,*

$$\Omega = \left\{ N(S_h, E_h, T_h, I_h, S_b, I_b) \in \mathbb{R}^6_+ : N(t) \leqslant \frac{\Lambda_h}{\mu_h} + \frac{\Lambda_b}{\mu_b} \right\} \tag{4.2}$$

The wildlife reservoir system (4.1) is therefore bounded. Additionally, since $\limsup_{t\to\infty} N(t)$ *is independent of the initial conditions then the system is said to be uniformly bounded.*

As all solutions beginning in our positive invariant region Ω are trapped there, the analysis will therefore be restricted to this region. Now that we have shown that solutions are bounded the next stage is to show that the wildlife reservoir model solutions are well posed (i.e. exist and are unique depending on initial conditions).

Theorem 4.2.2 *The wildlife host system (4.1) is well posed.*

Proof 4.2.2 *Similarly to previous proofs, the Lipschitz continuity condition permits the use of the Picard Lindelöf theorem which implies the system is well posed. The right hand side of the wildlife reservoir system 4.1 are continuously differentiable functions on*

$$\mathbb{R}^6_+ = \{N(S_h, E_h, T_h, I_h, S_b, I_b) | S_h \geqslant 0, E_h \geqslant 0, T_h \geqslant 0, I_h \geqslant 0, S_b \geqslant 0, I_b \geqslant 0\}$$

and as the above theorem indicates that the first derivative of our system is uniformly bounded. This condition implies that the system equation are Lipschitz continuous and with this condition, we can apply the Picard Lindelöf theorem that proves a unique solution exists for the wildlife reservoir system 4.1.

The following positive invariant region Ω bounds the wildlife reservoir system (4.1) solutions and our future analysis will be restricted to this domain.

4.2.2.1 *Disease Free Equilibrium's and it's Stability*

Theorem 4.2.3 *For the given wildlife host system (4.1), where initial conditions originate in the positively invariant set* Ω*, the disease free equilibrium* $\mathcal{DFE}$ *is locally asymptotically stable (LAS) in* Ω *whenever* $\mathcal{R}_0 < 1$*. Where* $\mathcal{R}_0$ *is defined as follows:*

$$\mathcal{R}_0 = \frac{\gamma_h \sigma_h}{\kappa_1 \kappa_2} \left(\frac{\beta_{bh}\beta_{hb}}{\mu_h \mu_b} + \frac{\beta_{hh}}{\mu_h} \right)$$

Where the following two parameter expression κ_1 *and* κ_2 *are defined as follows*

$$\kappa_1 = \gamma_h + \mu_h \qquad \kappa_2 = \sigma_h + \mu_h$$

Proof 4.2.3 *The local asymptotically stability of the disease free equilibrium can be examined through analysing the linearised system around the disease free equilibrium ($\mathcal{DFE}$). The Jacobian of our wildlife host system (4.1) is given below:*

$$J(\mathcal{DFE}) = \begin{pmatrix} -\mu_h & 0 & 0 & -\beta_{hh} & 0 & -\beta_{bh} \\ 0 & -\kappa_1 & 0 & \beta_{hh} & 0 & \beta_{bh} \\ 0 & \gamma_h & -\kappa_2 & 0 & 0 & 0 \\ 0 & 0 & \sigma_h & -\mu_h & 0 & 0 \\ 0 & 0 & 0 & -\beta_{hb} & -\mu_b & 0 \\ 0 & 0 & 0 & \beta_{hb} & 0 & -\mu_b \end{pmatrix}$$

Recall, at the disease free equilibrium the entire population is completely comprised of susceptible hosts, therefore, $\frac{S_h}{N_h} = 1$ and $\frac{S_b}{N_b} = 1$.

The associated characteristic equation for the the Jacobian $J(\mathcal{DFE})$ is

$$(\lambda+\mu_h)(\lambda+\mu_b)\Big((\lambda+\kappa_1)(\lambda+\kappa_2)(\lambda+\mu_h)(\lambda+\mu_b) - \beta_{hh}\gamma_h\sigma_h(\lambda+\mu_b) - \gamma_h\sigma_h\beta_{hb}\beta_{bh}\Big) = 0$$

For the disease free equilibrium $\mathcal{DFE}$ to be locally stable asymptotically, all corresponding eigenvalues of the Jacobian must have negative real part. Clearly, two eigenvalues for the system are $\lambda_1 = -\mu_h$ and $\lambda_2 = -\mu_b$, using the Routh-Hurwitz condition, it can be shown the other four eigenvalues are negative. The other four eigenvalues correspond to the four roots of the following function $f(\lambda)$:

$$f(\lambda) = (\lambda+\kappa_1)(\lambda+\kappa_2)(\lambda+\mu_h)(\lambda+\mu_b) - \gamma_h\sigma_h(\beta_{bh}\beta_{hb} + \beta_{hh}(\lambda+\mu_b))$$

After expanding the brackets the following coefficients are made evident,

$$f(\lambda) = \lambda^4 + a_1\lambda^3 + a_2\lambda^2 + a_3\lambda + a_4$$

Where the coefficients are defined as follows:

$$a1 = \kappa_1 + \kappa_2 + \mu_h + \mu_b$$
$$a2 = \kappa_1(\kappa_2 + \mu_h + \mu_b) + \kappa_2(\mu_h + \mu_b) + \mu_h\mu_b$$
$$a3 = -\beta_{hh}\sigma_h\gamma_h + \kappa_1\kappa_2(\mu_h + \mu_b) + \mu_h\mu_b(\kappa_1 + \kappa_2)$$
$$a4 = \kappa_1\kappa_2\mu_b\mu_h - \beta_{bh}\beta_{hb}\sigma_h\gamma_h - \mu_b\beta_{hh}\sigma_h\gamma_h$$

After some manipulation of a_4, we can obtain the tipping point of the system:

$$a4 = \kappa_1\kappa_2\mu_b\mu_h\left(1 - \frac{\sigma_h\gamma_h}{\kappa_1\kappa_2}\left(\frac{\beta_{bh}\beta_{hb}}{\mu_h\mu_b} + \frac{\beta_{hh}}{\mu_h}\right)\right) = \kappa_1\kappa_2\mu_b\mu_h(1-\mathcal{R}_0)$$

Therefore, the basic reproductive number is given by:

$$\mathcal{R}_0 = \frac{\sigma_h\gamma_h}{\kappa_1\kappa_2}\left(\frac{\beta_{bh}\beta_{hb}}{\mu_h\mu_b} + \frac{\beta_{hh}}{\mu_h}\right)$$

The Routh-Hurwitz condition implies the disease free equilibrium is locally asymptotically stable if:

1. *All coefficients* a_i *for* $i = 1, 2, 3, 4$ *are positive* $a_i > 0$.

2. $a_1 a_2 - a_3 > 0$

3. $a_3(a_1 a_2 - a_3) - a_1^2 a_4 > 0$

If the basic reproductive number is less than unity ($\mathcal{R}_0 < 1$) *then clearly* a_1, a_2, *and* a_4 *are positive. Notice that* a_3 *can be manipulated into the following form:*

$$a_3 = \mu_b(\kappa_1\kappa_2) + \mu_h\mu_b(\kappa_1 + \kappa_2) + (\kappa_1\kappa_2\mu_h - \beta_{hh}\sigma_h\gamma_h)$$

Where if the basic reproductive number is less than unity, then the following inequality holds:

$$\mathcal{R}_0 < 1 \implies \frac{\sigma_h\gamma_h}{\kappa_1\kappa_2}\left(\frac{\beta_{bh}\beta_{hb}}{\mu_h\mu_b} + \frac{\beta_{hh}}{\mu_h}\right) < 1 \implies \frac{\sigma_h\gamma_h}{\kappa_1\kappa_2}\left(\frac{\beta_{hh}}{\mu_h}\right) < 1 \implies \kappa_1\kappa_2\mu_h > \beta_{hh}\sigma_h\gamma_h$$

By showing that $a_3 > 0$ *if* $\mathcal{R}_0 < 1$ *this shows that all coefficient's of our characteristic equation* a_i *for* $i = 1, 2, 3, 4$ *are all positive* $a_i > 0$.

The next condition that must be proven is $a_1 a_2 - a_3 > 0$. *Notice, that as* a_3 *can be arranged into the following form* $a_3 = \kappa_1\kappa_2 + (\kappa_1 + \kappa_2)(\mu_h + \mu_b) + \mu_h\mu_b - \beta_{hh}\sigma_h\gamma_h$, *and by expanding when* a_3 *is in this form we obtain:*

$$\begin{aligned} a_1 a_2 - a_3 = {} & a_1 a_2 - && -a_3 \\ & \kappa_1\kappa_2(\kappa_1 + \kappa_2 + \mu_h + \mu_b) && -\kappa_1\kappa_2(\mu_h + \mu_b) \\ & + (\kappa_1 + \kappa_2)(\mu_h + \mu_b)(\kappa_1 + \kappa_2 + \mu_h + \mu_b) && \\ & + \mu_h\mu_b(\kappa_1 + \kappa_2 + \mu_h + \mu_b) && -\mu_h\mu_b(\kappa_1 + \kappa_2) \\ & && +\beta_{hh}\sigma_h\gamma_h \end{aligned}$$

Hence, the non-negative restriction of parameters implies that $a_1 a_2 - a_3 > 0$ *is clearly positive as demonstrated below:*

$$a_1 a_2 - a_3 = \kappa_1\kappa_2(\kappa_1 + \kappa_2) + (\kappa_1 + \kappa_2)(\mu_h + \mu_b)(\kappa_1 + \kappa_2 + \mu_h + \mu_b) + \mu_h\mu_b(\mu_h + \mu_b) + \beta_{hh}\sigma_h\gamma_h > 0$$

The last condition that must be shown is $a_3(a_1 a_2 - a_3) - a_1^2 a_4 > 0$. *In order to show this condition* $a_3(a_1 a_2 - a_3) - a_1^2 a_4 > 0$, *we will focus on only one segment of* $a_3(a_1 a_2 - a_3)$ *and show that this is greater than* $a_1^2 a_4$. *Let us first examine only part of the expression* $a_3(a_1 a_2 - a_3)$, *namely let us examine* $a_3((\kappa_1 + \kappa_2)(\mu_h + \mu_b)(\kappa_1 + \kappa_2 + \mu_h + \mu_b))$.

$$\begin{aligned} (\kappa_1 + \kappa_2)(\mu_h + \mu_b)a_1 a_3 = {} & (\kappa_{12}\mu_h - \beta_{hh}\sigma_h\gamma_h)(\kappa_1 + \kappa_2)(\mu_h + \mu_b)a_1 \\ & + \kappa_1\kappa_2\mu_b(\kappa_1 + \kappa_2)(\mu_h + \mu_b)a_1 \\ & + \mu_h\mu_b(\kappa_1 + \kappa_2)^2(\mu_h + \mu_b)a_1 \end{aligned}$$

Where if we examined the following term $\kappa_1\kappa_2\mu_b(\kappa_1+\kappa_2)(\mu_h+\mu_b)a_1$ *we obtain the following:*

$$\kappa_1\kappa_2\mu_b(\kappa_1+\kappa_2)(\mu_h+\mu_b)a_1 = \kappa_1\kappa_2\mu_h\mu_b(\kappa_1+\kappa_2)a_1 + \kappa_1\kappa_2\mu_b^2(\kappa_1+\kappa_2)a_1$$

Similarly, if we examined the following term $\mu_h\mu_b(\kappa_1+\kappa_2)^2(\mu_h+\mu_b)a_1$ *we obtain the following by expanding* $(\kappa_1+\kappa_2)^2$*:*

$$\mu_h\mu_b(\kappa_1+\kappa_2)^2(\mu_h+\mu_b)a_1 = \kappa_1\kappa_2\mu_h\mu_b(\mu_h+\mu_b)a_1 + \mu_h\mu_b(\kappa_1^2+\kappa_2^2+\kappa_1\kappa_2)(\mu_h+\mu_b)a_1$$

Therefore, let us now sum both these expressions, $G = \kappa_1\kappa_2\mu_b(\kappa_1+\kappa_2)(\mu_h+\mu_b)a_1 + \mu_h\mu_b(\kappa_1+\kappa_2)^2(\mu_h+\mu_b)a_1$*, we obtain the following expressions for G:*

$$\begin{aligned}
G &= \kappa_1\kappa_2\mu_h\mu_b(\kappa_1+\kappa_2)a_1 + \kappa_1\kappa_2\mu_h\mu_b(\mu_h+\mu_b)a_1 \\
&\quad + \kappa_1\kappa_2\mu_b^2(\kappa_1+\kappa_2)a_1 + (\kappa_1^2+\kappa_2^2+\kappa_1\kappa_2)\mu_h\mu_b(\mu_h+\mu_b)a_1 \\
G &= \kappa_1\kappa_2\mu_h\mu_b a_1^2 + \kappa_1\kappa_2\mu_b^2(\kappa_1+\kappa_2)a_1 + (\kappa_1^2+\kappa_2^2+\kappa_1\kappa_2)\mu_h\mu_b(\mu_h+\mu_b)a_1
\end{aligned}$$

Therefore, by subbing this expression back in we obtain the following expression for $a_3(a_1a_2-a_3)$*:*

$$\begin{aligned}
a_3(a_1a_2-a_3) = a_3(&\kappa_1\kappa_2(\kappa_1+\kappa_2)+\mu_h\mu_b(\mu_h+\mu_b)+\beta_h h\gamma_h\sigma_h) \\
&+ (\kappa_1\kappa_2\mu_h-\beta_{hh}\gamma_h\sigma_h)(\kappa_1+\kappa_2)(\mu_h+\mu_b)a_1 \\
&+ \kappa_1\kappa_2\mu_b^2(\kappa_1+\kappa_2)a_1 + (\kappa_1^2+\kappa_2^2+\kappa_1\kappa_2)\mu_h\mu_b(\mu_h+\mu_b)a_1 \\
&+ \kappa_1\kappa_2\mu_h\mu_b a_1^2
\end{aligned}$$

Where clearly our last term of the expression for $a_3(a_1a_2-a_3)$*, namely* $\kappa_1\kappa_2\mu_h\mu_b a_1^2$ *is larger than* $a_1^2a_4$ *as:*

$$\begin{aligned}
\kappa_1\kappa_2\mu_h\mu_b a_1^2 - a_1^2a_4 &= \kappa_1\kappa_2\mu_h\mu_b a_1^2(1-(1-\mathcal{R}_0)) \\
&= \kappa_1\kappa_2\mu_h\mu_b a_1^2\mathcal{R}_0
\end{aligned}$$

Therefore, the expression for $a_3(a_1a_2-a_3)-a_1^2a_4$ *is as follows:*

$$\begin{aligned}
a_3(a_1a_2-a_3)-a_1^2a_4 = a_3(&\kappa_1\kappa_2(\kappa_1+\kappa_2)+\mu_h\mu_b(\mu_h+\mu_b)+\beta_h h\gamma_h\sigma_h) \\
&+ (\kappa_1\kappa_2\mu_h-\beta_{hh}\gamma_h\sigma_h)(\kappa_1+\kappa_2)(\mu_h+\mu_b)a_1 \\
&+ \kappa_1\kappa_2\mu_b^2(\kappa_1+\kappa_2)a_1 + (\kappa_1^2+\kappa_2^2+\kappa_1\kappa_2)\mu_h\mu_b(\mu_h+\mu_b)a_1 \\
&+ \kappa_1\kappa_2\mu_h\mu_b a_1^2\mathcal{R}_0
\end{aligned}$$

From above it has been shown that $\mathcal{R}_0 < 1$ *implies* $\kappa_1\kappa_2\mu_h > \beta_{hh}\gamma_h\sigma_h$*. This implies that the above expression for* $a_3(a_1a_2-a_3)-a_1^2a_4$ *is positive, proving last condition required by the Routh-Hurwitz condition. Therefore, the disease free equilibrium* $\mathcal{DFE}$ *is locally asymptotically stable (LAS) in* Ω *whenever* $\mathcal{R}_0 < 1$*.*

4.2.3 *Backward Bifurcation*

The wildlife host system (4.1) is different compared to the previous system discussed, as under certain parameter values there exist multiple endemic equilibria, indicating this system undergoes a backward bifurcation. In order to obtain the exact endemic equilibrium, the wildlife reservoir system (4.1) must first be solved in terms of a single variable (e.g. I_h). Through inserting these variable expression back into our system equations we obtain a quadratic equation, the roots of this quadratic represent the explicit endemic equilibria in terms of system parameters.

The endemic equilibrium ($\mathcal{EE}$) represents disease being maintained in the system at a particular endemic level and for the wildlife host system (4.1) it is given by:

$$\begin{aligned}
\mathcal{EE} &= (\overline{S_h}, \overline{E_h}, \overline{T_h}, \overline{I_h}, \overline{S_b}, \overline{I_b}) \\
\overline{S_h} &= \frac{\Lambda_h}{\overline{\lambda^{**}}_h + \mu_h} \\
\overline{E_h} &= \frac{\kappa_2}{\gamma_h}\overline{T_h} = \frac{\kappa_2\mu_h}{\gamma_h\sigma_h}\overline{I_h} \\
\overline{T_h} &= \frac{\mu_h}{\sigma_h}\overline{I_h} \\
\overline{S_b} &= \frac{N_h\Lambda_b}{\beta_{hb}\overline{I_h} + N_h\mu_b} \\
\overline{I_b} &= \left(\frac{\beta_{hb}N_b\overline{I_h}}{\beta_{hb}\overline{I_h} + N_h\mu_b}\right)
\end{aligned} \tag{4.3}$$

Where we define the force of infection for the host population as:

$$\overline{\lambda^{**}}_h = \beta_{hh}\frac{\bar{I}_h}{N_h} + \beta_{bh}\frac{\bar{I}_b}{N_b}$$

Moreover, recall the following parameter κ_1 and κ_2 are defined as:

$$\kappa_1 = (\gamma_h + \mu_h) \qquad\qquad \kappa_2 = (\sigma_h + \mu_h)$$

Through substituting our expressions for $\overline{E}_h$ into the exposed compartments differential equation at equilibrium (i.e. $\frac{dE_h}{dt} = 0$) we obtain the following relationship:

$$\overline{\lambda^{**}}_h\overline{S}_h = \kappa_1\overline{E}_h = \frac{\kappa_1\kappa_2\mu_h}{\gamma_h\sigma_h}\overline{I_h}$$

Through rearranging and inserting our equilibrium expressions, we obtain the following:

$$\overline{S_h} = \frac{\kappa_1\kappa_2}{\gamma_h\sigma_h}\left(\frac{\Lambda_h(\beta_{hb}\overline{I_h} + \mu_b N_h)}{\beta_{hh}(\beta_{hb}\overline{I_h} + \mu_b N_h) + \beta_{bh}\beta_{hb}N_h}\right)$$

4.2.3.1 *The Backward Bifurcation Quadratic Equation*

Now that we have obtained the endemic equilibrium expression for all variables in terms of a I_h, we must substitute these variable expression back into our system equations to obtain our

quadratic equation $f(\bar{I}_h)$. The roots of this quadratic represent the explicit endemic equilibria for the system.

Let us first start by considering the susceptible hosts at the endemic equilibrium (i.e. $\dot{S_h} = 0$):

$$\dot{S_h} = 0 = \Lambda_h - \beta_{hh}\bar{S}_h\frac{\bar{I}_h}{N_h} - \beta_{bh}\bar{S}_h\frac{\bar{I}_h}{N_b} - \mu_h\bar{S}_h$$

Let us define the numerator (i_h) and denominator (j_h) of the susceptible host population at equilibrium (i.e. $\bar{S}_h = \frac{i_h}{j_h}$) by the parameter i_h and j_h.

Where i_h and j_h both are defined as follows:

$$i_h = \kappa_1\kappa_2\Lambda_h(\beta_{hb}\bar{I}_h + \mu_b N_h)$$
$$j_h = \gamma_h\sigma_h\beta_{hh}(\beta_{hb}\overline{I_h} + \mu_b N_h) + \gamma_h\sigma_h\beta_{bh}\beta_{hb}N_h$$

Now let us define our quadratic $f(\bar{I}_h)$, we construct this quadratic by multiplying the susceptible host population at the endemic equilibrium by $-j_h$:

$$f(\bar{I}_h) = 0 = -\Lambda_h j_h + \beta_{hh}i_h\bar{I}_h - \beta_{bh}i_h\bar{I}_h - \mu_h i_h$$

where by substituting in our expression for i_h and j_h into the above quadratic $f(\bar{I}_h)$, we obtain the following expressions:

$$-\Lambda_h j_h = -\Lambda_h\gamma_h\sigma_h\beta_{hh}\beta_{hb}\overline{I_h} - \Lambda_h N_h\gamma_h\sigma_h(\mu_b\beta_{hh} + \beta_{bh}\beta_{hb})$$
$$\frac{\beta_{hh}}{N_h}i_h\bar{I}_h = \kappa_1\kappa_2\mu_h\beta_{hh}\beta_{hb}\bar{I}_h^2 + \kappa_1\kappa_2\mu_b\beta_{hh}\Lambda_h\bar{I}_h$$
$$\frac{\beta_{bh}}{N_b}i_h\bar{I}_b = \kappa_1\kappa_2\beta_{bh}\beta_{hb}\Lambda_h\bar{I}_h$$
$$\mu_h i_h = \kappa_1\kappa_2\Lambda_h\mu_h(\beta_{hb}\bar{I}_h + \mu_b N_h)$$

By substituting these variable expressions back into $f(\bar{I}_h)$, we obtain the following quadratic function:

$$f(I_h) = aI_h^2 + bI_h + c$$

where the coefficient of our quadratic are given by:

$$a = \beta_{hh}\beta_{hb}\kappa_1\kappa_2\mu_h$$
$$b = -\Lambda_h\gamma_h\sigma_h\beta_{hh}\beta_{hb} + \kappa_1\kappa_2\mu_b\beta_{hh}\Lambda_h + \kappa_1\kappa_2\beta_{bh}\beta_{hb}\Lambda_h + \kappa_1\kappa_2\Lambda_h\mu_h\beta_{hb}$$
$$c = \kappa_1\kappa_2\mu_h\mu_b\Lambda_h N_h - \Lambda_h N_h\gamma_h\sigma_h(\mu_b\beta_{hh} + \beta_{bh}\beta_{hb})$$

After some manipulation it can be shown that the coefficient c can be also be written as:

$$c = \kappa_1\kappa_2\mu_h\mu_b\Lambda_h N_h\left(1 - \frac{\sigma_h\gamma_h}{\kappa_1\kappa_2}\left(\frac{\beta_{bh}\beta_{hb}}{\mu_h\mu_b} + \frac{\beta_{hh}}{\mu_h}\right)\right) = \kappa_1\kappa_2\mu_b\Lambda_h^2\left(1 - \mathcal{R}_0\right) \tag{4.4}$$

As there exist two roots of a quadratic equation, there may exist two corresponding endemic equilibrium points. However, the existence of these equilibrium points in our feasibility region depends on the sign of these equilibrium points, which depends on the quadratic equation's coefficients a, b, c. There can exist a maximum of two endemic equilibrium points corresponding to the two roots of this quadratic:

$$I_1 = \frac{-b - \sqrt{b^2 - 4ac}}{2a}, \qquad I_2 = \frac{-b + \sqrt{b^2 - 4ac}}{2a}$$

Theorem 4.2.4 *The wildlife reservoir system (4.1) has the following equilibrium in our feasibility region Ω:*

1. *There exist a singular unique endemic equilibrium if the quadratic coefficients c is negative which occurs if and only if $\mathcal{R}_0 > 1$.*
2. *There exist a singular unique endemic equilibrium if the quadratic coefficients b is negative and either the discriminant or c is zero (either $b^2 - 4ac = 0$ or $c = 0$).*
3. *Two endemic equilibrium exist if $b < 0$, $b^2 - 4ac > 0$, and $c > 0$*
4. *Under all other conditions, no endemic equilibrium exist.*

In our wildlife reservoir system (4.1) a is always positive and c signs depends explicitly on $\mathcal{R}_0$. In case 1, there exist a singular unique positive endemic equilibrium if the quadratic coefficients c is negative, as equation 4.4 shows, this only occurs if and only if $\mathcal{R}_0 > 1$. In case 1, the two roots of the quadratic function have the following form if $c < 0$:

$$I_1 = \frac{-b - \sqrt{b^2 + 4ac}}{2a}, \qquad I_2 = \frac{-b + \sqrt{b^2 + 4ac}}{2a}$$

Where our second root I_2 is the only positive endemic as $\sqrt{b^2 + 4ac} > b$, the other root is negative and therefore outside our feasibility region Ω. Therefore, if $\mathcal{R}_0 > 1$ there only exist one singular biologically feasible endemic equilibrium.

In case 2 where $b < 0$ and either $c = 0$, or $b^2 - 4ac = 0$, this implies that there exist one positive root described below.

$$I = \begin{cases} \frac{-b}{a} & \text{if } c = 0 \text{ and } b < 0 \\ \frac{-b}{2a} & \text{if } b^2 - 4ac = 0 \text{ and } b < 0 \end{cases}$$

In case 3, there exist two positive roots I_1 and I_2 if $b < 0$, $b^2 - 4ac > 0$, and $c > 0$ ($\mathcal{R}_0 < 1$). Consider the numerator of both our roots I_1 and I_2, clearly both roots are both positive, as under these conditions $b > \sqrt{b^2 - 4ac}$ therefore $-b \pm \sqrt{b^2 - 4ac} > 0$ for both the roots I_1

and I_2. Under this condition it is clear that there exists two unique endemic equilibrium in Ω.

In the other cases, such as $c > 0$ and either $b \geqslant 0$ or $b^2 - 4ac < 0$ there are no positive roots for the quadratic and therefore there exist no endemic equilibrium.

4.2.4 *Feasibility of backward bifurcation*

As discussed through out the literature review section 2.3.4, backward bifurcation occur in many epidemiological system, albeit, often at extreme parameter values that are outside realistic ranges. Let us consider the conditions which are required for a backward bifurcations in this wildlife reservoir system to occur.

For there to exist two endemic equilibria the following conditions must hold $b < 0$, $b^2 - 4ac$, and $c > 0$. From the condition $c > 0$ to be true, our basic reproductive number must be less than unity.

$$\mathcal{R}_0 = \frac{\gamma_h \sigma_h}{\kappa_1 \kappa_2}\left(\frac{\beta_{bh}\beta_{hb}}{\mu_h \mu_b} + \frac{\beta_{hh}\mu_b}{\mu_h}\right) < 1$$

However as we shall demonstrate below, if $c > 0$ this implies that $b > 0$, proving that for the wildlife reservoir system there exists at most one endemic equilibrium. Let us begin by examining b:

$$b = \Lambda_h\Big(\kappa_1\kappa_2(\beta_{hh}\mu_b + \beta_{hb}\mu_h + \beta_{hb}\beta_{bh}) - \gamma_h\sigma_h\beta_{hh}\beta_{hb}\Big)$$

Where after some manipulation, b takes on the following form:

$$\begin{aligned}
b &= \Lambda_h\Big(\kappa_1\kappa_2(\beta_{hh}\mu_b + \beta_{hb}\mu_h + \beta_{hb}\beta_{bh}) - \gamma_h\sigma_h\beta_{hh}\beta_{hb}\Big) \\
b &= \Lambda_h\Big(\kappa_1\kappa_2(\beta_{hh}\mu_b + \beta_{hb}\beta_{bh}) + \kappa_1\kappa_2\beta_{hb}\mu_h - \gamma_h\sigma_h\beta_{hh}\beta_{hb}\Big) \\
b &= \Lambda_h\Big(\kappa_1\kappa_2(\beta_{hh}\mu_b + \beta_{hb}\beta_{bh}) + \kappa_1\kappa_2\beta_{hb}\mu_h\Big(1 - \frac{\gamma_h\sigma_h}{\mu_h\mu_b}\Big(\frac{\beta_{hh}}{\mu_h}\Big)\Big)\Big)
\end{aligned}$$

Now, by our condition $c > 0$ this implies that $\mathcal{R}_0 < 1$, although this implies the following:

$$\begin{aligned}
\mathcal{R}_0 < 1 \quad \Longrightarrow \qquad & \frac{\gamma_h\sigma_h}{\kappa_1\kappa_2}\left(\frac{\beta_{bh}\beta_{hb}}{\mu_h\mu_b} + \frac{\beta_{hh}}{\mu_h}\right) < 1 \\
& \frac{\gamma_h\sigma_h}{\kappa_1\kappa_2}\left(\frac{\beta_{hh}}{\mu_h}\right) < 1
\end{aligned}$$

Hence, if we consider this inequality in relation to our expression for b we see that if $c > 0$ ($\mathcal{R}_0 < 1$) this implies $b > 0$:

$$b = \Lambda_h\Big(\kappa_1\kappa_2(\beta_{hh}\mu_b + \beta_{hb}\beta_{bh}) + \kappa_1\kappa_2\beta_{hb}\mu_h\Big(1 - \frac{\gamma_h\sigma_h}{\mu_h\mu_b}\Big(\frac{\beta_{hh}}{\mu_h}\Big)\Big)\Big) > 0$$

As we have shown just demonstrated, the wildlife reservoir system can have at most one endemic equilibrium point, as the condition required for two endemic equilibrium points is impossible. Moreover, in the next section through analysing the global stability of the disease free equilibrium $\mathcal{DFE}$, we will in fact show that the system does not backward bifurcate in our feasibility region Ω. As the disease free equilibrium $\mathcal{DFE}$ is globally asymptotically stable in our feasibility region Ω.

4.3 GLOBAL STABILITY ANALYSIS

Theorem 4.3.1 *For the given wildlife reservoir system (4.1), where initial conditions originate in the positively invariant set Ω, the disease free equilibrium $\mathcal{DFE}$ is globally asymptotically stable (GAS) in Ω whenever $\mathcal{R}_0 < 1$.*

Proof 4.3.1 *The following Lyapunov function establishes this global stable nature of the $\mathcal{DFE}$ given that $\mathcal{R}_0$*

$$\begin{aligned}\mathcal{F}(t) = {} & \frac{\gamma_h}{\kappa_1}\left(S_h - \overline{S_h} - \overline{S_h}\ln\frac{S_h}{\overline{S_h}}\right) + \frac{\gamma_h}{\kappa_1}E_h + T_h + \frac{\kappa_2}{\sigma_h}I_h \\ & + \left(\frac{\gamma_h\beta_{bh}}{\kappa_1\mu_b}\right)\left(\frac{N_h}{N_b}\right)\left(S_b - \overline{S_b} - \overline{S_b}\ln\frac{S_b}{\overline{S_b}}\right) + \left(\frac{\gamma_h\beta_{bh}}{\kappa_1\mu_b}\right)\left(\frac{N_h}{N_b}\right)I_b\end{aligned}$$

Let us begin by taking the time derivative of our Lyapunov function.

$$\mathcal{F}(t) = \frac{\gamma_h}{\kappa_1}\left(\frac{S_h - \overline{S_h}}{S_h}\right)\dot{S}_h + \frac{\gamma_h}{\kappa_1}\dot{E}_h + \dot{T}_h + \frac{\kappa_2}{\sigma_h}\dot{I}_h + \left(\frac{\gamma_h\beta_{bh}}{\kappa_1\mu_b}\right)\left(\frac{N_h}{N_b}\right)\left(\frac{S_b - \overline{S_b}}{S_b}\right)\dot{S}_b + \left(\frac{\gamma_h\beta_{bh}}{\kappa_1\mu_b}\right)\left(\frac{N_h}{N_b}\right)\dot{I}_b$$

Let us now expand the Lyapunov function:

$$\begin{aligned}\dot{\mathcal{F}}(t) = {} & \frac{\gamma_h}{\kappa_1}\left(\frac{S_h - \overline{S}_h}{S_h}\right)\left(\Lambda_h - \mu_h S_h - \left(\frac{\beta_{hh}I_hS_h}{N_h} + \frac{\beta_{bh}I_bS_h}{N_b}\right)\right) \\ & + \frac{\gamma_h}{\kappa_1}\left(\frac{\beta_{hh}I_hS_h}{N_h} + \frac{\beta_{bh}I_bS_h}{N_b} - \kappa_1 E_h\right) \\ & + \left(\gamma_h E_h - \kappa_2 T_h\right) \\ & + \frac{\kappa_2}{\sigma_h}\left(\sigma_h T_h - \mu_h I_h\right) \\ & + \frac{\gamma_h\beta_{bh}}{\kappa_1\mu_b}\left(\frac{N_h}{N_b}\right)\left(\frac{S_b - \overline{S}_b}{S_b}\right)\left(\Lambda_b - \mu_b S_b - \left(\frac{\beta_{hb}I_hS_b}{N_h}\right)\right) \\ & + \frac{\gamma_h\beta_{bh}}{\kappa_1\mu_b}\left(\frac{N_h}{N_b}\right)\left(\beta_{hb}S_b\frac{I_h}{N_h} - \mu_b I_b\right)\end{aligned}$$

If we use the following equalities $\overline{S_h} = \frac{\Lambda_h}{\mu_h}$ and $\overline{S_b} = \frac{\Lambda_b}{\mu_b}$ and substitute them in for Λ_h and Λ_b then we achieve the following equivalent expressions:

$$\begin{aligned}\frac{\gamma_h}{\kappa_1}\left(\frac{S_h - \overline{S}_h}{S_h}\right)\left(\Lambda_h - \mu_h S_h\right) &= \frac{\gamma_h}{\kappa_1}\left(\frac{S_h - \overline{S}_h}{S_h}\right)\left(\mu_h\overline{S}_h - \mu_h S_h\right) \\ &= -\mu_h\frac{\gamma_h}{\kappa_1}\left(\frac{(S_h - \overline{S}_h)^2}{S_h}\right)\end{aligned}$$

Similarly, for the badger population:

$$\frac{\gamma_h\beta_{bh}}{\kappa_1\mu_b}\left(\frac{N_h}{N_b}\right)\left(\frac{S_b-\overline{S}_b}{S_b}\right)\left(\Lambda_b-\mu_b S_b\right)=\frac{\gamma_h\beta_{bh}}{\kappa_1\mu_b}\left(\frac{N_h}{N_b}\right)\left(\frac{S_b-\overline{S}_b}{S_b}\right)\left(\mu_b\overline{S}_b-\mu_b S_b\right)$$
$$=-\mu_b\frac{\gamma_h\beta_{bh}}{\kappa_1\mu_b}\left(\frac{N_h}{N_b}\right)\left(\frac{(S_b-\overline{S}_b)^2}{S_b}\right)$$

Let us substitute these expressions into our Lyapunov function, while also collecting out terms for E_h *and* T_h*:*

$$\begin{aligned}\dot{\mathcal{F}}(t)=&-\mu_h\frac{\gamma_h}{\kappa_1}\left(\frac{(S_h-\overline{S}_h)^2}{S_h}\right)-\frac{\gamma_h}{\kappa_1}\left(\frac{S_h-\overline{S}_h}{S_h}\right)\left(\frac{\beta_{hh}I_hS_h}{N_h}+\frac{\beta_{bh}I_bS_h}{N_b}\right)\\&+\frac{\gamma_h}{\kappa_1}\left(\frac{\beta_{hh}I_hS_h}{N_h}+\frac{\beta_{bh}I_bS_h}{N_b}\right)\\&+E_h\left(\gamma_h-\kappa_1\frac{\gamma_h}{\kappa_1}\right)\\&+T_h\left(\frac{\kappa_2}{\sigma_h}\sigma_h-\kappa_2\right)-\frac{\kappa_2\mu_h}{\sigma_h}I_h\\&+-\mu_b\frac{\gamma_h\beta_{bh}}{\kappa_1\mu_b}\left(\frac{N_h}{N_b}\right)\left(\frac{(S_b-\overline{S}_b)^2}{S_b}\right)-\frac{\gamma_h\beta_{bh}}{\kappa_1\mu_b}\left(\frac{N_h}{N_b}\right)\left(\frac{S_b-\overline{S}_b}{S_b}\right)\left(\frac{\beta_{hb}I_hS_b}{N_h}\right)\\&+\frac{\gamma_h\beta_{bh}}{\kappa_1\mu_b}\left(\frac{N_h}{N_b}\right)\left(\beta_{hb}S_b\frac{I_h}{N_h}-\mu_bI_b\right)\end{aligned}$$

Therefore, the parameter associated with both E_h *and* T_h *both disappear, let us continue with simplify by collecting terms:*

$$\begin{aligned}\dot{\mathcal{F}}(t)=&-\mu_h\frac{\gamma_h}{\kappa_1}\left(\frac{(S_h-\overline{S}_h)^2}{S_h}\right)+\frac{\gamma_h}{\kappa_1}\left(1-1+\frac{\overline{S}_h}{S_h}\right)\left(\frac{\beta_{hh}I_hS_h}{N_h}+\frac{\beta_{bh}I_bS_h}{N_b}\right)-\frac{\kappa_2\mu_h}{\sigma_h}I_h\\&-\mu_b\frac{\gamma_h\beta_{bh}}{\kappa_1\mu_b}\left(\frac{N_h}{N_b}\right)\left(\frac{(S_b-\overline{S}_b)^2}{S_b}\right)+\frac{\gamma_h\beta_{bh}}{\kappa_1\mu_b}\left(\frac{N_h}{N_b}\right)\left(1-1+\frac{\overline{S}_b}{S_b}\right)\left(\frac{\beta_{hb}I_hS_b}{N_h}\right)\\&-\frac{\gamma_h\beta_{bh}}{\kappa_1\mu_b}\left(\frac{N_h}{N_b}\right)\mu_bI_b\end{aligned}$$

After some manipulation we obtain the following:

$$\begin{aligned}\dot{\mathcal{F}}(t)=&-\mu_h\frac{\gamma_h}{\kappa_1}\left(\frac{(S_h-\overline{S}_h)^2}{S_h}\right)+\frac{\gamma_h}{\kappa_1}\left(\frac{\beta_{hh}I_h\overline{S}_h}{N_h}+\frac{\beta_{bh}I_b\overline{S}_h}{N_b}\right)-\frac{\kappa_2\mu_h}{\sigma_h}I_h\\&-\mu_b\frac{\gamma_h\beta_{bh}}{\kappa_1\mu_b}\left(\frac{N_h}{N_b}\right)\left(\frac{(S_b-\overline{S}_b)^2}{S_b}\right)+\frac{\gamma_h\beta_{bh}}{\kappa_1\mu_b}\left(\frac{N_h}{N_b}\right)\left(\frac{\beta_{hb}I_h\overline{S}_b}{N_h}\right)\\&-\frac{\gamma_h\beta_{bh}}{\kappa_1\mu_b}\left(\frac{N_h}{N_b}\right)\mu_bI_b\end{aligned}$$

Now let us extract out the terms I_h *and* I_b*. Moreover, if we use the equality* $\overline{S_h}=\frac{\Lambda_h}{\mu_h}=N_h$ *and* $\overline{S_b}=\frac{\Lambda_b}{\mu_b}=N_b$ *then we see the following simplification:*

$$\begin{aligned}\dot{\mathcal{F}}(t)=&-\mu_h\frac{\gamma_h}{\kappa_1}\left(\frac{(S_h-\overline{S}_h)^2}{S_h}\right)-\frac{\gamma_h\beta_{bh}}{\kappa_1}\left(\frac{N_h}{N_b}\right)\left(\frac{(S_b-\overline{S}_b)^2}{S_b}\right)\\&+I_h\left(\frac{\gamma_h}{\kappa_1}\beta_{hh}+\frac{\gamma_h}{\kappa_1\mu_b}\beta_{bh}\beta_{hb}-\mu_h\frac{\kappa_2}{\sigma_h}\right)\\&+I_b\left(\frac{\gamma_h}{\kappa_1}\beta_{bh}\frac{N_h}{N_b}-\frac{\gamma_h}{\kappa_1\mu_b}\mu_b\beta_{bh}\frac{N_h}{N_b}\right)\end{aligned}$$

After noticing that the expression in front of I_b equals zero, the last remaining step is to extract the expression $\left(\frac{\mu_h \kappa_2}{\sigma_h}\right)$ from the I_h expression.

$$\dot{\mathcal{F}}(t) = -\mu_h \frac{\gamma_h}{\kappa_1}\left(\frac{(S_h - \overline{S}_h)^2}{S_h}\right) - \frac{\gamma_h \beta_{bh}}{\kappa_1}\left(\frac{N_h}{N_b}\right)\left(\frac{(S_b - \overline{S}_b)^2}{S_b}\right) + \mu_h \frac{\kappa_2}{\sigma_h} I_h \left(\frac{\gamma_h \sigma_h}{\kappa_1 \kappa_2}\left(\frac{\beta_{hh}}{\mu_h} + \frac{\beta_{bh}\beta_{hb}}{\mu_h \mu_b}\right) - 1\right)$$

Therefore,

$$\dot{\mathcal{F}}(t) = -\mu_h \frac{\gamma_h}{\kappa_1}\left(\frac{(S_h - \overline{S}_h)^2}{S_h}\right) - \mu_b \frac{\gamma_h \beta_{bh}}{\kappa_1 \mu_b}\left(\frac{N_h}{N_b}\right)\left(\frac{(S_b - \overline{S}_b)^2}{S_b}\right) + \mu_h \frac{\kappa_2}{\sigma_h} I_h \left(\mathcal{R}_0 - 1\right)$$

Clearly, if $\mathcal{R}_0 < 1$ then $\dot{\mathcal{F}} \leqslant 0$ with $\dot{\mathcal{F}} = 0$ if and only if all other parameters other than susceptible host (S_h) and susceptible badgers (S_b) are zero (i.e. $E_h = T_h = I_H = I_b = 0$). Hence, LaSalle invariance principle implies every solution to the wildlife reservoir system (4.1) with initial conditions in Ω asymptotically converge to $\mathcal{DFE}$ as time tends to infinity. Hence, the disease free equilibrium is globally asymptotically stable in Ω if $\mathcal{R}_0 < 1$.

The global nature of this theorem indicates that in our feasibility region Ω, there only exist two equilibrium; a unique endemic equilibrium $\mathcal{EE}$ which exists if $\mathcal{R}_0 > 1$ and a globally stable disease free equilibrium $\mathcal{DFE}$ when $\mathcal{R}_0 < 1$. The last step in our analysis is to determine the stability of the endemic equilibrium.

4.4 STABILITY OF THE ENDEMIC EQUILIBRIUM

As previously discussed, the endemic equilibrium ($\mathcal{EE}$) represents disease being maintained in the system at a particular endemic level. Recall, this has been calculated for the wildlife host system (4.1) and it is given by:

$$\begin{aligned}
\mathcal{EE} &= (\overline{S_h}, \overline{E_h}, \overline{T_h}, \overline{I_h}, \overline{S_b}, \overline{I_b}) \\
\overline{S_h} &= \frac{\Lambda_h}{\overline{\lambda^{**}}_h + \mu_h} \\
\overline{E_h} &= \frac{\kappa_2}{\gamma_h}\overline{T_h} = \frac{\kappa_2 \mu_h}{\gamma_h \sigma_h}\overline{I_h} \\
\overline{T_h} &= \frac{\mu_h}{\sigma_h}\overline{I_h} \\
\overline{S_b} &= \frac{N_h \Lambda_b}{\beta_{hb}\overline{I_h} + N_h \mu_b} \\
\overline{I_b} &= \left(\frac{\beta_{hb} N_b \overline{I_h}}{\beta_{hb}\overline{I_h} + N_h \mu_b}\right)
\end{aligned} \tag{4.5}$$

Where we define the force of infection for the host population as:

$$\overline{\lambda^{**}}_h = \beta_{hh}\frac{\overline{I}_h}{N_h} + \beta_{bh}\frac{\overline{I}_b}{N_b}$$

Moreover, recall the following parameter κ_1 and κ_2 are defined as:

$$\kappa_1 = (\gamma_h + \mu_h) \qquad \kappa_2 = (\sigma_h + \mu_h)$$

Through substituting our expressions for $\overline{E}_h$ into the exposed compartments differential equation at equilibrium (i.e. $\dot{E_h} = 0$) we obtain the following relationship:

$$\overline{\lambda^{**}}_h \overline{S}_h = \kappa_1 \overline{E}_h = \frac{\kappa_1 \kappa_2 \mu_h}{\gamma_h \sigma_h} \overline{I_h}$$

Through rearranging and inserting the above equilibrium expressions we obtain:

$$\overline{S_h} = \frac{\kappa_1 \kappa_2}{\gamma_h \sigma_h} \left(\frac{\Lambda_h (\beta_{hb} \overline{I_h} + \mu_b N_h)}{\beta_{hh} (\beta_{hb} \overline{I_h} + \mu_b N_h) + \beta_{bh} \beta_{hb} N_h} \right)$$

Let us now show the endemic equilibrium is locally asymptotically stable when the basic reproductive number is above unity $\mathcal{R}_0 > 1$.

Theorem 4.4.1 *For the given wildlife reservoir system (4.1), where initial conditions originate in the positively invariant set Ω, the endemic equilibrium $\mathcal{EE}$ is locally asymptotically stable (LAS) in Ω whenever $\mathcal{R}_0 > 1$.*

Proof 4.4.1 *The local asymptotically stability of the endemic equilibrium $\mathcal{EE}$ can be examined through analysing the linearised wildlife reservoir system (4.1). The Jacobian evaluated at the endemic equilibrium $\mathcal{EE}$ for our wildlife reservoir system (4.1) is given below:*

$$J(\mathcal{EE}) = \begin{pmatrix} -(\beta_{hh} \frac{\overline{I_h}}{N_h} + \beta_{bh} \frac{\overline{I_b}}{N_b} + \mu_h) & 0 & 0 & -\beta_{hh} \frac{\overline{S_h}}{N_h} & 0 & -\beta_{bh} \frac{\overline{S_h}}{N_b} \\ \beta_{hh} \frac{\overline{I_h}}{N_h} + \beta_{bh} \frac{\overline{I_b}}{N_b} & -\kappa_1 & 0 & \beta_{hh} \frac{\overline{S_h}}{N_h} & 0 & \beta_{bh} \frac{\overline{S_h}}{N_b} \\ 0 & \gamma_h & -\kappa_2 & 0 & 0 & 0 \\ 0 & 0 & \sigma_h & -\mu_h & 0 & 0 \\ 0 & 0 & 0 & -\beta_{hb} \frac{\overline{S_b}}{N_h} & -\beta_{hb} \frac{\overline{I_h}'}{N_h} - \mu_b & 0 \\ 0 & 0 & 0 & \beta_{hb} \frac{\overline{S_b}}{N_h} & \beta_{hb} \frac{\overline{I_h}'}{N_h} & -\mu_b \end{pmatrix}$$

Let us define a useful shortcut expression for the following analysis:

$$e_1 = \overline{\lambda_h^{**}} + \mu_h = \beta_{hh} \frac{\overline{I_h}}{N_h} + \beta_{bh} \frac{\overline{I_b}}{N_b} + \mu_h$$

The following elementary row operations are preformed on the Jacobian:

$$R_2' \leftarrow R_2 + \left(1 - \frac{\mu_h}{e_1}\right) R_1, \qquad R_3' \leftarrow R_3 + \frac{\gamma_h}{\kappa_1} R_2,$$
$$R_4' \leftarrow R_4 + \frac{\sigma_h}{\kappa_2} R_3, \qquad R_5' \leftarrow R_5 + R_6,$$
$$R_6' \leftarrow R_6 - \frac{\overline{S_b} \beta_{hb}}{N_h \mu_h} \left(\frac{\kappa_1 \kappa_2 N_h e_1}{\overline{S_h} \beta_{hh} \gamma_h \sigma_h - \kappa_1 \kappa_2 N_h e_1} \right) R_4$$

Where R_i' indicates that the new i^{th} row is obtained by combining scalar multiple of other rows. The Jacobian of the matrix obtained after these row operations is presented below:

$$J(\mathcal{EE}) = \begin{pmatrix} -e_1 & 0 & 0 & -\beta_{hh}\frac{\overline{S_h}}{N_h} & 0 & -\beta_{bh}\frac{\overline{S_h}}{N_b} \\ 0 & -\kappa_1 & 0 & \beta_{hh}\frac{\overline{S_h}}{N_h}(\frac{\mu_h}{e_1}) & 0 & \beta_{bh}\frac{\overline{S_h}}{N_b}(\frac{\mu_h}{e_1}) \\ 0 & 0 & -\kappa_2 & \beta_{hh}\frac{\overline{S_h}}{N_h}(\frac{\mu_h\gamma_h}{\kappa_1 e_1}) & 0 & \beta_{bh}\frac{\overline{S_h}}{N_b}(\frac{\mu_h\gamma_h}{\kappa_1 e_1}) \\ 0 & 0 & 0 & \beta_{hh}\mu_h(\frac{\overline{S_h}\gamma_h\sigma_h}{\kappa_1\kappa_2 N_h e_1}) - \mu_h & 0 & \beta_{bh}\frac{\overline{S_h}}{N_b}(\frac{\mu_h\gamma_h\sigma_h}{\kappa_1\kappa_2 e_1}) \\ 0 & 0 & 0 & 0 & -\beta_{hb}\frac{I_b}{N_h} & -\frac{\overline{S}_h\overline{S}_b\beta_{hb}\beta_{bh}\gamma_h\sigma_h}{N_b(\kappa_1\kappa_2 N_h e_1 - \overline{S_h}\beta_{hh}\gamma_h\sigma_h)} \\ 0 & 0 & 0 & 0 & 0 & -\mu_b\frac{\overline{S}_h\overline{S}_b\beta_{bh}\gamma_h\sigma_h}{\overline{I_b}N_b(\kappa_1\kappa_2 N_h e_1 - \overline{S_h}\beta_{hh}\gamma_h\sigma_h)} - \mu_b \end{pmatrix}$$

The corresponding eigenvalues of the Jacobian must all be negative to prove that the endemic equilibrium ($\mathcal{EE}$) is locally asymptotically stable.

$$\lambda_1 = -\left(\beta_{hh}\frac{\overline{I_h}}{N_h} + \beta_{bh}\frac{\overline{I_b}}{N_b} + \mu_h\right) < 0, \qquad \lambda_2 = -\kappa_1 < 0,$$

$$\lambda_3 = -\kappa_2 < 0, \qquad \lambda_4 = \beta_{hh}\left(\frac{\overline{S_h}\mu_h\gamma_h\sigma_h}{\kappa_1\kappa_2 N_h e_1}\right) - \mu_h,$$

$$\lambda_5 = -\beta_{hb}\frac{I_b}{N_h} < 0, \qquad \lambda_6 = -\mu_b\frac{\overline{S}_h\overline{S}_b\beta_{bh}\gamma_h\sigma_h}{\overline{I_b}N_b(\kappa_1\kappa_2 N_h e_1 - \overline{S_h}\beta_{hh}\gamma_h\sigma_h)} - \mu_b,$$

As the eigenvalues $\lambda_1 < 0, \lambda_2 < 0, \lambda_3 < 0, \lambda_5 < 0$ are all negative it remains to show that λ_4 and λ_6 are negative. Although, notice that both λ_4 and λ_6 are negative if the following inequality holds:

$$\kappa_1\kappa_2(\beta_{hh}\overline{I_h} + \beta_{bh}\overline{I_b} + \mu_h) - \beta_{hh}\gamma_h\sigma_h\overline{S_h} > 0$$

Let us first demonstrate that $\lambda_4 < 0$ if the above inequality holds:

$$\begin{aligned}\lambda_4 &= \beta_{hh}\left(\frac{\overline{S_h}\mu_h\gamma_h\sigma_h}{\kappa_1\kappa_2 N_h e_1}\right) - \mu_h \\ &= \mu_h\left(\frac{\overline{S_h}\beta_{hh}\gamma_h\sigma_h}{\kappa_1\kappa_2 N_h e_1} - 1\right) \\ &= \frac{\mu_h}{\kappa_1\kappa_2 N_h e_1}\left(\overline{S_h}\beta_{hh}\gamma_h\sigma_h - \kappa_1\kappa_2 N_h e_1\right)\end{aligned}$$

Clearly if $\kappa_1\kappa_2 N_h e_1 - \beta_{hh}\gamma_h\sigma_h\overline{S_h} > 0$ then this implies that λ_4 is negative. Similarly, this condition implies the denominator of λ_6 is positive and by the non-negative criterion of parameters this implies $\lambda_6 < 0$. In order to prove this inequality is correct, let us first re-define $\overline{S_h}$ in terms of new parameters e_2 & e_3:

$$\overline{S_h} = \frac{\kappa_1\kappa_2}{\gamma_h\sigma_h}\left(\frac{\Lambda_h(\beta_{hb}\overline{I_h} + \mu_b N_h)}{\beta_{hh}(\beta_{hb}\overline{I_h} + \mu_b N_h) + \beta_{bh}\beta_{hb}N_h}\right) = \frac{\Lambda_h\kappa_1\kappa_2 e_2}{e_3}$$

$$e_2 = \beta_{hb}I_h + N_h\mu_b$$

$$e_3 = \gamma_h\sigma_h(\beta_{hh}e_2 + N_h\beta_{hb}\beta_{bh})$$

Hence our inequality can be expressed in the following form:

$$\begin{aligned}\kappa_1\kappa_2 N_h e_1 - \beta_{hh}\gamma_h\sigma_h\overline{S_h} &= \kappa_1\kappa_2 N_h e_1 - \beta_{hh}\gamma_h\sigma_h\frac{\Lambda_h\kappa_1\kappa_2 e_2}{e_3}\\ &= \frac{\kappa_1\kappa_2}{e_3}\left(N_h e_1 e_3 - \beta_{hh}\gamma_h\sigma_h\Lambda_h e_2\right)\\ &= \frac{\kappa_1\kappa_2}{e_3}\left(N_h e_3\left(\beta_{hh}\frac{\overline{I_h}}{N_h} + \beta_{bh}\frac{\overline{I_b}}{N_b}\right) + N_h\mu_h e_3 - \beta_{hh}\gamma_h\sigma_h\Lambda_h e_2\right)\end{aligned}$$

Let us further examine the following expressions:

$$\begin{aligned}N_h\mu_h e_3 - \beta_{hh}\gamma_h\sigma_h\Lambda_h e_2 &= \Lambda_h\left(\gamma_h\sigma_h\left(\beta_{hh}e_2 + N_h\beta_{hb}\beta_{bh}\right)\right) - \beta_{hh}\gamma_h\sigma_h\Lambda_h e_2\\ &= \Lambda_h\gamma_h\sigma_h\left(\beta_{hh}e_2 + N_h\beta_{hb}\beta_{bh} - \beta_{hh}e_2\right)\\ &= \Lambda_h\gamma_h\sigma_h N_h\beta_{hb}\beta_{bh}\end{aligned}$$

Therefore, our inequality $\kappa_1\kappa_2 N_h(\beta_{hh}\overline{I_h} + \beta_{bh}\overline{I_b} + \mu_h) - \beta_{hh}\gamma_h\sigma_h\overline{S_h} > 0$ *holds as:*

$$\kappa_1\kappa_2 N_h e_1 - \beta_{hh}\gamma_h\sigma_h\overline{S_h} = \frac{\kappa_1\kappa_2}{e_3}\left(N_h e_3\left(\beta_{hh}\frac{\overline{I_h}}{N_h} + \beta_{bh}\frac{\overline{I_b}}{N_b}\right) + \Lambda_h\gamma_h\sigma_h N_h\beta_{hb}\beta_{bh}\right)$$

Therefore as shown above, this inequality $\kappa_1\kappa_2 N_h e_1 - \beta_{hh}\gamma_h\sigma_h\overline{S_h} > 0$ *demonstrates that all eigenvalues of the Jacobian have a negative real part which proves that the endemic equilibrium* $\mathcal{EE}$ *is locally asymptotically stable in* Ω*.*

The role of a wildlife reservoir in bTB is further discussed and analysed in chapter six, where using a simulation model we demonstrate the change in dynamics through partially removing the wildlife reservoir, representing a herd improving bio-security measures. The simulation model incorporates more model mechanisms and therefore gives a more realistic representation of the wildlife reservoir, therefore, to avoid duplication of results the wildlife reservoir mechanic analysis shall be completed in chapter six.

4.5 CONCLUSION

A mathematical model for wildlife reservoir disease transmission is proposed and investigated. The demographics of the model constrain both species to constant recruitment with an exponential natural death rate, where the system has been analysed when both species are at equilibrium. The analysis of the system has shown that if the disease's basic reproductive number is higher than unity (i.e. $\mathcal{R}_0 > 1$) the disease will be locally attracted to a unique endemic equilibrium. The wildlife host system can also be shown to backward bifurcate, however after further analyse it was shown that this could not occur in the feasibility region Ω that we restricted our analysis to. As a result, if the basic reproductive number is less than unity (i.e. $\mathcal{R}, < 1$) then the system solutions are attracted to the disease-free equilibrium.

5

CHAPTER 5: BOVINE TUBERCULOSIS' ENVIRONMENTAL CONTAMINATION

In this chapter, we investigate the biological contamination properties of bovine tuberculosis and incorporate them into our model. As discussed in the literature review chapter, M. bovis can contaminate soil, troughs, cattle feed, hay, and various other materials [82]. As a result, cattle may become infected by interacting with the different contaminated micro-environments seen within a farm. The literature indicates that cattle are notably more likely to contract the disease by interacting with contaminated sources for long exposure times or by ingesting contaminated materials [175]. As a result, cattle feed and water troughs are considered more potent contamination sources [85], as cattle consume food and/or drink closely with one another. Moreover, the proximity of infectious cattle's snouts to food and water sources increases the overall level of contamination, as nasal secretion is more concentrated on one particular object, leading to a more significant number of infections [20]. Similarly, cattle bedding (normally hay) is seen as a more potent contamination source due to cattle's long exposure time [62].

The model analysed and examined in this chapter extends the standard prototypical model by incorporating a compartment for the background environment $B(t)$. This background environmental compartment $B(t)$ attempts to quantify the level of contamination excreted by infectious cattle. Therefore, this multi-transmission pathway model considers cattle contracting bTB from two sources, either from direct cattle to cattle interaction or by cattle engaging with the contaminated environment $B(t)$. The fundamental qualities of this model are analysed; disease-free equilibrium, endemic equilibrium, the basic reproductive number, and the long term behaviour of our solutions. After which, we examine the SETIB system with bTB parameters through numerical analysis, comparing and contrasting how the system dynamics alter when examing different environmental contamination parameters.

5.1 BACKGROUND CONTAMINATION

As discussed extensively in the literature review chapter, infectious cattle spray fomites that contaminate the environment [19],[20]. The M. bovis bacterium can either aerosolise or contaminate surfaces (e.g. soil, pasture, and water sources). If M. bovis undergoes aerosolisation, it has been demonstrated experimentally that these contaminated aerosols linger in the air

for 12-24 hours and are resistant to the associated stresses [19]. Furthermore, this infection interval is expected to be considerably longer if cattle are housed indoors permanently due to the poor ventilation associated with housing pens [19].

Infected hosts can contaminate the various different environmental matrices seen within a farm (e.g. feed, hay, soil, or water), where this contamination period lasts for varying periods of time. The rate at which bTB is estimated to decay is exceptionally variable depending on the material, lasting anywhere between a couple of days to 2 years [16]. How then do these environmental matrices become contaminated? Infected cattle excrete M. bovis through their urine, faeces, saliva, nasal secretion, and sputum, where notably, the highest bacterial load is found in cattle sputum. One USA (Michigan) study found that M. bovis remains viable and pathogenic for 88 days in soil and 58 days in both water and hay [62]. In comparison, similar studies in the UK have found that the bacteria may remain present in pastures and soils for around six months. The survival and persistence of M. bovis increase in other mediums such as faeces (8-9 months) and dry cattle feed when stored indoors (9 months) [79],[19]. The differing bacterial time intervals exhibited above are likely due to UK's climate, multiple studies have found that tubercle bacilli best survive in cool and moist environments, shaded from direct sunlight. Under laboratory conditions, researchers have demonstrated that if M. bovis remains in a shaded environment, it remains viable for up to twice as long [20]. Consequentially, similar field studies imply longer survival times during the winter months; GB [85], New Zealand [81], Michigan [62] and Australia [175].

Contamination of drinking water has also been identified as a typical transmission pathway between local wildlife and cattle (white-tailed deer in the USA [62] and boar in Spain [84]). Infected hosts shed M. bovis through nasal and oral secretion into communal water sources, often supporting the disease spread through reservoir and target population interaction. In the UK, communal water sources are not considered a significant risk factor in reservoir and target population interactions, as most cattle drink from self-contained troughs. However, livestock troughs have yet to be examined thoroughly in the literature and various researchers have indicated troughs could be a more substantial source of contamination than current thought [16]. DEFRA suggests that troughs may be contaminated by saliva and sputum, advising regular cleaning and disinfection of water troughs and avoiding stagnation if possible [85]. Furthermore, in independent advice regarding badger biosecurity measures, DEFRA suggests raising water troughs to at least 80cm to prevent badger contamination [49]. DEFRA advises that similar measures should be implemented regarding feeder rings, as these have also been suggested as a potential source of contamination [85].

Therefore, environmental contamination is a decisive disease transmission mechanic and should undoubtedly be understood and incorporated into the wider bTB modelling literature. As environmental contamination can induce infections in a wholly susceptible herd, even after all infected animals are culled. However, even though the literature discusses bTB environmental contamination in great detail, where various papers have indicated the importance of this paramount disease mechanic, there are currently very little bTB modelling papers incorporating environmental contamination. The virtual non-existent discussion of environmental contamination within the bTB modelling literature means there is little discussion regarding contamination parameter values. Therefore, there are no parameters for environmental contamination for the numerical analysis section of this chapter. Hence, we shall assume different relative percentages of host infected (β_h and β_b) in the numerical analysis section. Let us now demonstrate the model and its system properties.

5.2 MATHEMATICAL MODEL FORMULATION

The inter-herd disease dynamics are described using a cattle population compartmental model similar to the SE_1E_2TIRC model. Where like before, the total cattle population at time t is denoted by $N(t)$ and cattle are separated into the following mutually distinct compartments; Susceptible $S(t)$, Exposed $E(t)$, Test sensitive $T(t)$, or Infected $I(t)$. Therefore, the first system constraint is the population dynamics;

$$N(t) = S(t) + E(t) + T(t) + I(t)$$

After accounting for newly recruited cattle Λ and natural deaths μ, the susceptible host population is reduced by susceptible cattle contracting the disease. Infection from both the background contamination and cattle to cattle transmission occurs according to the mass action principle. The effective transmission rate for cattle to cattle transmissions is given by β_h and similarly, the effective transmission rate for background contamination is given by β_b. The continuous non-linear differential equation therefore models the rate of change of the susceptible population:

$$\frac{dS}{dt} = \Lambda - \left(\beta_h \frac{I}{N} + \beta_b \frac{B}{N_B}\right) S - \mu S$$

Cattle that contract the disease progress to the exposed compartments $E(t)$ and remain there until the disease progresses to test sensitive compartment or until they die a natural death μ. The γ progression parameter is the transition rate between the exposed $E(t)$ to the test sensitive $T(t)$ compartment. The differential equation controlling the exposed compartments is therefore given by:

$$\frac{dE}{dt} = \left(\beta_h \frac{I}{N} + \beta_b \frac{B}{N_B}\right) S - (\mu + \gamma) E$$

The test sensitive population $T(t)$ is increased by those cattle progressing from the exposed compartment $E(t)$. The population is reduced by natural deaths μ and cattle progressing to the infected stage, which occurs at the rate σ.

$$\frac{dT}{dt} = \gamma E - (\mu + \sigma) T$$

As the test sensitive $T(t)$ cattle progress into the infected compartment $I(t)$, they enter into the last compartment of this system. The only way hosts are removed from the infected compartment is by dying a natural death occurring at rate μ.

$$\frac{dI}{dt} = \sigma T - \mu I$$

The background compartment $B(t)$ is not part of the infection cycle, rather it represents the environmental contamination exhibited on the farm. In our set of differential equations below, cattle contract the disease from the environment in a similar fashion to the mass action principle, where the force of infection is as follows:

$$\lambda_b^{**} = \beta_h \frac{I}{N} + \beta_b \frac{B}{N_B}$$

Where N_B represents the maximum total environmental contamination that a herd could produce. Therefore, the background compartment $B(t)$ represents the proportion of the maximum total environmental contamination seen on a farm. Where this parameter λ_b^{**} incorporate infections induced from cattle interacting/ingesting contaminated material and the inhalation of fomite (contaminated dust particles) from the air. Each individual infected cattle shed fomites and contaminate their nearby surroundings at a rate θ, as more M. bovis is shed into the environment, more cattle ingest/interact with M. bovis and become infectious themselves. Bovine tuberculosis decays at different rates depending on the media it is found within, although for the purpose of modelling, we have only one average decay rate for all mediums on the farm given by ξ.

$$\frac{dB}{dt} = \theta I - \xi B$$

We generate just the environmental force of infection $\beta_b \frac{B}{N_B}$ by normalising the environmental contamination parameter $B(t)$. However, for us to do so, we must find out what the maximum size that $B(t)$ can become. From later analysis, regarding the bounded nature of solutions, we shall see that the environmental contamination parameter $B(t)$ is at most:

$$N_B = \frac{\theta}{\xi}\left(\frac{\Lambda}{\mu}\right) = \frac{\theta}{\xi} N$$

Therefore, the non-linear set of differential equations has the following system equations:

$$\begin{aligned}
\frac{dS}{dt} &= \Lambda - \left(\beta_h \frac{I}{N} + \beta_b \frac{B}{N_B}\right) S - \mu S \\
\frac{dE}{dt} &= \left(\beta_h \frac{I}{N} + \beta_b \frac{B}{N_B}\right) S - (\mu + \gamma) E \\
\frac{dT}{dt} &= \gamma E - (\mu + \sigma) T \\
\frac{dI}{dt} &= \sigma T - \mu I \\
\frac{dB}{dt} &= \theta I - \xi B
\end{aligned} \tag{5.1}$$

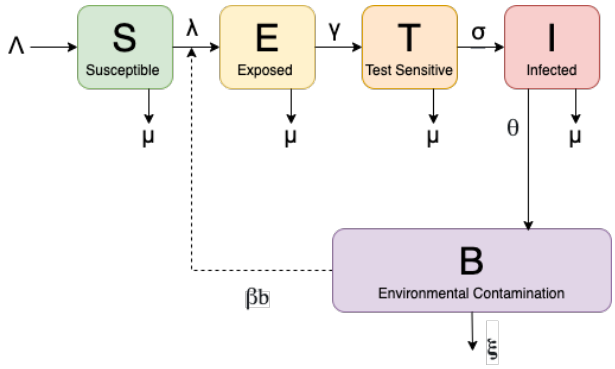

Figure 5.1: Flow chart of the transmission dynamics of the SETIB model.

5.2.1 *Mathematical Model Properties*

Let us now investigate the model properties of the SETIB system. In this section, we shall demonstrate the well posed nature of solutions and construct the system feasibility region.

Theorem 5.2.1 *All solutions for our SETIRB system 5.1 which have initial conditions originating within* $\mathbb{R}^5_+$ *are bounded.*

$$\mathbb{R}^5_+ = \{N(S, E, T, I, B) \mid S \geqslant 0, E \geqslant 0, T \geqslant 0, I \geqslant 0, B \geqslant 0\}$$

Proof 5.2.1 *Let* $N\big(S(t), E(t), T(t), I(t), B(t)\big)$ *be an arbitrary solution of the SETIB system 5.1 with a non-negative initial conditions. The population of the herd is given by* $N(t)$*, where*

$$N(t) = S(t) + E(t) + T(t) + I(t)$$

Hence,

$$\frac{dN}{dt} = \Lambda - \mu(S + E + T + I) = \Lambda - \mu N(t)$$

By Grönwall lemma, if $x(t)$ *is a function satisfying* $\frac{dx}{dt} \leqslant ax + b$*, where* $x(0) = x_0$ *and both* a *and* b *are constants then for all time* $t \geqslant 0$*. Hence,*

$$x(t) \leqslant x_0 e^{at} + \frac{b}{a}\left(e^{at} - 1\right)$$

therefore,

$$0 \leqslant N\big(S(t), E(t), T(t), I(t)\big) \leqslant \frac{\Lambda}{\mu}\left(1 - e^{-\mu t}\right) + N(0)e^{-\mu t}$$

Hence,

$$0 \leqslant \limsup_{t\to\infty} N(t) \leqslant \frac{\Lambda}{\mu}$$

It remains to show that our compartment representing background contamination $B(t)$ *is bounded. As shown above, the total population of the herd* $N(t)$ *is bounded by* $\frac{\Lambda}{\mu}$*, hence so is the number of hosts within the infected compartment (i.e.* $I(t) \leqslant \frac{\Lambda}{\mu}$*). As a result,*

$$\frac{dB}{dt} = \theta I_h - \xi B \leqslant \theta\frac{\Lambda}{\mu} - \xi B$$

Hence, using Grönwall lemma once again it can be shown that $B(t)$ *is bounded.*

$$\limsup_{t\to\infty} B(t) \leqslant \frac{\theta}{\xi}\left(\frac{\Lambda}{\mu}\right)$$

As discussed previously, we shall normalise $B(t)$ *by this maximum bound, where* $N_B = \frac{\theta}{\xi}N$.

Therefore all solutions of the SETIB system 5.1 that originate in $\mathbb{R}^5_+$ *are attracted to the following positive invariant region,*

$$\Omega = \left\{N(S, E, T, I, B) \in \mathbb{R}^5_+ | N(t) \leqslant \frac{\Lambda}{\mu}, B(t) \leqslant \frac{\theta}{\xi}\left(\frac{\Lambda}{\mu}\right)\right\} \tag{5.2}$$

The SETIB system 5.1 is therefore bounded. Additionally, since $\limsup_{t\to\infty} N(t)$ *is independent of the initial conditions then the system is said to be uniformly bounded. As all solutions beginning in our positive invariant region* Ω *are trapped there, the analysis will be restricted to this feasible region.*

Now that we have shown that solutions are bounded the next stage is to show that the SETIB model solutions are well posed (i.e. exist and are unique depending on initial conditions).

Theorem 5.2.2 *The SETIB system (5.1) is well posed.*

Proof 5.2.2 *As the right hand side of system 5.1 are continuously differentiable functions on*

$$\mathbb{R}^5_+ = \{N(S, E, T, I, B) \mid S \geqslant 0, E \geqslant 0, T \geqslant 0, I \geqslant 0, B \geqslant 0\}$$

and as the above theorem indicates that the first derivative of our system is uniformly bounded. This condition implies that the system equation are Lipschitz continuous and with this condition, we can apply the Picard Lindelöf theorem that proves a unique solution exists for the SETIB system 5.1.

The SETIB model 5.1 is therefore well posed and any solution with initial conditions originating in Ω will remain in this feasibility region for all future time. Now, lets turn our attention to the system equilibrium and the basic reproductive number that bifurcates the system.

5.2.2 *Basic Reproductive Number $\mathcal{R}_0$*

Theorem 5.2.3 *For the given SETIB system 5.1, where initial conditions originate in the positively invariant set Ω, the basic reproductive number is:*

$$\mathcal{R}_0 = \left(\frac{\gamma\sigma}{\kappa_1\kappa_2\mu}\right)\left(\beta_h + \beta_b\right)$$

Proof 5.2.3 *The basic reproductive number $\mathcal{R}_0$ is calculated using the next generation matrix using the Van den Driesche and Watmough approach. This method has been extensively discussed in section 2.3.3.3 and throughout this thesis so our analysis shall be condensed.*

The basic reproductive number $\mathcal{R}_0$ is given by the following:

$$\mathcal{R}_0 = \rho(FV^{-1})$$

Where the matrices F and V are defined below:

$$F = \begin{pmatrix} 0 & 0 & \beta_h & \beta_b\left(\frac{\xi}{\theta}\right) \\ 0 & 0 & 0 & 0 \\ 0 & 0 & 0 & 0 \\ 0 & 0 & 0 & 0 \end{pmatrix} \quad \textit{and} \quad V = \begin{pmatrix} k_1 & 0 & 0 & 0 \\ -\gamma & k_2 & 0 & 0 \\ 0 & -\sigma & \mu & 0 \\ 0 & 0 & -\theta & \xi \end{pmatrix}$$

Where in the linearised F matrix we have used removed demographic dependencies. As consider the result for $f_{[1,4]} \in F$, where $f_{[1,4]} = \frac{\partial E}{dB}$, this evaluated at the disease free equals:

$$\frac{\partial E}{dB} = \beta_b \frac{\overline{S}}{N_B} = \beta_b \frac{\overline{S}}{\frac{\theta}{\xi}N} = \beta_b \frac{\xi}{\theta}$$

Where as defined previously $N_b = \frac{\theta}{\xi}N$, moreover, at the disease free equilibrium the entire herd are susceptible cattle (i.e. $\overline{S} = \frac{\Lambda}{\mu}$).

The order in which these matrix have been attained are E,T,I,B and hence the matrix V^{-1} is calculated below.

$$V^{-1} = \begin{pmatrix} \frac{1}{\kappa_1} & 0 & 0 & 0 \\ \frac{\gamma}{\kappa_1\kappa_2} & \frac{1}{\kappa_2} & 0 & 0 \\ \frac{\gamma\sigma}{\kappa_1\kappa_2\mu} & \frac{\sigma}{\kappa_2\mu} & \frac{1}{\mu} & 0 \\ \frac{\gamma\sigma\theta}{\xi\kappa_1\kappa_2\mu} & \frac{\sigma\theta}{\xi\kappa_2\mu} & \frac{\theta}{\xi\mu} & \frac{1}{\xi} \end{pmatrix} \tag{5.3}$$

Therefore the next generation matrix for the SETIB system is defined as follows:

$$FV^{-1} = \begin{pmatrix} \left(\frac{\gamma\sigma}{\kappa_1\kappa_2\mu}\right)\left(\beta_h + \beta_b\right) & \left(\frac{\sigma}{\kappa_2\mu}\right)\left(\beta_h + \beta_b\right) & \left(\frac{1}{\mu}\right)\left(\beta_h + \beta_b\right) & \frac{\beta_b}{\theta} \\ 0 & 0 & 0 & 0 \\ 0 & 0 & 0 & 0 \\ 0 & 0 & 0 & 0 \end{pmatrix}$$

Thereby, the largest eigenvalue of the next generation matrix FV^{-1} *gives the corresponding* $\mathcal{R}_0$ *for the system.*

$$\mathcal{R}_0 = \rho(FV^{-1}) = \left(\frac{\gamma\sigma}{\kappa_1\kappa_2\mu}\right)\left(\beta_h + \beta_b\right)$$

5.2.3 *Disease Free Equilibrium and its Stability*

The disease free equilibrium $\mathcal{DFE}$ represents the system absent of both the disease and background contamination, hence for the SETIB system 5.1 the disease free equilibrium $\mathcal{DFE}$ is given by:

$$\mathcal{DFE} = (\overline{S}, \overline{E}, \overline{T}, \overline{I}, \overline{B}) = \left(\frac{\Lambda}{\mu}, 0, 0, 0, 0\right) \tag{5.4}$$

Theorem 5.2.4 *For the given SETIB system (5.1), where initial conditions originate in the positively invariant set* Ω*, the disease free equilibrium* $\mathcal{DFE}$ *is locally asymptotically stable (LAS) in* Ω *whenever* $\mathcal{R}_0 < 1$.

Where the $\mathcal{R}_0$ *for the system is defined as:*

$$\mathcal{R}_0 = \left(\frac{\gamma\sigma}{\kappa_1\kappa_2\mu}\right)\left(\beta_h + \beta_b\right)$$

Proof 5.2.4 *The local asymptotically stability of the disease free equilibrium can be examined through analysing the linearised system around the disease free equilibrium ($\mathcal{DFE}$). The Jacobian of our environmental contamination system (5.1) is given below:*

$$J(\mathcal{DFE}) = \begin{pmatrix} -\mu & 0 & 0 & -\beta_h \frac{\overline{S}}{N} & -\beta_b \frac{\overline{S}}{N_B} \\ 0 & -\kappa_1 & 0 & \beta_h \frac{\overline{S}}{N} & \beta_b \frac{\overline{S}}{N_B} \\ 0 & \gamma & -\kappa_2 & 0 & 0 \\ 0 & 0 & \sigma & -\mu & 0 \\ 0 & 0 & 0 & \theta & -\xi \end{pmatrix}$$

Where the following variable equalities exist $\overline{S} = \frac{\Lambda}{\mu}$, although as we examine the asymptotically autonomous system this means that $N = \frac{\Lambda}{\mu}$ for all time t, hence, as a result $\frac{\overline{S}}{N} = 1$.

The associated characteristic equation for the the Jacobian $J(\mathcal{DFE})$ is

$$(\lambda+\mu)\Big((\lambda+\kappa_1)(\lambda+\kappa_2)(\lambda+\mu)(\lambda+\xi) - \gamma\sigma(\xi\beta_b + \beta_h(\lambda+\xi))\Big) = 0$$

For the disease free equilibrium $\mathcal{DFE}$ to be locally stable asymptotically, all corresponding eigenvalues of the Jacobian must have negative real part. One eigenvalue for the system is $\lambda_1 = -\mu$ and using the Routh-Hurwitz condition we can show the other eigenvalues are negative. The other four eigenvalues correspond to the four roots of the following function $f(\lambda)$:

$$f(\lambda) = (\lambda+\kappa_1)(\lambda+\kappa_2)(\lambda+\mu)(\lambda+\xi) - \gamma\sigma(\xi\beta_b + \beta_h(\lambda+\xi))$$

After expanding the brackets the following coefficients are made evident:

$$f(\lambda) = \lambda^4 + a_1\lambda^3 + a_2\lambda^2 + a_3\lambda + a_4$$

Where,

$$a_1 = \kappa_1 + \kappa_2 + \mu + \xi$$
$$a_2 = \kappa_1(\kappa_2 + \mu + \xi) + \kappa_2(\mu + \xi) + \mu\xi$$
$$a_3 = -\beta_h\sigma\gamma + \kappa_1\kappa_2(\mu+\xi) + \mu\xi(\kappa_1+\kappa_2)$$
$$a_4 = \kappa_1\kappa_2\mu\xi - \sigma\gamma\xi(\beta_h + \beta_b)$$

After some manipulation of a_4, we can obtain the tipping point of the system:

$$a4 = \kappa_1\kappa_2\mu\xi\left(1 - \left(\frac{\gamma\sigma}{\kappa_1\kappa_2\mu}\right)\Big(\beta_h + \beta_b\Big)\right) = \kappa_1\kappa_2\mu\xi(1 - \mathcal{R}_0)$$

The Routh-Hurwitz condition implies the disease free equilibrium is locally asymptotically stable if the following conditions hold.

1. *All coefficient's a_i for i=1,2,3,4 are positive $a_i > 0$.*

2. $a_1 a_2 - a_3 > 0$

3. $a_3(a_1 a_2 - a_3) - a_1^2 a_4 > 0$

If the basic reproductive number is less than unity ($\mathcal{R}_0 < 1$) then clearly a_1, a_2, and a_4 are positive. Notice that a_3 can be manipulated into the following form:

$$a_3 = \kappa_1\kappa_2\xi + \mu\xi(\kappa_1 + \kappa_2) + (\kappa_1\kappa_2\mu - \beta_{hh}\sigma\gamma)$$

Where if the basic reproductive number is less than unity then the following inequality holds:

$$\mathcal{R}_0 < 1 \implies \qquad \kappa_1\kappa_2\mu > \beta_h\sigma\gamma$$

This inequality is derived as follows:

$$\begin{aligned}\mathcal{R}_0 < 1 \implies \left(\frac{\gamma\sigma}{\kappa_1\kappa_2\mu}\right)\Big(\beta_h + \beta_b\Big) &< 1 \\ \gamma\sigma\Big(\beta_h + \beta_b\Big) &< \kappa_1\kappa_2\mu \\ \gamma\sigma\beta_h &< \kappa_1\kappa_2\mu\end{aligned}$$

Therefore, a_3 is positive if our basic reproductive number is less than unity (i.e. $a_3 > 0$ if $\mathcal{R}_0 < 1$). This shows that all coefficient's of our characteristic equation a_i for i=1,2,3,4 are all positive $a_i > 0$.

The next condition that must be proven is $a_1 a_2 - a_3 > 0$.

$$\begin{aligned}a_1 a_2 - a_3 =&(\kappa_1 + \kappa_2 + \mu + \xi)(\kappa_1(\kappa_2 + \mu + \xi) + \kappa_2(\mu + \xi) + \mu\xi) \\ &- (-\beta_h\sigma\gamma + \kappa_1\kappa_2(\mu + \xi) + \mu\xi(\kappa_1 + \kappa_2))\end{aligned}$$

Notice, that a_2 can be separated into the following form:

$$a_2 = \kappa_1\kappa_2 + (\kappa_1 + \kappa_2)(\mu + \xi) + \mu\xi$$

Therefore, if we express the a_2 parameter in this form then the expression $a_1 a_2 - a_3$ becomes the following:

$$\begin{aligned}a_1 a_2 - a_3 =&\kappa_1\kappa_2(\kappa_1 + \kappa_2 + \mu + \xi) && -\kappa_1\kappa_2(\mu + \xi) \\ &+ (\kappa_1 + \kappa_2)(\mu + \xi)(\kappa_1 + \kappa_2 + \mu + \xi) && +\beta_h\sigma\gamma \\ &+ \mu\xi(\kappa_1 + \kappa_2 + \mu + \xi) && -\mu\xi(\kappa_1 + \kappa_2)\end{aligned}$$

Hence, after some manipulation this expression becomes the following:

$$\begin{aligned}a_1 a_2 - a_3 =&\kappa_1\kappa_2(\kappa_1 + \kappa_2) \\ &+ (\kappa_1 + \kappa_2)(\mu + \xi)(\kappa_1 + \kappa_2 + \mu + \xi) + \beta_h\sigma\gamma \\ &+ \mu\xi(\mu + \xi)\end{aligned}$$

Therefore, clearly our expression $a_1 a_2 - a_3 > 0$ *is positive due to the restriction of parameters to the feasibility region (i.e. non-negative).*

$$a_1 a_2 - a_3 = \kappa_1\kappa_2(\kappa_1+\kappa_2) + \mu\xi(\mu+\xi) + \beta_h\sigma\gamma + (\kappa_1+\kappa_2)(\mu+\xi)(\kappa_1+\kappa_2+\mu+\xi) > 0$$

The last condition that must be shown is $a_3(a_1 a_2 - a_3) - a_1^2 a_4 > 0$*. In order to show this is true lets first analysis* $a_3(a_1 a_2 - a_3)$*, by expanding some of its terms we can see that* $a_3(a_1 a_2 - a_3) - a_1^2 a_4 > 0$*.*

$$\begin{aligned} a_3(a_1 a_2 - a_3) &= a_3\big(\kappa_1\kappa_2(\kappa_1+\kappa_2) + \mu\xi(\mu+\xi) + \beta_h\sigma\gamma + (\kappa_1+\kappa_2)(\mu+\xi)(\kappa_1+\kappa_2+\mu+\xi)\big) \\ &= a_3\big((\kappa_1+\kappa_2)(\mu+\xi)(\kappa_1+\kappa_2+\mu+\xi)\big) + a_3\big(\kappa_1\kappa_2(\kappa_1+\kappa_2) + \mu\xi(\mu+\xi) + \beta_h\sigma\gamma\big) \\ &= a_3(\kappa_1+\kappa_2)(\mu+\xi)a_1 + a_3\big(\kappa_1\kappa_2(\kappa_1+\kappa_2) + \mu\xi(\mu+\xi) + \beta_h\sigma\gamma\big) \end{aligned}$$

Let focus our attention just to $a_3(\kappa_1+\kappa_2)(\mu+\xi)a_1$*. First let us separate* a_3 *into two parts, where* $a_3 = (\kappa_1\kappa_2\mu - \beta_h\sigma\gamma) + (\kappa_1\kappa_2\xi + \mu\xi(\kappa_1+\kappa_2))$*, therefore,*

$$\begin{aligned} a_3(\kappa_1+\kappa_2)(\mu+\xi)a_1 = \big(\kappa_1\kappa_2\mu - \beta_h\sigma\gamma\big)(\kappa_1+\kappa_2)(\mu+\xi)a_1 \\ + (\kappa_1\kappa_2\xi + \mu\xi(\kappa_1+\kappa_2))(\kappa_1+\kappa_2)(\mu+\xi)a_1 \end{aligned}$$

The next stage of analysis is to examine $(\kappa_1\kappa_2\xi + \mu\xi(\kappa_1+\kappa_2))(\kappa_1+\kappa_2)(\mu+\xi)a_1$*. As we shall see, this expression contains two terms* $\kappa_1\kappa_2\mu\xi(\kappa_1+\kappa_2)a_1$ *and* $\kappa_1\kappa_2\mu\xi(\mu+\xi)a_1$ *which together make* $\chi = \kappa_1\kappa_2\mu\xi(\kappa_1+\kappa_2+\mu+\xi)a_1$*, an expression larger than* $a_1^2 a_4$*. As demonstrated below:*

$$\chi = \kappa_1\kappa_2\mu\xi a_1^2 \geqslant \kappa_1\kappa_2\mu\xi a_1^2(1-\mathcal{R}_0) = a_1^2 a_4$$

Hence, let us extract χ *from the* $(\kappa_1\kappa_2\xi + \mu\xi(\kappa_1+\kappa_2))(\kappa_1+\kappa_2)(\mu+\xi)a_1$ *expression.*

$$\begin{aligned} (\kappa_1\kappa_2\xi + \mu\xi(\kappa_1+\kappa_2))(\kappa_1+\kappa_2)(\mu+\xi)a_1 &= \kappa_1\kappa_2\xi(\kappa_1+\kappa_2)(\mu+\xi)a_1 + \mu\xi(\kappa_1+\kappa_2)^2(\mu+\xi)a_1 \\ &= \kappa_1\kappa_2\mu\xi(\kappa_1+\kappa_2)a_1 + \kappa_1\kappa_2\xi^2(\kappa_1+\kappa_2)a_1 \\ &\quad + \mu\xi(\kappa_1^2+\kappa_2^2+2\kappa_1\kappa_2)(\mu+\xi)a_1 \\ &= \kappa_1\kappa_2\mu\xi(\kappa_1+\kappa_2)a_1 + \kappa_1\kappa_2\xi^2(\kappa_1+\kappa_2)a_1 \\ &\quad + \mu\xi\kappa_1\kappa_2(\mu+\xi)a_1 + \mu\xi(\kappa_1^2+\kappa_2^2+\kappa_1\kappa_2)(\mu+\xi)a_1 \\ &= \chi + \kappa_1\kappa_2\xi^2(\kappa_1+\kappa_2)a_1 + \mu\xi(\kappa_1^2+\kappa_2^2+\kappa_1\kappa_2)(\mu+\xi)a_1 \end{aligned}$$

Therefore, by backward substitution this expression for $(\kappa_1\kappa_2\xi + \mu\xi(\kappa_1+\kappa_2))(\kappa_1+\kappa_2)(\mu+\xi)a_1$ *into the expression for* $a_3(\kappa_1+\kappa_2)(\mu+\xi)a_1$*, we obtain the following expressions:*

$$\begin{aligned} a_3(\kappa_1+\kappa_2)(\mu+\xi)a_1 = \big(\kappa_1\kappa_2\mu - \beta_h\sigma\gamma\big)(\kappa_1+\kappa_2)(\mu+\xi)a_1 \\ + \chi + \kappa_1\kappa_2\xi^2(\kappa_1+\kappa_2)a_1 + \mu\xi(\kappa_1^2+\kappa_2^2+\kappa_1\kappa_2)(\mu+\xi)a_1 \end{aligned}$$

The next stage is to backward substitute this expression and into $a_3(a_1a_2 - a_3)$.

$$\begin{aligned}
a_3(a_1a_2 - a_3) &= a_3\big(\kappa_1\kappa_2(\kappa_1+\kappa_2) + \mu\xi(\mu+\xi) + \beta_h\sigma\gamma\big) + a_3(\kappa_1+\kappa_2)(\mu+\xi)a_1 \\
&= a_3\big(\kappa_1\kappa_2(\kappa_1+\kappa_2) + \mu\xi(\mu+\xi) + \beta_h\sigma\gamma\big) \\
&\quad + \big(\kappa_1\kappa_2\mu - \beta_h\sigma\gamma\big)(\kappa_1+\kappa_2)(\mu+\xi)a_1 \\
&\quad + x + \kappa_1\kappa_2\xi^2(\kappa_1+\kappa_2)a_1 + \mu\xi(\kappa_1^2+\kappa_2^2+\kappa_1\kappa_2)(\mu+\xi)a_1
\end{aligned}$$

Therefore, the expression for $a_3(a_1a_2 - a_3) - a_1^2a_4$ *is given below and is clearly positive as* $a_3(a_1a_2 - a_3)$ *contains* x *(i.e* $x \leqslant a_1^2a_4$*).*

$$\begin{aligned}
a_3(a_1a_2 - a_3) - a_1^2a_4 &= a_3\big(\kappa_1\kappa_2(\kappa_1+\kappa_2) + \mu\xi(\mu+\xi) + \beta_h\sigma\gamma\big) \\
&\quad + \big(\kappa_1\kappa_2\mu - \beta_h\sigma\gamma\big)(\kappa_1+\kappa_2)(\mu+\xi)a_1 \\
&\quad + \kappa_1\kappa_2\xi^2(\kappa_1+\kappa_2)a_1 + \mu\xi(\kappa_1^2+\kappa_2^2+\kappa_1\kappa_2)(\mu+\xi)a_1 \\
&\quad + \kappa_1\kappa_2\mu\xi a_1^2\mathcal{R}_0
\end{aligned}$$

From above, we have shown that $\mathcal{R}_0 < 1$ *implies* $\kappa_1\kappa_2\mu > \beta_h\sigma\gamma$*. This implies that the above expression for* $a_3(a_1a_2 - a_3) - a_1^2a_4$ *is positive, proving last condition required by the Routh-Hurwitz condition. Therefore, the disease free equilibrium* $\mathcal{DFE}$ *is locally asymptotically stable (LAS) in* Ω *whenever* $\mathcal{R}_0 < 1$*. Although, as the next theorem shows, we can prove this holds globally instead of locally.*

Theorem 5.2.5 *For the given SETIB system 5.1, where initial conditions originate in the positively invariant set* Ω*, the disease free equilibrium* $\mathcal{DFE}$ *is globally asymptotically stable (GAS) in* Ω *whenever* $\mathcal{R}_0 < 1$*.*

Proof 5.2.5 *This theorem shall be proved by the existence of the following Lyapunov function:*

$$\mathcal{F} = E + \frac{\kappa_1}{\gamma}T + \frac{\kappa_1\kappa_2}{\gamma\sigma}I + \frac{\beta_b}{\xi}B$$

Let us begin by differentiating the Lyapunov function:

$$\begin{aligned}
\dot{\mathcal{F}} &= \dot{E} + \frac{\kappa_1}{\gamma}\dot{T} + \frac{\kappa_1\kappa_2}{\gamma\sigma}\dot{I} + \frac{\beta_b}{\xi}\dot{B} \\
&= \left(\beta_h\frac{I}{N} + \beta_b\frac{B}{N_B}\right)S - \kappa_1 E + \frac{\kappa_1}{\gamma}(\gamma E - \kappa_2 T) + \frac{\kappa_1\kappa_2}{\gamma\sigma}(\sigma T - \mu I) + \frac{\beta_b}{\xi}(\theta I - \xi B)
\end{aligned}$$

After some manipulation and rearranging we obtain $\dot{F}$ *in the following form:*

$$\begin{aligned}
\dot{\mathcal{F}} &= E\big(\frac{\kappa_1}{\gamma}\gamma - \kappa_1\big) + T\big(\frac{\kappa_1\kappa_2}{\gamma\sigma}\sigma - \frac{\kappa_1}{\gamma}\kappa_2\big) + I\big(\beta_h\frac{S}{N} + \beta_b\frac{\theta}{\xi} - \frac{\kappa_1\kappa_2\mu}{\gamma\sigma}\big) + B\big(\beta_b\frac{S}{N} - \beta_b\big) \\
&= I\left(\beta_h\frac{S}{N} + \beta_b\frac{\theta}{\xi} - \frac{\kappa_1\kappa_2\mu}{\gamma\sigma}\right) + B\beta_b\left(\frac{S}{N} - 1\right) \\
&= \frac{\kappa_1\kappa_2\mu}{\gamma\sigma}I\left(\frac{\gamma\sigma}{\kappa_1\kappa_2\mu}\left(\beta_h\frac{S}{N} + \beta_b\frac{\theta}{\xi}\right) - 1\right) + B\beta_b\left(\frac{S}{N} - 1\right)
\end{aligned}$$

As we are restricting our analysis to the feasibility region Ω*, hence the following two expression hold:* $\left(\frac{S}{N}\right) < 1$ *and* $\left(\frac{\theta}{\xi}\right) < 1$*. The first is obvious although the second is less so. The reason for* $\left(\frac{\theta}{\xi}\right) < 1$ *is*

recall that N_B is the maximum proportion of the environment that the entire herd may contaminate. Therefore, the following inequality holds:

$$1 \geqslant N_B \quad \Longrightarrow \quad 1 \geqslant \frac{\theta}{\xi} N \quad \Longrightarrow \quad \xi \geqslant \theta N \quad \Longrightarrow \quad \frac{\theta}{\xi} \leqslant 1$$

As both these equalities hold $\left(\frac{S}{N}\right) < 1$ and $\left(\frac{\theta}{\xi}\right) < 1$, therefore:

$$\dot{\mathcal{F}} = \frac{\kappa_1\kappa_2\mu}{\gamma\sigma} I\left(\frac{\gamma\sigma}{\kappa_1\kappa_2\mu}\left(\beta_h \frac{S}{N} + \beta_b \frac{\theta}{\xi}\right) - 1\right) + B\beta_b\left(\frac{S}{N} - 1\right) \leqslant \frac{\kappa_1\kappa_2\mu}{\gamma\sigma} I\left(\mathcal{R}_0 - 1\right) - B\beta_b\left(1 - \frac{\overline{S}}{N}\right)$$

Therefore, clearly we have demonstrated that $\dot{\mathcal{F}} \leqslant 0$ for $\mathcal{R}_0 < 1$ as $\overline{S} \leqslant N$ in Ω. The lyapunov function has therefore shown that the $\mathcal{DFE}$ is globally asymptotically stable (GAS) if $\dot{\mathcal{F}} < 0$.

5.2.4 *Endemic Equilibrium and its Stability*

Let us now consider the SETIB system's dynamics when the basic reproductive number is greater than unity (i.e. $\mathcal{R}_0 > 1$), what does this mean for the long term solutions? The definition of the endemic equilibrium ($\mathcal{EE} = (\overline{S}, \overline{E}, \overline{E}, \overline{T}, \overline{I}, \overline{B})$) for the SETIB system 5.1 is given below:

$$\begin{aligned}
\overline{S} &= \frac{\Lambda}{(\overline{\lambda^{**}} + \mu)} \\
\overline{E} &= \frac{\overline{\lambda^{**}}}{\kappa_1}\overline{S} \\
\overline{T} &= \frac{\gamma}{\kappa_2}\overline{E} = \frac{\gamma\overline{\lambda^{**}}}{\kappa_1\kappa_2}\overline{S} \\
\overline{I} &= \frac{\sigma}{\mu}\overline{T} = \frac{\gamma\sigma\overline{\lambda^{**}}}{\kappa_1\kappa_2\mu}\overline{S} \\
\overline{B} &= \frac{\theta}{\xi}\overline{I} = \frac{\theta}{\xi}\left(\frac{\gamma\sigma\overline{\lambda^{**}}}{\kappa_1\kappa_2\mu}\overline{S}\right)
\end{aligned} \tag{5.5}$$

Where, the force of infection for the herd at the endemic equilibrium for the SETIB system 5.1 is denoted by the following expression:

$$\overline{\lambda^{**}} = \beta_h \frac{\overline{I}}{\overline{N}} + \beta_B \frac{\overline{B}}{\overline{N_B}}$$

As the below theorem indicates, if the basic reproductive number is greater than unity (i.e. $\mathcal{R}_0 > 1$) then this endemic equilibrium is locally asymptotically stable.

Theorem 5.2.6 *When the basic reproductive number is greater than unity (i.e. $\mathcal{R}_0 > 1$) the unique endemic equilibrium $\mathcal{EE}$ of the SETIB system with initial condition in the feasibility region Ω is locally asymptotically stable.*

Proof 5.2.6 *The local asymptotically stability of the endemic equilibrium $\mathcal{EE}$ can be examined through analysing the linearised SETIB system (5.1). This Jacobian of our environmental contamination model is given below:*

$$J(\mathcal{EE}) = \begin{pmatrix} -(\lambda^{**}+\mu) & 0 & 0 & -\beta_h\frac{\overline{S}}{N} & -\beta_b\frac{\overline{S}}{N_B} \\ \lambda^{**} & -\kappa_1 & 0 & \beta_h\frac{\overline{S}}{N} & \beta_b\frac{\overline{S}}{N_B} \\ 0 & \gamma & -\kappa_2 & 0 & 0 \\ 0 & 0 & \sigma & -\mu & 0 \\ 0 & 0 & 0 & \theta & -\xi \end{pmatrix}$$

Where λ^{**} is again the force of infection for the SETIB model (e.g. $\lambda^{**} = \beta_h\frac{\overline{I}}{N} + \beta_b\frac{\overline{B}}{N_B}$. The following elementary row operations are preformed on the Jacobian:

$$R_1' \leftarrow R_1 + R_2, \qquad R_2' \leftarrow R_2 + \frac{\lambda^{**}}{\mu}R_1,$$
$$R_3' \leftarrow R_3 + \frac{\gamma}{\kappa_1\left(1+\frac{\lambda^{**}}{\mu}\right)}R_2, \qquad R_4' \leftarrow R_4 + \frac{\sigma}{\kappa_2}R_3,$$
$$R_5' \leftarrow R_5 + \frac{\theta\kappa_1\kappa_2(\lambda^{**}+\mu)}{\mu(\frac{\overline{S}}{N})\beta_h\gamma\sigma - \kappa_1\kappa_2(\lambda^{**}+\mu)}R_4$$

Where R_i' indicates that the new i^{th} row is obtained by combining scalar multiple of other rows.

The Jacobian of the matrix obtained after these row operations is presented below:

$$J(\mathcal{EE}) = \begin{pmatrix} -\mu & -\kappa_1 & 0 & 0 & 0 \\ 0 & -\kappa_1\left(1+\frac{\lambda^{**}}{\mu}\right) & 0 & \beta_h\frac{\overline{S}}{N} & \beta_b\frac{\overline{B}}{N_B} \\ 0 & 0 & -\kappa_2 & \frac{\overline{S}}{N}\left(\frac{\beta_h\gamma\mu}{\kappa_1(\lambda^{**}+\mu)}\right) & \frac{\overline{B}}{N_B}\left(\frac{\beta_b\gamma\mu}{\kappa_1(\lambda^{**}+\mu)}\right) \\ 0 & 0 & 0 & \mu\left(\frac{\beta_h\gamma\sigma\frac{\overline{S}}{N}-\kappa_1\kappa_2(\lambda^{**}+\mu)}{\kappa_1\kappa_2(\lambda^{**}+\mu)}\right) & \frac{\overline{B}}{N_B}\left(\frac{\beta_b\gamma\sigma\mu}{\kappa_1\kappa_2(\lambda^{**}+\mu)}\right) \\ 0 & 0 & 0 & 0 & \xi\left(\frac{\frac{\overline{B}}{N_B}\beta_b\sigma\gamma\frac{\theta}{\xi}}{\kappa_1\kappa_2(\lambda^{**}+\mu)-\beta_h\gamma\sigma\frac{\overline{S}}{N}}-1\right) \end{pmatrix}$$

The corresponding eigenvalues of the Jacobian must all be negative to prove that the endemic equilibrium ($\mathcal{EE}$) is locally asymptotically stable.

$$\lambda_1 = -\mu < 0, \qquad \lambda_2 = -\kappa_1\left(1+\frac{\lambda^{**}}{\mu}\right) < 0,$$
$$\lambda_3 = -\kappa_2 < 0, \qquad \lambda_4 = \mu\left(\frac{\beta_h\gamma\sigma\frac{\overline{S}}{N} - \kappa_1\kappa_2(\lambda^{**}+\mu)}{\kappa_1\kappa_2(\lambda^{**}+\mu)}\right),$$
$$\lambda_5 = \xi\left(\frac{\frac{\overline{B}}{N_B}\beta_b\sigma\gamma\frac{\theta}{\xi}}{\kappa_1\kappa_2(\lambda^{**}+\mu) - \beta_h\gamma\sigma\frac{\overline{S}}{N}} - 1\right)$$

As the eigenvalues $\lambda_1 < 0, \lambda_2 < 0, \lambda_3 < 0$ are all negative it remains to show that λ_4 and λ_5 are negative.

Notice that both λ_4 and λ_5 are negative if:

$$\beta_h \gamma \sigma \frac{\overline{S}}{N} + \beta_b \gamma \sigma \frac{\overline{B}}{N_B} - \kappa_1 \kappa_2 (\lambda^{**} + \mu) < 0$$

If the above inequality holds then λ_4 is negative:

$$\beta_h \gamma \sigma \frac{\overline{S}}{N} + \beta_b \gamma \sigma \frac{\overline{B}}{N_B} - \kappa_1 \kappa_2 (\lambda^{**} + \mu) < 0 \implies \beta_h \gamma \sigma \frac{\overline{S}}{N} - \kappa_1 \kappa_2 (\lambda^{**} + \mu) < 0$$

Similarly, if we examine the λ_5 eigenvalue we shall see that if the following inequality holds then $\lambda_5 < 0$.

$$\frac{\frac{\overline{B}}{N_B} \beta_b \sigma \gamma \frac{\theta}{\xi}}{\kappa_1 \kappa_2 (\lambda^{**} + \mu) - \beta_h \gamma \sigma \frac{\overline{S}}{N}} < 1$$

Therefore, through rearrange this inequality we see that is equivalent to the following inequality stated above:

$$\beta_h \gamma \sigma \frac{\overline{S}}{N} + \beta_b \gamma \sigma \frac{\overline{B}}{N_B} - \kappa_1 \kappa_2 (\lambda^{**} + \mu) < 0$$

Before we show this inequality we require the following expression, notice by inputting our explicit endemic equilibrium values for $\left(\frac{\overline{S}}{N}\right)$ and $\left(\frac{\overline{B}}{N_B}\right)$ the following equivalent expression for $\left(\lambda^{**} + \mu\right)$ is obtained:

$$\begin{aligned}
\lambda^{**} &= \beta_h \frac{\overline{I}}{N} + \beta_b \frac{\overline{B}}{N_B} \\
&= \beta_h \frac{\sigma\gamma}{\kappa_1 \kappa_2} \left(\frac{\lambda^{**}}{\lambda^{**} + \mu} \right) + \beta_b \frac{\theta}{\xi} \left(\frac{\sigma\gamma}{\kappa_1 \kappa_2} \right) \left(\frac{\lambda^{**}}{\lambda^{**} + \mu} \right) \\
&= \left(\frac{\lambda^{**}}{\lambda^{**} + \mu} \right) \mu \left(\frac{\gamma\sigma}{\kappa_1 \kappa_2 \mu} \right) \left(\beta_h + \beta_b \left(\frac{\theta}{\xi} \right) \right) \\
&= \left(\frac{\lambda^{**}}{\lambda^{**} + \mu} \right) \mu \mathcal{R}_0
\end{aligned}$$

Therefore the following equality is obtained:

$$\lambda^{**} + \mu = \mu \mathcal{R}_0$$

With the above equality in hand, let us now demonstrate the following inequality:

$$\begin{aligned}
\beta_h \gamma \sigma \frac{\overline{S}}{N} + \beta_b \gamma \sigma \frac{\overline{B}}{N_B} - \kappa_1 \kappa_2 (\lambda^{**} + \mu) &= \beta_h \gamma \sigma \frac{\overline{S}}{N} + \beta_b \gamma \sigma \frac{\overline{B}}{N_B} - \kappa_1 \kappa_2 \mu \mathcal{R}_0 \\
&= \kappa_1 \kappa_2 \mu \left(\frac{\gamma\sigma}{\kappa_1 \kappa_2 \mu} \left(\beta_h \frac{\overline{S}}{N} + \beta_b \frac{\theta}{\xi} \frac{\overline{B}}{N_B} \right) - \mathcal{R}_0 \right)
\end{aligned}$$

This proves the inequality $\beta_h \gamma \sigma \frac{\overline{S}}{N} + \beta_b \gamma \sigma \frac{\overline{B}}{N_B} - \kappa_1 \kappa_2 (\lambda^{**} + \mu) < 0$. As both our expression $\left(\frac{\overline{S}}{N}\right)$ and $\left(\frac{\overline{B}}{N_B}\right)$ are less than or equal to one, hence the following relationship holds:

$$\frac{\gamma\sigma}{\kappa_1\kappa_2\mu}\left(\beta_h\frac{\overline{S}}{N}+\beta_b\frac{\theta}{\xi}\frac{\overline{B}}{N_B}\right)<\frac{\gamma\sigma}{\kappa_1\kappa_2\mu}\left(\beta_h+\beta_b\frac{\theta}{\xi}\right)=\mathcal{R}_0$$

This proves that both λ_4 and λ_5 are negative, hence all eigenvalues of the Jacobian have negative real part which proves that the endemic equilibrium $\mathcal{EE}$ is locally asymptotically stable in Ω.

5.3 MODEL ANALYSIS

Let us compare and contrast the different dynamics in the SETIB model by exploring how our contamination parameter alter the system dynamics. First, let point out that as discussed in the mathematical properties element of this chapter, the environmental contamination compartment of this model $B(t)$ is bounded:

$$\limsup_{t\to\infty} B(t)\leqslant\frac{\theta}{\xi}\left(\frac{\Lambda}{\mu}\right)$$

Where these two parameter control the relative size of both the herd population $\left(\frac{\Lambda}{\mu}\right)$ and the environmental contamination $\left(\frac{\theta}{\xi}\right)$. For our model to make sense, these two scales must represent the system accurately. If we were to non-dimensionalise the SETIB model and re-scale parameters so the population size was regarded as one instead of $\frac{\Lambda}{\mu}$, then our contamination parameter $B(t)$ would have a maximum bound of $\frac{\theta}{\xi}$. However, the underlying biology of $B(t)$ means it represents the proportion of the total maximal proportion of the environment that can be contaminated; therefore, a natural upper bound of the $B(t)$ compartment is one (hence $\frac{\theta}{\xi}\leqslant 1$). However, consider what this would mean if $\frac{\theta}{\xi}=1$, this would mean that a full herd of infected cattle would then contaminate the entire environment (i.e. $B(t)=1$). This does not make sense biologically as the entire environment would not become fully contaminated, therefore the parameter $(\frac{\theta}{\xi})$ should represent the proportion of the environment that would become contaminated if the entire herd is infected. One paper [175] had somewhat relevant data, this paper used molecular detection protocols and identified widespread environmental contamination on a Portuguese farm. Where out of a total of 248 environmental samples, 38 detected M. bovis, although the overall proportion of samples that detected M. bovis was higher in feeding areas.

Although without further biological investigation into the M. bovis contamination effects, it is unlikely that realistic parameters would be found for N_B, θ and ξ directly. If we cannot obtain realistic parameters, then we are forced to use the data that is obtainable. If we assume the maximum environmental contamination is the same as the Portuguese paper[175] then this implies $\frac{\theta}{\xi}=\frac{38}{248}$. As discussed in the literature review, on average M. bovis survives in the soil for around six months [19], this implies $\xi=\frac{1}{0.5\times 365}$, using these two parameters estimates in conjunction we can estimate the contamination level shed by an infectious cattle

$\theta = \frac{38}{248 \times 0.5 \times 365} = 8.3959 \times 10^{-4}$.

The only remaining parameter that we need to find is β_b, although there is no available data to estimate this parameter. Let us achieve an estimate of this parameter indirectly, if instead we consider what the environmental contamination parameter β_b must be, if we consider that a proportion of infected cattle p result from environmental contamination. If we consider that only a modest number of cattle are infected by the environment (e.g. $p = 0.05$) then if we consider the force of infection at the endemic equilibrium, then the following equality is obtained

$$\frac{\frac{\beta_b \overline{B}}{N_B}}{\frac{\beta_h \overline{I}}{N}} = p \qquad \Longrightarrow \qquad \frac{\beta_b \overline{B}}{N_B} = p \frac{\beta_h \overline{I}}{N} \qquad \Longrightarrow \qquad \beta_b = p \beta_h$$

Therefore, lets use the model parameters from [64] and use a proportion $p = 0.05$ then we obtain the following estimate for $\beta_b = 2.2831 \times 10^{-4}$. Using these estimates in conjunction with the other model parameters from [64] the following data table gives our parameter estimates.

Parameter	Description	Baseline Value	Reference/Comment
Λ	Cattle Recruitment	4.56621×10^{-2}	[64]
μ	Natural Death Rate	4.56621	[64]
β_h	Cattle Infection rate	1.64383×10^{-3}	[64]
γ	Exposure Progression Rate	2.27945×10^{-2}	[64]
σ	Test Sensitive Progression Rate	9.47945×10^{-4}	[64]
ν	Infected Progression Rate	1.369863×10^{-3}	[64]
α	Relapsing Progression Rate	1.369863×10^{-3}	[64]
ξ	Contamination Decay Rate	5.47945×10^{-3}	Estimate/[20]
θ	Shedding Rate	8.3959×10^{-4}	Estimate
β_b	Environment Infection Rate	2.2831×10^{-4}	Estimate
N_B	Maximum Contamination Level	0.153226	Estimate/[175]

Substituting these parameters into the SETIB differential equations 5.1 and numerically simulating the disease spread we obtain the following results.

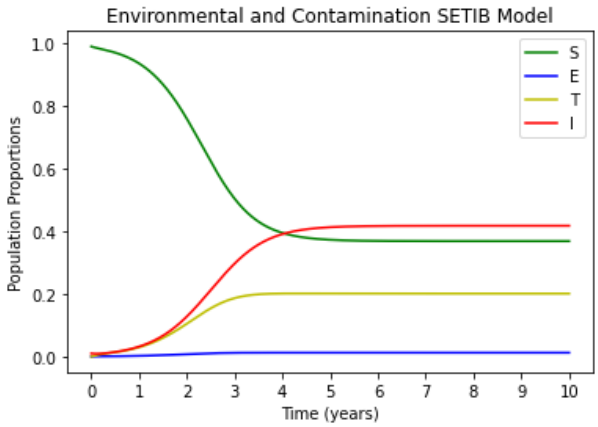

Figure 5.2: Transmission Dynamics of the SETIB model.

The basic reproductive number for the system $\mathcal{R}_0 = 2.7127$, as a result the endemic equilibrium is locally asymptotically stable which can be seen from figure 5.2. The proportional endemic equilibrium level for the different disease compartment on the farm are the following:

$$\frac{\overline{S}}{N} = 0.36863, \qquad \frac{\overline{E}}{N} = 0.01240, \qquad \frac{\overline{T}}{N} = 0.20123, \qquad \frac{\overline{I}}{N} = 0.417745,$$

The role of environmental contamination in bTB is further discussed and analysed in chapter six, where using a simulation model we aim to further understand the role of environmental contamination in persistent reinfections. As infected cattle contaminate the environment, this contamination lingers even if the animal is subsequently culled. In the simulation model, we examine the dual dynamics of environmental contamination and culling, where, by altering the level of environmental contamination we aim to further understand how this reinfects cattle. The simulation model incorporates more model mechanisms and therefore gives a more realistic representation than this environmental contamination SETIB model, therefore further analysis shall be completed in chapter six.

5.4 CONCLUSION

Cattle infected with bTB shed fomites and infect not just each other but also contaminate the environment, where the environment will continuously reinfect the herd with the disease. Therefore, after the herd has been tested and all subsequent positively detected hosts are removed, the contaminated environment may still infect susceptible cattle within the herd. In this chapter a mathematical model called the SETIB model for both direct and indirect transmission is proposed and investigated. The analyse of the system has shown that if the diseaseâs basic reproductive number is lower than unity (i.e. $\mathcal{R}_0 < 1$) the disease will be globally attracted to the unique disease free equilibrium. Similarly, when the basic reproductive

number increases past unity (i.e. $\mathcal{R}_0 > 1$ the endemic equilibrium becomes locally asymptotically stable. In the model analysis section of this chapter, we discussed the environmental contamination system parameters β_b, θ, and ξ, and as there are very few bTB modelling papers that examine environmental contamination, there exist no parameter values in the literature. In an effort to understand how the SETIB model operates, we estimate these parameters from the sparse data sources in the literature and then numerically simulated the disease dynamics.

The SETIB model represents the first step in furthering our understanding of the role of environmental contamination in the spread of bovine tuberculosis. Environmental contamination may be a significant factor in the spread of bovine tuberculosis and without further investigation, this factor may be under-represented in future research. From examining the literature on bTB in Cattle, there remain various gaps regarding the role of environmental contamination in the spread of bovine tuberculosis. While considering the limited cross-species direct interaction [66], continual disease resurgence in areas without badgers, the high longevity of bovine tuberculosis in different materials, and the close proximity of the confined herd during winter periods, there remains a strong possibility that environmental contamination could be an under-represented transmission pathway.

Overall, the methodology incorporates a fundamental notation of environmental contamination in a mathematical form that remains sufficiently mathematically tractable to produce the systemâs equilibriums and mathematically understand their behaviour. This is an important first step in understanding the role of environmental contamination, however, there remain many open questions. The main obstacle in furthering the mathematical modelling of the environmental contamination mechanic is data and its inherent limitation. Due to difficulties in quantifying how likely bTB may infect hosts as it decays, this model was forced to re-parameterise this model by normalising the environmental contamination using a theoretical maximum. However, if further data regarding environmental survival and infectivity of bTB were to become available, this model could be reformatted to incorporate this data.

Additionally, with further data sources, the underlying methodology governing the model could be enhanced to further incorporate the underlying environmental contamination drivers. The current model incorporates environmental contamination in a rudimental way, where all factors governing this contamination are aggregated into a singular infection rate and decay rate. However, environmental contamination is unlikely to act homogeneously across the farm, as there will likely be disease hotspots (e.g water troughs) through the various micro-environments of the farm. Further study should examine how to incorporate these micro-environments into the model, understanding how their varied environmental matrices

mediums and their different decay will further enhance this model.

To further understand the role of the environment in bTB infections other modelling methodologies could also be incorporated. Particularly, an agent-based PDE diffusion simulation may provide insights, each cow could be simulated to sheds bTB fomites into a farm representation. This methodology has the added advantage of being able to be tailored to exact farm layouts, allowing further research into infection-resistant architecture, as potential farms' layouts may enhance disease transmission. Through possible readjustment and added biosecurity measures, farms could be designed to reduce not just bTB but all livestock diseases.

6

CHAPTER 6: SIMULATING BOVINE TUBERCULOSIS TRANSMISSION

Throughout Mathematical epidemiology, simulation models have been extensively used to examine disease dynamics and to investigate control strategies, examples include bovine spongiform encephalopathy (BSE; e.g. Anderson et al., 1996), foot and mouth disease (FMD; e.g. Keeling et al., 2001; Morris et al., 2001), avian influenza (e.g. Sharkey et al., 2008), and classical swine fever (e.g. Boklund et al., 2009). A particularly strong advantage of simulations is their usefulness in supporting the decision-making process, simulations can explore disease prevention and eradication programmes by simulating plausible real-world scenarios (Merl et al., 2009; Szmaragd et al., 2010; Brooks-Pollock et al., 2014). In this chapter, through the use of simulations and their techniques we examine how the different model mechanics expressed throughout this thesis work in conjunction. The other mechanics were contemplated and considered through the lens of ODE dynamical systems, if this model was analysed using the same methods, the resulting inherent complexity of the set of differential equations would make the system very complicated to analyse, if not impossible with currently available methods. However, through the use of simulations and their techniques, much of the underlying complexity can be mitigated.

Computational models provide a flexible framework for designing different disease control and prevention strategies that would be incredibly complicated to analyse using dynamical system techniques. This framework provides researchers with the ability to incorporate a larger range of disease mechanics without significantly increasing the overall complexity of the simulation. For example, in this simulation we explicitly incorporate the UK test and detect strategy into this simulation, a feat that would be incredibly complicated using the ODE dynamical system framework. Moreover, simulations provide public health officials and other stakeholders with obtainable predictions to base decisions on, granting them the ability to design and test different control strategies.

The layout of this chapter starts with a concise and succinct description of the Gillespie algorithm, the computational techniques used to simulate the inter-herd dynamics of bTB. From there, we discuss and develop our computational model, where we explicitly incorporate the different mechanics discussed through this thesis; realistic latency period, wildlife reservoir, and environmental contamination. After the description of the material and methods behind the construction of the simulation, two main research themes are explored and investigated:

1. Infection Proportion and Residual Disease: In this section, we investigate the model predictions in terms of infection proportion and residual disease under two different scenarios (with and without culling). Firstly, this simulation quantifies and analysis the different infection proportions, trying to understand the main routes of infection. Secondly, as discussed in depth in the literature review chapter, after culling occurs on a farm there is often residue disease left on the farm. What are the sources of the residual disease remaining on a farm? This section shall quantify the proportions of future infections that occur when the herd is in lockdown (e.g. latency, wildlife reservoir, and environmental contamination). Through a better understanding of these proportions, researchers will gain further insight into how to mitigate persistent infections.

2. Badger's Contribution: The second theme examines how an associated wildlife reservoir contributes to the disease dynamics. This section investigates the change in dynamics in the model by both fully and partially excluding the wildlife reservoir. This partial removal of the wildlife reservoir and its influences is achievable in real-world scenarios, as this represents what would occur if a farm were to increase bio-security measures.

This chapter then concluded by discussing the simulation predictions and implications for the UK cattle industry bTB control strategy; followed by a discussion regarding the simulation and its data limitations and a concise summary.

6.1 GILLESPIE ALGORITHM

This section reviews the Gillespie algorithm's mathematical concepts, describing what this algorithm is and what they are used for. Simply put, Gillespie algorithms generate one possible trajectory to a set of stochastic equations. Originally developed by Dan Gillespie in 1977 [176], to simulate biochemical reaction systems both efficiently and accurately while using limited computational power. This development sparked a modelling revolution and Gillespie algorithms are now used throughout mathematical biology and various other fields to simulate complex systems [86]. For example, one use case of Gillespie algorithms pertaining to this chapter is the modelling of stochastic epidemic dynamics of a population, in which the number of infectious individuals varies over time. These Gillespie algorithms simulate the disease dynamics according to a predefined parameterised mathematical model, where this set of rules governs how the system or individual changes over time. In the previous chapter, the focus was on deterministic dynamical systems, as these models are deterministic then given the same initial conditions the model behaves the same each time. Gillespie algorithms simulate stochastic processes, primarily driven by discrete events taking place in continuous time, therefore each model output will generally differ.

The general idea of how the Gillespie algorithm works is twofold; firstly the Gillespie algorithm selects the next event to occur out of all possible future events. The selection process is achieved by randomly selecting one event from all possible events, where the probability of an event being selected is weighted according to its proportional probability. Secondly, the Gillespie algorithm determines when this event occurs. For example, suppose it is currently time t, the Gillespie algorithm determines the time step until this event τ, where τ is a random number according to the exponential distribution scaled by the sum of all possible process rates. The Gillespie algorithm will then randomly select an event, where the probability of selection is weighted by the relative likelihood that event will occur. This process is then iterated continuously for a given time period or until one particular event occurs.

There are numerous texts dedicated to explaining Gillespie algorithms, for further discussion and concrete examples see [176],[177]. The Gillespie algorithm is now a standard tool used throughout mathematical epidemiology. The next section discusses the construction of our simulation and how the various disease mechanics are incorporated.

6.2 MATERIALS AND METHODS

The disease dynamics of a herd are modelled by employing a non-linear stochastic multi-agent model and by using a Gillespie algorithm we can generate a statistically correct trajectory (possible solutions) of the stochastic equation system. The description of this model is split into two main sections; firstly, we explain the underlying mechanisms behind the model. Where we inspect each incorporated mechanic and investigate how they operate in conjunction with each other. The second half of this description focuses on the data parameters associated with the different components of the model. As discussed throughout the previous chapter, the literature has various data inconsistencies and inaccuracies, this section explains how the various epidemiological parameters have been generated.

6.2.1 *Simulation Model Methods*

An overview of our non-linear Gillespie algorithm-based simulation works primarily through the use of differential equations with modified environmental contamination, culling procedure, and demographics. In this simulation, the cattle disease cycle is based on the SE^nT^mIRC model, therefore cattle can either be susceptible, exposed, test sensitive, infected, or relapsed, where there are an n and m arbitrary number of exposed and test sensitive compartments. Unless otherwise stated the number of compartments (n and m) in the simulation are equal to one. Whereas, the wildlife reservoir disease cycle operates on a reduced form, as badgers

may only be susceptible S_B, exposed E_B or infected I_B.

The different transmission pathways for cattle are as follows; cattle to cattle transmission, badger to cattle transmission, and environmental contamination transmissions, where each operates under the mass action principle, therefore the force of infection for this model is given by:

$$S_h\left(\beta_{hh}\frac{I_h}{N_h}+\beta_{bh}\frac{I_b}{N_b}+\beta_{hB}\frac{B}{N_B}\right)$$

Similarly, for badgers the force of infection is given by:

$$S_b\left(\beta_{bb}\frac{I_b}{N_b}+\beta_{hb}\frac{I_h}{N_h}+\beta_{bB}\frac{B}{N_B}\right)$$

The deterministic versions of the differential equations that govern disease progression for this simulation are given below, although, as discussed in the forthcoming section, other mechanics such as demographics are altered.

Cattle Differential Equations

$$\frac{dS_h}{dt} = \mu_h N_h - \left(\beta_{hh}\frac{I_h}{N_h} + \beta_{bh}\frac{I_b}{N_b} + \beta_{hB}\frac{B}{N_B}\right)S_h - (\mu_h + \tau_1)S_h$$
$$\frac{dE_{h1}}{dt} = \left(\beta_{hh}\frac{I_h}{N_h} + \beta_{bh}\frac{I_b}{N_b} + \beta_{hB}\frac{B}{N_B}\right)S_h - (\mu_h + \tau_1 + \gamma_h)E_1$$
$$\frac{dE_{h2}}{dt} = \gamma_h E_{h1} - (\mu_h + \tau_1 + \gamma_h)E_{h2}$$
$$\dots$$
$$\frac{dE_{hn}}{dt} = \gamma_h E_{hn-1} - (\mu_h + \tau_1 + \gamma_h)E_{hn}$$
$$\frac{dT_{h1}}{dt} = \gamma_h E_{hn} - (\mu_h + \tau_2 + \sigma)T_{h1}$$
$$\frac{dT_{h2}}{dt} = \sigma T_{h1} - (\mu_h + \tau_2 + \sigma)T_{h2}$$
$$\dots$$
$$\frac{dT_{hm}}{dt} = \gamma_h T_{hm-1} - (\mu_h + \tau_2 + \gamma_h)T_{hm}$$
$$\frac{dI_h}{dt} = \sigma T_{hm} + \alpha R_h - (\mu_h + \tau_2 + \nu)I_h$$
$$\frac{dR_h}{dt} = \nu I_h - (\mu_h + \tau_2 + \alpha)R_h$$
$$\frac{dC_h}{dt} = \tau_1\left(S_h + \sum_{i=1}^{n} E_{hi}\right) + \tau_2\left(\sum_{j=1}^{m} T_{hj} + I_h + R_h\right) - \mu_h C_h$$

Badger Differential Equations

$$\frac{dS_b}{dt} = \mu_b N_b - \left(\beta_{bb}\frac{I_b}{N_b} + \beta_{hb}\frac{I_h}{N_h} + \beta_{bB}\frac{B}{N_B}\right)S_b - \mu_b S_b$$
$$\frac{dE_b}{dt} = \left(\beta_{bb}\frac{I_b}{N_b} + \beta_{hb}\frac{I_h}{N_h} + \beta_{bB}\frac{B}{N_B}\right)S_b - (\mu_b + \gamma_{hb})E_b$$
$$\frac{dI_b}{dt} = \gamma_b E_b - \mu_b I_b$$

Environmental Contamination Differential Equations

$$\frac{dB}{dt} = \theta_h I_h + \theta_b I_b - \xi B$$

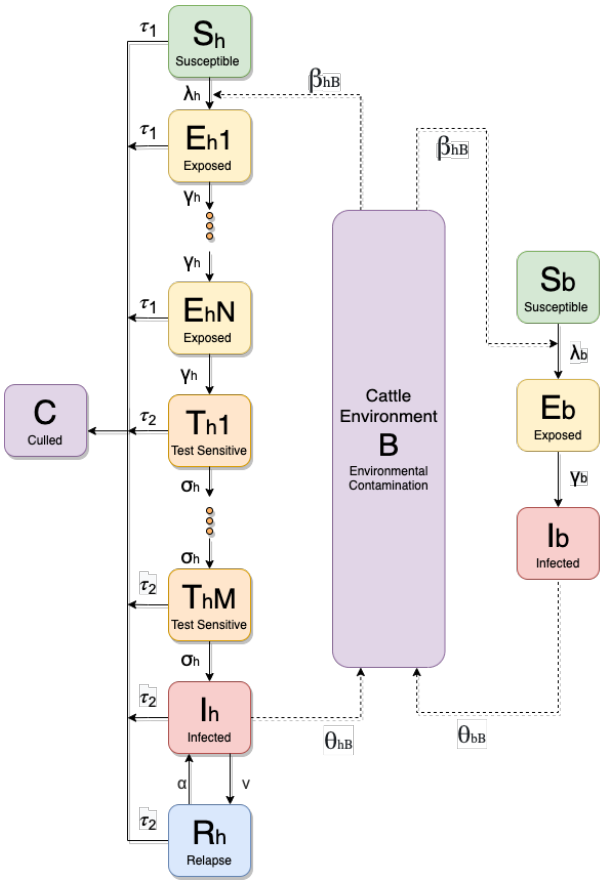

Figure 6.1: A flow diagram model representation of the interconnected dynamics of bTB flowing between the cattle and badgers populations.

6.2.1.1 *Demographics*

In an attempt to focus on the internal dynamics on the farm, without considering the added complexity of demographic dynamics, this simulation keeps the demographics component to a minimal. As a result, the livestock and wildlife reservoir populations are kept constant. In the Gillespie algorithm, when either a host from the cattle or badger population dies of natural deaths μ, the host is immediately replaced with a new susceptible host. A host's natural death rate (μ_h or μ_B) depends on the individual being considered; cattle (μ_h) or badgers (μ_B).

6.2.1.2 *Environmental Contamination*

In the simulation, badgers transmit the disease directly and indirectly, as they infect cattle by contributing to contamination of the joint landscape $B(t)$. Infected cattle and badgers contribute to environmental contamination, after each time period the cattle and badgers contaminate the environment at rates θ_h and θ_b respectively, where this contamination decays

according to the ξ. Hence, the continuous differential equations that govern environmental contamination is given by:

$$\frac{dB}{dt} = \theta_h I_h + \theta_b I_b - \xi B$$

Unlikely the other disease mechanics, environmental contamination works continuously and not stochastically. In the Gillespie algorithm, other disease mechanics such as transmission work stochastically, for example, the rate at which a cattle transition from the exposed compartment is random. In contrast, environmental contamination mechanics is better suited to a continuous approach, so the environmental contamination level is continuously updated between events. Otherwise, if no distinction between environmental contamination and other disease mechanics is made, then it would be possible for long period to occur where infectious cattle do not contaminate the environment which is biologically unrealistic.

This mixed modelling approach permits infected cattle and badgers to continuously contaminate the environment at every time period. In the Gillespie algorithm, the environmental contamination level is updated after every selected event, where the jump time and the environmental contamination parameters are used to inform the updated contamination level.

6.2.1.3 *Culling*

Culling operates differently in the simulation compared to how culling has been implemented previously in this thesis. The culling mechanic should be modelled as close as possible to the underlying biological situation in order to accurately capture the actual dynamics of the bTB dynamics within a UK cattle herd. In the simulation, the UK's test and slaughter strategy are no longer models culling at a constant rate, instead culling is operated accustom to the UK test and detection strategy.

Herds are subjected to whole herd testing at least once every two years, representing a herd in a low incidence area [93]. All hosts detected with bTB are culled immediately and replaced with susceptible cattle. In the simulation, once a herd is identified as infectious then the herd is continuously tested every 30 days until two consecutive whole herd tests are passed. Once cleared, the same herd is then tested again two years later.

6.2.2 *Simulation Model Data Values and Time Step*

All parameters in this model related to time are defined on a daily basis, where this model time step variable depends on the number of possible events. The time step used in the model is a random exponentially distributed variable depending on the total probability of all possible next events. Otherwise, if we instead fixed the time step, the arbitrary nature of the n

and m number of compartments in the exposed and test sensitive stages means that the time step can become arbitrary short, increasing computation time.

In order to account for the bTB dynamics simulated scenarios, each simulation is repeated using different seed numbers 250 times. This number of iterations allows us to be confident that the simulation result accurately represents the true underlying distribution of results.

Parameter	Description	Baseline Value	Comment/Reference
μ_h	Cattle Natural Death Rate	4.56621×10^{-2}	[64]
μ_b	Badger Natural Death Rate	3.044140×10^{-4}	[178]
γ_h	Cattle Exposure Progression Rate	2.27945×10^{-2}	Exponential Value/[179]
γ_b	Badger Exposure Progression Rate	7.692307×10^{-3}	[179]
σ_h	Test Sensitive Progression Rate	9.47945×10^{-4}	Exponential Value/[179]
ν_h	Infected Progression Rate	1.369863×10^{-3}	[64]
α_h	Relapsing Progression Rate	1.369863×10^{-3}	[64]
ξ	Contamination Decay Rate	5.47945×10^{-3}	Estimate/[20]
θ_h,θ_b	Shedding Rate	5.997×10^{-7}	Estimate
β_{Bh}, β_{Bb}	Environment Infection Rate	2.2831×10^{-5}	Estimate
N_B	Maximum Contamination Level	0.153226	Estimate/[175]
β_{hh}	Cattle to Cattle	6.3×10^{-6}	[179]
β_{hb}	Cattle to Badger	2.45×10^{-6}	[179]
β_{bh}	Badger to Cattle	4.39×10^{-6}	[179]
β_{bb}	Badger to Badger	1.64383×10^{-6}	[179]
τ_2	SICCT Detection rate	0.506	[179]

Likewise to chapter five, we must estimate the environmental contamination parameters θ_h, θ_b, β_{Bb}, β_{Bh}, ξ and N_B. Let us use the same estimation as discussed within that chapter, although N_B must be changed to account for the wildlife reservoir. Chapter five indicated that N_B should represent the maximum upper bound of environmental contamination, although this bound must be altered if we incorporate a wildlife reservoir as they also contaminate the environment. The maximum bound for environmental contamination $B(t)$ in this simulation is:

$$N_B = \frac{\theta_h N_h + \theta_b N_b}{\xi}$$

Similarly, without further biological investigation into the M. bovis contamination effects, it is unlikely that realistic parameters would be found for N_B, θ and ξ in the literature. If we cannot obtain realistic parameters, then we are forced to use the data that is obtainable. If we assume the maximum environmental contamination is the same as the Portuguese paper [175] then this implies $N_B = \frac{38}{248}$. Similarly, as discussed in the literature review, on average M. bovis survives in the soil for around six months [79], this implies $\xi = \frac{1}{0.5\times 365}$. Using these two parameter estimates in conjunction, we can estimate the contamination level shed by both infectious cattle and badgers if we assume they both contaminate at the same rate (i.e. $\theta_h = \theta_b$).

$$N_B = \frac{\theta_h N_h + \theta_b N_b}{\xi} \quad \Longrightarrow \quad \frac{38}{248} = \theta_h \frac{110+30}{\frac{1}{0.5\times 365}} \quad \Longrightarrow \quad \theta_h = \theta_b = 5.997 \times 10^{-6}.$$

6.2.2.1 *Initialisation*

All scenarios are initiated under the same initial conditions unless otherwise stated. The system variable's initial conditions are as follows: out of the average UK herd size of 110 [49], ten cattle are considered infectious, with the rest being susceptible. For the wildlife reservoir population, this population is initialised with 30 susceptible badgers with no infected badgers [49]. The Gillespie algorithm's time step between events depends on the number of possible events. This simulation uses the standard Gillespie algorithm approach of generating a random time step, this random time step is an exponentially distributed variable with a shape parameter equal to the total probability of all possible next events. At the beginning of the simulation ($t = 0$), the simulation is initialised with the above conditions and is left to continuously jump forward until either one of two events occurs, 100 years pass or all infectious sources are removed from the system.

In this chapter, various different scenarios are investigated in order to compare and contrast the bTB dynamics of each scenario accurately; each different scenario is repeated 250 times with the same initial conditions. The first of our research themes is analysed in the next section.

6.3 INFECTION PROPORTION AND RESIDUAL DISEASE

This section investigates two main questions related to the infection proportion and residual disease found on a farm:

- Infection Proportion: In order to construct a base case that we can compare the other scenarios to we will first begin by simply generating the system with described initial conditions. This base case is calculated under two different circumstances; one version

incorporates the culling mechanic while the other does not. In this section, we shall compare and contrast the overall infection numbers of these two circumstances and discuss the culling strategy's effectiveness.

- Residual Disease and Persistent Infections: As discussed in depth in the literature review chapter, after culling occurs on a farm there is often residue disease left on the farm. What are the sources of the residual disease remaining on a farm? This section shall quantify the proportions of future infections that occur when the herd is in and out of lockdown (e.g. latency, wildlife reservoir, and environmental contamination). By better understanding these proportions, researchers will gain further insight into how to mitigate persistent infections.

6.3.1 *Infection Proportion Results*

The first base case we shall discuss is the infection proportion with no culling.

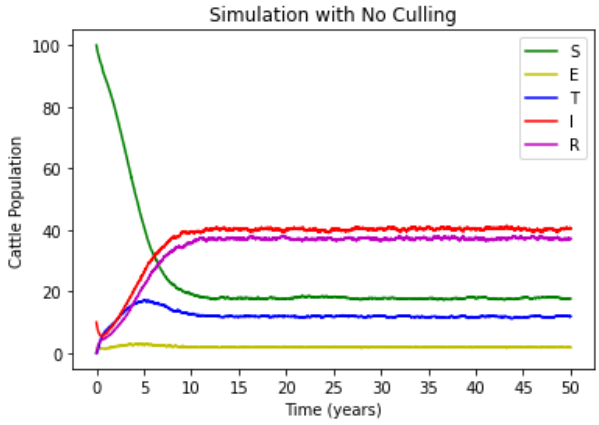

Figure 6.2: The disease dynamics of the simulation model with no culling.

Figure 6.2 above represents the average compartment proportions for this simulation model with no culling. This graphic clearly depicts that infection level tends to some endemic equilibrium with the following herd percentages:

$$\mathcal{EE}\Big(S_h, E_h, T_h, I_h, R_h\Big) = \mathcal{EE}\Big(17.36, 1.931, 12.13, 40.38, 37.32\Big)$$

Under the literature parameters, this simulation indicates that without intervention, once disease is introduced to a herd it will continue to grow and spread until it reaches the endemic equilibrium. In only one out of 250 independent simulations, the disease goes extinct. Let us now turn our attention to the differing disease transmission pathways that infect cattle; on average cattle to cattle transmission accounted for 90.1% of all cattle infections, badger to cattle caused 4.2% of infections, and lastly 5.7% were caused by environmental contamination.

Let us now compare and contrast this model results with the same simulation, however in this simulation, a realistic representation of the UK test and cull strategy is incorporated. The main difference that culling introduces is that the disease is more likely to go extinct. In a singular simulation iteration, a disease is deemed to have gone extinct if there are currently only susceptible hosts and the environmental contamination level (B(t)) is below 0.1% of its theoretical maximum. Out of the 250 simulation runs with culling, the disease went extinct in 76 simulations.

Further investigation of disease extinction revealed an interesting phenomenon, as demonstrated in figure 6.4, if we look at the distribution of extinction times below, we see that all simulations went extinct within the first 22 years, with the distribution peaking at 10 years.

Further analysis of this behaviour indicated that the wildlife reservoir disease mechanic prevented infection extinction from occurring later. Within all simulations in which the disease went extinct, the infection had not been transmitted to the wildlife reservoir or if it was transmitted to the badger population, the disease died out before it could gather a foothold. As simulation time increases over 22 years, it becomes increasingly unlikely that the disease had not spread to the wildlife population. After the badger population becomes infectious, this prevents a herd from achieving disease extinction, as the disease continually spills over from the badger population onto the herd.

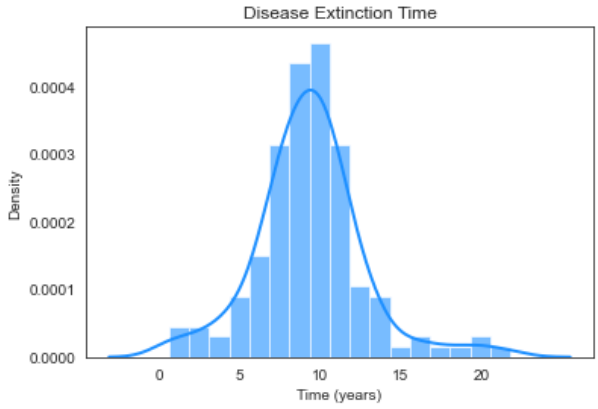

Figure 6.3: The distribution of the extinction time of the disease.

The disease continued to re-emerge in the simulation runs in which bTB became endemic in the wildlife reservoir. The adjusted disease dynamics are represented below, where this graphic depicts the average compartment proportions for simulations in which the epidemic did not die out.

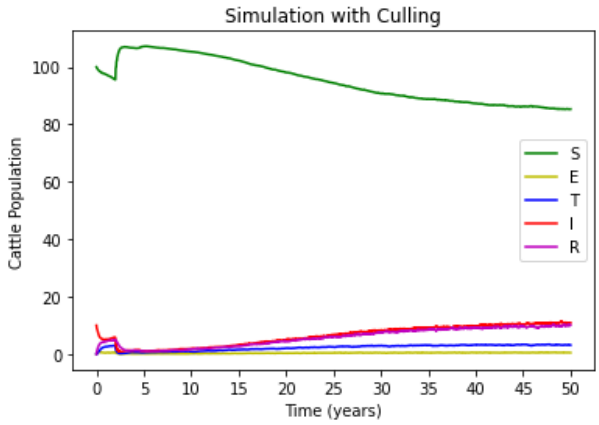

Figure 6.4: The disease dynamics of the simulation model with culling.

Similar to the previous graphic, the disease dynamics depict that infection tends to some endemic equilibrium with the following herd percentages:

$$\mathcal{EE}\Big(S_h, E_h, T_h, I_h, R_h\Big) = \mathcal{EE}\Big(84.2, 0.541, 3.36, 11.3, 10.6\Big)$$

If we compare the two graphics (Figure 6.2 and 6.4), we do see a stark difference in the endemic equilibrium values, clearly indicating the effectiveness of the UK culling strategy.

Cattle's transmission pathways also change if the simulation incorporates culling. In the simulations, cattle to cattle transmission accounted for 87.05% of all cattle infections on average, badger to cattle transmission caused 4.85% of all infections, and lastly 8.1% were caused by environmental contamination transmission. Clearly, incorporating the UK test and surveillance strategy does affect the infection proportion, as demonstrated by the differences in the infection proportion between the simulation with culling and without. Further analysis indicates that during herd lockdown periods, these infection proportions change once again, as on average cattle to cattle transmission dropped to 78.97%, badger to cattle transmission increased to 6.35%, and lastly, 14.68% of all cattle infections were caused by environmental contamination.

This analysis indicated a fundamental property of persistent infection, indeed, cattle to cattle transmission is the dominant factor in bTB transmission even when a herd is in lockdown. However, interestingly environmental contamination transmission proportion increased around threefold when only considering the lockdown period. Recall from the previous section in which we discussed the epidemiological parameters for this simulation, environmental contamination was constructed to be only around 5% as infectious when compared to cattle to cattle transmission. However during herd lockdown, both environmental contamination and badger to cattle transmission pathways began infecting a relatively higher percentage of cattle. Suppose this 5% under-represents the environmental contamination parameters (many

researchers do believe this is the case) then the relative proportion of new infections caused by environmental contamination during lockdown could be significantly larger.

In the section, we compared and constructed the average level of infections in cattle, infection proportion, and disease extinction for the system with and without culling. The results indicate that the UK test and surveillance strategy is effective, although there is still considerable room for improvement. In the scenario where no test and surveillance strategy was implemented, the disease was maintained in nearly all simulation iterations. Moreover, the average infection level for the 250 iterations was substantial throughout all simulations, the average percentage of cattle that were susceptible at the end was only 17.36%, while the other 82.64% of the herd were some form of infected. The situation completely changed if the UK test and surveillance strategy is implemented, as on average 84.2% of all cattle remained susceptible, clearly implying that culling substantially reduced the average level of infection. Further analysis demonstrated that culling also changes the overall infection proportion for each disease transmission, as culling reduced the relative percentage of infection from cattle to cattle transmission. This is particularly apparent if we only consider infections induced during lockdown periods, as the portion of infections caused by environmental contamination substantially increased from 8.1% to 14.68%.

6.4 BADGER'S CONTRIBUTION

In this section, we focus on the role of the wildlife reservoir and how the system dynamics change through both fully and partially excluding the wildlife reservoir. The decoupling of the badger and cattle populations represents how a herd's disease dynamics change by increasing biosecurity measures. In our analysis, we pay particular attention to how decoupling badgers and cattle can affect disease extinction levels.

To investigate the effects of wildlife reservoir decoupling, the simulation is repeated under five different scenarios, each further reducing the influence of the wildlife reservoir from the system. The reduction of the wildlife reservoir's impact is achieved by lowering badger parameters ($\beta_{bh}, \beta_{hb}, \theta_b, \beta_{Bb}$) by the factor p, where p is one of the following values $[1.0, 0.75, 0.5, 0.25, 0]$. By reducing p through these parameters, the behaviour ranges from no increased biosecurity measures ($p = 1.0$), slight improvement in biosecurity measures ($p = 0.75$), medium improvement in biosecurity measures ($p = 0.50$), significant improvement in biosecurity measures ($p = 0.25$), complete decoupling of these populations ($p = 0$). The figure below represents the different distribution of extinction time for the different scenarios:

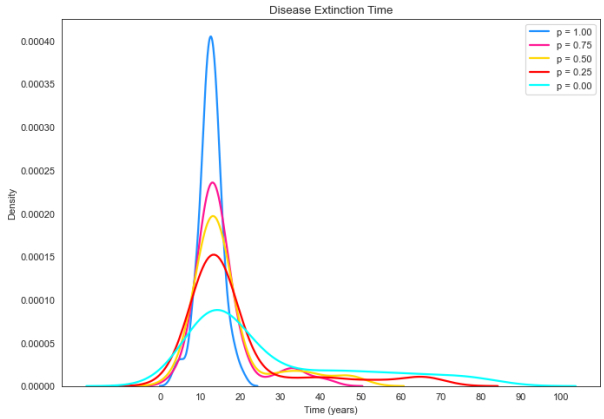

Figure 6.5: The differing distribution of extinction time of our five scenarios, where we vary decouple the wildlife and reservoir populations.

The simulation demonstrates a crucial principle related to the control of bTB, if we decouple the badger and cattle populations, on average, the probability that bTB will go extinct increases.

As discussed in the previous section, if $p = 1$, then the disease goes extinct in 76 out of the 250 simulations, which means that 30.4% of our simulations do not reach the 100 year iteration time. The corresponding values for the other p values are as follows:

- For $p = 0.75$, out of 250 different iterations, in 93 the disease becomes extinct (37.3%).
- For $p = 0.50$, out of 250 different iterations, in 109 the disease becomes extinct (43.6%).
- For $p = 0.25$, out of 250 different iterations, in 152 the disease becomes extinct (60.8%).
- For $p = 0.00$, out of 250 different iterations, in 175 the disease becomes extinct (70%).

Examination of figure 6.5 paints a detailed picture, when $p = 1.00$ extinctions rarely happen after the first 20 years as previously discussed. In this discussion, further analysis demonstrated that bTB had most likely not achieved a foothold in the wildlife reservoir after this point. However, as we reduce p and decouple the cattle and badger populations, then the wildlife reservoir has less influence on the dynamics, allowing the disease to become extinct in more herds and at a later point in time. This simulation indicates that increasing biosecurity measures would profoundly affect disease dynamics, as a larger portion of herds would be able to eradicate the disease.

6.5 SENSITIVITY ANALYSIS

In this section, we analyse and discuss the underlying sensitivity of our parameter to perturbation with some sensitivity analysis. In this section we examine the sensitivity of parameters in two main themes:

1. **Domestic Cattle Average Lifespan:** In this section we examine the effects of extending and subtracting the average lifespan of both cattle and badgers, in an effort to further understand the relationship between shortened domestic cattle lifespan and the lifeline burden of bovine tuberculosis extensive latency period.

2. **Cross Pathway Transmission Rates:** In this subsection we examine the overall infection rates utilised in the simulation model; Cattle, Badger, Cross Species and Environmental. Attempting to understand how increases and decreases in each of the infection rates, contribute and affect the overall infection level of the simulation.

The metric used to understand the sensitivity analysis results is the average proportion of the total herd proportion made up of susceptible cattle in the 15 years. The 15-year cut-off period was constructed from some experimental analysis of the simulation, this period gives enough room for the average distribution and its characteristics to alter without being weighted down from results where the system is at equilibrium. For a baseline the simulation was run 1000 times to generate the average whiteout any alteration. The average of these simulations indicates that on average the total average proportion of susceptible in the first 15 years of bTB being introduced was 93.92985%.

In the forthcoming analysis, each different parameter will be examined in relation to this metric, where we shall examine what effects an increase and decrease of 10% will cause.

6.5.1 *Domestic Cattle Average Lifespan:*

This section aims to understand the effects of extending and subtracting the average lifespan of both cattle and badgers. By understanding the relationship between shortened domestic cattle lifespan and the lifeline burden of bovine tuberculosis's extensive latency period, farmers will be more able to actively monitor herd duration. Three different pieces of sensitivity analysis were conducted; increased/decreased domestic cattle lifespan only, altering badger lifespan only, and altering both of these simultaneously. In the analysis below, we predominately focus on the result that only altered cattle lifespan only. As while examining the results, we see that increasing and decreasing badger lifespan had virtually no effect on overall results. Where the largest magnitude of difference that badger contributed was an average increase of 0.00023% in infection proportion.

If we compare this to the overall effect of altering cattle's lifespan, we see that altering cattleâs lifespan has a more material influence, but still ill a relatively small impact. There was an 0.02717% increase in disease portion when cattle lives were 10% longer on average.

Similarly, there was a 0.02465% decrease in disease portion when cattle lives were 10% shorter on average. Further analysis of these results showed that when livestock lived longer, there is a higher chance of the infected cattle becoming infected and infecting other cattle. Whereas, when cattle have a shorter lifespan, there is a marginally higher chance of the exposed host dying before becoming infected and infecting other hosts. From this perspective, these marginal changes follow the expected rank ordering, and the overall magnitude of these alterations makes intuitive sense.

6.5.2 *Cross Pathway Transmission Rates:*

The model is significantly more sensitive to alterations of Cross Pathway Transmission Rates compared to altering the average lifespan of cattle. In this section, we investigate the given sensitivity of four given scenarios, altering the cattle to cattle transmission, badger-to-badger transmission, cross-species transmission, and lastly, we alter environmental transmission. Where alteration to the cross-species transmission includes a 10% increase or decrease to both cattle to badger transmission and badger to cattle transmission. Let us begin with the model most sensitive parameter, the cattle to cattle transmission parameter:

If the beta used to model infection between cattle is increased by 10% we see a compensatory decrease of the susceptible proportion of 2.3690%. Whereas, if this cattle transmission beta is decreased, there is a corresponding increase to the average susceptible proportion of 1.6781%. This alteration of infection proportion shows that infection numbers are indeed sensitive to changes in cattle transmission rates, this makes intuitive sense as the literature indicates that cattle transmission is the largest component of infection. The model is inherently sensitive to alteration of this parameter, where similar to the previous analysis, the increases and decreases align with intuition. As an overall increase in the cattle transmission parameter corresponds to a decrease of overall susceptible levels of the model. Similarly, an overall decrease of cattle transmission parameters corresponds to an increase in the number of susceptible hosts within the system.

Two important differences stood out when we analysed the altered cattle transmission beta:

1. These alterations correspond to the largest magnitude changes in the model and hence represent the most sensitive model parameter to these changes in cattle transmission beta. As these overall changes in the model infection proportion represent the largest in our given analysis.

2. When comparing the different infection proportions under the different scenarios considered, we see that Cross Pathway Transmission Rates have the highest variance in

results. Where the standard deviation for the 1000 simulation runs of the average infection proportion was around 0.632% for the case when infection rates increased. Similarly, for the scenarios where we decreased the infection beta transmission parameter, we see there is similar standard deviation of around 0.5892%.

If we instead compare the difference in cattle-to-cattle transmission to the other scenarios considered (badger to badger, cross-species, and environmental transmission), we see the model is less sensitive to changes to either badger-to-badger transmission or cross-species transmission. For example, if we consider the badger-to-badger alterations, we see this makes virtually no difference to the overall infection proportion. As, if the badger-to-badger transmission is increased by 10% we see a compensatory decrease of the susceptible proportion of 0.02821%. Similarly, if the badger-to-badger transmission is decreased by 10% we see a compensatory increase of the susceptible proportion of 0.01393%. Again, comparisons between cattle-to-cattle transmission and cross-species transmission show that the model is not very sensitive to changes in cross-species transmissions. As, if the cross-species transmission is increased by 10% we see a compensatory decrease of the susceptible proportion of 0.043522%. Similarly, if the cross-species transmission is decreased by 10% we see a compensatory increase of the susceptible proportion of 0.02337%. Lastly, by increasing the environmental beta transmission by 10% we see a marginal increase to the average infection portion (0.0034291%) if the beta is increased, and a similar marginal decrease to the infection proportion if the environment is decreased (0.002776%).

After some reflection this analysis makes sense from an intuitive perspective, cross-species, badger-to-badger, and environmental transmission pathways should have a smaller material impact for two reasons:

1. Both cross-species and badger-to-badger transmission parameters infect very few cattle compared to cattle-to-cattle, instead their detrimental role focus on disease continuation. These factors cause overflow from the reservoir to continuously preserve or reinfect the cattle hosts. The small increase in transmission parameters will only cause continuation in very few herds and as a result, have little influence on infection proportion.

2. Secondly, the sensitivity analysis metric used to compare results (average proportion of the total herd proportion made up by susceptible cattle in the 15 years) will intrinsically pick up the difference in cattle population more effectively than the difference in the badger population. By creating a metric with a similar focus to the UK cattle industry, we intrinsically focus on cattle infection numbers. A more accurate depiction of how these other beta transmissions influence the disease proportion would be to analyse bTB lifespan within the system for the different transmission parameters. As these transmission parameters are increased and decreased, there would be a corresponding

extension or shrinkage of disease survival time. However, similar issues would affect this metric, as badger and cross-species transmissions would more heavenly influence this metric. After some consideration, our original metric (average proportion of the total herd proportion made up by susceptible cattle in the 15 years) was selected to match the focus of the UK cattle industry.

6.5.3 *Sensitivity Analysis Summary*

The sensitive analysis conducted on this simulation at an overall level replicates the findings of the literature, the model is most sensitive to changes in the cattle-to-cattle beta transmission. Where a 10% increase in this parameter induces a 2.3690% increase in the average infection proportion in the first 15 years. Cattle-to-Cattle transmission beta has by far the largest increase in the average infection proportion, as the next largest increase was 0.043522% caused by a 10% increase in cross-species transmission. During discussions regarding the results of this analysis, the model was less sensitive to changes in other transmission parameters partly because of the nature of the model but also by the nature of the sensitive analysis metric used to analyse the results. Alternative metrics could have been examined, however each metric would intrinsically focus on one model characteristic over another. In the end, this metric was selected to focus on the factors important for the UK cattle industry. Examination of the model sensitivity metric was deemed out of scope of this thesis and is one avenue of future improvement.

6.6 SIMULATION MODEL WEAKNESSES

There exist a variety of advantages and disadvantages of the model methodology with inherited model limitations given by the model structure. In this section we analyse and discuss various of these weaknesses and limitations, particularly focusing on how these could be enhanced in future.

6.6.1 *Data Limitations*

There exists an important caveat to the preceding simulation predictions, related to the data and parameter estimation techniques used to generate our epidemiological parameters. The quantifying and modelling of bTB dynamics while considering our different mechanics; latency, wildlife reservoir, and environmental contamination is not a trivial task (Godfray et al. 2013). The literature uses statistical and analytical methods to analyse existing data rigorously.

However, the data gaps, significant variation, and discrepancies seen within these data sets generate parameters with poor predictive powers. Additionally, a compounding factor that exasperates this problem is the considerable variation in the parameter values used within the modelling literature. Many models use techniques such as Bayesian partial-likelihood inference to estimate parameters for specific models (e.g. [179] and [**?**]). However, the epidemiological parameters generated from such techniques may provide accurate model predictions for that exact model, however, these parameters typically do not represent the underlying biology accurately. As a result, when these parameters are utilised in other models, they may not generate realistic predictions.

The above simulation has analysed various different underlying aspects of the disease, although these results rely on these literature epidemiological parameters. Additionally, the methods used to construct the epidemiological parameters could be significantly improved after further biological investigation of M. bovis and its survivability in nature. The exact predictions of the simulation may not perfectly represent the future outcomes of bTB, although they do indicate general trends and likely possible directions that the disease dynamics may take. In future, as the availability of accurate and biologically based data increases, these could be used to improve the accuracy of this simulation's predictions.

6.6.2 *National Infection Spread*

One of the greatest weaknesses of this simulation approach is its singular herd view of this simulation. This simulation model represents a disease spread among a single herd, however, instead bTB spread occurs at a national level, with spread occurring by livestock trading. The model was designed to specifically to complement the other transmission pathways discussed in this thesis, allowing us to examine and understand the different pathways in combination, otherwise incredibly difficult using the previous dynamical system approach. However, one aspect that would enhance this model is my incorporating many such herds and implementing livestock-inducing transmission. Allowing us to view the disease not from a singular herd but rather from a national level.

One future direction of this chapter therefore would be to alter the simulation to monitor such regional spread. To complete such an update to this simulation wouldn't require much reconstruction, as the model could be run in parallel with N independent systems, each running in step. All infection induced by livestock trading intervention could be completed by a simple out of sequence livestock addition, where one host is moved between farms. After which, by the differential equation viewpoint of these systems, the N-independent parallel systems could be continued until the next cow is traded. This would represent a simulated

spread at a national level. However, the high level of complexity and abstraction of this model would potentially obscure the overall network influence behind other mechanics. Deeper analysis would be required to examine the overall role of cattle livestock trading in disease spread.

To further examine the role of livestock trading using a dynamical systems approach, would be difficult but there are currently existing methods to analyse the spread of disease from a network perspective. There exist several techniques, however, the most prominent such technique is Mean-field modelling. This approach utilises network modelling to provide a more flexible framework, where individuals (nodes) may only spread disease to others only if connected to them in the network. The method works by understanding that calculating how likely a node is to become infected, relies on pairs. Similarly, to calculating the infection occur at a pair level required knowledge of triples etc. Mean field modelling works by breaking this requirement of higher order structure by imposing some structure on this calculation (called a closure), used to create an approximation for the system. As closures allow the expression of higher-order groups of nodes (triples, quads, etc) in simpler lower-order structures (pairs and singles), overall disease movement can therefore be approximated by solving the system with the given closure.

Mean-field modelling provides an alternative to simulation, allowing us to understand how disease travels through a network from a dynamical system approach. Similar techniques as the ones used throughout this thesis can be applied to this system to understand the underlying equilibrium of the system, and understand how these network systems bifurcate. The main detriment to the mean-field modelling approach is that the inherent additional complexity of the network often flows through this process, and the dynamical systems this method produces are also complex. The additional complexity of these dynamical systems often acts as a barrier, preventing useful insights from being easily accessible. There is currently significant research in designing techniques to incorporate multi-host systems and more complex dynamical structures with network models, that still allow meaningful insights about the system. One future direction of my work would be to incorporate such new techniques, allowing the characteristics

6.6.3 *Farm Microenvironments*

The methodology used to examine the environmental contamination in this thesis represents an initial step in exploration into the shedding and contraction of bTB from the shared landscape. As demonstrated in the literature review, clearly contamination of the shared landscape is an important and opaque transmission pathway. As the literature demonstrates, direct transmission between cattle and badger interaction is extremely rare, as shown through

extensive GPS monitoring collars and contact collars study [66] and some other ecologists have gone as far to even suggest non-existent [80]. However, Phenotype studies indicate that bTB is continuously in a state of spilling over and spilling back between the target population and reservoir [75]. Clearly, transmission is occurring in the shared landscape, where infected hosts shed fomites, contaminating the shared landscape.

The methodology implemented in the simulation was designed to act as a comparison for the dynamical system approach used in this thesis. However, the approach of only considering the entire landscape as one compartment, this approach has various unrealistic assumptions that we will discuss below:

- Equal Proximity Assumption: By the assumptions made in the model, we assume that each cattle interact with others and the joint environment equally. This assumption clearly does consider possible segmentation of herds (pre and post-parturition cattle) or the local preference of cattle. A more advanced environmental mechanism would consider the different micro-environments of the farm and the selective localisation that different hosts occupy. There are a variety of ways to better integrate the local disease dispersion within a farm. The simplest of these is to separate the compartments, each representing the different microenvironments of the farm. However, a more mathematically sophisticated approach is to utilise some diffusion PDE models to map the continuous spread of fomites [**?**].

- Temporal Element: In order to accurately consider how bTB is shed throughout the farm it is important to understand the potential temporal implication. Direct transmission introduces a seasonal component to transmission due to farm housing practices. The bulk of UK cattle are permanently housed indoors during the winter months, whereas cattle graze on pastures during the spring and summer months. When housed indoors, the increased average herd density caused by cramped conditions elevates direct inhalation risk [19]. Moreover, cattle contaminate/interact with the shared environment with greater frequency when housed indoors [19]. Where conversely, the improved ventilation and roaming area of pastures during the summer months imply a lower incidence rate among cattle. Models within the literature rarely consider this seasonality effect and often omit the differences in transmission between indoor and outdoor. One possible future direction of this work is to incorporate seasonality and incorporate the different micro-environments within a farm; herd separation in livestock barns, birthing pens, isolated cattle and milk processing areas.

6.6.4 *Residual Disease*

Earlier discussions indicated the associated data limitations regarding the model parameters required to accurately examine the spread of bTB. Currently, the model has various errors induced by the poor quality of data, if further studies collected and cleaned new biometric data this would increase the model performance. If the data was more accurate then the next avenue of study would be to try and accurately quantify the disease proportion of each transmission pathway.

The direction I would focus this analysis would be to further understand the roots of re-infection. What factors are responsible for preventing disease eradication and how can these be mitigated? Using this model with standard UK practices (disease surveillance, culling, pre and post-movement test etc), I would simulate herds to understand what is the average bTB lifespan with a farm and understand how the other transmission pathways (Cross species interactions, contamination of the shared landscape, or cattle livestock trading, etc) influence disease survivability and resurgence. This would be a simplistic alteration to this simulation, where results would not just calculate if an infection occurs but would also categorise that type of infection. This analysis would provide researchers with an understanding of the most important pathways and allow the construction of optimal disease eradication protocols. However, due to these data limitations, accurately producing this analysis is not possible with this method.

6.7 CONCLUSION

In this chapter, we developed a computational model based on the Gillespie algorithm framework to simulate bTB in a herd of UK cattle. This simulation explicitly incorporated the mechanics discussed in this thesis; realistic latency period, wildlife reservoir, and environmental contamination. The simulation aimed to further understand the following research themes; infection proportions and residual disease, badger's contribution and the effect of improving bio-security.

A succinct and concise summary of results shows that culling is adequate, but there still exists room for improvement. The simulation demonstrated that the residual disease is still predominately caused by cattle to cattle transmission under the current epidemiological parameters from the literature. However, badger to cattle transmission and environmental contamination becomes more substantial factors when the herd is in lockdown. The next theme we investigated was biosecurity and wildlife reservoirs, the result showed that increasing biosecurity measures also increased the probability of extinction. By decoupling the badger

and cattle populations, we reduce the spillover and spillback between these populations, increasing the likelihood that the disease will become extinct. The last theme investigated was the relationship between the test sensitivity of the SICCT test and realistic latency periods. The result demonstrated that more test-sensitive cattle were identified and culled by altering the latency period distribution (Erlang distributed) shape parameter, subsequently reducing infection levels.

Part III

DISCUSSION AND CONCLUSION

7

CHAPTER 7: GENERAL DISCUSSION AND CONCLUSION

The primary aim of this thesis was to gain further qualitative and quantitative insights into bovine tuberculosis's (bTB's) persistent disease cycle. In each chapter, we have constructed mathematical models aiming to understand why bovine tuberculosis (bTB) remains a complex and challenging livestock disease in the UK's cattle industry. In the following sections of this chapter, we shall discuss the various limitation of this thesis, focusing predominately on data limitation and their effect on model predictions. After which, we will summarise the insight gained from each chapter while also illustrating both, possible future directions and the associated obstacles hindering these directions. This chapter will then conclude with a short thesis summary, recapping key issues addressed and examining the current UK's bTB control strategy.

7.1 DATA LIMITATION

In order to utilise the models constructed in this thesis, various data sets from governing bodies (DEFRA), invested parties (e.g. OIE, WHO), and the wider literature must be collected, processed and then implemented. These datasets enable modellers to answer high-impact questions without investing a considerable amount of time and resources in primary data collection themselves [147], although there are limitations in using data for purposes beyond its original scope.

Several challenges arose in my attempts to gather data parameters that accurately depict the underlying biological situation. Firstly, data sets that aimed to accurately capture the underlying biology for various integral epidemiological parameters were either scarce, non-existent, or not freely available. Without informative quantitative predictions of parameters, there can be little faith in our model's predictions. However, how do researchers obtain estimations for the epidemiological parameters for their models?

Throughout the literature, hard to obtain epidemiological parameters have increasingly been estimated using parameter interference techniques such as bayesian likelihood methods. These methods have been employed throughout the bovine tuberculosis literature to generate many modelling parameters. Most of these techniques use DEFRA's bTB incidences data to estimate epidemiological parameters for a given epidemiological model. There lie two main

problems with this approach:

Firstly, for these methods to produce accurate and informative epidemiological parameters, the underlying data source must be clear with no inconsistencies. However, as discussed extensively in the literature review, the bTB properties of a particular farm depend on numerous factors; farm management type and style, herd characteristics, the proximity of associated wildlife reservoir, etc. Moreover, the poor sensitivity and specificity of the SICCT test means that we can not be confident in the overall accuracy of the incidence of disease rates. As a result, incident rates of bTB are an exceptionally poor data source to estimate parameters from.

Secondly, parameter inference techniques create estimations of our epidemiological parameters for specific underlying models. The significant variability of mechanisms included and excluded from different bTB models is extreme, as model complexity varies from simplistic models (SETIRC model) to models incorporating a multitude of competing disease mechanics. As a result, the estimation of the epidemiological parameters varies wildly based on the different epidemiological mechanisms incorporated. For example, a bTB epidemiological model examining persistent reinfections, which excludes the effect of a wildlife reservoir, would likely have a significant reduction in the estimation of sensitivity and specificity of the SICCT test. This model would only consider reinfection from undetected cattle and would exclude the spillover from a wildlife reservoir. As a result, there exists a myriad of inconsistent estimations for the various epidemiological parameters for bTB models within the literature. Making it extremely challenging to pick valid disease parameters for the models used in this thesis.

In the future, more experimental data collection is required to fully understand the interworkings of bovine tuberculosis. Understandably, these experiments would take a considerable amount of time and resources, however, they would be a prudent investment, as with this knowledge researchers could mitigate some of bTB associated costs. Moreover, a more realistic suggestion, that could be enacted in a shorter time frame, is for the modelling literature to become more transparent regarding parameter origins. The entire mathematical modelling community should improve their transparency regarding modelling parameters' origins. Modelling papers could achieve this by simply adding an additional key in data tables, stating where this data came from and how it was generated. Researchers would then be able to quickly determine if the associated parameter is applicable to their model or not.

7.2 model limitations

Throughout this thesis, epidemiological models have been used to understand disease transmission mechanisms and to assess the impact of alternative control strategies. Generally, the overall effectiveness of control mechanisms are typically assumed from expert opinions rather than from model predictions. The actively managed nature of bTB means it should be potentially possible to estimate the efficiency of control strategies directly from epidemiological data. However, imperfect data sources that obscure a model's ability to make accurate predictions are not the only modelling limitation. As we shall see, mathematical models will always be subject to limitations due to their construction.

By the nature of modelling, some form of simplifying assumptions about the complex processes that drive disease transmission dynamics must be made [180]. As no matter how realistic a model is, it will never be perfect. A model will always have to make some assumptions and simplifications regarding its own mechanics; therefore, all models will inherently have limitations and as a consequence, their prediction will never be perfect. However, the power of mathematical modelling doesn't lie in just its predictions, as scientific models represent a system of ideas, events, or processes in an informative manner, allowing insights to be gathered about their patterns, structures, or functions. Modelling insights regarding how a system operates are equally, if not more helpful, as researchers can translate these scientific discoveries into practical applications. In the case of the UK's cattle industry, insights and understanding of bTB mechanics from modelling enhances humans' knowledge base regarding the disease. From this knowledge base, researchers draw conclusions on how best to construct control strategies, allowing humans to mitigate and ultimately eradicate bTB once and for all.

7.3 thesis summary and possible future directions

The model limitation seen within this thesis will require considerable further refinement before directly informing government policy. These models aimed to address and create further understanding regarding one of bTB's primary open questions:

"What are the underlying mechanics of bTB that facilitate persistent reinfections exhibited in UK's cattle herds?"

Through further understanding of the qualitative and quantitative factors that influence persistent reinfections, government officials will be able to translate these scientific insights into practical interventions that will ultimately reduce the burden of endemic disease on cattle

production systems [180]. In the forthcoming sections, we discuss the different mechanics examined throughout this thesis (e.g. latency, wildlife reservoir, and environmental contamination), discussing the insights gained from each chapter and what future work should be carried out.

However before progressing onto this summary, let us illustrate one consistent improvement for all models seen in this thesis. In the above discussion we have illustrated the imperfect nature of parameter estimation by using bTB's incident rates. The high variance, competing factors, and unobserved nature of many of the different transmission pathways make incidence rates an inadequate data source. However, to properly investigate each of the mechanics discussed throughout this thesis, similar parameter estimation techniques would need to be performed for each model. This analysis would improve model parameters accuracy, compared to those available within the literature. Such analysis would be particularly important for our simulation, as this simulation incorporates the most significant number of modelling mechanisms; therefore, its current parameters are most likely to have compounding parameter errors. Moreover, this analysis would produce relevantly realistic parameter estimation for our other models studying the other modelling mechanics. Furthermore, as high resolution detailed epidemiological data that focus on the underlying biological mechanisms become available, then these could be incorporated into this analysis, further improving our parameter estimation.

7.3.1 *bTB Latency Mechanic*

Throughout chapter three, we examined how latency influences persistent infections. As the literature indicates, one of the major recurring themes of the infection cycle is 'undiagnosed infections', these have a profound effect on both the disease transmission dynamics and the surveillance performance at the industry level. Undiagnosed infections contributed to the 'silent' spread of the disease both within and between cattle herds. At a herd level, there is evidence that many factors including host characteristics, testing interval, and physiological stresses, can potentially contribute to a lack of response from the standard diagnostic test. Moreover, the high variability in the latency period obscures disease transmission, as cattle may harbour the infection for years before becoming infectious themselves. In this chapter, we further incorporated the variable latency mechanic into the standard prototypical model by altering the latency period distribution from the standard exponential distribution to the Erlang distribution. As demonstrated from the model's analysis, this does alter the dynamics by drawing out the time until solutions reach the endemic equilibrium. However, the system still bifurcates according to a transcritical bifurcation, where the long term behaviour of solu-

tions depends entirely on the basic reproductive number $\mathcal{R}_0$. Where the endemic equilibrium infection level is intrinsically tied to this threshold value, as the basic reproductive level reduces to one, the infection level reduces to zero.

The main limitation of this model is the lack of data regarding latency period distribution. There is an extensive discussion in the literature regarding latency period distribution and the various factors that affect it, although remarkably little in the way of quantitive discussion of the range. Further investigation of such latency period distribution is required to enhance this model's potential predictive power.

7.3.2 *Wildlife Reservior*

In chapter four, we examined the influence of the wildlife reservoir, attempting to understand the dual dynamics of spillover and spillback between the badger and cattle population. The presence of a wildlife reservoir complicates disease surveillance, as their presence masks the true roots of infection. In this chapter, we developed a wildlife reservoir system close to a vector host system; in this model analysis we described the long term behaviour of the system's solutions from the perspective of system equilibrium. This analysis focuses on the system's equilibria and under what conditions these equilibria are stable.

This model could see considerable improvement, as some of the model assumptions do not accurately reflect bTB's true dynamics. In future, to better understand the transmission of bovine tuberculosis this model should be reframed as a patch model. In these patch models, hosts and wildlife interact in distinct and discrete spatial patches where the wildlife hosts would be able to migrate between the different patches infecting other badgers setts and cattle herds. Moreover, these models would incorporate not just the migration disease mechanics but could also be adapted to incorporate environmental contamination as well.

7.3.3 *bTB Environmental Contamination*

In chapter five, we turned our attention to bTB's environmental contamination. A vital aspect of this thesis was trying to understand the role in which environmental contamination in the within-herd spread of bTB. Environmental contamination is heavily discussed throughout the literature, although this factor is almost excluded from the modelling literature. The literature clearly discusses that cattle herds and badgers don't interact directly, rather the two populations maintain the disease by interacting with the shared landscape. For example, recall from the literature review that in a longitudinal observational study [66], ecologists monitored 421 collared cattle for a total of 8551 collar days, 53 contact-collared badgers for

8308 collar days, and 54 GPS-collared badgers for 7176 days. The results of this longitudinal observational study found no cattle and badger interactions.

Conversely, phenotype studies indicate that bTB is continuously in a state of spilling over and spilling back, as in [181], as 40% of the badger samples taken were indistinguishable from the sample sequenced in cattle implying close inter-community spreading occurs [181]. Undoubtlfully, cattle and badgers interact through the shared landscape, although this factor has been almost excluded from the modelling literature. In the literature, most reinfections are assumed to be caused by either undiagnosed cattle or badger reinfection.

Environmental contamination is an essential avenue for further exploration as currently there remain numerous open questions. In future, like the other disease mechanisms, more data collection is required, which is especially true for environmental contamination, as within the literature the is very little data regarding modelling parameters. Moreover, similar work needs to be completed in the modelling side of the literature, as various crucial factors are excluded from the literature models. Our SETIB environmental contamination model could be improved in future by incorporating the level of bacterium concentration in which cattle contract the disease, as it is unlikely to be linear as our model suggests. Similarly, the different micro-environments on a farm should be investigated, as the infection level from contamination with likely vary. For example, contamination hot spots will likely exist; water troughs, cattle feeders, and bedding areas.

7.4 SIMULATION MODEL

In chapter six, we use simulations and their techniques to examine how the different model mechanics expressed throughout this thesis work in conjunction (e.g. latency distribution, wildlife reservoir, and environmental contamination). The results indicate that the UK's surveillance and cull strategy is adequate, but there still exists room for improvement. Bovine tuberculosis is predominately caused by cattle to cattle transmission, using current epidemiological parameters from the literature. However, the other factors still exert a substantial influence (e.g. badger to cattle and environmental contamination transmission), especially when the herd is in lockdown. In our investigation of biosecurity measures and wildlife reservoirs, we determined that increasing biosecurity measures radically reduces infections as the biosecurity measures increase the probability of extinction. Through decoupling the badger and cattle population, we reduce the spillover and spillback between these populations, increasing the likelihood that the disease will become extinct.

To truly leverage the scientific capacity of this simulation, parameter estimation techniques would need to be performed on this simulation. In future, as data sets that accurately represent the underlying biology become available, we could incorporate these within the simulation to answer further biological questions. Much more study into residual disease and environmental contamination is needed to truly understand the hidden disease pathways of bTB.

7.5 THESIS CONCLUSION

Bovine tuberculosis continues to undermine the sustainability of the UK's cattle industry, despite enormous advances in our understanding of its critical epidemiological features. Overall, an essential criterion for designing effective bTB control programs relies on a clear understanding of the underlying disease mechanism. To stop the cycle of persistent reinfection seen with cattle herds throughout the southwest of England, requires a transparent picture of the associated route of reinfection. This thesis has only begun to reveal the underlying qualitative and quantitative route of reinfection and much more work is needed. For public health officials to meet the UK's target of being "Officially Bovine Tuberculosis Free (OTF) status for England by 2038", various problems must be addressed. Overall, the analysis in this thesis has demonstrated that the key to creating a more effective bTB control programme is to address infection in wildlife hosts to prevent sporadic re-introductions. By decoupling wildlife reservoirs and host populations, we would mitigate a substantial factor in the reinfection cycle. This could be achieved through a two-fold approach, firstly the UK government could force farmers to improve biosecurity, preventing infectious badgers from entering farm pastures. Secondly, further investigation and investment in a wildlife vaccine are needed.

The analysis also indicates that further research and data collection are required concerning the transmission pathways, particularly regarding the effect of environmental contamination. By increasing the availability of high-quality datasets that aim to model the underlying biology of epidemiological parameters accurately, researchers would enhance their parameter estimations. Moreover, this data would shed light on the various transmission mechanisms contributing to persistent reinfection. Notably, further analysis of environmental contamination must be conducted, as currently, very little analysis of its quantitive effects on disease transmission has been performed. With this research, public health officials could develop more targeted and cost-effective approaches to controlling bTB at the herd and industry levels. What we can say with some certainty; bovine tuberculosis is a complex disease and without a change in strategy, new diagnostic tools, vaccine discovery, or an enhanced understanding of transmission pathways, bTB is likely to remain problematic for many years to come.

BIBLIOGRAPHY

[1] Louise H Taylor, Sophia M Latham, and Mark EJ Woolhouse. Risk factors for human disease emergence. *Philosophical Transactions of the Royal Society of London. Series B: Biological Sciences*, 356(1411):983–989, 2001.

[2] Sarah Cleaveland, M Karen Laurenson, and Louise H Taylor. Diseases of humans and their domestic mammals: pathogen characteristics, host range and the risk of emergence. *Philosophical Transactions of the Royal Society of London. Series B: Biological Sciences*, 356(1411):991–999, 2001.

[3] Kate E Jones, Nikkita G Patel, Marc A Levy, Adam Storeygard, Deborah Balk, John L Gittleman, and Peter Daszak. Global trends in emerging infectious diseases. *Nature*, 451(7181):990–993, 2008.

[4] James M Hughes. Emerging infectious diseases: a cdc perspective. *Emerging Infectious Diseases*, 7(3 Suppl):494, 2001.

[5] Katherine F Smith, Karina Acevedo-Whitehouse, and Amy B Pedersen. The role of infectious diseases in biological conservation. *Animal conservation*, 12(1):1–12, 2009.

[6] Daniel T Haydon, Sarah Cleaveland, Louise H Taylor, and M Karen Laurenson. Identifying reservoirs of infection: a conceptual and practical challenge. *Emerging infectious diseases*, 8(12):1468–1473, 2002.

[7] Peter Daszak, Andrew A Cunningham, and Alex D Hyatt. Emerging infectious diseases of wildlife–threats to biodiversity and human health. *science*, 287(5452):443–449, 2000.

[8] Christian Gortazar, Iratxe Diez-Delgado, Jose Angel Barasona, Joaquin Vicente, Jose De La Fuente, and Mariana Boadella. The wild side of disease control at the wildlife-livestock-human interface: a review. *Frontiers in veterinary science*, 1:27, 2015.

[9] MV Palmer. Mycobacterium bovis: characteristics of wildlife reservoir hosts. *Transboundary and emerging diseases*, 60:1–13, 2013.

[10] Siv Aina J Leendertz, Jan F Gogarten, Ariane Düx, Sebastien Calvignac-Spencer, and Fabian H Leendertz. Assessing the evidence supporting fruit bats as the primary reservoirs for ebola viruses. *EcoHealth*, 13(1):18–25, 2016.

[11] Gretchen Vogel. Sequence offers clues to deadly flu. *Science*, 279(5349):324–324, 1998.

[12] Martin Enserink. New virus fingered in malaysian epidemic. 1999.

[13] CA Donnelly, NM Ferguson, AC Ghani, MEJ Woolhouse, CJ Watt, and RM Anderson. The epidemiology of bse in cattle herds in great britain. i. epidemiological processes, demography of cattle and approaches to control by culling. *Philosophical Transactions of the Royal Society of London. Series B: Biological Sciences*, 352(1355):781–801, 1997.

[14] David Whyte Macdonald et al. *Rabies and wildlife-a biologist's perspective.* University Press., 1980.

[15] Elise Uberoi. Bovine tb statistics: Great britain. *House of Commons: Briefing paper*, 1(6081), Jul 2019.

[16] JM Broughan, J Judge, E Ely, RJ Delahay, G Wilson, RS Clifton-Hadley, AV Goodchild, H Bishop, JE Parry, and SH Downs. A review of risk factors for bovine tuberculosis infection in cattle in the uk and ireland. *Epidemiology & Infection*, 144(14):2899–2926, 2016.

[17] Robin A Skuce, Adrian R Allen, Stanley WJ McDowell, and Bacteriology Branch. Bovine tuberculosis (tb): a review of cattle-to-cattle transmission, risk factors and susceptibility. *Bacteriology Branch Veterinary Sciences Division Agrifood and Biosciences Institute*, 1:115–167, 2011.

[18] Robin A Skuce, Adrian R Allen, and Stanley WJ McDowell. Herd-level risk factors for bovine tuberculosis: a literature review. *Veterinary medicine international*, 2012, 2012.

[19] BW Gannon, CM Hayes, and JM Roe. Survival rate of airborne mycobacterium bovis. *Research in veterinary science*, 82(2):169–172, 2007.

[20] B Winkler and F Mathews. Environmental risk factors associated with bovine tuberculosis among cattle in high-risk areas. *Biology letters*, 11(11):20150536, 2015.

[21] Graham J Hickling. Dynamics of bovine tuberculosis in wild white-tailed deer in michigan. 2002.

[22] David SL Ramsey and Murray G Efford. Management of bovine tuberculosis in brushtail possums in new zealand: predictions from a spatially explicit, individual-based model. *Journal of Applied Ecology*, 47(4):911–919, 2010.

[23] M De Garine-Wichatitsky, Alexandre Caron, Richard Kock, R Tschopp, Musso Munyeme, Markus Hofmeyr, and A Michel. A review of bovine tuberculosis at the wildlife–livestock–human interface in sub-saharan africa. *Epidemiology & Infection*, 141(7):1342–1356, 2013.

[24] R Tschopp, J Zinsstag, E Schelling, D Waltner-Toews, M Whittaker, and M Tanner. Bovine tuberculosis at the human–livestock–wildlife interface in sub-saharan africa. *One Health: the theory and practice of integrated health approaches*, pages 163–175, 2015.

[25] Anita Luise Michel, Borna Müller, and Paul David Van Helden. Mycobacterium bovis at the animal–human interface: A problem, or not? *Veterinary microbiology*, 140(3-4):371–381, 2010.

[26] WY Ayele, SD Neill, J Zinsstag, MG Weiss, and I Pavlik. Bovine tuberculosis: an old disease but a new threat to africa. *The International Journal of Tuberculosis and Lung Disease*, 8(8):924–937, 2004.

[27] Noel H Smith, Stephen V Gordon, Ricardo de la Rua-Domenech, Richard S Clifton-Hadley, and R Glyn Hewinson. Bottlenecks and broomsticks: the molecular evolution of mycobacterium bovis. *Nature Reviews Microbiology*, 4(9):670–681, 2006.

[28] Debby V Cousins, Ricardo Bastida, Angel Cataldi, Viviana Quse, Sharon Redrobe, Sue Dow, Padraig Duignan, Alan Murray, Christine Dupont, Niyaz Ahmed, et al. Tuberculosis in seals caused by a novel member of the mycobacterium tuberculosis complex: Mycobacterium pinnipedii sp. nov. *International journal of systematic and evolutionary microbiology*, 53(5):1305–1314, 2003.

[29] Wolfgang M Prodinger, Anita BrandstaÌtter, Ludmila Naumann, Maria Pacciarini, Tanja Kubica, Maria Laura Boschiroli, Alicia Aranaz, GyoÌrgy Nagy, Zeljko Cvetnic, Matjaz Ocepek, et al. Characterization of mycobacterium caprae isolates from europe by mycobacterial interspersed repetitive unit genotyping. *Journal of Clinical Microbiology*, 43(10):4984–4992, 2005.

[30] Borna Müller, Salome Dürr, Silvia Alonso, Jan Hattendorf, Cláudio JM Laisse, Sven DC Parsons, Paul D Van Helden, and Jakob Zinsstag. Zoonotic mycobacterium bovis–induced tuberculosis in humans. *Emerging infectious diseases*, 19(6):899, 2013.

[31] David G Russell, Clifton E Barry 3rd, and JoAnne L Flynn. Tuberculosis: what we donât know can, and does, hurt us. *Science*, 328(5980):852–856, 2010.

[32] Isabelle Suárez, Sarah Maria Fünger, Stefan Kröger, Jessica Rademacher, Gerd Fätkenheuer, and Jan Rybniker. The diagnosis and treatment of tuberculosis. *Deutsches Aerzteblatt International*, 116(43), 2019.

[33] Philippe Sudre, G Ten Dam, and Arata Kochi. Tuberculosis: a global overview of the situation today. *Bulletin of the World Health Organization*, 70(2):149, 1992.

[34] Rein MGJ Houben and Peter J Dodd. The global burden of latent tuberculosis infection: a re-estimation using mathematical modelling. *PLoS medicine*, 13(10):e1002152, 2016.

[35] Dag Gundersen Storla, Solomon Yimer, and Gunnar Aksel Bjune. A systematic review of delay in the diagnosis and treatment of tuberculosis. *BMC public health*, 8(1):1–9, 2008.

[36] P Konch, B Dutta, S Goswami, AG Barua, and GK Saikia. Pathology of bovine tuberculosis. *Indian J. Anim. Res*, 53(10):1377–1381, 2019.

[37] Rea Tschopp, Esther Schelling, Jan Hattendorf, Abraham Aseffa, and Jakob Zinsstag. Risk factors of bovine tuberculosis in cattle in rural livestock production systems of ethiopia. *Preventive veterinary medicine*, 89(3-4):205–211, 2009.

[38] SD Neill, RA Skuce, and JM Pollock. Tuberculosis-new light from an old window. *Journal of applied microbiology*, 98(6):1261–1269, 2005.

[39] Sabrina Rodriguez-Campos, Noel H Smith, Maria B Boniotti, and Alicia Aranaz. Overview and phylogeny of mycobacterium tuberculosis complex organisms: implications for diagnostics and legislation of bovine tuberculosis. *Research in veterinary science*, 97:S5–S19, 2014.

[40] News Desk. Meat from tb-positive cows sold as food in uk, Jul 2018. Available online at: `https://www.foodsafetynews.com/2013/07/meat-from-tb-positive-cows-sold-as-food-in-uk/#:~:text=%E2%80%9CThe%20Food%20Standards%20Agency%20has,is%20killed%20by%20cooking%20meat.`

[41] Ottorino Cosivi, John M Grange, Chris J Daborn, Mario C Raviglione, T Fujikura, D Cousins, RA Robinson, HF Huchzermeyer, Isabel de Kantor, and François-Xavier Meslin. Zoonotic tuberculosis due to mycobacterium bovis in developing countries. *Emerging infectious diseases*, 4(1):59, 1998.

[42] Robert F Kelly, Saidou M Hamman, Kenton L Morgan, Egbe F Nkongho, Victor Ngu Ngwa, Vincent Tanya, Walters N Andu, Melissa Sander, Lucy Ndip, Ian G Handel, et al. Knowledge of bovine tuberculosis, cattle husbandry and dairy practices amongst pastoralists and small-scale dairy farmers in cameroon. *PLoS One*, 11(1):e0146538, 2016.

[43] R De la Rua-Domenech, AT Goodchild, HM Vordermeier, RG Hewinson, KH Christiansen, and RS Clifton-Hadley. Ante mortem diagnosis of tuberculosis in cattle: a review of the tuberculin tests, γ-interferon assay and other ancillary diagnostic techniques. *Research in veterinary science*, 81(2):190–210, 2006.

[44] Matthew B Huante, Rebecca J Nusbaum, and Janice J Endsley. Co-infection with tb and hiv: converging epidemics, clinical challenges, and microbial synergy. In *Tuberculosis host-pathogen interactions*, pages 123–153. Springer, 2019.

[45] Paul R Torgerson and David J Torgerson. Public health and bovine tuberculosis: what's all the fuss about? *Trends in microbiology*, 18(2):67–72, 2010.

[46] F Boelaert, A Stoicescu, G Amore, W Messens, M Hempen, V Rizzi, SE Antoniou, F Baldinelli, E Dorbek-Kolin, Y VanderStede, et al. European food safety authority. *European Centre for Disease Prevention and Control The European Union One Health*, 2019.

[47] ML Monaghan, ML Doherty, JD Collins, JF Kazda, and PJ Quinn. The tuberculin test. *Veterinary microbiology*, 40(1-2):111–124, 1994.

[48] MV Palmer, WR Waters, and TC Thacker. Lesion development and immunohistochemical changes in granulomas from cattle experimentally infected with mycobacterium bovis. *Veterinary pathology*, 44(6):863–874, 2007.

[49] Defra. The strategy for achieving officially bovine tuberculosis free status for england. 2014.

[50] Sebastian G Kurz, Jennifer J Furin, and Charles M Bark. Drug-resistant tuberculosis: challenges and progress. *Infectious Disease Clinics*, 30(2):509–522, 2016.

[51] RS Morris, DU Pfeiffer, and R Jackson. The epidemiology of mycobacterium bovis infections. *Veterinary microbiology*, 40(1-2):153–177, 1994.

[52] Charles O Thoen, James H Steele, and Michael J Gilsdorf. *Mycobacterium bovis infection in animals and humans*. John Wiley & Sons, 2008.

[53] Daniel J OâBrien, Stephen M Schmitt, Scott D Fitzgerald, Dale E Berry, and Graham J Hickling. Managing the wildlife reservoir of mycobacterium bovis: the michigan, usa, experience. *Veterinary microbiology*, 112(2-4):313–323, 2006.

[54] Johanna Judge, Gavin J Wilson, Roy Macarthur, Robbie A McDonald, and Richard J Delahay. Abundance of badgers (meles meles) in england and wales. *Scientific Reports*, 7(1):1–8, 2017.

[55] TB FREE England. History of bovine tb. Technical report, Tech. rep., TB Free England, 2008.

[56] FD Menzies and SD Neill. Cattle-to-cattle transmission of bovine tuberculosis. *The Veterinary Journal*, 160(2):92–106, 2000.

[57] JE Shitaye, B Getahun, T Alemayehu, M Skoric, F Treml, P Fictum, V Vrbas, and I Pavlik. A prevalence study of bovine tuberculosis by using abattoir meat inspection and tuberculin skin testing data, histopathological and is6110 pcr examination of tissues with tuberculous lesions in cattle in ethiopia. *VETERINARNI MEDICINA-PRAHA-*, 51(11):512, 2006.

[58] RR Kao, Michael B Gravenor, Bryan Charleston, JC Hope, M Martin, and CJ Howard. Mycobacterium bovis shedding patterns from experimentally infected calves and the effect of concurrent infection with bovine viral diarrhoea virus. *Journal of the Royal Society Interface*, 4(14):545–551, 2007.

[59] AM Perez, MP Ward, and V Ritacco. Modelling the feasibility of bovine tuberculosis eradication in argentina. *Revue Scientifique et Technique-OIE*, 30(2):635, 2011.

[60] Christl A Donnelly, Gao Wei, W Thomas Johnston, DR Cox, Rosie Woodroffe, F John Bourne, CL Cheeseman, Richard S Clifton-Hadley, George Gettinby, Peter Gilks, et al. Impacts of widespread badger culling on cattle tuberculosis: concluding analyses from a large-scale field trial. *International Journal of Infectious Diseases*, 11(4):300–308, 2007.

[61] Darren M Green, Istvan Z Kiss, Andrew P Mitchell, and Rowland R Kao. Estimates for local and movement-based transmission of bovine tuberculosis in british cattle. *Proceedings of the Royal Society B: Biological Sciences*, 275(1638):1001–1005, 2008.

[62] Amanda E Fine, Carole A Bolin, Joseph C Gardiner, and John B Kaneene. A study of the persistence of mycobacterium bovis in the environment under natural weather conditions in michigan, usa. *Veterinary medicine international*, 2011, 2011.

[63] Monika Boehm, Michael R Hutchings, and Piran CL White. Contact networks in a wildlife-livestock host community: identifying high-risk individuals in the transmission of bovine tb among badgers and cattle. *PloS one*, 4(4):e5016, 2009.

[64] Folashade B Agusto, Suzanne Lenhart, Abba B Gumel, and Agricola Odoi. Mathematical analysis of a model for the transmission dynamics of bovine tuberculosis. *Mathematical Methods in the Applied Sciences*, 34(15):1873–1887, 2011.

[65] RR Kao, MG Roberts, and TJ Ryan. A model of bovine tuberculosis control in domesticated cattle herds. *Proceedings of the Royal Society of London. Series B: Biological Sciences*, 264(1384):1069–1076, 1997.

[66] Rosie Woodroffe, Christl A Donnelly, Cally Ham, Seth YB Jackson, Kelly Moyes, Kayna Chapman, Naomi G Stratton, and Samantha J Cartwright. Badgers prefer cattle pasture but avoid cattle: implications for bovine tuberculosis control. *Ecology letters*, 19(10):1201–1208, 2016.

[67] Gillian S Dean, Shelley G Rhodes, Michael Coad, Adam O Whelan, Paul J Cockle, Derek J Clifford, R Glyn Hewinson, and H Martin Vordermeier. Minimum infective dose of mycobacterium bovis in cattle. *Infection and immunity*, 73(10):6467–6471, 2005.

[68] Irene Schiller, W RayWaters, H Martin Vordermeier, Thomas Jemmi, Michael Welsh, Nicolas Keck, Adam Whelan, Eamonn Gormley, Maria Laura Boschiroli, Jean Louis Moyen, et al. Bovine tuberculosis in europe from the perspective of an officially tuberculosis free country: trade, surveillance and diagnostics. *Veterinary microbiology*, 151(1-2):153–159, 2011.

[69] Liliana CM Salvador, Michael Deason, Jessica Enright, Paul R Bessell, and Rowland R Kao. Risk-based strategies for surveillance of tuberculosis infection in cattle for low-risk areas in england and scotland. *Epidemiology & Infection*, 146(1):107–118, 2018.

[70] RM Christley, SE Robinson, B Moore, C Setzkorn, and I Donald. Responses of farmers to introduction in england and wales of pre-movement testing for bovine tuberculosis. *Preventive Veterinary Medicine*, 100(2):126–133, 2011.

[71] Fraser D Menzies, Darrell A Abernethy, Lesley A Stringer, Nick Honhold, and Alan W Gordon. A matched cohort study investigating the risk of mycobacterium bovis infection in the progeny of infected cows. *The Veterinary Journal*, 194(3):299–302, 2012.

[72] CJC Phillips, CRW Foster, PA Morris, and R Teverson. The transmission of mycobacterium bovis infection to cattle. *Research in veterinary science*, 74(1):1–15, 2003.

[73] Frances C Flower and Daniel M Weary. Effects of early separation on the dairy cow and calf:: 2. separation at 1 day and 2 weeks after birth. *Applied Animal Behaviour Science*, 70(4):275–284, 2001.

[74] C Garro, S Garbaccio, M Cobos Roldán, and S Oriani. Tuberculosis in calves: results of a prospective study. *Redvet*, 12:121108, 2011.

[75] Hannah Trewby, David Wright, Eleanor L Breadon, Samantha J Lycett, Tom R Mallon, Carl McCormick, Paul Johnson, Richard J Orton, Adrian R Allen, Julie Galbraith, et al. Use of bacterial whole-genome sequencing to investigate local persistence and spread in bovine tuberculosis. *Epidemics*, 14:26–35, 2016.

[76] Roman Biek, Anthony O'Hare, David Wright, Tom Mallon, Carl McCormick, Richard J Orton, Stanley McDowell, Hannah Trewby, Robin A Skuce, and Rowland R Kao. Whole genome sequencing reveals local transmission patterns of mycobacterium bovis in sympatric cattle and badger populations. *PLoS pathogens*, 8(11):e1003008, 2012.

[77] Rosie Woodroffe, Christl A Donnelly, DR Cox, F John Bourne, CL Cheeseman, RJ Delahay, George Gettinby, John P Mcinerney, and W Ivan Morrison. Effects of culling on badger meles meles spatial organization: implications for the control of bovine tuberculosis. *Journal of Applied Ecology*, 43(1):1–10, 2006.

[78] JA Drewe, HM O'connor, N Weber, RA McDonald, and RJ Delahay. Patterns of direct and indirect contact between cattle and badgers naturally infected with tuberculosis. *Epidemiology & Infection*, 141(7):1467–1475, 2013.

[79] R Stenhouse Williams and WA Hoy. The viability of b. tuberculosis (bovinus) on pasture land, in stored faeces and in liquid manure. *Epidemiology & Infection*, 30(4):413–419, 1930.

[80] DT OâMahony. Badger-cattle interactions in the rural environment: implications for bovine tuberculosis transmission. *Northern Ireland*, 2014.

[81] R Jackson, GW De Lisle, and RS Morris. A study of the environmental survival of mycobacterium bovis on a farm in new zealand. *New Zealand Veterinary Journal*, 43(7):346–352, 1995.

[82] BJ Duffield and DA Young. Survival of mycobacterium bovis in defined environmental conditions. *Veterinary microbiology*, 10(2):193–197, 1985.

[83] Kurt C VerCauteren, Michael J Lavelle, and Henry Campa III. Persistent spillback of bovine tuberculosis from white-tailed deer to cattle in michigan, usa: Status, strategies, and needs. *Frontiers in Veterinary Science*, page 301, 2018.

[84] Victoria Naranjo, Christian Gortazar, Joaquín Vicente, and José de la Fuente. Evidence of the role of european wild boar as a reservoir of mycobacterium tuberculosis complex. *Veterinary microbiology*, 127(1-2):1–9, 2008.

[85] Dealing with tb in your herd: What to do if bovine tb is detected in your herd in wales. Available online at: `https://www.gov.uk/government/publications/what-happens-if-tb-is-identified-in-your-herd/dealing-with-tb-in-your-herd-what-to-do-if-bovine-tb-is-detected-in-your-herd-in-wales`, journal=GOV.UK.

[86] Maia Martcheva. *An introduction to mathematical epidemiology*, volume 61. Springer, 2015.

[87] Aneesh Thakur, Mandeep Sharma, Vipin C Katoch, Prasenjit Dhar, and RC Katoch. A study on the prevalence of bovine tuberculosis in farmed dairy cattle in himachal pradesh. *Veterinary World*, 3(9):408, 2010.

[88] Mairead L Bermingham, Susan Brotherstone, Donagh P Berry, Simon J More, Margaret Good, Andrew R Cromie, Ian White, Isabella M Higgins, Mike Coffey, Sara H Downs, et al. Evidence for genetic variance in resistance to tuberculosis in great britain and irish holstein-friesian populations. In *BMC proceedings*, volume 5, pages 1–4. Springer, 2011.

[89] Ian W Richardson, Dan G Bradley, Isabella M Higgins, Simon J More, Jennifer McClure, and Donagh P Berry. Variance components for susceptibility to mycobacterium bovis infection in dairy and beef cattle. *Genetics Selection Evolution*, 46(1):1–11, 2014.

[90] H Dobson, SL Walker, MJ Morris, JE Routly, and RF Smith. Why is it getting more difficult to successfully artificially inseminate dairy cows? *Animal*, 2(8):1104–1111, 2008.

[91] Ellen Brooks-Pollock, Andrew JK Conlan, Andy P Mitchell, Ruth Blackwell, Trevelyan J McKinley, and James LN Wood. Age-dependent patterns of bovine tuberculosis in cattle. *Veterinary research*, 44(1):1–9, 2013.

[92] FO Inangolet, B Demelash, J Oloya, J Opuda-Asibo, and E Skjerve. A cross-sectional study of bovine tuberculosis in the transhumant and agro-pastoral cattle herds in

the border areas of katakwi and moroto districts, uganda. *Tropical animal health and production*, 40(7):501–508, 2008.

[93] DAR EN ETHIOPIE DE BAHIR. Bovine pulmonary tuberculosis at bahir dar municipality abattoir, ethiopia. *Animal Health and Production*, 56:223–229, 2008.

[94] Louis M O'Reilly and CJ Daborn. The epidemiology of mycobacterium bovis infections in animals and man: a review. *Tubercle and Lung disease*, 76:1–46, 1995.

[95] ML Bermingham, SJ More, M Good, AR Cromie, IM Higgins, and DP Berry. Genetic correlations between measures of mycobacterium bovis infection and economically important traits in irish holstein-friesian dairy cows. *Journal of Dairy Science*, 93(11):5413–5422, 2010.

[96] Michael L Doherty, Michael L Monaghan, Hugh F Bassett, Patrick J Quinn, and William C Davis. Effect of dietary restriction on cell-mediated immune responses in cattle infected with mycobacterium bovis. *Veterinary immunology and immunopathology*, 49(4):307–320, 1996.

[97] E Costello, ML Doherty, ML Monaghan, FC Quigley, and PF O'Reilly. A study of cattle-to-cattle transmission of mycobacterium bovis infection. *The Veterinary Journal*, 155(3):245–250, 1998.

[98] CM Sauter and RS Morris. Behavioural studies on the potential for direct transmission of tuberculosis from feral ferrets (mustela furo) and possums (trichosurus vulpecula) to farmed livestock. *New Zealand veterinary journal*, 43(7):294–300, 1995.

[99] Stefano Marangon, Marco Martini, Manuela Dalla Pozza, and Josè Ferreira Neto. A case-control study on bovine tuberculosis in the veneto region (italy). *Preventive Veterinary Medicine*, 34(2-3):87–95, 1998.

[100] Andrew JK Conlan, Trevelyan J McKinley, Katerina Karolemeas, Ellen Brooks Pollock, Anthony V Goodchild, Andrew P Mitchell, Colin PD Birch, Richard S Clifton-Hadley, and James LN Wood. Estimating the hidden burden of bovine tuberculosis in great britain. 2012.

[101] AV Goodchild and RS Clifton-Hadley. Cattle-to-cattle transmission of mycobacterium bovis. *Tuberculosis*, 81(1-2):23–41, 2001.

[102] LA Reilly and O Courtenay. Husbandry practices, badger sett density and habitat composition as risk factors for transient and persistent bovine tuberculosis on uk cattle farms. *Preventive Veterinary Medicine*, 80(2-3):129–142, 2007.

[103] Isabelle Carbonell. The ethics of big data in big agriculture. *Internet Policy Review*, 5(1), 2016.

[104] AM Ramírez-Villaescusa, GF Medley, S Mason, and LE Green. Risk factors for herd breakdown with bovine tuberculosis in 148 cattle herds in the south west of england. *Preventive Veterinary Medicine*, 95(3-4):224–230, 2010.

[105] Sam AJ Strain, James McNair, Stanley WJ McDowell, and Bacteriology Branch. Bovine tuberculosis: a review of diagnostic tests for m. bovis infection in badgers. *Report: Agri-Food and Biosciences Institute. Available online: http://www. dardni. gov. uk/afbi-literature-review-tb-reviewdiagnostic-tests-badgers.pdf (accessed 22 March 2016)*, 2011.

[106] JM Pollock and SD Neill. Mycobacterium boviss infection and tuberculosis in cattle. *The Veterinary Journal*, 163(2):115–127, 2002.

[107] Ulrich E Schaible and Stefan H E Kaufmann. Malnutrition and infection: complex mechanisms and global impacts. *PLoS medicine*, 4(5):e115, 2007.

[108] ML Monaghan, ML Doherty, JD Collins, JF Kazda, and PJ Quinn. The tuberculin test. *Cattle Practice*, 13:337–345, 2005.

[109] William Amos, Ellen Brooks-Pollock, Ruth Blackwell, Erin Driscoll, Martha Nelson-Flower, and Andrew JK Conlan. Genetic predisposition to pass the standard sicct test for bovine tuberculosis in british cattle. *PLoS One*, 8(3):e58245, 2013.

[110] Bo Norby, Paul C Bartlett, Scott D Fitzgerald, Larry M Granger, Colleen S Bruning-Fann, Diana L Whipple, and Janet B Payeur. The sensitivity of gross necropsy, caudal fold and comparative cervical tests for the diagnosis of bovine tuberculosis. *Journal of veterinary diagnostic investigation*, 16(2):126–131, 2004.

[111] Bovine tuberculosis - oie - world organisation for animal health, Jul 2021. Available online at: `https://www.oie.int/en/disease/bovine-tuberculosis/`.

[112] Nikki M Parrish, James D Dick, and William R Bishai. Mechanisms of latency in mycobacterium tuberculosis. *Trends in microbiology*, 6(3):107–112, 1998.

[113] Piran CL White and James KA Benhin. Factors influencing the incidence and scale of bovine tuberculosis in cattle in southwest england. *Preventive Veterinary Medicine*, 63(1-2):1–7, 2004.

[114] Michael Coad, Derek Clifford, Shelley G Rhodes, R Glyn Hewinson, H Martin Vordermeier, and Adam O Whelan. Repeat tuberculin skin testing leads to desensitisation in naturally infected tuberculous cattle which is associated with elevated interleukin-10 and decreased interleukin-1 beta responses. *Veterinary research*, 41(2):1–12, 2010.

[115] M Thom, JH Morgan, JC Hope, B Villarreal-Ramos, M Martin, and CJ Howard. The effect of repeated tuberculin skin testing of cattle on immune responses and disease

following experimental infection with mycobacterium bovis. *Veterinary immunology and immunopathology*, 102(4):399–412, 2004.

[116] AP Mitchell, LE Green, R Clifton-Hadley, J Mawdsley, R Sayers, GF Medley, et al. An analysis of single intradermal comparative cervical test (sicct) coverage in the gb cattle population. In *Society for Veterinary Epidemiology and Preventive Medicine. Proceedings of a meeting held at Exeter, UK, 29-31 March 2006*, pages 70–86. Society for Veterinary Epidemiology and Preventive Medicine, 2006.

[117] Council of European Union. Council regulation (EU) no 80/219/1980, 1980. `https://eur-lex.europa.eu/LexUriServ/LexUriServ.do?uri=CONSLEG:1964L0432:20071113:EN:PDF`.

[118] E Gormley, MB Doyle, T Fitzsimons, K McGill, and JD Collins. Diagnosis of mycobacterium bovis infection in cattle by use of the gamma-interferon (bovigam®) assay. *Veterinary microbiology*, 112(2-4):171–179, 2006.

[119] Angela Lahuerta-Marin, James McNair, Robin Skuce, Stewart McBride, Michelle Allen, Sam AJ Strain, Fraser D Menzies, Stanley JW McDowell, and Andrew W Byrne. Risk factors for failure to detect bovine tuberculosis in cattle from infected herds across northern ireland (2004–2010). *Research in veterinary science*, 107:233–239, 2016.

[120] W. Lilenbaum, J. C. Schettini, G. N. Souza, E. R. Ribeiro, E. C. Moreira, and L. S. Fonseca. Comparison between a γ-ifn assay and intradermal tuberculin test for the diagnosis of bovine tuberculosis in field trials in brazil. *Journal of Veterinary Medicine, Series B*, 46(5):353â358, 1999.

[121] Julio Alvarez, Lucia de Juan, Javier Bezos, Beatriz Romero, Jose Luis Saez, Sergio Marques, Concepcion Dominguez, Olga Minguez, Baudilio Fernandez-Mardomingo, Ana Mateos, and et al. Effect of paratuberculosis on the diagnosis of bovine tuberculosis in a cattle herd with a mixed infection using interferon-gamma detection assay. *Veterinary Microbiology*, 135(3-4):389â393, 2009.

[122] Irene Schiller, H. Martin Vordermeier, W. Ray Waters, Mitchell Palmer, Tyler Thacker, Adam Whelan, Roland Hardegger, Beatrice Marg-Haufe, Alex Raeber, Bruno Oesch, and et al. Assessment of mycobacterium tuberculosis ompatb as a novel antigen for the diagnosis of bovine tuberculosis. *Clinical and Vaccine Immunology*, 16(9):1314â1321, 2009.

[123] I. Schiller, B. Oesch, H. M. Vordermeier, M. V. Palmer, B. N. Harris, K. A. Orloski, B. M. Buddle, T. C. Thacker, K. P. Lyashchenko, W. R. Waters, and et al. Bovine tuberculosis: A review of current and emerging diagnostic techniques in view of their relevance for disease control and eradication. *Transboundary and Emerging Diseases*, 2010.

[124] Lina Awada, Paolo Tizzani, Elisabeth Erlacher-Vindel, Simona Forcella, and Paula Caceres. Bovine tuberculosis: worldwide picture. *Bovine tuberculosis. Oxfordshire: CABI. p*, pages 1–15, 2018.

[125] MA Skinner, DN Wedlock, and BM Buddle. Vaccination of animals against mycobacterium bovis. *Revue Scientifique et Technique-Office International des Epizooties*, 20(1):112–132, 2001.

[126] Martin Vordermeier, Gareth J Jones, and Adam O Whelan. Diva reagents for bovine tuberculosis vaccines in cattle. *Expert review of vaccines*, 10(7):1083–1091, 2011.

[127] Stephen P Carter, Mark A Chambers, Stephen P Rushton, Mark DF Shirley, Pia Schuchert, Stephane Pietravalle, Alistair Murray, Fiona Rogers, George Gettinby, Graham C Smith, et al. Bcg vaccination reduces risk of tuberculosis infection in vaccinated badgers and unvaccinated badger cubs. *PloS one*, 7(12):e49833, 2012.

[128] Christian Gortazar, Joaquín Vicente, Mariana Boadella, Cristina Ballesteros, Ruth C Galindo, Joseba Garrido, Alicia Aranaz, and Jose De la Fuente. Progress in the control of bovine tuberculosis in spanish wildlife. *Veterinary microbiology*, 151(1-2):170–178, 2011.

[129] Ellen Brooks-Pollock, Gareth O Roberts, and Matt J Keeling. A dynamic model of bovine tuberculosis spread and control in great britain. *Nature*, 511(7508):228–231, 2014.

[130] AR Renwick, PCL White, and Roy G Bengis. Bovine tuberculosis in southern african wildlife: a multi-species host–pathogen system. *Epidemiology & Infection*, 135(4):529–540, 2007.

[131] D Hutcheon. Tering, consumption, tables mesenterica. *Annual Report, Colonial Veterinary Surgeon, Cape of Good Hope*, 1880.

[132] Thomas M Daniel, Joseph H Bates, and Katharine A Downes. History of tuberculosis. *Tuberculosis: pathogenesis, protection, and control*, pages 13–24, 1994.

[133] F Boland, GE Kelly, M Good, and SJ More. Bovine tuberculosis and milk production in infected dairy herds in ireland. *Preventive veterinary medicine*, 93(2-3):153–161, 2010.

[134] Ellie JC Goldstein, Elsie Lee, and Robert S Holzman. Evolution and current use of the tuberculin test. *Clinical infectious diseases*, 34(3):365–370, 2002.

[135] DR Cox, Christl A Donnelly, F John Bourne, George Gettinby, John P McInerney, W Ivan Morrison, and Rosie Woodroffe. Simple model for tuberculosis in cattle and badgers. *Proceedings of the National Academy of Sciences*, 102(49):17588–17593, 2005.

[136] Bovine tuberculosis statistics and costs. Available online at: `http://www.bovinetb.info/`.

[137] John Kerb. Badger culling is ineffective, says architect of 10-year trial, Jul 2011. Available online at: https://www.theguardian.com/environment/2011/jul/11/badger-culling-ineffective-krebs.

[138] JJ Carrique-Mas, GF Medley, and LE Green. Risks for bovine tuberculosis in british cattle farms restocked after the foot and mouth disease epidemic of 2001. *Preventive Veterinary Medicine*, 84(1-2):85–93, 2008.

[139] Tuberculosis (tb) in cattle in great britain. Available online at: https://www.gov.uk/government/statistical-data-sets/tuberculosis-tb-in-cattle-in-great-britain.

[140] Sara H Downs, Alison Prosser, Adam Ashton, Stuart Ashfield, Lucy A Brunton, Adam Brouwer, Paul Upton, Andrew Robertson, Christl A Donnelly, and Jessica E Parry. Assessing effects from four years of industry-led badger culling in england on the incidence of bovine tuberculosis in cattle, 2013–2017. *Scientific reports*, 9(1):1–14, 2019.

[141] Kathryn A Glatter and Paul Finkelman. History of the plague: An ancient pandemic for the age of covid-19. *The American Journal of Medicine*, 134(2):176–181, 2021.

[142] Agence France-Presse. 500 years later, scientists discover what probably killed the aztecs. *Guardian*, Jan 2018.

[143] Who coronavirus (covid-19) dashboard. Available online at: https://covid19.who.int/.

[144] Tao Zhang, Qunfu Wu, and Zhigang Zhang. Probable pangolin origin of sars-cov-2 associated with the covid-19 outbreak. *Current biology*, 30(7):1346–1351, 2020.

[145] Nicolas Bacaër. Daniel bernoulli, dâalembert and the inoculation of smallpox (1760). In *A short history of mathematical population dynamics*, pages 21–30. Springer, 2011.

[146] WILLIAM HEATON Hamer. *Epidemic disease in England: the evidence of variability and of persistency of type*. Bedford Press, 1906.

[147] David L Smith, Katherine E Battle, Simon I Hay, Christopher M Barker, Thomas W Scott, and F Ellis McKenzie. Ross, macdonald, and a theory for the dynamics and control of mosquito-transmitted pathogens. *PLoS pathogens*, 8(4):e1002588, 2012.

[148] William Ogilvy Kermack and Anderson G McKendrick. A contribution to the mathematical theory of epidemics. *Proceedings of the royal society of london. Series A, Containing papers of a mathematical and physical character*, 115(772):700–721, 1927.

[149] A Deria, Z Jezek, K Markvart, P Carrasco, and J Weisfeld. The world's last endemic case of smallpox: surveillance and containment measures. *Bulletin of the World Health Organization*, 58(2):279, 1980.

[150] Donald Ainslie Henderson. *Smallpox: the death of a disease: the inside story of eradicating a worldwide killer*. Prometheus Books, 2009.

[151] Stephen Wiggins. *Introduction to applied nonlinear dynamical systems and chaos*, volume 2. Springer Science & Business Media, 2003.

[152] Adolf Hurwitz. Ueber die bedingungen, unter welchen eine gleichung nur wurzeln mit negativen reellen theilen besitzt. *Mathematische Annalen*, 46(2):273–284, 1895.

[153] AM Lyapunov. A general task about the stability of motion. *PhD Thesis*, 1892.

[154] Emilia Vynnycky and Richard White. *An introduction to infectious disease modelling*. OUP oxford, 2010.

[155] Odo Diekmann, Johan Andre Peter Heesterbeek, and Johan AJ Metz. On the definition and the computation of the basic reproduction ratio r o in models for infectious diseases in heterogeneous populations. *Journal of mathematical biology*, 28(4):365–382, 1990.

[156] Carlos Castillo-Chavez, Zhilan Feng, and Wenzhang Huang. On the computation of ro and its role on global stability. *Mathematical approaches for emerging and reemerging infectious diseases: an introduction*, 1:229, 2002.

[157] Pauline Van den Driessche and James Watmough. Reproduction numbers and subthreshold endemic equilibria for compartmental models of disease transmission. *Mathematical biosciences*, 180(1-2):29–48, 2002.

[158] B Buonomo and Deborah Lacitignola. On the backward bifurcation of a vaccination model with nonlinear incidence. *Nonlinear Analysis: Modelling and Control*, 16(1):30–46, 2011.

[159] Christopher M Kribs-Zaleta and Jorge X Velasco-Hernández. A simple vaccination model with multiple endemic states. *Mathematical biosciences*, 164(2):183–201, 2000.

[160] Wendi Wang. Backward bifurcation of an epidemic model with treatment. *Mathematical biosciences*, 201(1-2):58–71, 2006.

[161] O Sharomi and AB Gumel. Re-infection-induced backward bifurcation in the transmission dynamics of chlamydia trachomatis. *Journal of Mathematical Analysis and Applications*, 356(1):96–118, 2009.

[162] Z Mukandavire, W Garira, and JM Tchuenche. Modelling effects of public health educational campaigns on hiv/aids transmission dynamics. *Applied Mathematical Modelling*, 33(4):2084–2095, 2009.

[163] Timothy C Reluga, Jan Medlock, and Alan S Perelson. Backward bifurcations and multiple equilibria in epidemic models with structured immunity. *Journal of theoretical biology*, 252(1):155–165, 2008.

[164] Toshikazu Kuniya. Global stability of a multi-group svir epidemic model. *Nonlinear Analysis: Real World Applications*, 14(2):1135–1143, 2013.

[165] P Van Den Driessche, Lin Wang, and Xingfu Zou. Modeling diseases with latency and relapse. *Mathematical Biosciences & Engineering*, 4(2):205, 2007.

[166] ND Barlow, JM Kean, G Hickling, PG Livingstone, and AB Robson. A simulation model for the spread of bovine tuberculosis within new zealand cattle herds. *Preventive veterinary medicine*, 32(1-2):57–75, 1997.

[167] SD Neill, J Hanna, DP Mackie, and TG Bryson. Isolation of mycobacterium bovis from the respiratory tracts of skin test-negative cattle. *The Veterinary Record*, 131(3):45–47, 1992.

[168] Angela Lahuerta-Marin, MG Milne, James McNair, RA Skuce, SH McBride, FD Menzies, SJW McDowell, AW Byrne, IG Handel, and BM de C Bronsvoort. Bayesian latent class estimation of sensitivity and specificity parameters of diagnostic tests for bovine tuberculosis in chronically infected herds in northern ireland. *The Veterinary Journal*, 238:15–21, 2018.

[169] Gary Stoneham. Australian brucellosis and tuberculosis eradication campaign. 1986.

[170] A Essl. Longevity in dairy cattle breeding: a review. *Livestock production science*, 57(1):79–89, 1998.

[171] Angel H Alvarez. Revisiting tuberculosis screening: An insight to complementary diagnosis and prospective molecular approaches for the recognition of the dormant tb infection in human and cattle hosts. *Microbiological Research*, 252:126853, 2021.

[172] JM Kean, ND Barlow, and GJ Hickling. Evaluating potential sources of bovine tuberculosis infection in a new zealand cattle herd. *New Zealand Journal of Agricultural Research*, 42(1):101–106, 1999.

[173] H_H Kleeberg. The tuberculin test in cattle. *Journal of the South African Veterinary Association*, 31(2):213–225, 1960.

[174] Dennis S. Bernstein. *Matrix mathematics: Theory, facts, and formulas*. Princeton Press, 2 edition, 2009.

[175] Nuno Santos, Catarina Santos, Teresa Valente, Christian Gortázar, Virgílio Almeida, and Margarida Correia-Neves. Widespread environmental contamination with mycobacterium tuberculosis complex revealed by a molecular detection protocol. *PLoS One*, 10(11):e0142079, 2015.

[176] Daniel T Gillespie. Exact stochastic simulation of coupled chemical reactions. *The journal of physical chemistry*, 81(25):2340–2361, 1977.

[177] Naoki Masuda and Luis EC Rocha. A gillespie algorithm for non-markovian stochastic processes. *Siam Review*, 60(1):95–115, 2018.

[178] European badger. Available online at: `https://www.wildlifetrusts.org/wildlife-explorer/mammals/european-badger`.

[179] Anthony O'Hare, Daniel Balaz, David M. Wright, Carl McCormick, Stanley McDowell, Hannah Trewby, Robin A. Skuce, and Rowland R. Kao. A new phylodynamic model of mycobacterium bovis transmission in a multi-host system uncovers the role of the unobserved reservoir. *PLOS Computational Biology*, 17(6), Jun 2021.

[180] Maureen Carolyn Gates. Controlling endemic disease in cattle populations: current challenges and future opportunities. 2014.

[181] A. OHare, R. J. Orton, P. R. Bessell, and R. R. Kao. Estimating epidemiological parameters for bovine tuberculosis in british cattle using a bayesian partial-likelihood approach. *Proceedings of the Royal Society B: Biological Sciences*, 281(1783), Mar 2014.

Part IV

APPENDICES

APPENDIX A

In this appendix we investigate the model properties of the SE^nT^mIRC system (3.4), wWhere we preform the same system analysis as was applied in the SE^nTIRC system (3.3), on the SE^nT^mIRC system (3.4).

Theorem A.0.1 *All solutions for our SE^nT^mIRC system 3.4 which have initial conditions originating within $\mathbb{R}_+^{n+m+4}$ are bounded.*

$$\mathbb{R}_+^{n+m+4} = \{N(S, E_1, \ldots, E_n, T_1, \ldots, T_m, I, R, C) \mid S \geqslant 0, E_i \geqslant 0, T_m \geqslant 0, I \geqslant 0, R \geqslant 0, C \geqslant 0\}$$
$$\forall i \in \{1, \ldots, n\}, \quad \forall j \in \{1, \ldots, m\}$$

Proof A.0.1 *Let $N\big(S(t), E_1(t), \ldots, E_n(t), T_1(t), \ldots, T_m(t), I(t), R(t), C(t)\big)$ be an arbitrary solution of the SE^nT^mIRC system 3.4 with a non-negative initial conditions. The population of the herd is given by $N(t)$, where*

$$N(t) = S(t) + \sum_{i=1}^{n} E_i(t) + \sum_{j=1}^{m} T_j(t) + I(t) + R(t) + C(t)$$

Hence,

$$\frac{dN}{dt} = \Lambda - \mu(S + \sum_{i=1}^{n} E_i(t) + \sum_{j=1}^{m} T_j(t) + I + R + C) = \Lambda - \mu N(t)$$

By Grönwall lemma, if $x(t)$ is a function satisfying $\frac{dx}{dt} \leqslant ax + b$, where $x(0) = x_0$ and both a and b are constants then for all time $t \geqslant 0$,

$$x(t) \leqslant x_0 e^{at} + \frac{b}{a}\big(e^{at} - 1\big)$$

therefore,

$$0 \leqslant N\big(S(t), E_1(t), \ldots, E_n(t), T_1(t), \ldots, T_m(t), I(t), R(t), C(t)\big) \leqslant \frac{\Lambda}{\mu}\big(1 - e^{-\mu t}\big) + N(0)e^{-\mu t}$$

Hence,

$$0 \leqslant \limsup_{t\to\infty} N(t) \leqslant \frac{\Lambda}{\mu}$$

Therefore all solutions of the SE^nT^mIRC system 3.4 that originate in $\mathbb{R}_+^{n+m+4}$ are attracted to the following positive invariant region,

$$\Omega_{n+m} = \Big\{N(S(t), E_1(t), \ldots, E_n(t), T_1(t), \ldots, T_m(t), I(t), R(t), C(t)) \in \mathbb{R}_+^{n+m+4} : N \leqslant \frac{\Lambda}{\mu}\Big\}$$

The SE^nT^mIRC system 3.4 is therefore bounded. Additionally, since $\limsup N(t)$ *is independent of the initial conditions then the system is said to be uniformly bounded. As all solutions beginning in our positive invariant region* Ω_{n+m} *are trapped there, the analysis will be restricted to this feasibility region.*

Now that we have shown that the solutions are bounded the next stage is to show that the SE^nT^mIRC model solutions are well posed (i.e. exist and are unique depending on initial conditions).

Theorem A.0.2 *The SE^nT^mIRC system (3.4) is well posed.*

Proof A.0.2 *As the right hand side of system 3.4 are continuously differentiable functions on*

$$\mathbb{R}_+^{n+m+4} = \{N(S, E_1, \ldots, E_n, T_1, \ldots, T_j, I, R, C) \mid S \geqslant 0, E_i \geqslant 0, T_m \geqslant 0, I \geqslant 0, R \geqslant 0, C \geqslant 0\}$$
$$\forall i \in \{1, \ldots, n\}, \quad \forall j \in \{1, \ldots, m\}$$

and as the above theorem indicates that the first derivative of our system is uniformly bounded. This condition implies that the system equation are Lipschitz continuous and with this condition, we can apply the Picard Lindelöf theorem that proves a unique solution exists for the SE^nT^mIRC system (3.4).

The SE^nT^mIRC model is therefore well posed and any solution with initial conditions originating in Ω_{n+m} will remain in this feasibility region for all future time. Now, lets turn our attention the the system equilibrium and the basic reproductive number that bifurcates the system.

A.0.1 *Disease free equilibrium $\mathcal{DFE}$ and the Basic Reproductive Number $\mathcal{R}_0$*

The disease-free equilibrium $\mathcal{DFE}$ for the SE^nT^mIRC system (3.4) is given by:

$$\mathcal{DFE} = (\overline{S}, \overline{E_1}, \ldots, \overline{E_n}, \overline{T_1}, \ldots, \overline{T_m}, \overline{I}, \overline{R}, \overline{C}) = \left(\frac{\Lambda}{\mu}, 0, \ldots, 0\right)$$

Where, the over line notation denote that the compartment is at equilibrium (e.g. $\overline{S}$ represents the susceptible compartment at equilibrium).

Theorem A.0.3 *For the given SE^nT^mIRC system (3.4), where initial conditions originate in the positively invariant set* Ω_{n+m}*, the basic reproductive number is:*

$$\mathcal{R}_0 = \left(\frac{\gamma^n}{\kappa_1^n}\right)\left(\frac{\sigma^m}{\kappa_2^m}\right)\frac{\beta\kappa_4}{(\kappa_3\kappa_4 - \nu\alpha)}$$

Proof A.0.3 *The basic reproductive number $\mathcal{R}_0$ is calculated by the next generation matrix approach using the Van den Driesche and Watmough approach. This method has been extensively discussed in*

section 2.3.3.3 and therefore this analysis shall be condensed.

The basic reproductive number $\mathcal{R}_0$ *is the spectral radius of the next generation matrix given by* FV^{-1}*, hence the basic reproductive number is denoted by:*

$$\mathcal{R}_0 = \rho(FV^{-1})$$

Where the matrices F and V are generated from the linearization of the system equations evaluated at the disease free equilibrium. Where the two matrices F and V decouple the system, as F's compartment are only the parameters which induce new infections and the matrix V compartments are all other parameters. Although, lets consider the form that the F *matrix for our arbitrary system that has n-dimensional latency compartment. If the matrix order is considered to be in order* $E_1, \ldots, E_n, T_1, \ldots, T_m, I, R, C$ *then the matrix F will be a* $n + m + 3$ *dimensional square matrix. Although as there exist only a single infection transmission pathway (cattle to cattle) in the F matrix, therefore, it has the following simple formula,*

$$F_{[i,j]} = \begin{cases} \beta & \textit{if i=1 and j=n+m+1} \\ 0 & \textit{otherwise} \end{cases}$$

Where this simply confirms that all new infectious enter into the first exposure compartment E_1 *and are subsequently recorded as such.*

$$F = \begin{pmatrix} 0 & \ldots & 0 & \beta & 0 & 0 \\ 0 & \ldots & 0 & 0 & 0 & 0 \\ \vdots & \vdots & \vdots & \vdots & \vdots & \vdots \\ 0 & 0 & 0 & 0 & 0 & 0 \end{pmatrix}$$

Therefore, as there only exist one non-zero element of matrix F*, the next generational matrix* FV^{-1} *will entirely consist of one row of the inverse of the matrix V. Namely, as the only non-zero element (*β*) of F is positioned as* $F[1, n + m + 1]$ *this implies the next generation matrix will consist of* β *times the* $n + m + 1$ *row of the inverse of matrix V. Hence, the next generation matrix has the following form:*

$$FV^{-1} = \beta \begin{pmatrix} V^{-1}_{[n+m+1,1]} & V^{-1}_{[n+m+1,2]} & \cdots & V^{-1}_{[n+m+1,n+m+3]} \\ 0 & 0 & \ldots & 0 \\ \vdots & \vdots & \vdots & \vdots \\ 0 & 0 & 0 & 0 \end{pmatrix}$$

By the properties of eigenvalues, if the next generation matrix FV^{-1} *has the above form then the spectral radius of this matrix* FV^{-1} *is given by the first element of the next generation matrix (i.e.*

$\rho(FV^{-1}) = a_{11} \in FV^{-1}$*). This element corresponds to the the first element of the* $n + m + 1$ *row of the inverse of matrix V and hence, the basic reproductive number for the system* $\mathcal{R}_0$ *is given by:*

$$\mathcal{R}_0 = \rho(FV^{-1}) = \beta V^{-1}_{[n+m+1,1]}$$

Lets us now turn our focus to generating the inverse of the system V matrix for the system with n *arbitrary exposure compartments and* m *test sensitive compartments. First let us begin my commenting on the last row of our matrix V, this corresponds to the cull compartment and it wont effect the* $n + m + 1$ *row of the inverse of matrix V. As a result, we will excluded this row to reduce matrix size in this discussion.*

In our analyse of matrix V, we consider the matrix in its associated block form. Where a block matrix is a matrix whose elements are themselves matrices, which are called sub-matrices. By allowing a matrix to be viewed at different levels of abstraction, the block matrix viewpoint enables elegant proofs of results. Let us first define our matrix V as a block matrix, consisting of 4 sub-matrices , namely A,B,C,D.

$$V = \begin{pmatrix} A & B \\ C & D \end{pmatrix}$$

The sub-matrix A only incorporates the associated exposure compartments and the test sensitive compartments. As a result, the matrix is the dimension $n + m$ *square matrix, that is in a lower triangular form.*

$$A = \begin{pmatrix}
\kappa_1 & 0 & 0 & & & & & & \\
-\gamma & \kappa_1 & 0 & & & & & & \\
0 & -\gamma & \kappa_1 & & & & & & \\
 & & & \ddots & & & & & \\
 & & & & \kappa_1 & 0 & 0 & & \\
 & & & & -\gamma & \kappa_2 & 0 & & \\
 & & & & 0 & -\sigma & \kappa_2 & & \\
 & & & & & & & \ddots & \\
 & & & & & & & \kappa_2 & 0 & 0 \\
 & & & & & & & -\sigma & \kappa_2 & 0 \\
 & & & & & & & 0 & -\sigma & \kappa_2
\end{pmatrix}$$

Where the matrix is generated using the following function:

$$A_{[i,j]} = \begin{cases} \kappa_1 & \textit{if } i = j \qquad \forall i,j \in \{1,\dots,n\} \\ -\gamma & \textit{if } i = j+1 \qquad \forall i,j \in \{1,\dots,n\} \\ \kappa_2 & \textit{if } i = j \qquad \forall i,j \in \{n+1,\dots,n+m\} \\ -\sigma & \textit{if } i = j+1 \qquad \forall i,j \in \{n+1,\dots,n+m-1\} \\ 0 & \textit{otherwise} \end{cases}$$

The sub-matrix B represents the transfer (excluding new infected hosts) of hosts coming from either the infected or relapse compartments to the exposure and test sensitive compartments. As the system of differential equation for the SE^nT^mIRC system (3.4) show, no such transfer occur. Therefore, it should be clear to see that the sub-matrix B is a zero matrix of dimensions $[n+m, 2]$:

$$B = \begin{pmatrix} 0 & 0 \\ \vdots & \vdots \\ 0 & 0 \end{pmatrix}$$

The sub-matrix C similarly represents the transfer of hosts from the exposure and test sensitive compartments to either infected or relapse compartments. Through examining the SE^nT^mIRC differential equations, it can be seen that this only occurs when host progress from the test sensitive T_n compartment to the infected compartment I. Therefore, the sub-matrix C has only one non-zero element σ at the position $[1, n+m]$.

$$C = \begin{pmatrix} 0 & \dots & 0 & -\sigma \\ 0 & \dots & 0 & 0 \end{pmatrix} \qquad C_{[i,j]} = \begin{cases} -\sigma & \textit{if } i = 1 \textit{ and } j = n+m \\ 0 & \textit{otherwise} \end{cases}$$

Lastly the sub-matrix D represents the transfer between the infected or relapse compartments. Through examining the SE^nT^mIRC differential equations, it can be seen that the sub-matrix D has the following form:

$$D = \begin{pmatrix} \kappa_3 & -\alpha \\ -\nu & \kappa_4 \end{pmatrix}$$

In this block form, the next step in the analysis is to use a standard block form inversion, where the following formula allows us to obtain the inverse for our matrix V.

Theorem A.0.4 *Let $A \in \mathbb{F}^{n\times n}, B \in \mathbb{F}^{n\times m}, C \in \mathbb{F}^{m\times n}$, and $D \in \mathbb{F}^{m\times m}$. If A and $D - CA^{-1}B$ are non-singular, then the following formula holds:*

$$\mathbf{V^{-1}} = \begin{bmatrix} \mathbf{A} & \mathbf{B} \\ \mathbf{C} & \mathbf{D} \end{bmatrix}^{-1} = \begin{bmatrix} \mathbf{A^{-1}} + \mathbf{A^{-1}B}\left(\mathbf{D} - \mathbf{CA^{-1}B}\right)^{-1}\mathbf{CA^{-1}} & -\mathbf{A^{-1}B}\left(\mathbf{D} - \mathbf{CA^{-1}B}\right)^{-1} \\ -\left(\mathbf{D} - \mathbf{CA^{-1}B}\right)^{-1}\mathbf{CA^{-1}} & \left(\mathbf{D} - \mathbf{CA^{-1}B}\right)^{-1} \end{bmatrix}$$

For a proof of this statement please see [174]. As our block matrix B is the zero matrix, therefore we must show that A *and* D *are non-singular for this formula to hold, which will be completed in this analysis. Additional as the block matrix B is the zero matrix, this above condition can be simplified to the following:*

$$\mathbf{V^{-1}} = \begin{bmatrix} \mathbf{A} & \mathbf{B} \\ \mathbf{C} & \mathbf{D} \end{bmatrix}^{-1} = \begin{bmatrix} \mathbf{A^{-1}} & 0 \\ -\mathbf{DCA^{-1}} & \mathbf{D^{-1}} \end{bmatrix}$$

Therefore, let us begin by constructing the inverses for the our defined sub-matrices A, D *to construct* A^{-1}, D^{-1}*, and* $-DCA^{-1}$*.*

By the properties of matrices, the inverses of our sub-matrix A is defined as follows:

$$A^{-1} = \begin{pmatrix} \frac{1}{\kappa_1} & 0 & 0 & \cdots & \cdots & 0 \\ \frac{\gamma}{\kappa_1^2} & \frac{1}{\kappa_1} & 0 & & & \vdots \\ \frac{\gamma^2}{\kappa_1^3} & \frac{\gamma}{\kappa_1^2} & \frac{1}{\kappa_1} & & & \vdots \\ \vdots & \vdots & \vdots & \ddots & & \vdots \\ \left(\frac{\gamma^n}{\kappa_1^n}\right)\left(\frac{\sigma^{m-3}}{\kappa_2^{m-2}}\right) & \left(\frac{\gamma^{n-1}}{\kappa_1^{n-1}}\right)\left(\frac{\sigma^{m-3}}{\kappa_2^{m-2}}\right) & \left(\frac{\gamma^{n-2}}{\kappa_1^{n-2}}\right)\left(\frac{\sigma^{m-3}}{\kappa_2^{m-2}}\right) & \cdots & \frac{1}{\kappa_2} & 0 & 0 \\ \left(\frac{\gamma^n}{\kappa_1^n}\right)\left(\frac{\sigma^{m-2}}{\kappa_2^{m-1}}\right) & \left(\frac{\gamma^{n-1}}{\kappa_1^{n-1}}\right)\left(\frac{\sigma^{m-2}}{\kappa_2^{m-1}}\right) & \left(\frac{\gamma^{n-2}}{\kappa_1^{n-2}}\right)\left(\frac{\sigma^{m-2}}{\kappa_2^{m-1}}\right) & & \frac{\sigma}{\kappa_2^2} & \frac{1}{\kappa_2} & 0 \\ \left(\frac{\gamma^n}{\kappa_1^n}\right)\left(\frac{\sigma^{m-1}}{\kappa_2^m}\right) & \left(\frac{\gamma^{n-1}}{\kappa_1^{n-1}}\right)\left(\frac{\sigma^{m-1}}{\kappa_2^m}\right) & \left(\frac{\gamma^{n-2}}{\kappa_1^{n-2}}\right)\left(\frac{\sigma^{m-1}}{\kappa_2^m}\right) & \cdots & \frac{\sigma^2}{\kappa_2^3} & \frac{\sigma}{\kappa_2^2} & \frac{1}{\kappa_2} \end{pmatrix}$$

Where this inverse can easily be verified and can be proven using straight forward induction.

The next sub-matrix we find the inverse for is D:

$$D = \begin{pmatrix} \kappa_3 & -\alpha \\ -\nu & \kappa_4 \end{pmatrix} \quad \textit{and} \quad D^{-1} = \frac{1}{\kappa_4\kappa_3 - \nu\alpha}\begin{pmatrix} \kappa_4 & \alpha \\ \nu & \kappa_3 \end{pmatrix}$$

Given the inverse for both our sub-matrices A and D, the next step to obtain the next generation matrix is to calculate $-D^{-1}CA^{-1}$*, and given that* $-D^{-1}C$ *is given by:*

$$-D^{-1}C = \frac{1}{\kappa_4\kappa_3 - \nu\alpha}\begin{pmatrix} 0 & \dots & 0 & \kappa_4\sigma \\ 0 & \dots & 0 & \nu\sigma \end{pmatrix}$$

Hence,

$$-D^{-1}CA^{-1} = \frac{1}{\kappa_4\kappa_3 - \nu\alpha}\begin{pmatrix} \frac{\gamma^n\sigma^m}{\kappa_1^n\kappa_2^m}\kappa_4 & \frac{\gamma^n\sigma^{m-1}}{\kappa_1^n\kappa_2^{m-1}}\kappa_4 & \dots & \frac{\kappa_4\sigma}{\kappa_2} \\ \frac{\gamma^n\sigma^m}{\kappa_1^n\kappa_2^m}\nu & \frac{\gamma^n\sigma^{m-1}}{\kappa_1^n\kappa_2^{m-1}}\nu & \dots & \frac{\nu\sigma}{\kappa_2} \end{pmatrix}$$

Therefore, this last result is the final step in calculating the next inverse of our matrix V, therefore we are finally able to calculate the next generation matrix FV^{-1}. *As discussed previously, the next generation matrix consists of the* $n+m$ *row of the inverse of V, therefore it consists of the first row of both* $-D^{-1}CA^{-1}$ *and* $D^{-}1$.

$$FV^{-1} = \frac{\beta}{\kappa_4\kappa_3 - \nu\alpha}\begin{pmatrix} \frac{\gamma^n\sigma^m}{\kappa_1^n\kappa_2^m}\kappa_4 & \frac{\gamma^n\sigma^{m-1}}{\kappa_1^n\kappa_2^{m-1}}\kappa_4 & \dots & \frac{\kappa_4\sigma}{\kappa_2} & \frac{\kappa_4}{\beta} & \frac{\alpha}{\beta} \\ 0 & 0 & \dots & 0 & 0 & 0 \\ \vdots & \vdots & \ddots & \vdots & \vdots & \vdots \\ 0 & 0 & 0 & 0 & 0 & 0 \end{pmatrix}$$

Finally by the products of eigenvalues, the spectral radius of the next generation matrix is clearly its first element and hence the basic reproductive number for the SE^nT^mIRC *system (3.4) is as follows:*

$$\mathcal{R}_0 = \rho(FV^{-1}) = \left(\frac{\gamma^n}{\kappa_1^n}\right)\left(\frac{\gamma^m}{\kappa_2^m}\right)\frac{\beta\kappa_4}{\kappa_4\kappa_3 - \nu\alpha}$$

The basic reproductive number $\mathcal{R}_0$ for the given $n+m$ dimensional SE^nT^mIRC system correctly corresponds to the basic reproductive number given for the SE_1E_2TIRC system and the SE^nTIRC system (3.3).

We have therefore shown that given the basic reproductive number is less than unity ($\mathcal{R}_0 < 1$) then the disease free equilibrium $\mathcal{DFE}$ is locally asymptotically stable. In the remaining of this section, we examine the globally asymptotically stable nature of all solutions in the feasibility region Ω_{n+m} given that $\mathcal{R}_0 < 1$.

By the properties of the next generation matrix, we have shown that given the basic reproductive number is less than unity ($\mathcal{R}_0 < 1$) then the disease free equilibrium $\mathcal{DFE}$ is locally asymptotically stable. Although, as the remaining of this section will show this analysis can be extended. As given that our basic reproductive number is less than unity (i.e. $\mathcal{R}_0 < 1$), then the following theorem proves all solutions in the feasibility region Ω_{n+m} are globally asymptotically attracted to the $\mathcal{DFE}$.

Theorem A.0.5 *For the given* SE^nT^mIRC *system 3.4, where initial conditions originate in the positively invariant set* Ω_{n+m}, *the disease free equilibrium* $\mathcal{DFE}$ *is globally asymptotically stable (GAS) in* Ω_{n+m} *whenever* $\mathcal{R}_0 < 1$.

Proof A.0.4 *This theorem shall be proved by the existence of the following Lyapunov function:*

$$\mathcal{F} = \sum_{i=1}^{n} X_i E_i + \sum_{j=1}^{m} Y_j T_j + Z_1 I + Z_2 R$$

Where the expressions X_i, Y_j, Z_1, Z_2 *for all* $i \in \{1, \ldots, n\}$ *and* $j \in \{1, \ldots, m\}$ *are defined as follows:*

$$\begin{aligned}
X_i &= \beta\sigma\kappa_4 \frac{\kappa_1^{i-1}}{\gamma^{i-2}} && \forall i \in \{1, \ldots, n+1\} \\
Y_j &= \beta\kappa_4 \frac{\kappa_1^{n}}{\gamma^{n-1}} \frac{\kappa_2^{j-1}}{\sigma^{j-2}} && \forall j \in \{1, \ldots, m+1\} \\
Z_1 &= \beta\kappa_4 \frac{\kappa_1^{n}}{\gamma^{n-1}} \frac{\kappa_2^{m}}{\sigma^{m-1}} \\
Z_2 &= \beta\alpha \frac{\kappa_1^{n}}{\gamma^{n-1}} \frac{\kappa_2^{m}}{\sigma^{m-1}}
\end{aligned}$$

Notice, that our expression are linked in the cross over points, for example if you consider what X_{n+1} *is you will see that it is equivalent to* Y_1*. Similarly, for the variable* Y*, we see that* $Y_{m+1} = Z_1$*. Let us now differentiate our Lyapunov function* $\mathcal{F}$ *with respect to time. After expanding the Lyapunov function and some rearrangement we obtain* $\mathcal{F}$ *in the following form:*

$$\begin{aligned}
\dot{\mathcal{F}} = X_1 \beta I\left(\frac{S}{N}\right) + \sum_{i=1}^{n} \left(\gamma X_{i+1} - \kappa_1 X_i\right) E_i + \sum_{j=1}^{m} \left(\sigma Y_{j+1} - \kappa_2 Y_j\right) T_j + \\
+ \left(\nu Z_2 - \kappa_3 Z_1\right) I + \left(\alpha Z_1 - \kappa_4 Z_2\right) R
\end{aligned}$$

Where this expression can be simplified to the following form:

$$\dot{\mathcal{F}} = X_1 \beta I\left(\frac{S}{N}\right) + \left(\nu Z_2 - \kappa_3 Z_1\right) I$$

As a result of our choice of $X_{i,j}, _1, Z_2$ *expressions, the following expression are equal to zero.*

$$\begin{aligned}
&\sum_{i=1}^{n} \left(\gamma X_{i+1} - \kappa_1 X_i\right) E_i = 0 && \text{as } \gamma X_{i+1} = \beta\sigma\kappa_4 \left(\frac{\kappa_1^{i}}{\gamma^{i-2}}\right) = \kappa_1 X_i \quad \forall i \in \{1, \ldots, n\} \\
&\sum_{j=1}^{m} \left(\sigma Y_{j+1} - \kappa_2 Y_j\right) T_j = 0 && \text{as } \sigma Y_{j+1} = \beta\kappa_4 \left(\frac{\kappa_1^{n}}{\gamma^{n-1}}\right)\left(\frac{\kappa_2^{j}}{\sigma^{j-2}}\right) = \kappa_2 Y_j \quad \forall j \in \{1, \ldots, m\} \\
&\left(\alpha Z_1 - \kappa_4 Z_2\right) R = 0 && \text{as } \alpha Z_1 = \beta\alpha\kappa_4 \left(\frac{\kappa_1^{n}}{\gamma^{n-1}}\right)\left(\frac{\kappa_2^{m}}{\sigma^{m-1}}\right) = \kappa_4 Z_2
\end{aligned}$$

The next step in the analysis is to enter the our system parameter values instead of X_i, Y_j, Z *parameters. After doing so the Lyapunov function has the following form:*

$$
\begin{aligned}
\dot{\mathcal{F}} &= X_1 \beta I\left(\frac{S}{N}\right) + \left(\nu Z_2 - \kappa_3 Z_1\right) I \\
&= \beta\gamma\sigma\kappa_4\left(\beta\frac{SI}{N}\right) + \left(\beta\alpha\nu\left(\frac{\kappa_1^n}{\gamma^{n-1}}\right)\left(\frac{\kappa_2^m}{\sigma^{m-1}}\right) - \beta\kappa_3\kappa_4\left(\frac{\kappa_1^n}{\gamma^{n-1}}\right)\left(\frac{\kappa_2^m}{\sigma^{m-1}}\right)\right) I \\
&= \left(\beta\gamma\sigma\kappa_4\left(\frac{S}{N}\right) + \left(\frac{\kappa_1^n}{\gamma^{n-1}}\right)\left(\frac{\kappa_2^m}{\sigma^{m-1}}\right)(\alpha\nu - \kappa_3\kappa_4)\right)\beta I \\
&= \left(\frac{\kappa_1^n}{\gamma^{n-1}}\right)\left(\frac{\kappa_2^m}{\sigma^{m-1}}\right)\left(\beta\kappa_4\left(\frac{\gamma^n}{\kappa_1^n}\right)\left(\frac{\sigma^m}{\kappa_2^m}\right)\left(\frac{S}{N}\right) - (\kappa_3\kappa_4 - \alpha\nu)\right)\beta I \\
&= \left(\frac{\kappa_1^n}{\gamma^{n-1}}\right)\left(\frac{\kappa_2^m}{\sigma^{m-1}}\right)\left(\kappa_3\kappa_4 - \alpha\nu\right)\left(\frac{\beta\kappa_4}{(\kappa_3\kappa_4 - \alpha\nu)}\left(\frac{\gamma^n}{\kappa_1^n}\right)\left(\frac{\sigma^m}{\kappa_2^m}\right)\left(\frac{S}{N}\right) - 1\right)\beta I \\
&= \left(\frac{\kappa_1^n}{\gamma^{n-1}}\right)\left(\frac{\kappa_2^m}{\sigma^{m-1}}\right)(\kappa_3\kappa_4 - \alpha\nu)\left(\mathcal{R}_0\left(\frac{S}{N}\right) - 1\right)\beta I \\
&\leqslant \left(\frac{\kappa_1^n}{\gamma^{n-1}}\right)\left(\frac{\kappa_2^m}{\sigma^{m-1}}\right)(\kappa_3\kappa_4 - \alpha\nu)\left(\mathcal{R}_0 - 1\right)\beta I
\end{aligned}
$$

Therefore, our Lyapunov function is negative if our basic reproductive number is less than one (i.e. $\dot{\mathcal{F}} \leqslant 0$ *for* $\mathcal{R}_0 < 1$*, as* $S \leqslant N$ *in* Ω_{n+m}*). As the Lyapunov function has shown that the* $\mathcal{DFE}$ *is globally asymptotically stable (GAS) if* $\dot{\mathcal{F}} < 0$ *then it remains to show when* $\dot{\mathcal{F}} = 0$*.*

Notice that $\dot{\mathcal{F}} = 0$ *if and only is* $I = 0$*. As the model parameters are non-negative and given initial condition in* Ω_{n+m} *then it follows that, if* $I = 0$ *then by the system differential equations* 3.4 *then* $(E_1, \ldots, E_n, T_1, \ldots, T_m, I, R, C) \to (0, 0, \ldots, 0)$ *as* $t \to \infty$*. Hence, as the total population* $N(t)$ *is a conserved quantity then* $S \to N$ *and* $C \to 0$ *as* $t \to \infty$*. Thereby by the LaSalle's invariance principle,* $\dot{\mathcal{F}} = 0$ *implies that system 3.4's disease free equilibrium* $\mathcal{DFE}$ *is asymptotically stable. Hence, as this is true for both* $I > 0$ *and* $I = 0$*, the disease free equilibrium* $\mathcal{DFE}$ *is globally asymptotically stable (GAS) in* Ω_{n+m} *whenever* $\mathcal{R}_0 < 1$*.*

A.0.2 *Endemic Equilibrium and its Stability*

Let now examine the case when the basic reproductive number is greater than unity (i.e. $\mathcal{R}_0 > 1$), what does this mean for the long term solutions? As we shall show in this section, solutions are attracted to the endemic equilibrium ($\mathcal{EE}$). Where the endemic equilibrium represents disease being maintained in the system at a particular endemic level, that continuous depends on system parameters. The definition of the endemic equilibrium for the SE^nT^mIRC system 3.4 is given below:

$$\mathcal{EE} = (\overline{S}, \overline{E_1}, \ldots, \overline{E_n}, \overline{T_1}, \ldots, \overline{T_m}, \overline{I}, \overline{R}, \overline{C})$$

$$
\begin{aligned}
\overline{S} &= \frac{\Lambda}{(\lambda^{**}+\kappa_0)},\\
\overline{E_i} &= \frac{\gamma}{\kappa_1}\overline{E_{i-1}} = \frac{\gamma^{i-1}}{\kappa_1^{i-1}}\overline{E_1} = \frac{\gamma^{i-1}}{\kappa_1^{i}}\lambda^{**}\overline{S},\\
\overline{T_j} &= \frac{\sigma}{\kappa_2}\overline{T_{j-1}} = \frac{\sigma^{j-1}}{\kappa_2^{j-1}}\overline{T_1} = \frac{\sigma^{j-1}}{\kappa_2^{j}}\left(\frac{\gamma^n}{\kappa_1^n}\right)\lambda^{**}\overline{S},\\
\overline{I} &= \left(\frac{\sigma\kappa_4}{\kappa_3\kappa_4-\alpha\nu}\right)\overline{T_m} = \left(\frac{\kappa_4}{\kappa_3\kappa_4-\alpha\nu}\right)\left(\frac{\gamma^n}{\kappa_1^n}\right)\left(\frac{\sigma^m}{\kappa_2^m}\right)\lambda^{**}\overline{S}\\
\overline{R} &= \frac{\nu}{\kappa_4}\overline{I} = \left(\frac{\nu}{\kappa_3\kappa_4-\alpha\nu}\right)\left(\frac{\gamma^n}{\kappa_1^n}\right)\left(\frac{\sigma^m}{\kappa_2^m}\right)\lambda^{**}\overline{S}\\
\overline{C} &= \frac{\tau_1}{\mu}\left(\overline{S}+\sum_{i=1}^{n}\overline{E_i}\right)+\frac{\tau_2}{\mu}\left(\sum_{j=1}^{m}\overline{T_j}+\overline{I}+\overline{R}\right)
\end{aligned}
$$

Where, the following parameter are described the same as before:

$$\kappa_0 = (\mu+\tau_1) \qquad \kappa_1 = (\mu+\tau_1+\gamma) \quad \kappa_2 = (\mu+\tau_2+\sigma) \qquad \kappa_3 = (\mu+\tau_2+\nu) \quad \kappa_4 = (\mu+\tau_2+\alpha)$$

Similarly to the previous analysis, let us now determine the stability condition to the endemic equilibrium $(\mathcal{EE})$ through the use of Lyapunov functions.

Theorem A.0.6 *For the given SE^nT^mIRC system 3.4, where initial conditions originate in the positively invariant set Ω_{n+m}, the endemic equilibrium $\mathcal{EE}$ is globally asymptotically stable (GAS) in Ω_{n+m} whenever $\mathcal{R}_0 > 1$.*

Proof A.0.5 *If the basic reproductive number is above unity ($\mathcal{R}_0 > 1$) then our unique endemic equilibrium exists ($\mathcal{EE} < 1$) and the following non-linear Lyapunov function proves it is globally asymptotically stable (GAS).*

$$
\begin{aligned}
\mathcal{F} = \overline{S}\left(\frac{S}{\overline{S}}-\ln\frac{\overline{S}}{S}\right) &+ \sum_{i=1}^{n}\left(\frac{\kappa_1^{i-1}}{\gamma^{i-1}}\right)\overline{E_i}\left(\frac{E_i}{\overline{E_i}}-\ln\frac{\overline{E_i}}{E_i}\right) + \sum_{j=1}^{m}\left(\frac{\kappa_1^n}{\gamma^n}\right)\left(\frac{\kappa_2^{j-1}}{\sigma^{j-1}}\right)\overline{T_j}\left(\frac{T_j}{\overline{T_j}}-\ln\frac{\overline{T_j}}{T_j}\right)\\
&+\left(\frac{\kappa_1^n}{\gamma^n}\right)\left(\frac{\kappa_2^m}{\sigma^m}\right)\overline{I}\left(\frac{I}{\overline{I}}-\ln\frac{\overline{I}}{I}\right)+\left(\left(\frac{\kappa_1^n}{\gamma^n}\right)\left(\frac{\kappa_2^m}{\sigma^m}\right)\frac{\kappa_3}{\nu}-\frac{\beta\overline{S}}{N\nu}\right)\overline{R}\left(\frac{R}{\overline{R}}-\ln\frac{\overline{R}}{R}\right)
\end{aligned}
$$

Therefore, the differentiated Lyapunov Function is given by:

$$
\begin{aligned}
\dot{\mathcal{F}} = \left(1-\frac{\overline{S}}{S}\right)\dot{S} &+ \sum_{i=1}^{n}\left(\frac{\kappa_1^{i-1}}{\gamma^{i-1}}\right)\left(1-\frac{\overline{E_i}}{E_i}\right)\dot{E_i} + \sum_{j=1}^{m}\left(\frac{\kappa_1^n}{\gamma^n}\right)\left(\frac{\kappa_2^{j-1}}{\sigma^{j-1}}\right)\left(1-\frac{\overline{T_j}}{T_j}\right)\dot{T_j}\\
&+\left(\frac{\kappa_1^n}{\gamma^n}\right)\left(\frac{\kappa_2^m}{\sigma^m}\right)\left(1-\frac{\overline{I}}{I}\right)\dot{I}+\left(\left(\frac{\kappa_1^n}{\gamma^n}\right)\left(\frac{\kappa_2^m}{\sigma^m}\right)\frac{\kappa_3}{\nu}-\frac{\beta\overline{S}}{N\nu}\right)\left(1-\frac{\overline{R}}{R}\right)\dot{R}
\end{aligned}
$$

By expanding the brackets we obtain,

$$
\begin{aligned}
\dot{\mathcal{F}} &= \dot{S} - \left(\frac{\overline{S}}{S}\right)\dot{S} \\
&+ \sum_{i=1}^{n}\left(\frac{\kappa_1^{i-1}}{\gamma^{i-1}}\right)\dot{E_i} - \sum_{i=1}^{n}\left(\frac{\kappa_1^{i-1}}{\gamma^{i-1}}\right)\left(\frac{\overline{E_i}}{E_i}\right)\dot{E_i} \\
&+ \sum_{j=1}^{m}\left(\frac{\kappa_1^{n}}{\gamma^{n}}\right)\left(\frac{\kappa_2^{j-1}}{\sigma^{j-1}}\right)\dot{T_j} - \sum_{j=1}^{m}\left(\frac{\kappa_1^{n}}{\gamma^{n}}\right)\left(\frac{\kappa_2^{j-1}}{\sigma^{j-1}}\right)\left(\frac{\overline{T_j}}{T_j}\right)\dot{T_j} \\
&+ \left(\frac{\kappa_1^{n}}{\gamma^{n}}\right)\left(\frac{\kappa_2^{m}}{\sigma^{m}}\right)\dot{I} - \left(\frac{\kappa_1^{n}}{\gamma^{n}}\right)\left(\frac{\kappa_2^{m}}{\sigma^{m}}\right)\left(\frac{\overline{I}}{I}\right)\dot{I} \\
&+ \left(\left(\frac{\kappa_1^{n}}{\gamma^{n}}\right)\left(\frac{\kappa_2^{m}}{\sigma^{m}}\right)\frac{\kappa_3}{\nu} - \frac{\beta\overline{S}}{N\nu}\right)\dot{R} - \left(\left(\frac{\kappa_1^{n}}{\gamma^{n}}\right)\left(\frac{\kappa_2^{m}}{\sigma^{m}}\right)\frac{\kappa_3}{\nu} - \frac{\beta\overline{S}}{N\nu}\right)\left(\frac{\overline{R}}{R}\right)\dot{R}
\end{aligned}
$$

Lets define the following sub-functions, $\dot{\mathcal{F}_1}$ and $\dot{\mathcal{F}_2}$.

$$\dot{\mathcal{F}} = \dot{\mathcal{F}_1} + \dot{\mathcal{F}_2}$$

$$\dot{\mathcal{F}_1} = \frac{\beta I\overline{S}}{N} - \frac{\beta IS}{N} + \sum_{i=1}^{n}\left(\frac{\kappa_1^{i-1}}{\gamma^{i-1}}\right)\dot{E_i} + \sum_{j=1}^{m}\frac{\kappa_1^{n}}{\gamma^{n}}\left(\frac{\kappa_2^{j-1}}{\sigma^{j-1}}\right)\dot{T_j} + \left(\frac{\kappa_1^{n}}{\gamma^{n}}\right)\left(\frac{\kappa_2^{m}}{\sigma^{m}}\right)\dot{I} + \left(\left(\frac{\kappa_1^{n}}{\gamma^{n}}\right)\left(\frac{\kappa_2^{m}}{\sigma^{m}}\right)\frac{\kappa_3}{\nu} - \frac{\beta\overline{S}}{N\nu}\right)\dot{R}$$

$$
\begin{aligned}
\dot{\mathcal{F}_2} = \dot{S} &- \left(\frac{\overline{S}}{S}\right)\dot{S} - \frac{\beta I\overline{S}}{N} + \frac{\beta IS}{N} - \sum_{i=1}^{n}\left(\frac{\kappa_1^{i-1}}{\gamma^{i-1}}\right)\left(\frac{\overline{E_i}}{E_i}\right)\dot{E_i} - \sum_{j=1}^{m}\frac{\kappa_1^{n}}{\gamma^{n}}\left(\frac{\kappa_2^{j-1}}{\sigma^{j-1}}\right)\left(\frac{\overline{T_j}}{T_j}\right)\dot{T_j} \\
&- \left(\frac{\kappa_1^{n}}{\gamma^{n}}\right)\left(\frac{\kappa_2^{m}}{\sigma^{m}}\right)\left(\frac{\overline{I}}{I}\right)\dot{I} - \left(\left(\frac{\kappa_1^{n}}{\gamma^{n}}\right)\left(\frac{\kappa_2^{m}}{\sigma^{m}}\right)\frac{\kappa_3}{\nu} - \frac{\beta\overline{S}}{N\nu}\right)\left(\frac{\overline{R}}{R}\right)\dot{R}
\end{aligned}
$$

In order to understand our sub-functions in greater detail ($\dot{\mathcal{F}_1}$ and$\dot{\mathcal{F}_2}$), we will use the following equalities to aid our analysis.

$$
\begin{aligned}
\left(\frac{\kappa_1^{i}}{\gamma^{i-1}}\right)\overline{E_i} = \left(\frac{\kappa_1^{i-1}}{\gamma^{i-1}}\right)\left(\kappa_1\overline{E_i}\right) = \left(\frac{\kappa_1^{i-1}}{\gamma^{i-1}}\right)\left(\gamma\overline{E}_{i-1}\right) = \kappa_1\overline{E_1} = \cdots = \frac{\beta\overline{S}\overline{I}}{N} \\
\left(\frac{\kappa_1^{n}}{\gamma^{n}}\right)\left(\frac{\kappa_2^{j}}{\sigma^{j-1}}\right)\overline{T_j} = \left(\frac{\kappa_1^{n}}{\gamma^{n}}\right)\left(\frac{\kappa_2^{j-1}}{\sigma^{j-1}}\right)\left(\kappa_2\overline{T_j}\right) = \left(\frac{\kappa_1^{n}}{\gamma^{n}}\right)\left(\frac{\kappa_2^{j-1}}{\sigma^{j-1}}\right)\left(\sigma\overline{T}_{j-1}\right) = \cdots = \left(\frac{\kappa_1^{n}}{\gamma^{n}}\right)\kappa_2\overline{T_1} \\
\left(\frac{\kappa_1^{n}}{\gamma^{n}}\right)\kappa_2\overline{T_1} = \left(\frac{\kappa_1^{n}}{\gamma^{n}}\right)\gamma\overline{E_n} = \left(\frac{\kappa_1^{n-1}}{\gamma^{n-1}}\right)\kappa_1\overline{E_n} = \frac{\beta\overline{S}\overline{I}}{N} \\
\kappa_3\overline{I} = \alpha\overline{R} + \sigma\overline{T_m} \\
\nu\overline{I} = \kappa_4\overline{R}
\end{aligned}
$$

Using the equalities, the following relations can be obtained:

$$\dot{S} - \left(\frac{\overline{S}}{S}\right)\dot{S} - \frac{\beta I\overline{S}}{N} + \frac{\beta IS}{N} = \frac{\beta I\overline{S}}{N}\left(1 - \frac{\overline{S}}{S}\right) + \kappa_0\overline{S}\left(2 - \frac{\overline{S}}{S} - \frac{S}{\overline{S}}\right)$$

$$-\left(\frac{\overline{E_1}}{E_1}\right)\dot{E_1} = \frac{\beta I\overline{S}}{N}\left(1 - \frac{\overline{E_1}}{E_1}\frac{S}{\overline{S}}\frac{I}{\overline{I}}\right)$$

$$-\frac{\kappa_1^{i-1}}{\gamma^{i-1}}\left(\frac{\overline{E_i}}{E_i}\right)\dot{E_i} = \frac{\beta I\overline{S}}{N}\left(1 - \frac{\overline{E_i}}{E_i}\frac{E_{i-1}}{\overline{E_{i-1}}}\right)$$

$$-\frac{\kappa_1^n}{\gamma^n}\left(\frac{\overline{T_1}}{T_1}\right)\dot{T_1} = \frac{\beta I\overline{S}}{N}\left(1 - \frac{\overline{T_1}}{T_1}\frac{E_n}{\overline{E_n}}\right)$$

$$-\frac{\kappa_1^n}{\gamma^n}\frac{\kappa_2^{j-1}}{\sigma^{j-1}}\left(\frac{\overline{T_j}}{T_j}\right)\dot{T_j} = \frac{\beta I\overline{S}}{N}\left(1 - \frac{\overline{T_j}}{T_j}\frac{T_{j-1}}{\overline{T_{j-1}}}\right)$$

$$-\frac{\kappa_1^n}{\gamma^n}\frac{\kappa_2^m}{\sigma^m}\left(\frac{\overline{I}}{I}\right)\dot{I} = \frac{\beta I\overline{S}}{N}\left(1 - \frac{\overline{I}}{I}\frac{T_m}{\overline{T_m}}\right) + \frac{\kappa_1^n}{\gamma^n}\frac{\kappa_2^m}{\sigma^m}\alpha\overline{R}\left(1 - \frac{\overline{I}}{I}\frac{R}{\overline{R}}\right)$$

$$-\left(\left(\frac{\kappa_1^n}{\gamma^n}\right)\left(\frac{\kappa_1^m}{\sigma^m}\right)\frac{\kappa_3}{\nu} - \frac{\beta\overline{S}}{N\nu}\right)\left(\frac{\overline{R}}{R}\right)\dot{R} = \left(\frac{\kappa_1^n}{\gamma^n}\right)\left(\frac{\kappa_2^m}{\sigma^m}\right)\alpha\overline{R}\left(1 - \frac{I}{\overline{I}}\frac{\overline{R}}{R}\right)$$

Therefore, our sub-function $\dot{\mathcal{F}_2}$ can be written in the following form:

$$\begin{aligned}\dot{\mathcal{F}_2} = {} & \frac{\beta I\overline{S}}{N}\left(n + m + 2 - \frac{\overline{S}}{S} - \frac{\overline{E_1}}{E_1}\frac{S}{\overline{S}}\frac{I}{\overline{I}} - \sum_{i=2}^{n}\frac{\overline{E_i}}{E_i}\frac{E_{i-1}}{\overline{E_{i-1}}} - \frac{\overline{T_1}}{T_1}\frac{E_n}{\overline{E_n}} - \sum_{j=2}^{m}\frac{\overline{T_j}}{T_j}\frac{T_{j-1}}{\overline{T_{j-1}}} - \frac{\overline{I}}{I}\frac{T_m}{\overline{T_m}}\right) \\ & + \left(\frac{\kappa_1^n}{\gamma^n}\right)\left(\frac{\kappa_2^m}{\sigma^m}\right)\alpha\overline{R}\left(2 - \frac{\overline{I}}{I}\frac{R}{\overline{R}} - \frac{I}{\overline{I}}\frac{\overline{R}}{R}\right) \\ & + \kappa_0\overline{S}\left(2 - \frac{\overline{S}}{S} - \frac{S}{\overline{S}}\right)\end{aligned}$$

Lets now consider our other sub-function $\dot{\mathcal{F}_1}$. Using the equalities from above, the similar relationship from the analysis of the SE^{n}TIRC model is attained:

$$\begin{aligned}\left(\frac{\kappa_1^n}{\gamma^n}\right)\left(\frac{\kappa_2^m}{\sigma^m}\right)\left(\frac{\kappa_3\kappa_4}{\nu}\right)\overline{R} &= \left(\frac{\kappa_1^n}{\gamma^n}\right)\left(\frac{\kappa_2^m}{\sigma^m}\right)\kappa_3\overline{I} \\ &= \left(\frac{\kappa_1^n}{\gamma^n}\right)\left(\frac{\kappa_2^m}{\sigma^m}\right)\left(\alpha\overline{R} + \sigma\overline{T}_m\right) \\ &= \left(\frac{\kappa_1^n}{\gamma^n}\right)\left(\frac{\kappa_2^m}{\sigma^m}\right)\alpha\overline{R} + \left(\frac{\kappa_1^n}{\gamma^n}\right)\left(\frac{\kappa_2^m}{\sigma^m}\right)\sigma\overline{T}_m \\ &= \left(\frac{\kappa_1^n}{\gamma^n}\right)\left(\frac{\kappa_2^m}{\sigma^m}\right)\alpha\overline{R} + \frac{\beta\overline{S}}{N\nu}\kappa_4\overline{R}\end{aligned}$$

This is used below to show that the sub-function is equal to zero ($\dot{\mathcal{F}_1} = 0$).

$$
\begin{aligned}
\dot{\mathcal{F}}_1 &= \frac{\beta I\overline{S}}{N} - \frac{\beta IS}{N} + \sum_{i=1}^{n}\left(\frac{\kappa_1^{i-1}}{\gamma^{i-1}}\right)\dot{E}_i + \sum_{j=1}^{m}\left(\frac{\kappa_1^n}{\gamma^n}\right)\left(\frac{\kappa_2^{j-1}}{\sigma^{j-1}}\right)\dot{T}_j + \left(\frac{\kappa_1^n}{\gamma^n}\right)\left(\frac{\kappa_2^m}{\sigma^m}\right)\dot{I} \\
&\quad + \left(\left(\frac{\kappa_1^n}{\gamma^n}\right)\left(\frac{\kappa_2^m}{\sigma^m}\right)\frac{\kappa_3}{\sigma\nu} - \frac{\beta\overline{S}}{N\nu}\right)\dot{R} \\
&= -\frac{\beta IS}{N} + \left(\frac{\beta IS}{N} - \kappa_1 E_1\right) + \sum_{i=2}^{n}\left(\frac{\kappa_1^{i-1}}{\gamma^{i-1}}\right)\left(\gamma E_{i-1} - \kappa_1 E_i\right) \\
&\quad + \left(\frac{\kappa_1^n}{\gamma^n}\right)\left(\gamma E_n - \kappa_2 T_1\right) + \sum_{j=2}^{m}\left(\frac{\kappa_1^n}{\gamma^n}\right)\left(\frac{\kappa_2^{j-1}}{\sigma^{j-1}}\right)\left(\sigma T_{j-1} - \kappa_2 T_i\right) \\
&\quad + \left(\frac{\kappa_1^n}{\gamma^n}\right)\left(\frac{\kappa_2^m}{\sigma^m}\right)\left(\sigma T_m + \alpha R - \kappa_3 I\right) + \frac{\beta I\overline{S}}{N} + \left(\left(\frac{\kappa_1^n}{\gamma^n}\right)\left(\frac{\kappa_2^m}{\sigma^m}\right)\frac{\kappa_3}{\nu} - \frac{\beta\overline{S}}{N\nu}\right)\left(\nu I - \kappa_4 R\right) \\
&= \sum_{i=1}^{n} E_i\left(\frac{\kappa_1^{i-1}}{\gamma^{i-1}}\right)\left(\frac{\kappa_1}{\gamma}\gamma - \kappa_1\right) + \sum_{j=1}^{m} T_j\left(\frac{\kappa_1^n}{\gamma^n}\right)\left(\frac{\kappa_2^{j-1}}{\sigma^{j-1}}\right)\left(\frac{\kappa_2}{\sigma}\sigma - \kappa_2\right) \\
&\quad + I\left(\left(\frac{\kappa_1^n}{\gamma^n}\right)\left(\frac{\kappa_2^m}{\sigma^m}\right)\frac{\kappa_3}{\nu}\nu - \left(\frac{\kappa_1^n}{\gamma^n}\right)\left(\frac{\kappa_2^m}{\sigma^m}\right)\kappa_3 - \frac{\beta\overline{S}}{N\nu}\nu + \frac{\beta\overline{S}}{N}\right) \\
&\quad + R\left(-\left(\frac{\kappa_1^n}{\gamma^n}\right)\left(\frac{\kappa_2^m}{\sigma^m}\right)\left(\frac{\kappa_3\kappa_4}{\nu}\right) + \left(\frac{\kappa_1^n}{\gamma^n}\right)\left(\frac{\kappa_2^m}{\sigma^m}\right)\alpha + \frac{\beta\overline{S}}{N\nu}\kappa_4\right) \\
&= \left(\frac{R}{\overline{R}}\right)\left(-\left(\frac{\kappa_1^n}{\gamma^n}\right)\left(\frac{\kappa_2^m}{\sigma^m}\right)\left(\frac{\kappa_3\kappa_4}{\nu}\right)\overline{R} + \left(\frac{\kappa_1^n}{\gamma^n}\right)\left(\frac{\kappa_2^m}{\sigma^m}\right)\alpha\overline{R} + \frac{\beta\overline{S}}{N\nu}\kappa_4\overline{R}\right) \\
&= 0
\end{aligned}
$$

Therefore, the original Lyapunov function $\dot{\mathcal{F}}$ such that $\dot{\mathcal{F}} = \dot{\mathcal{F}}_1 + \dot{\mathcal{F}}_2$, is the following:

$$
\begin{aligned}
\dot{\mathcal{F}} &= \frac{\beta I\overline{S}}{N}\left(n + m + 2 - \frac{\overline{S}}{S} - \frac{\overline{E_1}}{E_1}\frac{S}{\overline{S}}\frac{I}{\overline{I}} - \sum_{i=2}^{n}\frac{\overline{E_i}}{E_i}\frac{E_{i-1}}{\overline{E_{i-1}}} - \frac{\overline{T_1}}{T_1}\frac{E_n}{\overline{E_n}} - \sum_{j=2}^{m}\frac{\overline{T_j}}{T_j}\frac{T_{j-1}}{\overline{T_{j-1}}} - \frac{\overline{I}}{I}\frac{T_m}{\overline{T_m}}\right) \\
&\quad + \left(\frac{\kappa_1^n}{\gamma^n}\right)\left(\frac{\kappa_2^m}{\sigma^m}\right)\alpha\overline{R}\left(2 - \frac{\overline{I}}{I}\frac{R}{\overline{R}} - \frac{I}{\overline{I}}\frac{\overline{R}}{R}\right) \\
&\quad + \kappa_0\overline{S}\left(2 - \frac{\overline{S}}{S} - \frac{S}{\overline{S}}\right)
\end{aligned}
$$

Using the fact that the arithmetic mean is greater than or equal to the geometric mean, the following inequalities hold:

$$
\begin{aligned}
n + m + 2 - \frac{\overline{S}}{S} - \frac{\overline{E_1}}{E_1}\frac{S}{\overline{S}}\frac{I}{\overline{I}} - \sum_{i=2}^{n}\frac{\overline{E_i}}{E_i}\frac{E_{i-1}}{\overline{E_{i-1}}} - \frac{\overline{T_1}}{T_1}\frac{E_n}{\overline{E_n}} - \sum_{j=2}^{m}\frac{\overline{T_j}}{T_j}\frac{T_{j-1}}{\overline{T_{j-1}}} - \frac{\overline{I}}{I}\frac{T_m}{\overline{T_m}} &\leqslant 0 \\
2 - \frac{\overline{I}}{I}\frac{R}{\overline{R}} - \frac{I}{\overline{I}}\frac{\overline{R}}{R} &\leqslant 0 \\
2 - \frac{\overline{S}}{S} - \frac{S}{\overline{S}} &\leqslant 0
\end{aligned}
$$

The above Lyapunov function $\dot{\mathcal{F}} < 0$ therefore shows that given that model parameters are non-negative and given initial condition in Ω_{n+m}, then the unique endemic equilibrium $\mathcal{EE}$ is globally asymptotically stable (GAS) when it exists (i.e. when $\mathcal{R}_0 > 1$).